Dipolar Liquids and Their Mixtures: Equilibrium and Nonequilibrium Properties with Field-Theoretic Approaches

Thesis by

Bilin Zhuang

In Partial Fulfillment of the Requirements for the

Degree of

Doctor of Philosophy

CALIFORNIA INSTITUTE OF TECHNOLOGY

Pasadena, California

2017

(Defended May 23, 2016)

To my mother, who embodied the greatest of a mother,
and whose love has carved an initial on every aspect of me

谨以这份论文献给我深爱的母亲，
对她在过去三十个逝去的春夏秋冬里为我辛勤而默默的付出与无微不至的爱，
致以微不足道的感谢

Acknowledgements

Six years have passed since I came to Caltech. It has been six years filled with much joy and sorrow. It has also been six years that have made a true transformation in me. I am indebted to many people for making these six years a rewarding and unforgettable experience, and at this moment, it is a pleasant task to thank all those for their continuous encouragement, support, and guidance.

First of all, I am extremely grateful to my advisor, Professor Zhen-Gang Wang. It is impossible to put in words how many ways he has influenced me, both in my professional development and in my personal growth. Over the past six years, in addition to guiding me with his impressive understanding, insights, and intuitions of statistical mechanics, he has also given me much freedom and independence to explore the unknown. When the tasks were challenging, he told me that "it is okay, we can work on other things", which has given me the reassurance and the time and space to eventually tackle the difficult problems. I am also grateful to all the hours that we sat in front of our papers together, pondering over them word by word – his meticulousness and perfectionism with developing the logic and the language in every word and punctuation always made me feel that the writing process is like crafting a delicate art piece. With his guidance, I have found much enjoyment in all the bits and pieces of research. Beyond research, he often shares with us much wisdom for life, and always encourages us to enjoy our hobbies and interests beyond work. During times of difficulties, he is the most understanding and accommodating, and the most caring and supportive. He has been a great mentor, teacher, and friend, and I feel truly fortunate to have had him as my advisor in the past six years.

I would also like to express my gratitude to members of my dissertation committee:

Professors David Tirrell, Thomas Miller, and Rudolph A. Marcus. Every meeting that I had with them was met with critical assessments of my work and many helpful suggestions. Professor Tirrell is the only experimental scientist in the committee; his comments and suggestions always pointed to the key issues that I need to improve on in my theory. As the chair of the committee, he has always been encouraging, with a reassuring broad smile during intense discussions during committee meetings and whenever we met in the hallway. Professor Miller has given me many valuable suggestions and constructive criticisms on my work. I have benefited from many discussions with him on my projects, especially when I was stumbling on technical difficulties; his suggestions always directed me to solve the crux of problems. It was also a true pleasure and privilege to have had many discussions with Professor Marcus, whose wealth of knowledge and insights cumulated over almost a century always brought me to think about my work in a broader scope.

I would also like to thank members of the Wang group. It is a cohesive group where members care for one another, and it has been a privilege to get to know and to work with them over the last several years. During my time in the Wang group, I met Issei Nakamura, Xiaofei Xu, Christina Ting, Rui Wang, Kevin Shen, Issac Fees, Ahmad Omar, Rachel Krueger, Umi Yamamoto, Jian Jiang, and Pengfei Zhang. It is not exaggerating to say that everyone in the group has been a good friend as well as an inspiration to me. I would like to specially thank Issei for laying the foundation for the work in this thesis, for countless helpful discussions, and for telling me that "if something is very confusing, that means there is a lot to be worked on". I would also like to thank Rui and Kevin for many of their helpful suggestions over the course of my research, which have been crucial to the work developed in this thesis. I also appreciate Christina for her help with my transition to Caltech during my first two years, and thank Xiaofei, Kevin, Umi, Jian, and Pengfei for being such caring friends beyond the scope of work and for supporting me through the most difficult times. It is also a true privilege to work with Ahmad, whose strength and optimism are a constant source of inspiration.

Outside the group, I would like to thank many of my friends, including Sijia

Dong, Connie Wang, Wendy Gu, Boyu Li, Caitlin Scott, and many others, who have given me lots of support over the past six years. I would also like to gratefully acknowledge the Agency for Science, Technology and Research (A*STAR), Singapore for the National Science Scholarship, without which I would not have the opportunity to have had the privilege of a fruitful education here. Acknowledgment is also made to the donors of the American Chemical Society Petroleum Research Fund for partial support of my research.

Throughout my life, the love and encouragement from my family have been of utmost importance in my growth. At this moment as I am completing my thesis, I would like to pay a homage to my most wonderful mother, Zhu Liqiong. I thank her for bringing me to this world, for raising me up with her love and care, and for always protecting me and shielding me from worries. Unfortunately, she left us for another world last year, leaving my mind still searching for her at moments of awakeness at night. Even though I will never be able to thank her enough, I dedicate this thesis to my mother, in the smallest way of saying thanks for all she has done and beyond.

In addition, I thank my father deeply for all his strength, optimism, and wisdom. It has been a truly difficult time, but he has stayed calm and held us tight through the storm. I also have to thank my younger brother specially for delaying a year of his college education to be with my father this past year – without his sacrifice, I would not have the peace of mind to complete the work in this thesis. I would also like to thank my parents-in-law and sisters-in-law, whose support have been instrumental in this journey.

Last but foremost, I am deeply thankful to my husband, Ding Ding, for being one that I could never find anywhere else. In the past eight years, we have sailed through many hard times together. Ding, thank you for being my pillar of support, for holding onto me tight when I am lost, and for knowing me deepest inside my heart. Thank you for making me a better and happier person each and every day that we spend together. With the impending arrival of our first child, I have a lot to look forward to in the life ahead with you.

Abstract

Liquid is a state of matter that is intermediate between the gas state and the solid state. Though it is an ordinary state of matter, the application of statistical mechanics for understanding its properties is far from complete. Compared to the solid state, the liquid state has molecules that can move around freely, and yet, unlike that in the gas state, the intermolecular correlations are significant in the liquid state. Therefore, the distance dependent correlations in a liquid need to be taken into account to properly describe a liquid. In particular, all molecules are polarizable. The polarizable nature allows the molecules to induce polarization in surrounding molecules, giving rise to van der Waals interactions that have important consequences on the properties of a liquid. In addition to polarizability, many molecules are intrinsically polar. The long-ranged dipole-dipole correlations contribute to the complexity of interactions and lead to a myriad of interesting properties special to a liquid.

In recent years, field-theoretic technique has emerged as a convenient and systematic tool for deriving coarse-grained theories for a wide range of complex-fluid and soft-matter systems while preserving the essential physics. In this thesis, we present the application of field-theoretic approaches to two problems of liquids and their mixtures. The first problem is to describe the dielectric properties of an ordinary liquid or liquid mixture under equilibrium condition, where current field-theoretic methods are inadequate. In this problem, we apply a variational field-theoretic approach to develop a statistical field theory of the liquid, and predict the dielectric constant and the miscibility of liquids using the variational free energies derived. The second problem involves the nonequilibrium solvent composition and orientational polarization surrounding some charged solute in the context of electron transfer reactions.

Using a self-consistent-field theory with constrained coarse-grained fields, we derive expressions for the nonequilibrium solvation energy, and apply it to compute the reorganization energy of electron transfer reactions. The theories presented in this thesis lead to simple analytical expressions for the equilibrium and the nonequilibrium free energies, making it possible to theoretically survey a wide range of liquids. In addition, our models involve only a few readily-available molecular parameters and avoid the use of any adjustable parameters, allowing one to make *a priori* predictions on the properties of liquids and their mixtures. Liquid is a state of matter that is intermediate between the gas state and the solid state. Though it is an ordinary state of matter, the application of statistical mechanics for understanding its properties is far from complete. Compared to the solid state, the liquid state has molecules that can move around freely, and yet, unlike that in the gas state, the intermolecular correlations are significant in the liquid state. Therefore, the distance dependent correlations in a liquid need to be taken into account to properly describe a liquid. In particular, all molecules are polarizable. The polarizable nature allows the molecules to induce polarization in surrounding molecules, giving rise to van der Waals interactions that have important consequences on the properties of a liquid. In addition to polarizability, many molecules are intrinsically polar. The long-ranged dipole-dipole correlations contribute to the complexity of interactions and lead to a myriad of interesting properties special to a liquid.

In recent years, field-theoretic technique has emerged as a convenient and systematic tool for deriving coarse-grained theories for a wide range of complex-fluid and soft-matter systems while preserving the essential physics. In this thesis, we present the application of field-theoretic approaches to two problems of liquids and their mixtures. The first problem is to describe the dielectric properties of an ordinary liquid or liquid mixture under equilibrium condition, where current field-theoretic methods are inadequate. In this problem, we apply a variational field-theoretic approach to develop a statistical field theory of the liquid, and predict the dielectric constant and the miscibility of liquids using the variational free energies derived. The second problem involves the nonequilibrium solvent composition and orientational polariza-

tion surrounding some charged solute in the context of electron transfer reactions. Using a self-consistent-field theory with constrained coarse-grained fields, we derive expressions for the nonequilibrium solvation energy, and apply it to compute the reorganization energy of electron transfer reactions. The theories presented in this thesis lead to simple analytical expressions for the equilibrium and the nonequilibrium free energies, making it possible to theoretically survey a wide range of liquids. In addition, our models involve only a few readily-available molecular parameters and avoid the use of any adjustable parameters, allowing one to make *a priori* predictions on the properties of liquids and their mixtures.

Published Content and Contributions

[1] Zhuang, B.; Wang, Z.-G. A Molecularly Based Theory for Electron Transfer Reorganization Energy. *J. Chem. Phys.* **2015,** *143,* 224502. DOI: 10.1063/1.4936586.

B.Z. participated in the conception of the project, derived the theory, performed the numerical calculations, analyzed the data, and participated in the writing of the manuscript.

[2] Zhuang, B.; Wang, Z.-G. Molecular-Based Theory for Electron-Transfer Reorganization Energy in Solvent Mixtures. *J. Phys. Chem. B* **2016,** *120,* 6373-6382. DOI: 10.1021/acs.jpcb.6b03295.

B.Z. participated in the conception of the project, derived the theory, performed the numerical calculations, analyzed the data, and participated in the writing of the manuscript.

Contents

List of Figures

List of Tables

Chapter 1

Introduction

The liquid state of matter is perceived as being intermediate in nature between the gas state and the solid state. However, in many aspects, the properties of a liquid are vastly different from a solid and a gas. In a liquid, there is a lack of translationally-ordered structure, and yet, the intermolecular interactions are strong and the molecules are constantly influencing the molecular state of one another. In particular, all molecules are polarizable, such that instantaneous induced dipole moments constantly appear and disappear as the molecules move towards and away from one another. Additionally, many molecules are polar, and their permanent dipole moments have significant effects on the correlations between the molecules. The presence of dipole moments gives rise to strong and long-ranged electrostatic interactions that have important consequences on the macroscopic properties of liquids. Therefore, to properly describe the basic nature of a liquid, one must carefully account for the effects of dipole-dipole interactions, which, at present, are still of great theoretical complexity to modern statistical-mechanical treatments of liquids.

In addition to pure liquids, there has also been long-standing interest in liquid mixtures due to their technological and industrial importance, as they offer virtually endless possibilities as tunable reaction media. Macroscopic properties such as dielectric constants, refractive indices, and transport properties of liquid mixtures can all be conveniently tuned by varying their mixture composition. Scientifically, liquid mixtures are interesting because they often exhibit complex structural and dynamical features that are not present in pure liquids. For example, charge solvation in a liquid

mixture is profoundly influenced by the phenomenon of preferential solvation, where the local composition of the solvent around a charged solute is significantly different from the bulk composition of the mixture.[2] In the realm of liquid mixtures, the development of simple, convenient, and yet robust theories is particularly helpful, because the sheer number of different solvent mixtures makes it too expensive to be surveyed through experimental methods or computational simulations. To facilitate the search of new reaction media for technological applications, a convenient and predictive theoretical framework for liquid mixtures is desirable. Presently, the generalization of liquid theories to liquid mixtures remains challenging, because the additional interactions and features in liquid mixtures often make the theories intractably complex.

The application of statistical mechanics to the study of liquids has progressed through the past century, but the theoretical framework is far from being complete.[3] Early attempts describe liquids as disordered solids with lattice model;[4,5] they were popular from the mid-1930s until the early 1960s, but they fail to predict a sufficiently large entropy. An alternative and more fundamental approach is to model the liquids using integral equation methods.[6–8] The approach starts by writing down exact equations for the molecular distribution function, and then introduces approximations to obtain a solution for the distribution function. This approach is able to provide the distribution functions directly, and is applicable to a wide variety of properties, but the theory often results in an integral equation that must be numerically solved in most cases, and the computation for numerical solutions can be particularly cumbersome for molecular liquids (for which the distribution functions involve orientational dependence) and liquid mixtures (for which mixture distribution functions are involved). Furthermore, the approach is often model-dependent, or includes adjustable parameters for liquids that cannot be determined *a priori*. Another successful theoretical framework is based on the thermodynamic perturbation theories.[6,7,9,10] In this approach, a reference fluid is chosen, and the free energy of the system is written as a perturbation from that of the reference system. However, the drawback in the approach is that the reference system must be close enough to the actual system, and as a result, it is difficult to apply the theory to general liquid systems.

Presently, one of the great difficulties for statistical-mechanical treatment of liquid is to account for the effects of molecular polarizability, which causes fluctuating instantaneous dipoles to constantly appear and disappear in the molecules. For integral-equation theories and perturbative approaches, it is a daunting task to include the induced-dipole dependence in the correlation functions. Therefore, most work treats solvent molecules as nonpolarizable molecules, for example, in the recently developed molecular density functional theories.[11,12] Other researchers approximate the effects of induced dipoles by considering renormalized systems/energies of nonpolarizable solvent.[13] The challenge in treating solvent polarizability poses a particular difficulty in the description of nonequilibrium properties of the solvent in the context of electron transfer reactions, where the permanent dipole moments and the induced dipole moments respond to the charge transfer on different time scales. Therefore, it is desirable to develop a convenient theoretical framework to treat both the permanent and the induced dipole moments explicitly without adding much complexity to the theory.

This thesis presents an alternative approach for the description of liquids and their mixtures, based on field-theoretic methods. In recent years, field-theoretic approach has been applied to a wide range of complex-fluid and soft-matter systems,[14–16] including polymeric systems,[14,16] biomolecular systems,[17,18] interfacial phenomena,[19] and amphiphiles,[20] and liquid crystals.[21] In a general field-theoretic approach, through a series of identity transformations, the particle-particle interactions can be decoupled by the introduction of a fluctuating field, such that each particle interacts with the fluctuating field instead of one another. The procedure may also introduce fluctuating densities (such as number density, charge density, or polarization density) that can serve as convenient coarse-grained order parameters for the state of the system. In a field-based partition function, the fluctuating fields and the fluctuating densities, instead of the individual particle degrees of freedom, are integrated over in the configurational integral. In addition, the fluctuating fields and the fluctuating densities may serve to describe the coarse-grained states of the system on the macroscopic scale. In the context of liquids, field-theoretic methods can provide a convenient and

systematic coarse-graining procedure so that we can explicitly account for the molecular permanent dipoles and induced dipoles without introducing much complexity to the theory. The procedure also enables us to circumvent the difficulty of describing molecular interactions through correlation functions, allowing the theory to be conveniently generalized to liquid mixtures. If a robust field-theoretical framework is developed for dipolar solvents and their mixtures, we can readily incorporate the framework to a myriad of other complex-fluid systems that has already been treated with field-theoretic approach.

The thesis considers two main systems. The first system is an equilibrium system of liquids or liquid mixtures. Presently, most field-theoretic approaches for equilibrium liquids have only been able to describe the liquid in the limit of dilute gases, without taking into account how a dipole moment influences its surrounding, which then exerts a field back on the dipole. In this thesis, we present a variational field-theoretic approach for the dipolar liquid systems, such that the effects of reaction field in the liquid can be taken into account. We apply the theory to calculate the dielectric constants of pure liquids and liquid mixtures and to predict the miscibility between liquids. Our development of the variational field-theoretic approach is presented in Part I (Chapters 2 and 3) of this thesis.

The second system that we consider is a system of nonequilibrium pure solvent or solvent mixtures around charged solutes, in the context of electron transfer reactions. In an electron transfer reaction, the electronic transition is a very fast process. While the solvent electronic degrees of freedom (represented by their induced dipoles) can react to the electronic transition on the same time scale, the solvent nuclear degrees of freedom (represented by their positions and their permanent dipoles) respond on a much slower time scale. Due to the different time scales for the fast electronic and the slow nuclear response in the solvent, the electron transfer process involves a nonequilibrium solvation state, where the solvent nuclear degrees of freedom are out-of-equilibrium with the charge on the solute and with the solvent electronic degrees of freedom. The problem of nonequilibrium solvation requires one to separate the electronic and nuclear degrees of freedom of the solvent. Our field-theoretic ap-

proach provides a simple framework for naturally treating the solvent permanent and induced dipoles as independent degrees of freedom. The orientational and electronic polarizations are described as independent coarse-grained fields, at the same level of approximation. This provides great convenience for treating the problem of nonequilibrium charge solvation. In this thesis, we present our development of a self-consistent-field theory for nonequilibrium charge solvation in Part II (Chapters 4 to 6).

In developing the field-theoretic approaches for both the equilibrium and the nonequilibrium systems, we describe the solvent molecules using only a few parameters that are readily available from physicochemical tables; the parameters include the permanent dipole moment and the polarizability for each solvent molecule, as well as the volume for each molecule. Our goal is to develop theories that use a minimal set of parameters but account for the most important effects and provide the key physical insights. By limiting the dependent variables to a few simple and non-adjustable parameters, the theories are more convenient for making *a priori* predictions than more elaborate theories that are based on detailed molecular models and require a large set of model-dependent, fitting parameters. Furthermore, since detailed molecular models are not available for general liquids, the theories presented in this thesis would serve as convenient tools for surveying properties of general liquids and mixtures mixtures.

The thesis is organized as follows. In Chapter 2, using a variational field-theoretic approach, we derive a theory for calculating the dielectric constants of a pure liquid, allowing the effect of reaction field to be taken into account without casting a cavity in the homogeneous system. The resulting theory evaluates the dielectric constant of a liquid with two simple algebraic equations, based on readily-available molecular quantities including the gas-phase permanent dipole moment, the molecular isotropic polarizability, and the volume of each molecule in the liquid. Though free of any adjustable parameters, the theory calculates dielectric constants of liquids in better agreement with experimental values compared to earlier theories based on field-theoretic methods with saddle-point approximation.

In Chapter 3, we present a variational field-theoretical approach for studying polar liquid mixtures, and apply the theory to compute the dielectric constants and miscibility of liquid mixtures. The theory results in a simple analytical expression for the free energy of a mixture. Using only the dielectric constants and the molar volumes of the pure-solvent components as inputs, and not any adjustable parameters, the theory predicts the dielectric constants and miscibility of liquid mixtures in impressive agreements with experimentally observed results. In addition, a short-ranged polarization distribution function is introduced for each solvent molecule, removing the divergence problems in the field-theoretic treatment.

In Chapter 4, we develop a molecularly-based dipolar self-consistent-field theory (DSCFT) for charge solvation in pure solvents under equilibrium and nonequilibrium conditions, and apply it to the reorganization energy of electron transfer reactions. The DSCFT uses a set of molecular parameters, such as the solvent molecule's permanent dipole moment and polarizability, thus avoiding approximations that are inherent in treating the solvent as a linear dielectric medium. A simple, analytical expression for the free energy is obtained in terms of the equilibrium and nonequilibrium electrostatic potential profiles and electric susceptibilities, which are obtained by solving a set of self-consistent equations. With no adjustable parameters, the DSCFT predicts activation energies and reorganization energies in good agreement with previous experiments and calculations for the electron transfer reorganization energies between metallic ions. Because the DSCFT is able to describe the properties of the solvent in the immediate vicinity of the charges, it is unnecessary to distinguish between the inner-sphere and outer-sphere solvent molecules in the calculation of the reorganization energy as in previous work. Furthermore, examining the nonequilibrium free energy surfaces of electron transfer, we find that the nonequilibrium free energy is well approximated by a double parabola for self-exchange reactions, but the curvature of the nonequilibrium free energy surface depends on the charges of the electron-transferring species, contrary to the prediction by the linear dielectric theory.

In Chapter 5, we extend the DSCFT for liquid mixtures under equilibrium and

nonequilibrium conditions, and apply it to compute the solvent reorganization energy of electron transfer reactions. In addition to the nonequilibrium orientational polarization, the reorganization energy in liquid mixtures is also determined by the out-of-equilibrium solvent composition around the reacting species due to preferential solvation. Using molecular parameters that are readily available, the DSCFT naturally accounts for the dielectric saturation effect and the spatially varying solvent composition in the vicinity of the reacting species. We identify three general categories of binary solvent mixtures, classified by the relative optical and static dielectric constants of the solvent components. Each category of mixture is shown to produce a characteristic local solvent composition profile in the vicinity of the reacting species, which gives rise to the distinctive composition dependence of the reorganization energy that cannot be predicted using the bulk dielectric constants of the solvent mixtures.

In Chapter 6, using both the DSCFT and molecular dynamics simulations, we calculate the solvent reorganization energies for the Fe^{2+}/Fe^{3+} electron exchange reaction in binary solvent mixtures, that are classified into three types based on the relative magnitudes of permanent dipole moments and polarizabilities of the components. Due to preferential solvation, the solvent reorganization energy in a mixed solvent not only includes contributions from the nonequilibrium orientational polarization, but also contributions from the nonequilibrium solvent composition around the charged redox centers. Both theory and simulations suggest that solvent reorganization energy in mixtures is predominantly determined by the solvent composition in the vicinity of redox centers.

Finally, in Chapter 7, we offer some concluding remarks and point to some directions for future work.

Part I

Equilibrium Properties

Chapter 2

Dielectric Constants of Pure Liquids: A Field-Theoretic Variational Approach

2.1 Introduction

Dielectric constant is one of the most basic properties of a liquid. Since a century ago, the computation of the dielectric constant from molecular properties has received a great deal of interest in the scientific community.[22,23] In 1912, Debye derived an equation relating the dielectric constant with the molecular permanent dipole moment and the isotropic polarizability. As Debye assumed the "internal field" that acts on each dipole to be equal to the external field, intermolecular dipole-dipole interactions are completely ignored, and therefore, the Debye equation is only applicable for dilute systems such as gases.[24,25] In 1936, Onsager developed an improved model by considering a point dipole at the center of a spherical cavity that is embedded in a homogeneous dielectric continuum. The model accounts for the fact that the point dipole instantaneously rearranges the dipoles in its surrounding medium, and the resulting polarization in the surrounding gives rise to a *reaction field* that tends to enhance the magnitude of the dipole moment in the cavity.[26] The Onsager equation provides better predictions of the dielectric constants than the Debye equation for condensed systems such as liquids.[27] Shortly after, Kirkwood extended Onsager's model by introducing a g-factor that accounts for the short-range orientational correlation between

the molecules.[28] While Kirkwood's formulation has become especially relevant for determining dielectric constants with computer simulations,[29] it is often difficult to evaluate the g-factor analytically because detailed information about molecular interactions is needed for calculation.[27,30] Since then, more sophisticated theories for dielectric constants have been developed based on perturbative expansions,[31–33] cluster expansions,[34–36] and integral-equation theories,[13,37–39] but the Debye equation and the Onsager equation remain popular due to their simplicity.

Despite the large body of theoretical literature on the computation of dielectric constants, the development of a simple parameter-free theory for calculating dielectric constants based on readily-available molecular parameters remains a challenge. Methods based on perturbative expansions are unsatisfactory because the series do not converge with increasing number of terms.[40] Cluster expansion methods are able to relate dielectric constants to molecular properties, but the required correlation functions are cumbersome to evaluate. Integral-equation theories often describe polarizable molecules using an effective permanent dipole moment with zero polarizability, even though molecular polarizability has shown to have significant effect on the dielectric property of a fluid.[41–43] More recently, dielectric theories of liquids have been developed using field-theoretic approaches with saddle-point approximation,[44,45] providing a mean-field description for the system, whose results are comparable to the predictions of the Dybye equation. In addition, Levy *et. al.*[46,47] introduces a higher-level field-theoretic treatment and derived an expression for the dielectric constant at the one-loop level, but the resulting theory is very sensitive to the parameter chosen for the momentum cut-off. Despite the downsides, a field-theoretic dielectric theory has the advantage that it can be conveniently integrated into studies for a wide range of soft-matter systems,[14–16] and therefore, it is desirable to develop an accurate theory for the dielectric constant based on field-theoretic methods.

In this work, our goal is to derive a field-theoretic theory for calculating the dielectric constant of a pure liquid using a variational approach.[48,49] By introducing a physically meaningful reference potential, the variational approach allows us to take into account the effects of reaction field. The resulting field-theoretic variational the-

ory (FTVT) presented in this work consists of simple analytical equations that allows one to calculate the dielectric constant of a liquid based on readily-available molecular parameters, including the gas-phase permanent dipole moment, the molecular isotropic polarizability, and the average volume of a molecule, with the use of no adjustable parameters. We compare the FTVT-calculated dielectric constants with the experimentally-measured values for common liquid solvents, and observe that the agreement between the theory and the experiment is satisfactory. For non-hydrogen-bonding liquids, the slope of the best-fit line for the FTVT-calculated vs. experimental values of dielectric constant is close to 1. Furthermore, unlike the Onsager derivation, which casts a cavity in the system and treats the molecule in the cavity as a special one, the FTVT does not involve the construction of a cavity. This feature makes it straightforward to extend the FTVT to liquid mixtures, for which analytical models are particularly desirable since it is inefficient to explore the huge parameter space of mixture compositions with computer simulations.

Another feature of the theory is the introduction of a short-ranged polarization distribution function for each molecule. The advantage of introducing such a short-ranged polarization distribution function is that the molecules are not described as point dipoles, and thus, the approach yields a theory that is free of divergences (which is a common issue in field-theoretic treatments of electrostatic problems). Where no divergence is caused, the short-ranged polarization distribution function can be taken to the point-dipole limit to simplify the theory.

The chapter is organized as follows. In Section 2.2, we describe the model and formulate the exact partition function in the field-theoretic representation. Then, we introduce a Gaussian reference action and apply the variational approach based on the Gibbs-Feynman-Bogoliubov variational principle. We solve the variational equations in the limit of zero external field, and find the relation between the polarization and the external field to calculate the dielectric constant. In Section 2.3, we apply the FTVT to calculate the dielectric constants of common organic liquids, and compare the results to the values calculated by the Onsager equation and the the dipolar self-consistent-field theory (DSCFT) in Ref. 44, both of which compute dielectric

constants with no adjustable parameters. Finally, in Section 2.4, we summarize the key features of the FTVT and offer some concluding remarks.

2.2 The Field-Theoretic Variational Theory for Dipolar Liquids

2.2.1 The System

We consider a system of N dipolar molecules in a field $\mathbf{E}_0(\mathbf{r})$ applied by external sources. Each dipolar molecule is characterized by its molecular volume v, its permanent dipole with magnitude $\bar{\mu}$, and its molecular isotropic polarizability α. We let $\mathbf{r}_i$, $\boldsymbol{\mu}_i$, and $\mathbf{p}_i$ denote the position, the permanent dipole moment (where $|\boldsymbol{\mu}_i| = \bar{\mu}$), and the induced dipole moment of the ith molecule, respectively. The total dipole moment of the ith molecule can be written as $\mathbf{m}_i = \boldsymbol{\mu}_i + \mathbf{p}_i$. To avoid numerical divergences caused by the point-dipole approximation for the molecules, we assume that the dipole moment finitely spread around the center of each molecule described by a short-ranged function $h(\mathbf{r})$. At this point, we do not specify the form of $h(\mathbf{r})$, and only require that the integral over $h(\mathbf{r})$ in space is unity, i. e. $\int d\mathbf{r}\, h(\mathbf{r}) = 1$. With these, the instantaneous polarization of the ith molecule, $\hat{\mathbf{P}}_i(\mathbf{r})$, can be expressed as

$$\hat{\mathbf{P}}_i(\mathbf{r}) = \mathbf{m}_i h(\mathbf{r} - \mathbf{r}_i) = (\boldsymbol{\mu}_i + \mathbf{p}_i) h(\mathbf{r} - \mathbf{r}_i) \tag{2.1}$$

The electrostatic energy U of the system can be expressed as

$$\begin{aligned} U &= \frac{1}{2} \sum_{i=1}^{N} \sum_{\substack{j=1 \\ i \neq j}}^{N} \int d\mathbf{r} \int d\mathbf{r}'\, \hat{\mathbf{P}}_i(\mathbf{r}) \mathbf{T}(\mathbf{r} - \mathbf{r}') \hat{\mathbf{P}}_j(\mathbf{r}') + \sum_{i=1}^{N} \frac{\mathbf{p}_i^2}{2\alpha} \\ &\quad - \sum_{i=1}^{N} \int d\mathbf{r}\, \hat{\mathbf{P}}_i(\mathbf{r}) \cdot \mathbf{E}_0(\mathbf{r}) \end{aligned} \tag{2.2}$$

where $\mathbf{T}(\mathbf{r}) = -\nabla\nabla(1/4\pi\varepsilon_0|\mathbf{r}|)$ is the dipole-dipole interaction tensor. The first term in U is the sum of the pairwise dipole-dipole interaction energy between the molecules,

the second term is the distortion energy of the induced dipoles written within the harmonic approximation,[50,51] and the third term describes the interactions between the dipoles and the applied external field $\mathbf{E}_0$. To proceed, we define $\hat{\mathbf{P}}(\mathbf{r}) = \sum_{i=1}^{N} \hat{\mathbf{P}}_i(\mathbf{r})$ to be the instantaneous polarization of the entire system, and rewrite the energy U in terms of $\hat{\mathbf{P}}(\mathbf{r})$ as:

$$\begin{aligned} U &= \frac{1}{2}\int d\mathbf{r}\int d\mathbf{r}'\,\hat{\mathbf{P}}(\mathbf{r})\mathbf{T}(\mathbf{r}-\mathbf{r}')\hat{\mathbf{P}}(\mathbf{r}') - \sum_{i=1}^{N}\frac{1}{2}\int d\mathbf{r}\int d\mathbf{r}'\,\hat{\mathbf{P}}_i(\mathbf{r})\mathbf{T}(\mathbf{r}-\mathbf{r}')\hat{\mathbf{P}}_i(\mathbf{r}') \\ &\quad + \sum_{i=1}^{N}\frac{\mathbf{p}_i^2}{2\alpha} - \int d\mathbf{r}\,\hat{\mathbf{P}}(\mathbf{r})\cdot\mathbf{E}_0(\mathbf{r}) \end{aligned} \tag{2.3}$$

As improper integrals involving the dipole-dipole interaction tensor $\mathbf{T}(\mathbf{r})$ is nonunique, careful interpretation is required. In fact, the nature and the origin of problem has been addressed in the literature, and the required interpretation that is consistent with the Maxwell equations is to express the dipole-dipole interaction tensor as[52]

$$\mathbf{T}(\mathbf{r}) = \lim_{\delta\to 0}\left[H(|\mathbf{r}|-\delta)\left(\frac{1}{4\pi\varepsilon_0 r^3}\left[\mathbb{1} - \frac{3\mathbf{r}\mathbf{r}}{r^3}\right]\right) + \frac{1}{3\varepsilon_0}\mathbb{1}\delta(\mathbf{r})\right] \tag{2.4}$$

where $H(x)$ is the Heaviside step function, and $\mathbb{1}$ is the unit tensor. We understand that the $\delta \to 0$ limit is eventually taken.

For convenience, we choose to work with the grand canonical ensemble of the system under chemical potential μ, inverse temperature $\beta = 1/k_B T$, and volume V. The particle-based grand partition function of the system is given by

$$\Xi = \sum_{N=0}^{\infty}\frac{\lambda^N}{N!}Z(N) \tag{2.5}$$

with $Z(N)$ being the canonical partition function in which the Boltzmann factor is integrated over the configuration space of N particles and given by

$$Z(N) = \left(\prod_i \int d\mathbf{r}_i \int d\Omega_i \int d\mathbf{p}_i\right) e^{-\beta U(N)} \tag{2.6}$$

where Ω_i indicates the solid angle of the permanent dipole $\boldsymbol{\mu}_i$. $\lambda = e^{\beta\mu}$ is the fugacity of the molecule. The grand potential W of the system is

$$\beta W = -\ln \Xi \tag{2.7}$$

Using standard field-theoretic techniques, we transform the particle-based grand partition function into the field-based grand partition function using the Faddeev-Popov method.[14,15,53] The transformation removes the quadratic terms of intermolecular interactions, and introduces terms describing particles interacting with an auxiliary field. The resulting grand partition function is written as functional integrals over the polarization and the auxiliary field, instead of over the molecular degrees of freedom. We defer the details of the transformation to Appendix 2.A and simply write down the resulting field-based grand partition function as

$$\Xi = \int \mathcal{D}\mathbf{P} \int \mathcal{D}\mathbf{G}\, e^{-\mathcal{L}[\mathbf{P},\mathbf{G}]} \tag{2.8}$$

where the field-theoretic action $\mathcal{L}$ is given by

$$\begin{aligned} \mathcal{L}[\mathbf{P},\mathbf{G}] \;=\; & \frac{1}{2}\langle \mathbf{P}|\, \boldsymbol{\mathcal{T}}\, |\mathbf{P}\rangle + i\,\langle \mathbf{P}|\, \mathbf{G}\rangle - \langle \mathbf{P}|\, \boldsymbol{\mathcal{E}}_0\rangle \\ & -\lambda \int d\mathbf{r} \int d\Omega \int d\mathbf{p}\, e^{i(\boldsymbol{\mu}+\mathbf{p})\cdot\mathbf{G}_h(\mathbf{r}) - \frac{\mathbf{p}^2}{2\bar{\alpha}} + \frac{1}{2}(\boldsymbol{\mu}+\mathbf{p})\cdot\boldsymbol{\mathcal{T}}_h(\mathbf{r})\cdot(\boldsymbol{\mu}+\mathbf{p})} \end{aligned} \tag{2.9}$$

where we have defined $\boldsymbol{\mathcal{T}} = \beta\mathbf{T}$, $\boldsymbol{\mathcal{E}}_0 = \beta\mathbf{E}_0$, and $\bar{\alpha} = \alpha/\beta$ for notational symplicity. The rules for the inner products are defined as

$$\langle \mathbf{v}_1|\, \mathbf{v}_2\rangle = \int d\mathbf{r}\, \mathbf{v}_1(\mathbf{r})\cdot\mathbf{v}_2(\mathbf{r}) \tag{2.10}$$

$$\langle \mathbf{v}_1|\, \mathbf{M}\, |\mathbf{v}_2\rangle = \int d\mathbf{r} \int d\mathbf{r}'\, \mathbf{v}_1(\mathbf{r})\mathbf{M}(\mathbf{r}-\mathbf{r}')\mathbf{v}_2(\mathbf{r}') \tag{2.11}$$

and $\mathbf{G}_h(\mathbf{r})$ and $\boldsymbol{\mathcal{T}}_h(\mathbf{r})$ are respectively the fluctuating field and the dipole interaction

tensor averaged over a single molecule, and they are given by

$$\mathbf{G}_h(\mathbf{r}) = \int d\mathbf{r}' h(\mathbf{r}' - \mathbf{r}) \mathbf{G}(\mathbf{r}') \tag{2.12}$$

$$\boldsymbol{\mathcal{T}}_h(\mathbf{r}) = \int d\mathbf{r}' \int d\mathbf{r}'' \, h(\mathbf{r}' - \mathbf{r}) \boldsymbol{\mathcal{T}}(\mathbf{r}' - \mathbf{r}'') h(\mathbf{r}'' - \mathbf{r}) \tag{2.13}$$

The field-based grand partition function Ξ in Eq. (2.8) is formally exact. However, since the last term in $\mathcal{L}$ – which is the partition function of a single molecule under the auxiliary field $\mathbf{G}$ – is not Gaussian, it is difficult to evaluate the partition function exactly. In the following section, we introduce a variational approach to provide an approximate treatment to the partition function.

2.2.2 Variational Treatment

We formulate the variational theory by introducing the reference action $\mathcal{L}_0$, which has the last term in $\mathcal{L}$ replaced with an expression of the Gaussian form:

$$\begin{aligned} \mathcal{L}_0[\mathbf{P}, \mathbf{G}] = \quad & \frac{1}{2} \langle \mathbf{P} | \, \boldsymbol{\mathcal{T}} \, | \mathbf{P} \rangle + i \langle \mathbf{P} | \, \mathbf{G} \rangle - \langle \mathbf{P} | \, \boldsymbol{\mathcal{E}}_0 \rangle \\ & + \frac{1}{2} \langle \mathbf{G} + i\mathbf{F} | \, \boldsymbol{\mathcal{A}}^{-1} \, | \mathbf{G} + i\mathbf{F} \rangle \end{aligned} \tag{2.14}$$

where $\boldsymbol{\mathcal{A}}(\mathbf{r}) = a \mathbb{1} \delta(\mathbf{r})$, with a and $\mathbf{F}$ being the variational parameters. The inverse of operator $\boldsymbol{\mathcal{A}}$ is $\boldsymbol{\mathcal{A}}^{-1}(\mathbf{r}) = \mathbb{1}\delta(\mathbf{r})/a$, such that the relation $\int d\mathbf{r}' \boldsymbol{\mathcal{A}}(\mathbf{r} - \mathbf{r}') \boldsymbol{\mathcal{A}}^{-1}(\mathbf{r}' - \mathbf{r}'') = \mathbb{1}\delta(\mathbf{r} - \mathbf{r}'')$ is satisfied. Because the last term in $\mathcal{L}$ involves only spatially local interactions, a δ-function on spatial variable is introduced in the Gaussian kernel in the last term of $\mathcal{L}_0$.

An upper bound for the field-based grand potential W can be obtained through the Gibbs-Feynman-Bogoliubov inequality:[54]

$$\beta W \leq \beta W_0 = -\ln \Xi_0 + \langle \mathcal{L} - \mathcal{L}_0 \rangle_0 \tag{2.15}$$

where Ξ_0 is given by

$$\Xi_0 = \int \mathcal{D}\mathbf{P} \int \mathcal{D}\mathbf{G}\, e^{-\mathcal{L}_0[\mathbf{P},\mathbf{G}]} \tag{2.16}$$

and $\langle \mathcal{O} \rangle_0$ is the average of observable $\mathcal{O}$ evaluated in the reference ensemble, i.e.,

$$\langle \mathcal{O} \rangle_0 = \frac{1}{\Xi_0} \int \mathcal{D}\mathbf{P} \int \mathcal{D}\mathbf{G}\, \mathcal{O}[\mathbf{P},\mathbf{G}] e^{-\mathcal{L}_0[\mathbf{P},\mathbf{G}]} \tag{2.17}$$

As W_0 is the upper bound for the grand potential W, we carry out the variational treatment by minimizing the upper bound W_0 with respect to variational parameters a and $\mathbf{F}$, and approximate W with the minimized upper bound. We present the details of the evaluation of W_0 in Appendix 2.B, and simply present the result here:

$$\begin{aligned} \beta W_0 \;=\; & -\ln\left(\frac{\det \boldsymbol{\mathcal{A}}}{\det(\boldsymbol{\mathcal{T}}+\boldsymbol{\mathcal{A}})}\right)^{\frac{1}{2}} - \frac{1}{2}\int d\mathbf{r}\, \frac{\beta}{v(\beta+\varepsilon_0 a)} \\ & -\frac{1}{2}\left(\frac{\varepsilon_0}{\beta+\varepsilon_0 a}\right)^2 \langle \boldsymbol{\mathcal{E}}_0 - \mathbf{F}|\, \boldsymbol{\mathcal{T}}\, |\boldsymbol{\mathcal{E}}_0 - \mathbf{F}\rangle \\ & -\lambda \int d\mathbf{r} \int d\Omega \int d\mathbf{p}\, e^{-f(\boldsymbol{\mu},\mathbf{p};\,\mathbf{r})} \end{aligned} \tag{2.18}$$

where $f(\boldsymbol{\mu}, \mathbf{p};\, \mathbf{r})$ is the effective potential experienced by a molecular at position $\mathbf{r}$, given by

$$f(\boldsymbol{\mu}, \mathbf{p};\, \mathbf{r}) = \frac{\mathbf{p}^2}{2\bar{\alpha}} + \frac{1}{2}\left(\frac{\varepsilon_0 a}{\beta+\varepsilon_0 a} - 1\right)(\boldsymbol{\mu}+\mathbf{p})\boldsymbol{\mathcal{T}}_h(\mathbf{r})(\boldsymbol{\mu}+\mathbf{p}) - (\boldsymbol{\mu}+\mathbf{p})\cdot\boldsymbol{\mathcal{E}}_{I,h}(\mathbf{r}) \tag{2.19}$$

where the field $\boldsymbol{\mathcal{E}}_{I,h}$ is given by

$$\boldsymbol{\mathcal{E}}_{I,h}(\mathbf{r}) = \int d\mathbf{r}'\, h(\mathbf{r}-\mathbf{r}')\boldsymbol{\mathcal{E}}_I(\mathbf{r}') \tag{2.20}$$

with $\boldsymbol{\mathcal{E}}_I$ being a linear combination of the applied field $\boldsymbol{\mathcal{E}}_0$ and the fluctuating field $\mathbf{F}$ defined as

$$\boldsymbol{\mathcal{E}}_I(\mathbf{r}) = \boldsymbol{\mathcal{E}}_0(\mathbf{r}) - \frac{\varepsilon_0}{\beta+\varepsilon_0 a}\int d\mathbf{r}'\boldsymbol{\mathcal{T}}(\mathbf{r}-\mathbf{r}')\left(\boldsymbol{\mathcal{E}}_0(\mathbf{r}') - \mathbf{F}(\mathbf{r}')\right) \tag{2.21}$$

In addition, the determinant of a general kernel $\mathbf{M}$ is given in terms of functional

integral as

$$(\det\mathbf{M})^{-\frac{1}{2}} = \int \mathcal{D}\boldsymbol{\xi} e^{-\frac{1}{2}\langle\boldsymbol{\xi}|\mathbf{M}|\boldsymbol{\xi}\rangle} \tag{2.22}$$

To further simplify the free energy, we now assume that the short-ranged polarization distribution function $h(\mathbf{r})$ is a spherically symmetrical function. The assumption allows us to reduce the tensor $\mathbf{T}_h$ to

$$\boldsymbol{\mathcal{T}}_h(\mathbf{r}) = \int d\mathbf{r}' \int d\mathbf{r}''\, h(\mathbf{r}'-\mathbf{r})\boldsymbol{\mathcal{T}}(\mathbf{r}'-\mathbf{r}'')h(\mathbf{r}''-\mathbf{r}) = t_h \mathbb{1} \tag{2.23}$$

with t_h being a scalar. With the simplification, the potential $f(\boldsymbol{\mu}, \mathbf{p};\, \mathbf{r})$ can be rewritten as

$$f(\boldsymbol{\mu}, \mathbf{p};\, \mathbf{r}) = \frac{\mathbf{p}^2}{2\bar{\alpha}} + \frac{1}{2}\left(\frac{\varepsilon_0 a}{\beta+\varepsilon_0 a} - 1\right) t_h(\boldsymbol{\mu}+\mathbf{p})^2 - (\boldsymbol{\mu}+\mathbf{p})\cdot\boldsymbol{\mathcal{E}}_{I,h}(\mathbf{r}) \tag{2.24}$$

Next, we minimize the variational free energy W_0 with respect to a and $\mathbf{F}(\mathbf{r})$. In this chapter, for simplicity, we assume that the variation in the electrostatic fields is much larger in length scale than the molecular size, such that $\mathbf{G}_h(\mathbf{r}) = \mathbf{G}(\mathbf{r})$ and $\boldsymbol{\mathcal{E}}_{I,h}(\mathbf{r}) = \boldsymbol{\mathcal{E}}_I(\mathbf{r})$. With the details of the minimization procedure presented in Appendix 2.C, the minimization procedure leads to the following set of two constitutive relations which can be solved simultaneously for the variational parameters a and $\mathbf{F}$:

$$\frac{\varepsilon_0}{\beta+\varepsilon_0 a}\left[\boldsymbol{\mathcal{E}}_0(\mathbf{r}) - \mathbf{F}(\mathbf{r})\right] = c(\mathbf{r})\bar{\alpha}C\left[1 + \frac{\bar{\mu}^2}{\bar{\alpha}}CG\left(\bar{\mu}C|\boldsymbol{\mathcal{E}}_I(\mathbf{r})|\right)\right]\boldsymbol{\mathcal{E}}_I(\mathbf{r}) \tag{2.25}$$

and

$$\frac{1}{a} = \frac{1}{3}c(\mathbf{r})\left\{3C\bar{\alpha} + C^2\bar{\mu}^2 + C^2\bar{\alpha}^2\left[1 + 2\frac{\bar{\mu}^2}{\bar{\alpha}}CG\left(\bar{\mu}C|\boldsymbol{\mathcal{E}}_I(\mathbf{r})|\right)\right]\boldsymbol{\mathcal{E}}_I(\mathbf{r})^2\right\} \tag{2.26}$$

where $C = \left(1 - \frac{\beta\bar{\alpha}t_h}{\beta+\varepsilon_0 a}\right)^{-1}$, and $G(x) = \left(\coth x - 1/x\right)/x$, and $c(\mathbf{r})$ is the number concentration of the particles in the system given by

$$c(\mathbf{r}) = \lambda \int d\Omega \int d\mathbf{p}\, e^{-f(\boldsymbol{\mu},\mathbf{p};\mathbf{r})} \tag{2.27}$$

2.2.3 Dielectric Constant of a Homogeneous System

The dielectric constant can be found from the linear relationship between the average polarization of the system and the applied field in the limit of zero applied field. In order to obtain a relationship between the polarization and the applied field, one needs to take the derivative of free energy of the system with respect to $\mathbf{E}_0(\mathbf{r})$. Furthermore, we assume that the polarization is distributed uniformly in a spherical region with molecular volume v, such that $h(\mathbf{r}) = 1/v$ inside the sphere and 0 otherwise. This short-ranged distribution function leads to the self-interaction factor $t_h = \beta/3\varepsilon_0 v$ (see Section 3.A for the derivation). To obtain the dielectric constant, we first take the derivative of the variational free energy with respect to $\mathbf{E}_0(\mathbf{r})$ to obtain a relationship between the polarization and the applied field:

$$\langle \mathbf{P}(\mathbf{r}) \rangle = \frac{\partial \ln Z}{\partial \beta \mathbf{E}_0(\mathbf{r})} \approx -\frac{\partial \beta W_0}{\partial \boldsymbol{\mathcal{E}}_0(\mathbf{r})} \tag{2.28}$$

To obtain an expression for the dielectric constant, we only need to know the expression for $\langle \mathbf{P}(\mathbf{r}) \rangle$ to linear order in $\mathbf{E}_0(\mathbf{r})$, because the dielectric constant relates to the polarization response in the limit of zero applied field. Evaluation of the derivative in Eq. (2.28) above leads us to

$$\begin{aligned}
&\langle \mathbf{P}(\mathbf{r}) \rangle \\
= \;& \left(\frac{\varepsilon_0}{\beta + \varepsilon_0 a} \right)^2 \int d\mathbf{r}' \int d\mathbf{r}'' \, \boldsymbol{\mathcal{T}}(\mathbf{r} - \mathbf{r}') \left[\mathbb{1}\delta(\mathbf{r}' - \mathbf{r}'') - \frac{\delta \mathbf{F}(\mathbf{r}')}{\delta \boldsymbol{\mathcal{E}}_0(\mathbf{r}'')} \right] (\boldsymbol{\mathcal{E}}_0(\mathbf{r}'') - \mathbf{F}(\mathbf{r}'')) \\
& + \int d\mathbf{r}' \int d\mathbf{r}'' \, c(\mathbf{r}'') \left\{ \left[\mathbb{1}\delta(\mathbf{r} - \mathbf{r}')\delta(\mathbf{r}' - \mathbf{r}'') \right.\right. \\
& \left.\left. - \frac{\varepsilon_0}{\beta + \varepsilon_0 a} \boldsymbol{\mathcal{T}}(\mathbf{r} - \mathbf{r}') \left(\mathbb{1}\delta(\mathbf{r}' - \mathbf{r}'') - \frac{\delta \mathbf{F}(\mathbf{r}')}{\delta \boldsymbol{\mathcal{E}}_0(\mathbf{r}'')} \right) \right] \langle \boldsymbol{\mu} + \mathbf{p} \rangle_{f(\mathbf{r}'')} \right\}
\end{aligned} \tag{2.29}$$

where $\langle \boldsymbol{\mu} + \mathbf{p} \rangle_{f(\mathbf{r})}$ is given by Eq. (2.65) as

$$\langle \boldsymbol{\mu} + \mathbf{p} \rangle_{f(\mathbf{r})} = \bar{\alpha} C \left[1 + \frac{\bar{\mu}^2}{\bar{\alpha}} C G \left(\bar{\mu} C |\boldsymbol{\mathcal{E}}_I(\mathbf{r})| \right) \right] \boldsymbol{\mathcal{E}}_I(\mathbf{r}) \tag{2.30}$$

To linear order, we let $\delta \mathbf{F}(\mathbf{r}) / \delta \boldsymbol{\mathcal{E}}_0(\mathbf{r}') = \mathbf{K}(\mathbf{r}, \mathbf{r}')$, and the Fourier transform of

Eq. (2.29) leads to

$$\begin{aligned}
&\langle \mathbf{P}(\mathbf{k}) \rangle \\
= \quad & \left(\frac{\varepsilon_0}{\beta + \varepsilon_0 a} \right)^2 \boldsymbol{\mathcal{T}}(\mathbf{k}) \left[\mathbb{1} - \mathbf{K}(\mathbf{k}) \right] \left[\mathbb{1} - \mathbf{K}(\mathbf{k}) \right] \boldsymbol{\mathcal{E}}_0(\mathbf{k}) \\
& + \frac{1}{a} \left[\mathbb{1} - \frac{\varepsilon_0}{\beta + \varepsilon_0 a} \boldsymbol{\mathcal{T}}(\mathbf{k}) \left(\mathbb{1} - \mathbf{K}(\mathbf{k}) \right) \right] \left[\mathbb{1} - \frac{\varepsilon_0}{\beta + \varepsilon_0 a} \boldsymbol{\mathcal{T}}(\mathbf{k}) \left(\mathbb{1} - \mathbf{K}(\mathbf{k}) \right) \right] \boldsymbol{\mathcal{E}}_0(\mathbf{k}) \quad (2.31)
\end{aligned}$$

To obtain an expression for the electric susceptibility $\boldsymbol{\chi}_0(\mathbf{k})$, we compare Eq. (2.31) with the following relation between the polarization of the system and the applied field:

$$\langle \mathbf{P}(\mathbf{k}) \rangle = \varepsilon_0 \boldsymbol{\chi}_0(\mathbf{k}) \boldsymbol{\mathcal{E}}_0(\mathbf{k}) = \frac{\varepsilon_0}{\beta} \boldsymbol{\chi}_0(\mathbf{k}) \boldsymbol{\mathcal{E}}_0(\mathbf{k}) \quad (2.32)$$

Thus, the expression for $\boldsymbol{\chi}_0(\mathbf{k})$ is given by

$$\begin{aligned}
\boldsymbol{\chi}_0(\mathbf{k}) \quad = \quad & \frac{\beta}{\varepsilon_0} \left(\frac{\varepsilon_0}{\beta + \varepsilon_0 a} \right)^2 \boldsymbol{\mathcal{T}}(\mathbf{k}) \left[\mathbb{1} - \mathbf{K}(\mathbf{k}) \right] \left[\mathbb{1} - \mathbf{K}(\mathbf{k}) \right] \\
& + \frac{\beta}{\varepsilon_0 a} \left[\mathbb{1} - \frac{\varepsilon_0}{\beta + \varepsilon_0 a} \boldsymbol{\mathcal{T}}(\mathbf{k}) \left(\mathbb{1} - \mathbf{K}(\mathbf{k}) \right) \right] \left[\mathbb{1} - \frac{\varepsilon_0}{\beta + \varepsilon_0 a} \boldsymbol{\mathcal{T}}(\mathbf{k}) \left(\mathbb{1} - \mathbf{K}(\mathbf{k}) \right) \right] \quad (2.33)
\end{aligned}$$

For a homogeneous system, the dependence on the spatial variable $\mathbf{r}$ could be dropped. As we are interested the linear relationship between the polarization and the applied electric field when the applied electric field is small, we solve the constitutive relations Eqs. (2.62) and (2.63) to first order in $\boldsymbol{\mathcal{E}}_0$. The result for solving the constitutive relations to first order in $\boldsymbol{\mathcal{E}}_0$ is

$$\frac{1}{a} = \frac{1}{3v} \left[3\bar{\alpha} C + C^2 \bar{\mu}^2 \right] \quad (2.34)$$

and

$$\mathbf{F} = -\frac{2\beta}{\beta + 3\varepsilon_0 a} \boldsymbol{\mathcal{E}}_0 \quad (2.35)$$

Therefore, from Eq. (2.35), we also have

$$\mathbf{K}(\mathbf{k} = 0) = -\frac{2\beta}{\beta + 3\varepsilon_0 a} \mathbb{1} \quad (2.36)$$

The dielectric constant ε can be calculated from the trace of the susceptibility matrix $\boldsymbol{\chi}_0(\mathbf{k})$ as[8]

$$\lim_{\mathbf{k}\to 0} \operatorname{tr} \boldsymbol{\chi}_0(\mathbf{k}) = \frac{(\varepsilon-1)(2\varepsilon+1)}{\varepsilon} \tag{2.37}$$

Substituting Eqs. (2.34) to (2.36) into the expression for electric susceptibility in Eq. (2.33), and evaluating the trace of $\boldsymbol{\chi}_0(\mathbf{k})$, we have

$$\frac{(\varepsilon-1)(2\varepsilon+1)}{\varepsilon} = \frac{3\beta\left(2\beta^2+3\beta\varepsilon_0 a+9\varepsilon_0^2 a^2\right)}{\varepsilon_0 a(\beta+3\varepsilon_0 a)^2} \tag{2.38}$$

In the next section, we apply the FTVT to calculate the dielectric constants for a range of fluids, and compare the values with those calculated using the Onsager equation and the DSCFT.

2.3 Results and Discussions

In this section, we calculate the dielectric constants of common liquid solvents using the FTVT, and compare the theory to the Onsager equation and the DSCFT. All three theories considered in this section calculate the dielectric constant without using adjustable parameters. To compare their performance, we examine the agreement between the theoretically predicted dielectric constants of a wide range of liquids with the corresponding experimentally-observed values.

The Onsager equation is derived by considering a single dipolar molecule in a spherical cavity and treating the outside of the cavity as a dielectric continuum under a uniform Maxwell field. A key insight of Onsager's picture is to recognize the presence of a reaction field, which describes the response of the surrounding dipoles to each dipole. The reaction field is parallel to the dipole, such that it enhances the electrostatic field on the dipole but does not contribute to the orienting force on the dipole. By carving a spherical cavity for a chosen dipole in the system, and solving for the dipole moment in the cavity self-consistently with the reaction field that it generates, the Onsager model predicts the dielectric constant through the following

relation:

$$\frac{(\varepsilon - \varepsilon_\infty)(2\varepsilon + \varepsilon_\infty)}{\varepsilon(\varepsilon_\infty + 2)^2} = \frac{\beta\bar{\mu}^2}{9v\varepsilon_0} \tag{2.39}$$

where ε_∞ is the optical dielectric constant, and one can relate ε_∞ to the isotropic polarizability of each molecule through the Clausius-Mossotti equation:

$$\frac{\varepsilon_\infty - 1}{\varepsilon_\infty + 2} = \frac{\alpha}{3\varepsilon_0 v} \tag{2.40}$$

As mentioned in the introduction, the DSCFT is a field-theoretic theory in which the dielectric constant is calculated at the saddle-point level. The theory considers an ion solvated in a dipolar solvent, but the dielectric constant can be recovered from the Eq. (7) in Ref. 44 by calculating the local dielectric constant at positions far away from the ion, where the local field approaches zero. Upon simplification, the dielectric constant of a solvent predicted by the DSCFT is given by

$$\varepsilon = 1 + \frac{3\alpha^2 + 6\beta\alpha\bar{\mu}^2 + \beta^2\bar{\mu}^4}{3\varepsilon_0 v(\alpha + \beta\bar{\mu}^2)} \tag{2.41}$$

In this work, we have chosen the DSCFT as a representative of field-theoretic theories at saddle-point level. Generally, field-theoretic methods at saddle-point level predicts values of dielectric constants comparable to the Debye equation, which is applicable only when the system is sufficiently dilute.

Let us denote the value of dielectric constant calculated by the FTVT, the Onsager equation, and the DSCFT by $\varepsilon_{\mathrm{FTVT}}$, $\varepsilon_{\mathrm{Ons}}$, and $\varepsilon_{\mathrm{DSCFT}}$, respectively. In Tables 2.1 and 2.2, we tabulate the values of theoretically predicted dielectric constants together with the experimental dielectric constants $\varepsilon_{\mathrm{exp}}$ for a wide range of common liquid solvents at 20°C. Table 2.1 contains liquids that do not form hydrogen bonds, and Table 2.2 contains liquids that form hydrogen bonds. In addition, the calculation parameters – the gas-phase permanent dipole moment $\bar{\mu}$, the molecular polarizability α, the molecular volume v – are also listed in the table for each liquid. The molecular volume v is calculated based on the density ρ of the liquid using $v = M/(\rho N_A)$, where M is the molar mass of the liquid and N_A is Avogadro's constant.

In Fig. 2.1, we plot $\varepsilon_{\mathrm{FTVT}}$, $\varepsilon_{\mathrm{Ons}}$, and $\varepsilon_{\mathrm{DSCFT}}$ vs. $\varepsilon_{\mathrm{exp}}$ for liquids that does not form hydrogen bonds, which are listed in Table 2.1. A logarithmic scale is used because the dielectric constant is often considered as a multiplicative screening factor for electrostatic interactions. For each set of theoretically calculated dielectric constants, we draw the line of best fit. If all data lies on the straight line with slope equal 1, the agreement between the theory and the experiment is perfect. We find the slopes for the line of best fit to be 1.04, 0.96, and 0.73 for $\varepsilon_{\mathrm{FTVT}}$, $\varepsilon_{\mathrm{Ons}}$, and $\varepsilon_{\mathrm{DSCFT}}$, respectively. This suggests that the FTVT predicts the dielectric constant much better than the DSCFT. In addition, the agreement between theoretically predicted values and the experimentally measured values are comparable for the FTVT and the Onsager equation.

In Fig. 2.2, we similarly plot the theoretically-calculated dielectric constants vs. the experimentally-measured values for liquids that form hydrogen bonds considered in Table 2.2. The slopes of the lines of best fit are 0.79, 0.72, and 0.53 for $\varepsilon_{\mathrm{FTVT}}$, $\varepsilon_{\mathrm{Ons}}$, and $\varepsilon_{\mathrm{DSCFT}}$, respectively. In this case, the FTVT predicts dielectric constants in closer agreements to the experimental values than the Onsager equation and the DSCFT.

From Figs. 2.1 and 2.2, we first observe that the agreement between the FTVT and experiment is much improved from the DSCFT. The DSCFT, at saddle-point level, predicts dielectric constants comparable to the Debye equation which is applicable when the system is sufficiently dilute. The key shortcoming in the saddle-point approximation is that the effect of reaction field is not accounted for, such that the inter-dipole interaction has not been taken into consideration. The improvement in the FTVT over the saddle-point approximation is due to the inclusion of the field $\mathbf{F}$ as the variational parameter, which allows the average field acting on a particle to fluctuate away from the conjugate field $\mathbf{G}$. If we instead carry out the variational treatment without introducing $\mathbf{F}$, i. e., by setting $\mathbf{F} = \mathbf{0}$, we obtain $\varepsilon = 1+\beta\bar{\mu}^2/(3\varepsilon_0 v)$ in the case of zero polarizability, which is exactly the Debye equation for a dilute gas of permanent dipoles.

With the construction of a cavity in a homogeneous medium, the Onsager equation accounts for the effect of reaction field by self-consistently solving for the magnitude

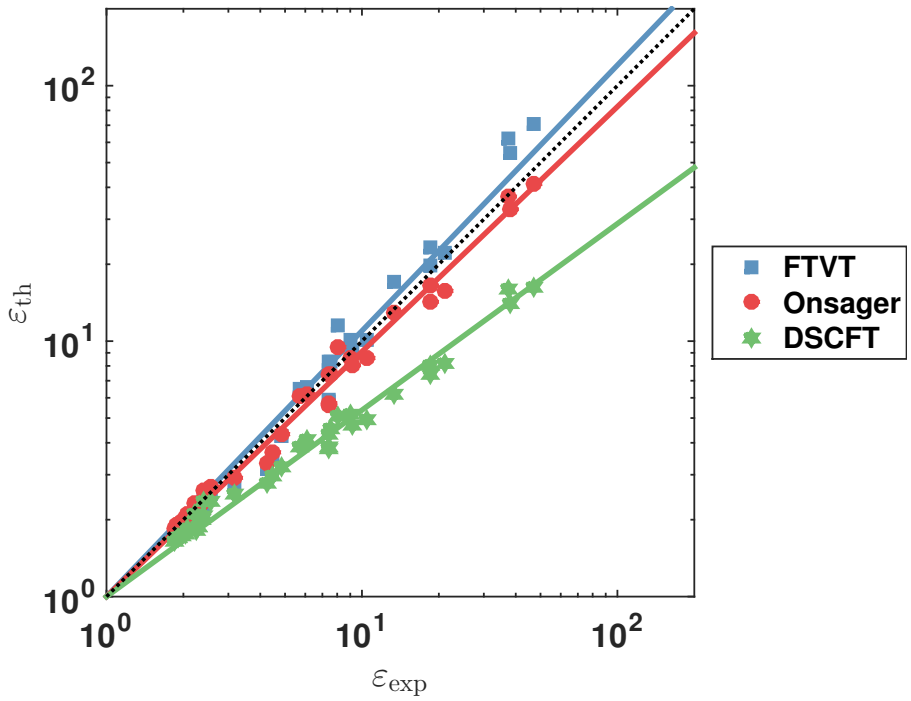

Figure 2.1: Theoretically-calculated dielectric constants ($\varepsilon_{\text{FTVT}}$, ε_{Ons}, and $\varepsilon_{\text{DSCFT}}$) vs. experimentally-measured dielectric constants ε_{exp} for liquids considered in Table 2.1, which do not form hydrogen bonds. The dashed line has slope equal to 1. The lines of best fit have slopes 1.04, 0.96, and 0.73 for the FVTV, the Onsager equation, and the DSCFT, respectively.

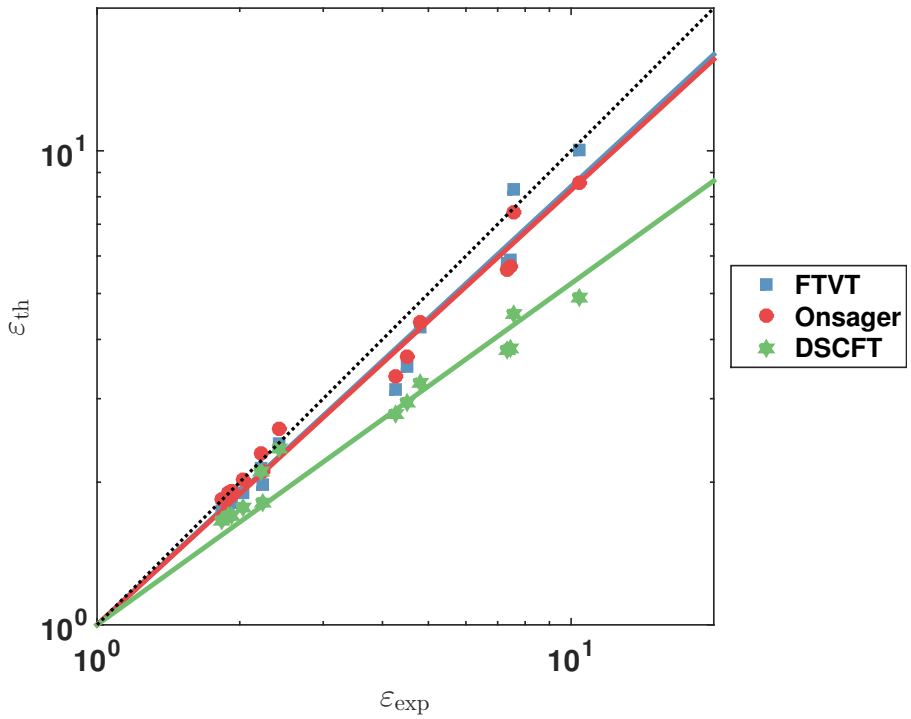

Figure 2.2: Theoretically-calculated dielectric constants ($\varepsilon_{\mathrm{FTVT}}$, $\varepsilon_{\mathrm{Ons}}$, and $\varepsilon_{\mathrm{DSCFT}}$) vs. experimentally-measured dielectric constants $\varepsilon_{\mathrm{exp}}$ for hydrogen-bonding liquids considered in Table 2.2. The dashed line has slope equal to 1. The lines of best fit have slopes 0.79, 0.72, and 0.53 for the FVTV, the Onsager equation, and the DSCFT, respectively.

Table 2.1: The calculated values of dielectric constants compared with the experimental values for common liquids that do not form hydrogen bonds. The values of $\varepsilon_{\mathrm{FTVT}}$, $\varepsilon_{\mathrm{Ons}}$, and $\varepsilon_{\mathrm{DSCFT}}$ are calculated from the FTVT, the Onsager equation, and the DSCFT, respectively. The calculation parameters, including the gas-phase permanent dipole moment $\bar{\mu}$, the molecular polarizability α, and the molecular volume v, are listed for each solvent.

Solvent	$\bar{\mu}$[D]	α[Å^3]	v[Å^3]	$\varepsilon_{\mathrm{exp}}$	$\varepsilon_{\mathrm{FTVT}}$	$\varepsilon_{\mathrm{Ons}}$	$\varepsilon_{\mathrm{DSCFT}}$
non-hydrogen-bonding liquids							
acetone	2.69	6.30	122.94	21.01	22.33	15.84	8.15
benzene	0.00	10.40	147.98	2.28	2.10	2.25	1.88
2-butanone	2.76	8.13	149.69	18.56	19.62	14.32	7.39
chlorobenzene	1.54	12.30	169.02	5.69	6.50	6.11	3.87
chloroform	1.15	8.40	134.05	4.81	4.25	4.35	3.23
cyclohexane	0.00	11.00	180.58	2.02	1.91	2.03	1.77
cyclopentane	0.00	9.15	156.17	1.97	1.86	1.98	1.74
cyclopentene	0.20	9.00	146.52	2.09	1.96	2.09	1.85
dibromomethane	1.78	8.68	115.61	7.46	8.35	7.42	4.31
1,2-dichloroethane	1.83	8.30	131.95	10.42	10.05	8.56	4.90
dichloromethane	1.14	6.48	106.31	9.15	9.22	8.02	4.72
diethyl ether	1.15	8.90	172.43	4.27	3.15	3.35	2.78
diglyme	1.92	13.90	236.17	7.36	5.82	5.61	3.78
1,2-dimethoxyethane	1.71	9.50	173.27	7.42	5.90	5.68	3.84
dimethyl sulfoxide	4.10	8.00	117.84	47.24	71.22	41.54	16.18
dimethylformamide	3.86	7.81	128.51	38.25	54.28	32.83	14.02
1,4-dioxane	0.45	8.60	141.53	2.22	2.15	2.30	2.10
ethyl acetate	1.88	8.62	162.51	6.08	6.61	6.21	4.09
furan	0.69	7.40	118.81	3.19	2.71	2.90	2.52
heptane	0.00	13.70	244.87	1.92	1.81	1.92	1.70
hexane	0.08	11.90	216.62	1.89	1.80	1.90	1.70
methyl formate	1.77	5.05	102.67	9.02	10.09	8.59	5.16
methyl t-butyl ether	1.32	10.70	199.05	4.50	3.49	3.68	2.94
nitromethane	3.46	5.00	89.14	37.27	61.71	36.66	16.07
o-xylene	0.45	14.20	201.36	2.56	2.52	2.71	2.34
m-xylene	0.31	14.20	205.04	2.36	2.17	2.33	2.00
p-xylene	0.00	14.20	205.83	2.27	2.07	2.22	1.87
pentane	0.00	10.00	191.32	1.84	1.74	1.84	1.66
propanal	2.52	6.40	111.40	18.50	23.43	16.45	8.09
pyridine	2.37	9.50	133.77	13.26	17.16	12.89	6.24
pyrrole	1.71	8.20	114.87	8.03	11.48	9.47	5.07
tetrachloromethane	0.00	10.50	160.24	2.24	2.00	2.14	1.82
tetrahydrofuran	1.75	7.90	135.55	7.56	8.29	7.39	4.51
toluene	0.31	12.30	177.43	2.39	2.23	2.40	2.08
triethylamine	0.87	13.30	230.97	2.42	2.41	2.60	2.35

Table 2.2: The calculated values of dielectric constants compared with the experimental values for common liquids that form hydrogen bonds. The values of $\varepsilon_{\mathrm{FTVT}}$, $\varepsilon_{\mathrm{Ons}}$, and $\varepsilon_{\mathrm{DSCFT}}$ are calculated from the FTVT, the Onsager equation, and the DSCFT, respectively. The calculation parameters, including the gas-phase permanent dipole moment $\bar{\mu}$, the molecular polarizability α, the molecular volume v are listed for each solvent.

Solvent	$\bar{\mu}$[D]	α[Å^3]	v[Å^3]	$\varepsilon_{\mathrm{exp}}$	$\varepsilon_{\mathrm{FTVT}}$	$\varepsilon_{\mathrm{Ons}}$	$\varepsilon_{\mathrm{DSCFT}}$
hydrogen-bonding liquids							
allyl alcohol	1.60	7.65	112.93	19.70	9.59	8.25	4.71
aziridine	1.89	5.00	85.96	18.97	16.56	12.55	6.54
1-butanol	1.75	8.88	152.05	17.84	7.38	6.76	4.26
2-butanol	1.41	8.80	152.65	17.26	6.55	6.16	4.02
ethanol	1.66	5.11	96.92	25.30	10.20	8.67	5.13
ethylene glycol	2.27	5.70	92.56	41.40	26.45	18.12	8.50
glycerol	2.56	8.10	121.24	46.53	25.18	17.42	7.97
hydrazine	1.75	3.60	53.02	52.94	27.63	18.76	8.38
methanol	1.70	3.32	67.23	33.00	15.02	11.64	6.47
1-propanol	1.55	6.90	124.78	20.80	6.74	6.31	4.10
2-propanol	1.66	6.97	127.79	20.18	7.48	6.83	4.33
water	1.87	1.50	30.00	80.10	48.67	29.92	14.10

of the dipole moment under the reaction field due to the surrounding induced polarization. Comparing $\varepsilon_{\mathrm{FTVT}}$ and $\varepsilon_{\mathrm{Ons}}$ in Figs. 2.1 and 2.2, we find that FTVT and the Onsager equation produce comparable dielectric constants. This observation suggests that the FTVT, like the Onsager model, has taken the effect of reaction field into consideration.

Hydrogen-bonding liquids, such as water and alcohols, have stronger angular correlations between the molecules due to the larger quadrupolar moment present,[55] and therefore, we expect a simple theory like the FTVT would underestimate the dielectric constant of hydrogen-bonding liquids. However, we note from Fig. 2.2 that the FTVT provides better predictions of the dielectric constants than the Onsager equation and the DSCFT. If we exclude the hydrogen-bonding liquids from our analysis and only consider the non-hydrogen-bonding liquids, the line of best fit for $\varepsilon_{\mathrm{FTVT}}$ vs. $\varepsilon_{\mathrm{exp}}$ in Fig. 2.1 has a slope of 1.04. Since the slope is very close to 1, this suggests that, on average, the FTVT produces reliable predictions of dielectric constants of non-hydrogen-bonding liquids. Also, the value of the slope for the FTVT is comparable

to that of the line of best fit for $\varepsilon_{\mathrm{Ons}}$ vs. $\varepsilon_{\mathrm{exp}}$ at 0.96.

2.4 Conclusions

In this work, we have developed a variational theory for dielectric constants of pure liquids using field-theoretic methods. By introducing a Gaussian reference action, with the interaction kernel and the average electrostatic field as variational parameters, the theory allows the reaction field in the system to be accounted for. In addition, as all particles are treated equivalently in the model and no particle is singled out in a cavity, the theory provides more intuitive description for dipolar liquids as no unphysical dielectric boundaries are introduced into the system. The resulting theory – which is based completely on readily-available molecular parameters, including the gas-phase permanent dipole moment, the molecular polarizability, and the volume of each molecule – consists of an analytical expression for the grand potential and two very simple algebraic constitutive relations, and it produces reliable estimates of the dielectric constants of common liquid solvents. In this work, we have focused on finding the dielectric constant when the applied field is small by solving the constitutive relations to linear order of the external field. However, we note that the nonlinear constitutive equations can be solved directly to study dielectric response under larger applied external field, where the effect of dielectric saturation become.

The calculation of dielectric constant of a liquid mixture is still one of the challenges in statistical mechanics. The Onsager formulation requires one dipolar molecule to be treated differently from the rest, and as a result, it is difficult to self-consistently generalize the theory to binary mixtures. In addition, for theories of dielectric constant based on integral equations, the generalization of the theory to liquid mixture is often complicated, as multiple correlation functions are required to be evaluated. However, in the FTVT, the derivation of the theory does not require any single molecule to be distinguished from the rest of the particles. This feature of the FTVT may allow the theory to be straightforwardly extended to the case of mixtures, for which an accurate theory would be most desirable due to the inefficiency of exploring

the mixture composition space with computer simulations.

In addition, by taking the effect of reaction field into consideration, the FTVT improves the prediction of dielectric constant from the DSCFT, a previous field-theoretic approach based on saddle-point approximation. Over the years, field-theoretic models of dielectric properties of soft matter have been hindered by inaccuracy due to the absence of reaction field at the saddle-point level. As such, the FTVT brings an important step forward towards better field-theoretic models for dielectric systems. Furthermore, in recent years, field-theoretic methods have been applied to a vast range of problems related to soft matter, including polymers and ionic solutions.[14,56] As the framework of the FTVT can be naturally integrated into the field-theoretic models for other systems of soft matter, it has a broad impact on the studies of soft-matter systems involving dielectric substances or medium.

Appendix 2.A Identity Transformation of the Grand Partition Function

As the dipole-dipole interaction tensor $\boldsymbol{\mathcal{T}}(\mathbf{r})$ does not have an inverse operator, we perform the identity transformations using the Faddeev-Popov method[14,15] by introducing the δ-functional into the partition function:

$$\begin{aligned} \mathbb{1} &= \int \mathcal{D}\mathbf{P}\, \delta[\mathbf{P}(\mathbf{r}) - \hat{\mathbf{P}}(\mathbf{r})] \\ &= \int \mathcal{D}\mathbf{P} \int \mathcal{D}\mathbf{G}\, e^{i\int d\mathbf{r}\, \mathbf{G}(\mathbf{r})\cdot[\mathbf{P}(\mathbf{r})-\hat{\mathbf{P}}(\mathbf{r})]} \end{aligned} \tag{2.42}$$

where $\delta[\mathbf{f}(\mathbf{r})]$ is the generalization of the multivariate δ-function which is zero unless $\mathbf{f}(\mathbf{r}) = \mathbf{0}$. Applying Eq. (2.42), we transform the Boltzmann factor as

$$\begin{aligned} e^{-\beta U} &= \int \mathcal{D}\mathbf{P} \int \mathcal{D}\mathbf{G}\, e^{-\frac{1}{2}\langle \mathbf{P}|\boldsymbol{\mathcal{T}}|P\rangle - i\langle \mathbf{P}|\,\mathbf{G}\rangle + \langle \mathbf{P}|\,\boldsymbol{\mathcal{E}}_0\rangle} \\ &\qquad \times e^{i\left\langle \hat{\mathbf{P}}\right|\mathbf{G}\rangle - \sum_{i=1}^{N}\frac{\mathbf{p}_i^2}{2\tilde{\alpha}} + \sum_{i=1}^{N}\frac{1}{2}\left\langle \hat{\mathbf{P}}_i\right|\boldsymbol{\mathcal{T}}\left|\hat{\mathbf{P}}_i\right\rangle} \end{aligned} \tag{2.43}$$

where only the exponent in the second line of Eq. (2.43) depends explicitly on the instantaneous molecular configurations of the system. Substituting Eq. (2.43) for the Boltzmann factor in $Z(N)$ leads to

$$\begin{aligned} Z(N) &= \int \mathcal{D}\mathbf{P} \int \mathcal{D}\mathbf{G}\, e^{-\frac{1}{2}\langle \mathbf{P}|\boldsymbol{\mathcal{T}}|\mathbf{P}\rangle - i\langle \mathbf{P}|\,\mathbf{G}\rangle + \langle \mathbf{P}|\,\boldsymbol{\mathcal{E}}_0\rangle} \\ &\quad \times \left\{ \int d\mathbf{r}_i \int d\Omega_i \int d\mathbf{p}_i\, e^{i\left\langle \hat{\mathbf{P}}_i\right|\mathbf{G}\rangle - \mathbf{p}_i^2/(2\bar{\alpha}) + \frac{1}{2}\left\langle \hat{\mathbf{P}}_i\right|\boldsymbol{\mathcal{T}}\left|\hat{\mathbf{P}}_i\right\rangle} \right\}^N \\ &= \int \mathcal{D}\mathbf{P} \int \mathcal{D}\mathbf{G}\, e^{-\frac{1}{2}\langle \mathbf{P}|\boldsymbol{\mathcal{T}}|\mathbf{P}\rangle - i\langle \mathbf{P}|\,\mathbf{G}\rangle + \langle \mathbf{P}|\,\boldsymbol{\mathcal{E}}_0\rangle} \\ &\quad \times \left\{ \int d\mathbf{r} \int d\Omega \int d\mathbf{p}\, e^{i(\boldsymbol{\mu}+\mathbf{p})\cdot\int d\mathbf{r}' h(\mathbf{r}'-\mathbf{r})\mathbf{G}(\mathbf{r}') - \mathbf{p}^2/(2\bar{\alpha})} \right. \\ &\qquad \left. \times e^{+\frac{1}{2}(\boldsymbol{\mu}+\mathbf{p})\cdot\left[\int d\mathbf{r}' \int d\mathbf{r}''\, h(\mathbf{r}'-\mathbf{r})\boldsymbol{\mathcal{T}}(\mathbf{r}'-\mathbf{r}'')h(\mathbf{r}''-\mathbf{r})\right]\cdot(\boldsymbol{\mu}+\mathbf{p})} \right\}^N \end{aligned} \tag{2.44}$$

Substitution of Eq. (2.44) into Eq. (2.5) leads to the field-based grand partition function given by Eqs. (2.8) and (2.9).

Appendix 2.B Evaluation of the Variational Bound

In this section, we present the evaluation of W_0, which is the variational upper bound for the grand free energy. The evaluation will involve the operator $\mathbf{Q} = \boldsymbol{\mathcal{T}} + \boldsymbol{\mathcal{A}}$ and its inverse $\mathbf{Q}^{-1}$ defined through the relation $\int d\mathbf{r}' \mathbf{Q}(\mathbf{r}-\mathbf{r}')\mathbf{Q}^{-1}(\mathbf{r}'-\mathbf{r}'') = \mathbb{1}\delta(\mathbf{r}-\mathbf{r}'')$. Let us start by deriving an expression for $\mathbf{Q}^{-1}$ in the Fourier space:

$$\begin{aligned} & \tilde{\mathbf{Q}}^{-1}(\mathbf{k}) \\ = \;& [\tilde{\boldsymbol{\mathcal{T}}}(\mathbf{k}) + \tilde{\boldsymbol{\mathcal{A}}}(\mathbf{k})]^{-1} = \frac{1}{a}[\mathbb{1} + a^{-1}\tilde{\boldsymbol{\mathcal{T}}}(\mathbf{k})]^{-1} \\ = \;& \frac{1}{a}[\mathbb{1} - a^{-1}\tilde{\boldsymbol{\mathcal{T}}}(\mathbf{k}) + a^{-2}\tilde{\boldsymbol{\mathcal{T}}}(\mathbf{k})^2 - a^{-3}\tilde{\boldsymbol{\mathcal{T}}}(\mathbf{k})^3 + \ldots] \\ = \;& \frac{1}{a}\left[\mathbb{1} - \left(\frac{\beta}{\varepsilon_0 a}\right)\frac{\mathbf{kk}}{k^2} + \left(\frac{\beta}{\varepsilon_0 a}\right)^2\frac{\mathbf{kk}}{k^2} - \left(\frac{\beta}{\varepsilon_0 a}\right)^3\frac{\mathbf{kk}}{k^2} + \ldots\right] \\ = \;& \frac{1}{a}\left[\mathbb{1} - \frac{\beta}{\varepsilon_0 a}\frac{1}{1+\frac{\beta}{\varepsilon_0 a}}\frac{\mathbf{kk}}{k^2}\right] \\ = \;& \frac{1}{a}\left[\mathbb{1} - \frac{\varepsilon_0}{\beta+\varepsilon_0 a}\tilde{\boldsymbol{\mathcal{T}}}(\mathbf{k})\right] \end{aligned} \tag{2.45}$$

We note that $\tilde{\boldsymbol{\mathcal{T}}}(\mathbf{k}) = \beta\mathbf{k}\mathbf{k}/(\varepsilon_0 k^2)$ is the Fourier transform of the dipole-dipole interaction tensor.[8,52] In the fourth equality above, we have used the fact that $\mathbf{k}\mathbf{k}/k^2$ is a projection operator and thus $(\mathbf{k}\mathbf{k}/k^2)^n = \mathbf{k}\mathbf{k}/k^2$ for positive integers n. Inverse Fourier transformation gives the expression of $\mathbf{Q}^{-1}$ in the real space:

$$\mathbf{Q}^{-1}(\mathbf{r}) = \frac{1}{a}\left[\mathbb{1}\delta(\mathbf{r}) - \frac{\varepsilon_0}{\beta + \varepsilon_0 a}\boldsymbol{\mathcal{T}}(\mathbf{r})\right] \tag{2.46}$$

Since the reference action $\mathcal{L}_0$ is Gaussian with respect to both $\mathbf{P}$ and $\mathbf{G}$, we can evaluate Ξ_0 using standard techniques for gaussian integrals. The result is

$$\Xi_0 = \left(\frac{\det \boldsymbol{\mathcal{A}}}{\det(\boldsymbol{\mathcal{T}} + \boldsymbol{\mathcal{A}})}\right)^{\frac{1}{2}} e^{\frac{1}{2}\langle \boldsymbol{\mathcal{E}}_0 - \mathbf{F} | \mathbf{Q}^{-1} | \boldsymbol{\mathcal{E}}_0 - \mathbf{F}\rangle} \tag{2.47}$$

The average $\langle \mathcal{L} - \mathcal{L}_0 \rangle_0$ can be expressed as

$$\begin{aligned}\langle \mathcal{L} - \mathcal{L}_0 \rangle_0 &= -\lambda \int d\mathbf{r} \int d\Omega \int d\mathbf{p}\, e^{-\frac{\mathbf{p}^2}{2\bar{\alpha}} + \frac{1}{2}(\boldsymbol{\mu}+\mathbf{p})\cdot\boldsymbol{\mathcal{T}}_h(\mathbf{r})\cdot(\boldsymbol{\mu}+\mathbf{p})} \left\langle e^{i(\boldsymbol{\mu}+\mathbf{p})\cdot\mathbf{G}_h(\mathbf{r})}\right\rangle_0 \\ &\quad -\frac{1}{2a}\int d\mathbf{r} \langle [\mathbf{G}(\mathbf{r}) + i\mathbf{F}(\mathbf{r})]^2 \rangle_0 \end{aligned} \tag{2.48}$$

The quantity $\langle e^{i(\boldsymbol{\mu}+\mathbf{p})\cdot\mathbf{G}_h(\mathbf{r})}\rangle_0$ can be evaluated using standard methods of Gaussian integrals. The result is

$$\begin{aligned} &\left\langle e^{i(\boldsymbol{\mu}+\mathbf{p})\cdot\mathbf{G}_h(\mathbf{r})}\right\rangle_0 \\ &= \exp\left\{(\boldsymbol{\mu}+\mathbf{p})\cdot\left[\int d\mathbf{r}'\, h(\mathbf{r}-\mathbf{r}')\mathbf{F}(\mathbf{r}')\right] - \frac{a}{2}(\boldsymbol{\mu}+\mathbf{p})^2\left[\int d\mathbf{r}'\, h(\mathbf{r}-\mathbf{r}')^2\right]\right. \\ &\quad + \frac{a^2}{2}(\boldsymbol{\mu}+\mathbf{p})\cdot\left[\int d\mathbf{r}'\int d\mathbf{r}''\, h(\mathbf{r}-\mathbf{r}')\mathbf{Q}^{-1}(\mathbf{r}'-\mathbf{r}'')h(\mathbf{r}''-\mathbf{r})\right]\cdot(\boldsymbol{\mu}+\mathbf{p}) \\ &\quad \left. + a\int d\mathbf{r}'\int d\mathbf{r}''\left[(\boldsymbol{\mathcal{E}}_0(\mathbf{r}') - \mathbf{F}(\mathbf{r}'))\mathbf{Q}^{-1}(\mathbf{r}'-\mathbf{r}'')h(\mathbf{r}''-\mathbf{r})\right]\cdot(\boldsymbol{\mu}+\mathbf{p})\right\} \\ &= \exp\left\{(\boldsymbol{\mu}+\mathbf{p})\cdot\boldsymbol{\mathcal{E}}_{I,h}(\mathbf{r}) - \frac{\varepsilon_0 a}{2(\beta+\varepsilon_0 a)}(\boldsymbol{\mu}+\mathbf{p})\cdot\boldsymbol{\mathcal{T}}_h(\mathbf{r})\cdot(\boldsymbol{\mu}+\mathbf{p})\right\} \end{aligned} \tag{2.49}$$

where the field $\boldsymbol{\mathcal{E}}_{I,h}$ is given by

$$\boldsymbol{\mathcal{E}}_{I,h}(\mathbf{r}) = \int d\mathbf{r}'\, h(\mathbf{r}-\mathbf{r}')\boldsymbol{\mathcal{E}}_I(\mathbf{r}') \tag{2.50}$$

with $\boldsymbol{\mathcal{E}}_I$ being a linear combination of the applied field $\boldsymbol{\mathcal{E}}_0$ and the fluctuating field $\mathbf{F}$:

$$\boldsymbol{\mathcal{E}}_I(\mathbf{r}) = \boldsymbol{\mathcal{E}}_0(\mathbf{r}) - \frac{\varepsilon_0}{(\beta+\varepsilon_0 a)} \int d\mathbf{r}' \boldsymbol{\mathcal{T}}(\mathbf{r}-\mathbf{r}')(\boldsymbol{\mathcal{E}}_0(\mathbf{r}') - \mathbf{F}(\mathbf{r}')) \tag{2.51}$$

On the other hand, $\langle [\mathbf{G}(\mathbf{r}) + i\mathbf{F}(\mathbf{r})]^2 \rangle_0$ can be evaluated as

$$\begin{aligned}
& \left\langle [\mathbf{G}(\mathbf{r}) + i\mathbf{F}(\mathbf{r})]^2 \right\rangle_0 \\
= \; & \frac{1}{\Xi_0} \int \mathcal{D}\mathbf{P} \int \mathcal{D}\boldsymbol{\Gamma}\, \boldsymbol{\Gamma}(\mathbf{r})^2 e^{-\frac{1}{2}\langle \mathbf{P}|\boldsymbol{\mathcal{T}}|\mathbf{P}\rangle + \langle \mathbf{P}|\,\boldsymbol{\mathcal{E}}_0 - \mathbf{F} - i\boldsymbol{\Gamma}\rangle - \frac{1}{2}\langle \boldsymbol{\Gamma}|\boldsymbol{\mathcal{A}}^{-1}|\boldsymbol{\Gamma}\rangle} \\
= \; & \frac{1}{\Xi_0} \frac{\delta}{i\delta \mathbf{J}(\mathbf{r})} \cdot \frac{\partial}{i\partial \mathbf{J}(\mathbf{r})} \int \mathcal{D}\mathbf{P} \int \mathcal{D}\boldsymbol{\Gamma}\; e^{-\frac{1}{2}\langle \mathbf{P}|\boldsymbol{\mathcal{T}}|\mathbf{P}\rangle + \langle \mathbf{P}|\,\boldsymbol{\mathcal{E}}_0 - \mathbf{F} - i\boldsymbol{\Gamma}\rangle - \frac{1}{2}\langle \boldsymbol{\Gamma}|\boldsymbol{\mathcal{A}}^{-1}|\boldsymbol{\Gamma}\rangle + i\langle \mathbf{J}|\,\boldsymbol{\Gamma}\rangle} \Big|_{\mathbf{J}=0} \\
= \; & \mathrm{tr}\boldsymbol{\mathcal{A}}(0) - a^2 \mathrm{tr}\mathbf{Q}^{-1}(0) - a^2 \left\{ \int d\mathbf{r}' \mathbf{Q}^{-1}(\mathbf{r}-\mathbf{r}')[\boldsymbol{\mathcal{E}}_0(\mathbf{r}') - \mathbf{F}(\mathbf{r}')] \right\}^2 \\
= \; & \frac{\beta a \delta(0)}{\beta + \varepsilon_0 a} - a^2 \left\{ \int d\mathbf{r}' \mathbf{Q}^{-1}(\mathbf{r}-\mathbf{r}')[\boldsymbol{\mathcal{E}}_0(\mathbf{r}') - \mathbf{F}(\mathbf{r}')] \right\}^2
\end{aligned} \tag{2.52}$$

We may further simplify the expression by noting that $\int d\mathbf{r} \boldsymbol{\mathcal{T}}(\mathbf{r}_1 - \mathbf{r}) \boldsymbol{\mathcal{T}}(\mathbf{r} - \mathbf{r}_2) = \frac{\beta}{\varepsilon_0} \boldsymbol{\mathcal{T}}(\mathbf{r}_1 - \mathbf{r}_2)$, which can be straightforwardly derived in the Fourier space.

In addition, we note that $\delta(0)$ is the continuum limit for $1/v$, as

$$\begin{aligned}
\delta(0) &= \frac{1}{(2\pi)^3} \int d\mathbf{k}\, e^{i\mathbf{k}\cdot\mathbf{r}} \Big|_{\mathbf{r}=\mathbf{0}} = \frac{1}{V} \sum_{\mathbf{k}} e^{i\mathbf{k}\cdot\mathbf{r}} \Big|_{\mathbf{r}=\mathbf{0}} \\
&= \frac{1}{V} (\text{number of modes in the } \mathbf{k}\text{-space}) \\
&= \frac{1}{V} \times \frac{V}{v} = \frac{1}{v}
\end{aligned} \tag{2.53}$$

where the second equality switches the integral over k-space in the continuum limit to the sum over k-space in the discrete limit.[57]

To obtain the variational free energy, we substitute Eqs. (2.47) to (2.52) into Eq. (2.15). Simplification of the expression leads to the variational grand potential in

Eq. (2.18):

$$\begin{aligned}
\beta W_0 &= -\ln\left(\frac{\det\boldsymbol{\mathcal{A}}}{\det(\boldsymbol{\mathcal{T}}+\boldsymbol{\mathcal{A}})}\right)^{\frac{1}{2}} - \frac{1}{2}\left\langle\boldsymbol{\mathcal{E}}_0-\mathbf{F}\right|\mathbf{Q}^{-1}\left|\boldsymbol{\mathcal{E}}_0-\mathbf{F}\right\rangle \\
&\quad -\lambda\int d\mathbf{r}\int d\Omega\int d\mathbf{p}\, e^{-\frac{\mathbf{p}^2}{2\tilde{\alpha}}+(\boldsymbol{\mu}+\mathbf{p})\cdot\boldsymbol{\mathcal{E}}_{I,h}(\mathbf{r})-\frac{1}{2}\left(\frac{\varepsilon_0 a}{(\beta+\varepsilon_0 a)}-1\right)(\boldsymbol{\mu}+\mathbf{p})\cdot\boldsymbol{\mathcal{T}}_h(\mathbf{r})\cdot(\boldsymbol{\mu}+\mathbf{p})} \\
&\quad -\frac{1}{2a}\int d\mathbf{r}\left\{\frac{\beta a\delta(0)}{\beta+\varepsilon_0 a}-a^2\left[\int d\mathbf{r}'\mathbf{Q}^{-1}(\mathbf{r}-\mathbf{r}')[\boldsymbol{\mathcal{E}}_0(\mathbf{r}')-\mathbf{F}(\mathbf{r}')]\right]^2\right\} \\
&= -\ln\left(\frac{\det\boldsymbol{\mathcal{A}}}{\det(\boldsymbol{\mathcal{T}}+\boldsymbol{\mathcal{A}})}\right)^{\frac{1}{2}} - \frac{1}{2}\int d\mathbf{r}\,\frac{\beta}{v(\beta+\varepsilon_0 a)} \\
&\quad -\lambda\int d\mathbf{r}\int d\Omega\int d\mathbf{p}\, e^{-\frac{\mathbf{p}^2}{2\tilde{\alpha}}+(\boldsymbol{\mu}+\mathbf{p})\cdot\boldsymbol{\mathcal{E}}_{I,h}(\mathbf{r})-\frac{1}{2}\left(\frac{\varepsilon_0 a}{(\beta+\varepsilon_0 a)}-1\right)(\boldsymbol{\mu}+\mathbf{p})\cdot\boldsymbol{\mathcal{T}}_h(\mathbf{r})\cdot(\boldsymbol{\mu}+\mathbf{p})} \\
&\quad -\frac{1}{2}\left(\frac{\varepsilon_0}{\beta+\varepsilon_0 a}\right)^2\int d\mathbf{r}\int d\mathbf{r}'\,[\boldsymbol{\mathcal{E}}_0(\mathbf{r})-\mathbf{F}(\mathbf{r})]\boldsymbol{\mathcal{T}}(\mathbf{r}-\mathbf{r}')[\boldsymbol{\mathcal{E}}_0(\mathbf{r}')-\mathbf{F}(\mathbf{r}')]
\end{aligned} \tag{2.54}$$

Appendix 2.C Minimization of the Variational Upper Bound of the Grand Potential

In this section, we minimize βW_0 with respect to the variational parameters a and $\mathbf{F}$. First, by expressing the determinants in terms of Gaussian functionals, we obtain

$$\begin{aligned}
&\frac{d}{da}\ln\left(\frac{\det\boldsymbol{\mathcal{A}}}{\det(\boldsymbol{\mathcal{T}}+\boldsymbol{\mathcal{A}})}\right)^{\frac{1}{2}} \\
&= \frac{1}{2a}\int d\mathbf{r}\int d\mathbf{r}'\boldsymbol{\mathcal{T}}(\mathbf{r}-\mathbf{r}'):\mathbf{Q}^{-1}(\mathbf{r}-\mathbf{r}') \\
&= \int d\mathbf{r}\,\frac{\beta}{2av(\beta+\varepsilon_0 a)}
\end{aligned} \tag{2.55}$$

where the last equality used the result $\int d\mathbf{r}\int d\mathbf{r}'\,\boldsymbol{\mathcal{T}}(\mathbf{r}-\mathbf{r}'):\boldsymbol{\mathcal{T}}(\mathbf{r}-\mathbf{r}')=\int d\mathbf{r}\,\beta^2/(v\varepsilon_0^2)$, which can be easily derived by expressing $\boldsymbol{\mathcal{T}}(\mathbf{r})$ as Fourier integrals. With this, the

derivative of βW_0 with respect to a is given by:

$$\begin{aligned}\frac{d\beta W_0}{da} &= -\int d\mathbf{r}\,\frac{\beta}{2av(\beta+\varepsilon_0 a)} + \int d\mathbf{r}\,\frac{\beta\varepsilon_0}{2v(\beta+\varepsilon_0 a)^2} \\ &\quad -\lambda\int d\mathbf{r}\int d\Omega\int d\mathbf{p}\,e^{-f(\boldsymbol{\mu},\mathbf{p};\mathbf{r})}\left[-\frac{\beta\varepsilon_0 t_h}{2(\beta+\varepsilon_0 a)^2}(\boldsymbol{\mu}+\mathbf{p})^2\right. \\ &\quad \left.+\left(\frac{\varepsilon_0}{\beta+\varepsilon_0 a}\right)^2\int d\mathbf{r}'(\boldsymbol{\mu}+\mathbf{p})\boldsymbol{\mathcal{T}}(\mathbf{r}-\mathbf{r}')[\boldsymbol{\mathcal{E}}_0(\mathbf{r}')-\mathbf{F}(\mathbf{r}')]\right] \\ &\quad +\left(\frac{\varepsilon_0}{\beta+\varepsilon_0 a}\right)^3\langle\boldsymbol{\mathcal{E}}_0-\mathbf{F}|\,\boldsymbol{\mathcal{T}}\,|\boldsymbol{\mathcal{E}}_0-\mathbf{F}\rangle \end{aligned} \tag{2.56}$$

On the other hand, the derivative of βW_0 with respect to $\mathbf{F}(\mathbf{r})$ is

$$\begin{aligned}\frac{\delta\beta W_0}{\delta\mathbf{F}(\mathbf{r})} &= \left(\frac{\varepsilon_0}{\beta+\varepsilon_0 a}\right)^2\int d\mathbf{r}'\boldsymbol{\mathcal{T}}(\mathbf{r}-\mathbf{r}')\,[\boldsymbol{\mathcal{E}}_0(\mathbf{r}')-\mathbf{F}(\mathbf{r}')] \\ &\quad -\lambda\int d\mathbf{r}'\int d\Omega\int d\mathbf{p}\,e^{-f(\boldsymbol{\mu},\mathbf{p};\mathbf{r})}\left[\frac{\varepsilon_0}{\beta+\varepsilon_0 a}\boldsymbol{\mathcal{T}}(\mathbf{r}-\mathbf{r}')(\boldsymbol{\mu}+\mathbf{p})\right] \end{aligned} \tag{2.57}$$

The constitutive relations are formed by setting

$$\frac{d\beta W_0}{da} = 0 \tag{2.58}$$

$$\frac{\delta\beta W_0}{\delta\mathbf{F}(\mathbf{r})} = \mathbf{0} \tag{2.59}$$

To further simplify the two constitutive relations, we introduce an expression for the number of particles in the system derived from the variational grand potential:

$$\begin{aligned}\langle N\rangle &= \lambda\frac{\partial\beta W_0}{\partial\lambda} \\ &= \lambda\int d\mathbf{r}\int d\Omega\int d\mathbf{p}\left\langle e^{i(\boldsymbol{\mu}+\mathbf{p})\cdot G(\mathbf{r})-\frac{p^2}{2\tilde{\alpha}}}\right\rangle_0 \end{aligned} \tag{2.60}$$

where the $\langle\mathcal{O}\rangle = \frac{1}{\Xi}\int\mathcal{D}\mathbf{P}\int\mathcal{D}\mathbf{G}\,\mathcal{O}[\mathbf{P},\mathbf{G}]e^{-\mathcal{L}[\mathbf{P},\mathbf{G}]}$. The particle concentration can be calculated through the relation $\langle N\rangle = \int d\mathbf{r}\,c(\mathbf{r})$. Using Eq. (2.49), we find the following expression for $c(\mathbf{r})$:

$$c(\mathbf{r}) = \lambda\int d\Omega\int d\mathbf{p}\,e^{-f(\boldsymbol{\mu},\mathbf{p};\mathbf{r})} \tag{2.61}$$

With the introduction of particle concentration $c(\mathbf{r})$, algebraic simplifications leads to the following constitutive relations:

$$\frac{1}{a} = \frac{1}{3} c(\mathbf{r}) \left\langle (\boldsymbol{\mu} + \mathbf{p})^2 \right\rangle_{f(\mathbf{r})} \tag{2.62}$$

and

$$\frac{\varepsilon_0}{\beta + \varepsilon_0 a} \left[\boldsymbol{\mathcal{E}}_0(\mathbf{r}) - \mathbf{F}(\mathbf{r}) \right] = c(\mathbf{r}) \left\langle \boldsymbol{\mu} + \mathbf{p} \right\rangle_{f(\mathbf{r})} \tag{2.63}$$

where $\langle \cdot \rangle_{f(\mathbf{r})}$ is the average value taken with respect to $f(\boldsymbol{\mu}, \mathbf{p}; \mathbf{r})$, and it is defined as

$$\left\langle \mathcal{O} \right\rangle_{f(\mathbf{r})} = \frac{\int d\Omega \int d\mathbf{p}\, \mathcal{O} e^{-f(\boldsymbol{\mu}, \mathbf{p}; \mathbf{r})}}{\int d\Omega \int d\mathbf{p}\, e^{-f(\boldsymbol{\mu}, \mathbf{p}; \mathbf{r})}} \tag{2.64}$$

The expectation values $\langle (\boldsymbol{\mu} + \mathbf{p})^2 \rangle_{f(\mathbf{r})}$ and $\langle \boldsymbol{\mu} + \mathbf{p} \rangle_{f(\mathbf{r})}$ can be algebraically evaluated, and the results are

$$\left\langle \boldsymbol{\mu} + \mathbf{p} \right\rangle_{f(\mathbf{r})} = \bar{\alpha} C \left[1 + \frac{\bar{\mu}^2}{\bar{\alpha}} C G \left(\bar{\mu} C |\boldsymbol{\mathcal{E}}_I(\mathbf{r})| \right) \right] \boldsymbol{\mathcal{E}}_I(\mathbf{r}) \tag{2.65}$$

and

$$\left\langle (\boldsymbol{\mu} + \mathbf{p})^2 \right\rangle_{f(\mathbf{r})} = 3C\bar{\alpha} + C^2 \bar{\mu}^2 + C^2 \bar{\alpha}^2 \left[1 + 2\frac{\bar{\mu}^2}{\bar{\alpha}} C G \left(\bar{\mu} C |\boldsymbol{\mathcal{E}}_I(\mathbf{r})| \right) \right] \boldsymbol{\mathcal{E}}_I(\mathbf{r})^2 \tag{2.66}$$

where $C = \left(1 - \frac{\beta \bar{\alpha} t_h}{\beta + \varepsilon_0 a} \right)^{-1}$ and $G(x) = (\coth x - 1/x)/x$.

Substituting Eqs. (2.65) and (2.66) into Eqs. (2.62) and (2.63) leads to the constitutive relations in Eqs. (2.25) and (2.26).

Chapter 3

A Variational Field-Theoretic Approach for Polar Liquid Mixtures: Miscibility and Dielectric Constants

3.1 Introduction

The study of liquid mixtures is essential in many aspects of science and of practical importance for miscellaneous technological applications. The sheer amount of different solvent mixtures has given us a vast amount of possibilities for reaction media. For example, if we create mixtures from a set of only about 50 common liquids, these liquids can make up about 1200 binary mixtures and 20,000 ternary mixtures; on top of that, each mixture can exist in different compositions. Given the immeasurable number of different mixtures, it is impossible and too expensive to explore the properties of general mixtures with experimental measurements or computer simulations. Therefore, in the realm of mixtures, the development of a robust theory is particularly important, and the goal of this chapter is to develop a reliable theory that captures the interactions between polar molecules in a mixture.

In Chapter 2, we have developed a field-theoretic variational theory for pure liquids. By introducing a physically meaningful reference potential, the variational approach allows us to take into account the effects of reaction field. In this chapter, we extend the framework developed in Chapter 2 to consider a mixture of polar liq-

uids. For simplicity, we consider each solvent component to be nonpolarizable in this chapter, and focus on capturing the interactions between permanent dipole moments. The resulting field-theoretic variational theory (FTVT) presented in this chapter consists of simple analytical equations that allow one to calculate the free energy of a mixture based on the permanent dipole moments and the molecular volumes of the solvent components and the mixture compositions. Without the use of any adjustable parameters, we are able to predict the dielectric constants and the miscibility for a wide range of liquid mixtures in good agreement with experimental observations. In particular, by computing the miscibility between liquids, we provide a quantitative explanation to the common saying "like dissolves like, and unlike does not."

This chapter is organized as follows. In Section 3.2, we introduce the model for the liquid mixture, and provide a detailed derivation for our theory. A reference field-based Hamiltonian is introduced to perform a field-theoretic variational treatment on the partition function of the system. Expressions for the mixing free energy and the mixture dielectric constant are derived. In Section 3.3, we apply the theory to calculate the dielectric constants and predict the miscibility of binary mixtures. The results are shown to be in good agreement with experimental observations. Finally, in Section 3.4, we provide some concluding remarks.

3.2 Theory

3.2.1 The Model and the Partition Functions

We consider a mixture of polar liquids in a canonical ensemble of volume V and temperature T, where there are N_s molecules of each solvent type s. For simplicity, we consider a binary solvent mixture, with $s = A, B$, but we note that the theory can be straightforwardly extended to multicomponent mixtures. Each molecule of solvent type s has a permanent dipole moment of magnitude $\bar{\mu}_s$ and an average molecular volume v_s. We assume that the dipole moment finitely spread around the center of each molecule, described by a short-ranged polarization distribution function $h_s(\mathbf{r})$.

For now, we do not specify the form of $h_s(\mathbf{r})$, but only require that its integral over space is 1, i. e. $\int d\mathbf{r}\, h_s(\mathbf{r}) = 1$. Let $\mathbf{r}_{s,i}$ and $\boldsymbol{\mu}_{s,i}$ denote the position and the permanent dipole moment of the ith molecule of type s, we write the instantaneous polarization of this molecule as:

$$\hat{\mathbf{P}}_{s,i}(\mathbf{r}) = \boldsymbol{\mu}_{s,i} h_s(\mathbf{r} - \mathbf{r}_{s,i}) \tag{3.1}$$

The instantaneous polarization $\hat{\mathbf{P}}(\mathbf{r})$of the system, given by the sum of instantaneous polarization of all molecules, is given by

$$\hat{\mathbf{P}}(\mathbf{r}) = \sum_{s=A,B} \sum_{i=1}^{N_s} \boldsymbol{\mu}_{s,i} h_s(\mathbf{r} - \mathbf{r}_{s,i}) \tag{3.2}$$

We apply an electric field $\mathbf{E}_0(\mathbf{r})$ to the system by external sources. The total energy of the system U can be written as the sum of the dipole-dipole interactions and the interaction between the dipoles and the external field as

$$\begin{aligned} \beta U &= \frac{\beta}{2} \int d\mathbf{r} \int d\mathbf{r}'\, \hat{\mathbf{P}}(\mathbf{r}) \mathbf{T}(\mathbf{r} - \mathbf{r}') \hat{\mathbf{P}}(\mathbf{r}') - \beta \int d\mathbf{r}\, \hat{\mathbf{P}}(\mathbf{r}) \cdot \mathbf{E}_0(\mathbf{r}) \\ &= \frac{1}{2} \int d\mathbf{r} \int d\mathbf{r}'\, \hat{\mathbf{P}}(\mathbf{r}) \boldsymbol{\mathcal{T}}(\mathbf{r} - \mathbf{r}') \hat{\mathbf{P}}(\mathbf{r}') - \int d\mathbf{r}\, \hat{\mathbf{P}}(\mathbf{r}) \cdot \boldsymbol{\mathcal{E}}_0(\mathbf{r}) \end{aligned} \tag{3.3}$$

where $\boldsymbol{\mathcal{E}} = \beta \mathbf{E}$ and $\boldsymbol{\mathcal{T}} = \beta \mathbf{T}$, with $\beta = 1/k_B T$ being the inverse temperature and $\boldsymbol{\mathcal{T}}(\mathbf{r})$ being the dipole-dipole interaction tensor scaled by the inverse temperature. The dipole-dipole interaction tensor can be expressed as[52]

$$\begin{aligned} \mathbf{T}(\mathbf{r}) &= -\nabla\nabla \frac{1}{4\pi\varepsilon_0 |\mathbf{r}|} \\ &= \lim_{\epsilon \to 0} \left[-H(|\mathbf{r}| - \epsilon) \nabla_{\mathbf{r}} \nabla_{\mathbf{r}} \frac{1}{4\pi\varepsilon_0 |\mathbf{r}|} + \frac{1}{3\varepsilon_0} \mathbb{1} \delta(\mathbf{r}) \right] \\ &= \lim_{\epsilon \to 0} \left[-H(|\mathbf{r}| - \epsilon) \frac{1}{4\pi\varepsilon_0 r^3} \left(\mathbb{1} - \frac{3\mathbf{r}\mathbf{r}}{r^2} \right) + \frac{1}{3\varepsilon_0} \mathbb{1} \delta(\mathbf{r}) \right] \end{aligned} \tag{3.4}$$

where $\mathbb{1}$ is the identity tensor, with its Fourier transform given by

$$\mathbf{T}(\mathbf{k}) = \frac{\mathbf{k}\mathbf{k}}{\varepsilon_0 k^2} \tag{3.5}$$

We note that the expression for total energy in Eq. (3.3) involves the self interaction energy of a dipole. However, because each molecule has a permanent dipole that is fixed in magnitude, the self interaction energy is a constant; the inclusion of self energy only shifts the energy scale and does not have physical consequences.

The canonical partition function of the system can be written as

$$\begin{aligned} Z &= \prod_{s=A,B}\prod_{i=1}^{N_s}\int \frac{d\mathbf{r}_{s,i}d\boldsymbol{\mu}_{s,i}}{\Lambda_s}\, e^{-\beta U} \\ &= \prod_{s=A,B}\prod_{i=1}^{N_s}\int \frac{d\mathbf{r}_{s,i}d\boldsymbol{\mu}_{s,i}}{\Lambda_s}\, \exp\left[-\frac{1}{2}\int d\mathbf{r}\int d\mathbf{r}'\,\hat{\mathbf{P}}(\mathbf{r})\boldsymbol{\mathcal{T}}(\mathbf{r}-\mathbf{r}')\hat{\mathbf{P}}(\mathbf{r}')\right. \\ &\quad \left. +\int d\mathbf{r}\,\hat{\mathbf{P}}(\mathbf{r})\cdot\boldsymbol{\mathcal{E}}_0(\mathbf{r})\right] \end{aligned} \tag{3.6}$$

To proceed, we transform the particle-based canonical partition function into a field-based one. The terms involving the instantaneous polarization density $\hat{\mathbf{P}}(\mathbf{r})$ can be transformed as

$$\begin{aligned} &\exp\left[-\frac{1}{2}\int d\mathbf{r}\int d\mathbf{r}'\,\hat{\mathbf{P}}(\mathbf{r})\boldsymbol{\mathcal{T}}(\mathbf{r}-\mathbf{r}')\hat{\mathbf{P}}(\mathbf{r}')+\int d\mathbf{r}\,\hat{\mathbf{P}}(\mathbf{r})\cdot\boldsymbol{\mathcal{E}}_0(\mathbf{r})\right] \\ =\ &\int \mathcal{D}\mathbf{P}\,\delta[\mathbf{P}-\hat{\mathbf{P}}]\exp\left[-\frac{1}{2}\int d\mathbf{r}\int d\mathbf{r}'\,\mathbf{P}(\mathbf{r})\boldsymbol{\mathcal{T}}(\mathbf{r}-\mathbf{r}')\mathbf{P}(\mathbf{r}')+\int d\mathbf{r}\,\mathbf{P}(\mathbf{r})\cdot\boldsymbol{\mathcal{E}}_0(\mathbf{r})\right] \\ =\ &\int \mathcal{D}\mathbf{P}\int \mathcal{D}\mathbf{G}\, e^{i\int d\mathbf{r},\mathbf{G}(\mathbf{r})\cdot[\mathbf{P}-\hat{\mathbf{P}}]} \\ &\qquad \times\exp\left[-\frac{1}{2}\int d\mathbf{r}\int d\mathbf{r}'\,\mathbf{P}(\mathbf{r})\boldsymbol{\mathcal{T}}(\mathbf{r}-\mathbf{r}')\mathbf{P}(\mathbf{r}')+\int d\mathbf{r}\,\mathbf{P}(\mathbf{r})\cdot\boldsymbol{\mathcal{E}}_0(\mathbf{r})\right] \\ =\ &\int \mathcal{D}\mathbf{P}\int \mathcal{D}\mathbf{G}\,\exp\left[-\frac{1}{2}\int d\mathbf{r}\int d\mathbf{r}'\,\mathbf{P}(\mathbf{r})\boldsymbol{\mathcal{T}}(\mathbf{r}-\mathbf{r}')\mathbf{P}(\mathbf{r}')-i\int d\mathbf{r}\,\mathbf{P}(\mathbf{r})\cdot\mathbf{G}(\mathbf{r})\right. \\ &\qquad \left. +\int d\mathbf{r}\,\mathbf{P}(\mathbf{r})\cdot\boldsymbol{\mathcal{E}}_0(\mathbf{r})+i\int d\mathbf{r}\,\hat{\mathbf{P}}(\mathbf{r})\cdot\mathbf{G}(\mathbf{r})\right] \end{aligned} \tag{3.7}$$

Substituting Eq. (3.7) into the particle-based canonical partition function Eq. (3.6)

and reorganizing the order of the terms, we arrive at

$$\begin{aligned} Z &= \int \mathcal{D}\mathbf{P} \int \mathcal{D}\mathbf{G} \, \exp\left[-\frac{1}{2} \int d\mathbf{r} \int d\mathbf{r}' \, \mathbf{P}(\mathbf{r}) \boldsymbol{\mathcal{T}}(\mathbf{r}-\mathbf{r}') \mathbf{P}(\mathbf{r}') \right. \\ &\qquad \left. -i \int d\mathbf{r} \, \mathbf{P}(\mathbf{r}) \cdot \mathbf{G}(\mathbf{r}) + \int d\mathbf{r} \, \mathbf{P}(\mathbf{r}) \cdot \boldsymbol{\mathcal{E}}_0(\mathbf{r}) \right] \prod_{s=A,B} q_s[\mathbf{G}(\mathbf{r})]^{N_s} \end{aligned} \tag{3.8}$$

where $q_s[\mathbf{G}]$ is the single-particle partition function for the solvent type s under the field $\mathbf{G}(\mathbf{r})$, given by

$$q_s[\mathbf{G}(\mathbf{r})] = \int \frac{d\mathbf{r} d\boldsymbol{\mu}_s}{\Lambda_s} \, \exp\left[i \int d\mathbf{r}' \, h_s(\mathbf{r}'-\mathbf{r}) \boldsymbol{\mu}_s \cdot \mathbf{G}(\mathbf{r}') \right] \tag{3.9}$$

It is more convenient to carry out variational treatments in the grand canonical ensemble. The grand partition function can be derived from the canonical partition function as follows:

$$\begin{aligned} \Xi &= \sum_{N_A=0}^{\infty} \sum_{N_B=0}^{\infty} \frac{e^{\beta\mu_A N_A}}{N_A!} \frac{e^{\beta\mu_B N_B}}{N_B!} Z(N_A, N_B) \\ &= \int \mathcal{D}\mathbf{P} \int \mathcal{D}\mathbf{G} \, \exp\left[-\frac{1}{2} \int d\mathbf{r} \int d\mathbf{r}' \, \mathbf{P}(\mathbf{r}) \boldsymbol{\mathcal{T}}(\mathbf{r}-\mathbf{r}') \mathbf{P}(\mathbf{r}') - i \int d\mathbf{r} \, \mathbf{P}(\mathbf{r}) \cdot \mathbf{G}(\mathbf{r}) \right. \\ &\qquad \left. + \int d\mathbf{r} \, \mathbf{P}(\mathbf{r}) \cdot \boldsymbol{\mathcal{E}}_0(\mathbf{r}) \right] \sum_{N_A=0}^{\infty} \frac{e^{\beta\mu_A N_A}}{N_A!} q_A[\mathbf{G}]^{N_A} \sum_{N_B=0}^{\infty} \frac{e^{\beta\mu_B N_B}}{N_B!} q_B[\mathbf{G}]^{N_B} \\ &= \int \mathcal{D}\mathbf{P} \int \mathcal{D}\mathbf{G} \, e^{-H_g[\mathbf{P},\mathbf{G}]} \end{aligned} \tag{3.10}$$

where $H_g[\mathbf{P}, \mathbf{G}]$ is the effective Hamiltonian in the grand canonical ensemble given by

$$\begin{aligned} H_g[\mathbf{P}, \mathbf{G}] &= \frac{1}{2} \int d\mathbf{r} \int d\mathbf{r}' \, \mathbf{P}(\mathbf{r}) \boldsymbol{\mathcal{T}}(\mathbf{r}-\mathbf{r}') \mathbf{P}(\mathbf{r}') + i \int d\mathbf{r} \, \mathbf{P}(\mathbf{r}) \cdot \mathbf{G}(\mathbf{r}) \\ &\quad - \int d\mathbf{r} \, \mathbf{P}(\mathbf{r}) \cdot \boldsymbol{\mathcal{E}}_0(\mathbf{r}) \\ &\quad - \sum_{s=A,B} \frac{e^{\beta\mu_s}}{\Lambda_s} \int d\mathbf{r} \int d\boldsymbol{\mu}_s \, \exp\left(i \int d\mathbf{r}' \, h_s(\mathbf{r}'-\mathbf{r}) \boldsymbol{\mu}_s \cdot \mathbf{G}(\mathbf{r}') \right) \end{aligned} \tag{3.11}$$

In the grand canonical ensemble, the grand potential W_g of the system is given by

$$\beta W_g = -\ln \Xi \tag{3.12}$$

3.2.2 Variational Treatment

In this subsection, we develop a variational approach to approximate the grand potential W_g. In the exact field-theoretic Hamiltonian in Eq. (3.11), only the last term is not Gaussian. We observe that this non-Gaussian term describes a single dipole interacting in the conjugate field $\mathbf{G}(\mathbf{r})$. Before we proceed, let us examine the value of $\mathbf{G}^*$ at the saddle point. By extremizing the effective Hamiltonian H_G with respect to $\mathbf{P}$, i. e. letting $\delta H_g/\delta \mathbf{P}(\mathbf{r}) = 0$, we have the following saddle point condition:

$$\begin{aligned} \int d\mathbf{r}' \boldsymbol{\mathcal{T}}(\mathbf{r}-\mathbf{r}')\mathbf{P}^*(\mathbf{r}') + i\mathbf{G}^*(\mathbf{r}) - \boldsymbol{\mathcal{E}}_0(\mathbf{r}) = 0 \\ i\mathbf{G}^*(\mathbf{r}) = \boldsymbol{\mathcal{E}}_0(\mathbf{r}) - \int d\mathbf{r}' \boldsymbol{\mathcal{T}}(\mathbf{r}-\mathbf{r}')\mathbf{P}^*(\mathbf{r}') \end{aligned} \tag{3.13}$$

where $\mathbf{P}^*$ and $\mathbf{G}^*$ are the saddle-point values of $\mathbf{P}$ and $\mathbf{G}$, respectively. From the above saddle-point constitutive relation, we see that the field $i\mathbf{G}(\mathbf{r})$ represents the *local field* at position $\mathbf{r}$ when the saddle-point approximation is used. In Onsager's theory for the dielectric constant, the insight is that only part of the local field is exerting a torque on the dipole moment. The other part is the reaction field, which always points in the same direction as the particle and thus does not exert a torque on the particle. Keeping this insight in mind, we propose the following variational Hamiltonian by modeling the last term in H as a Gaussian fluctuation around an average field $\mathbf{F}$:

$$\begin{aligned} H_0[\mathbf{P},\mathbf{G}] &= \frac{1}{2}\int d\mathbf{r}\int d\mathbf{r}'\,\mathbf{P}(\mathbf{r})\boldsymbol{\mathcal{T}}(\mathbf{r}-\mathbf{r}')\mathbf{P}(\mathbf{r}') + i\int d\mathbf{r}\,\mathbf{P}(\mathbf{r})\cdot\mathbf{G}(\mathbf{r}) \\ &\quad - \int d\mathbf{r}\,\mathbf{P}(\mathbf{r})\cdot\boldsymbol{\mathcal{E}}_0(\mathbf{r}) \\ &\quad + \frac{1}{2}\int d\mathbf{r}\int d\mathbf{r}'\,\left[\mathbf{G}(\mathbf{r})+i\mathbf{F}(\mathbf{r})\right]\boldsymbol{\mathcal{A}}^{-1}(\mathbf{r}-\mathbf{r}')\left[\mathbf{G}(\mathbf{r}')+i\mathbf{F}(\mathbf{r}')\right] \end{aligned} \tag{3.14}$$

where $\boldsymbol{\mathcal{A}}$ and $\mathbf{F}$ are the variational parameters. We then apply the Gibbs-Feynman-Bogoliubov inequality to obtain an upper bound W for the grand potential:

$$\beta W_g \leq \beta W = -\ln \Xi_0 + \langle H_g - H_0 \rangle_0 \tag{3.15}$$

where W is the variational grand potential, and

$$\Xi_0 = \int \mathcal{D}\mathbf{P} \int \mathcal{D}\mathbf{G}\, e^{-H_0[\mathbf{P},\mathbf{G}]} \tag{3.16}$$

$$\langle \mathcal{O} \rangle_0 = \frac{\int \mathcal{D}\mathbf{P} \int \mathcal{D}\mathbf{G}\, \mathcal{O}[\mathbf{P},\mathbf{G}] e^{-H_0[\mathbf{P},\mathbf{G}]}}{\int \mathcal{D}\mathbf{P} \int \mathcal{D}\mathbf{G}\, e^{-H_0[\mathbf{P},\mathbf{G}]}} \tag{3.17}$$

Our goal is to minimize W with respect to $\boldsymbol{\mathcal{A}}$ and $\mathbf{F}$ to obtain the upper bound of the grand potential.

The reference grand partition function Ξ_0 is a Gaussian integral, which can be evaluated to be

$$\Xi_0 = \left(\frac{\det \boldsymbol{\mathcal{A}}}{\det(\boldsymbol{\mathcal{T}} + \boldsymbol{\mathcal{A}})} \right)^{\frac{1}{2}} e^{\frac{1}{2} \int d\mathbf{r} \int d\mathbf{r}' \, [\boldsymbol{\mathcal{E}}_0(\mathbf{r}) - \mathbf{F}(\mathbf{r})][\boldsymbol{\mathcal{T}}(\mathbf{r}-\mathbf{r}') + \boldsymbol{\mathcal{A}}(\mathbf{r}-\mathbf{r}')]^{-1}[\boldsymbol{\mathcal{E}}_0(\mathbf{r}') - \mathbf{F}(\mathbf{r}')]} \tag{3.18}$$

where the determinant of a matrix $\boldsymbol{\mathcal{M}}$ is defined as

$$\begin{aligned} (\det \boldsymbol{\mathcal{M}})^{-\frac{1}{2}} &= (\det \boldsymbol{\mathcal{M}}^{-1})^{\frac{1}{2}} \\ &= \int \mathcal{D}\boldsymbol{\xi} \exp\left[-\frac{1}{2} \int d\mathbf{r} \int d\mathbf{r}' \, \boldsymbol{\xi}(\mathbf{r}) \boldsymbol{\mathcal{M}}^{-1}(\mathbf{r}-\mathbf{r}') \boldsymbol{\xi}(\mathbf{r}') \right] \end{aligned} \tag{3.19}$$

The term $\langle H_g - H \rangle_0$ in Eq. (3.15) can be simplified as

$$\begin{aligned} \langle H_g - H \rangle_0 = &- \sum_{s=A,B} \frac{e^{\beta \mu_s}}{\Lambda_s} \int d\mathbf{r} \int d\boldsymbol{\mu}_s \left\langle \exp\left(i \int d\mathbf{r}' \, h_s(\mathbf{r}'-\mathbf{r}) \boldsymbol{\mu}_s \cdot \mathbf{G}(\mathbf{r}') \right) \right\rangle_0 \\ &- \frac{1}{2} \int d\mathbf{r} \int d\mathbf{r}' \, \left\langle \mathbf{V}(\mathbf{r}) \boldsymbol{\mathcal{A}}^{-1}(\mathbf{r}-\mathbf{r}') \mathbf{V}(\mathbf{r}') \right\rangle_0 \end{aligned} \tag{3.20}$$

where $\mathbf{V} = \mathbf{G} + i\mathbf{F}$. The first expectation value with respect to the reference Hamiltonian involved in Eq. (3.20) can be exactly evaluated because it is a Gaussian integral;

the result of the evaluation is

$$\begin{aligned}
&\left\langle \exp\left(i \int d\mathbf{r}'\, h_s(\mathbf{r}'-\mathbf{r}_1)\boldsymbol{\mu}_s \cdot \mathbf{G}(\mathbf{r}') \right) \right\rangle_0 \\
= \;& \exp\left[\int d\mathbf{r}\, h_s(\mathbf{r}-\mathbf{r}_1)\boldsymbol{\mu}_s \cdot \mathbf{F}(\mathbf{r}) - \frac{1}{2}\int d\mathbf{r} \int d\mathbf{r}' \boldsymbol{\mu}_s h_s(\mathbf{r}-\mathbf{r}_1)\boldsymbol{\mathcal{A}}(\mathbf{r}-\mathbf{r}')h_s(\mathbf{r}'-\mathbf{r}_1)\boldsymbol{\mu}_s \right. \\
&+ \int d\mathbf{r} \int d\mathbf{r}' \int d\mathbf{r}''\, [\boldsymbol{\mathcal{E}}_0(\mathbf{r}) - \mathbf{F}(\mathbf{r})][\boldsymbol{\mathcal{T}}(\mathbf{r}-\mathbf{r}') + \boldsymbol{\mathcal{A}}(\mathbf{r}-\mathbf{r}')]^{-1}\boldsymbol{\mathcal{A}}(\mathbf{r}'-\mathbf{r}'')h_s(\mathbf{r}''-\mathbf{r}_1)\boldsymbol{\mu}_s \\
&+\frac{1}{2}\int d\mathbf{r} \int d\mathbf{r}' \int d\mathbf{r}'' \int d\mathbf{r}'''\, \boldsymbol{\mu}_s h_s(\mathbf{r}_1-\mathbf{r}'')\boldsymbol{\mathcal{A}}(\mathbf{r}''-\mathbf{r})[\boldsymbol{\mathcal{T}}(\mathbf{r}-\mathbf{r}') + \boldsymbol{\mathcal{A}}(\mathbf{r}-\mathbf{r}')]^{-1} \\
&\left. \cdot\boldsymbol{\mathcal{A}}(\mathbf{r}'-\mathbf{r}''')h_s(\mathbf{r}'''-\mathbf{r}_1)\boldsymbol{\mu}_s \right] \qquad (3.21)
\end{aligned}$$

The second expectation value with respect to the reference Hamiltonian involved in Eq. (3.20) can also be evaluated using derivatives of a Gaussian integral as:

$$\begin{aligned}
&\left\langle \mathbf{V}(\mathbf{r}_1)\boldsymbol{\mathcal{A}}^{-1}(\mathbf{r}_1-\mathbf{r}_2)\mathbf{V}(\mathbf{r}_2) \right\rangle_0 \\
= \;& \frac{1}{\Xi_0}\int \mathcal{D}\mathbf{P} \int \mathcal{D}\mathbf{V}\, \frac{\delta}{\delta i\mathbf{J}(\mathbf{r}_1)}\boldsymbol{\mathcal{A}}^{-1}(\mathbf{r}_1-\mathbf{r}_2)\frac{\delta}{\delta i\mathbf{J}(\mathbf{r}_2)} \left[e^{-\frac{1}{2}\int d\mathbf{r}\int d\mathbf{r}'\, \mathbf{P}(\mathbf{r})\boldsymbol{\mathcal{T}}(\mathbf{r}-\mathbf{r}')\mathbf{P}(\mathbf{r}')} \right. \\
&\left. \times e^{-i\int d\mathbf{r}\, \mathbf{P}(\mathbf{r})\cdot\mathbf{V}(\mathbf{r}) + \int d\mathbf{r}\, \mathbf{P}(\mathbf{r})\cdot[\boldsymbol{\mathcal{E}}_0(\mathbf{r})-\mathbf{F}(\mathbf{r})] - \frac{1}{2}\int d\mathbf{r}\int d\mathbf{r}'\, \mathbf{V}(\mathbf{r})\boldsymbol{\mathcal{A}}^{-1}(\mathbf{r}-\mathbf{r}')\mathbf{V}(\mathbf{r}') - i\int d\mathbf{r}\mathbf{J}(\mathbf{r})\cdot\mathbf{V}(\mathbf{r})} \right] \Big|_{\mathbf{J}=0} \\
= \;& \boldsymbol{\mathcal{A}}^{-1}(\mathbf{r}_1-\mathbf{r}_2) : \left\{ -\int d\mathbf{r}\int d\mathbf{r}'\, \boldsymbol{\mathcal{A}}(\mathbf{r}_1-\mathbf{r})[\boldsymbol{\mathcal{T}}(\mathbf{r}-\mathbf{r}') + \boldsymbol{\mathcal{A}}(\mathbf{r}-\mathbf{r}')]^{-1}\boldsymbol{\mathcal{A}}(\mathbf{r}'-\mathbf{r}_2) \right\} \\
&+\boldsymbol{\mathcal{A}}^{-1}(\mathbf{r}_1-\mathbf{r}_2) : \boldsymbol{\mathcal{A}}(\mathbf{r}_1-\mathbf{r}_2) \\
&-\int d\mathbf{r}\int d\mathbf{r}'\int d\mathbf{r}''\int d\mathbf{r}'''\, (\boldsymbol{\mathcal{E}}_0(\mathbf{r}) - \mathbf{F}(\mathbf{r}))\, [\boldsymbol{\mathcal{T}}(\mathbf{r}-\mathbf{r}') + \boldsymbol{\mathcal{A}}(\mathbf{r}-\mathbf{r}')]^{-1}\boldsymbol{\mathcal{A}}(\mathbf{r}'-\mathbf{r}_1) \\
&\cdot\boldsymbol{\mathcal{A}}^{-1}(\mathbf{r}_1-\mathbf{r}_2)\boldsymbol{\mathcal{A}}(\mathbf{r}_2-\mathbf{r}'')[\boldsymbol{\mathcal{T}}(\mathbf{r}''-\mathbf{r}''') + \boldsymbol{\mathcal{A}}(\mathbf{r}''-\mathbf{r}''')]^{-1}\, (\boldsymbol{\mathcal{E}}_0(\mathbf{r}''') - \mathbf{F}(\mathbf{r}''')) \qquad (3.22)
\end{aligned}$$

Substituting Eqs. (3.18), (3.20), (3.21), and (3.22) into the expression for varia-

tional free energy in (3.15), we write the variational free energy as

$$
\begin{aligned}
\beta W &= -\ln\left(\frac{\det \boldsymbol{\mathcal{A}}}{\det(\boldsymbol{\mathcal{T}}+\boldsymbol{\mathcal{A}})}\right)^{\frac{1}{2}} \\
&\quad -\frac{1}{2}\int d\mathbf{r}\int d\mathbf{r}'\,[\boldsymbol{\mathcal{E}}_0(\mathbf{r})-\mathbf{F}(\mathbf{r})][\boldsymbol{\mathcal{T}}(\mathbf{r}-\mathbf{r}')+\boldsymbol{\mathcal{A}}(\mathbf{r}-\mathbf{r}')]^{-1}[\boldsymbol{\mathcal{E}}_0(\mathbf{r}')-\mathbf{F}(\mathbf{r}')] \\
&\quad -\sum_{s=A,B}\frac{e^{\beta\mu_s}}{\Lambda_s}\int d\mathbf{r}_1\int d\boldsymbol{\mu}_s\, e^{\int d\mathbf{r}\, h_s(\mathbf{r}-\mathbf{r}_1)\boldsymbol{\mu}_s\cdot\mathbf{F}(\mathbf{r})-\frac{1}{2}\int d\mathbf{r}\int d\mathbf{r}'\boldsymbol{\mu}_s h_s(\mathbf{r}-\mathbf{r}_1)\boldsymbol{\mathcal{A}}(\mathbf{r}-\mathbf{r}')h_s(\mathbf{r}'-\mathbf{r}_1)\boldsymbol{\mu}_s} \\
&\quad \times e^{+\frac{1}{2}\int d\mathbf{r}\int d\mathbf{r}'\int d\mathbf{r}''\int d\mathbf{r}'''\,\boldsymbol{\mu}_s h_s(\mathbf{r}_1-\mathbf{r}'')\boldsymbol{\mathcal{A}}(\mathbf{r}''-\mathbf{r})[\boldsymbol{\mathcal{T}}(\mathbf{r}-\mathbf{r}')+\boldsymbol{\mathcal{A}}(\mathbf{r}-\mathbf{r}')]^{-1}\cdot\boldsymbol{\mathcal{A}}(\mathbf{r}'-\mathbf{r}''')h_s(\mathbf{r}'''-\mathbf{r}_1)\boldsymbol{\mu}_s} \\
&\quad \times e^{+\int d\mathbf{r}\int d\mathbf{r}'\int d\mathbf{r}''\,[\boldsymbol{\mathcal{E}}_0(\mathbf{r})-\mathbf{F}(\mathbf{r})][\boldsymbol{\mathcal{T}}(\mathbf{r}-\mathbf{r}')+\boldsymbol{\mathcal{A}}(\mathbf{r}-\mathbf{r}')]^{-1}\boldsymbol{\mathcal{A}}(\mathbf{r}'-\mathbf{r}'')h_s(\mathbf{r}''-\mathbf{r}_1)\boldsymbol{\mu}_s} \\
&\quad +\frac{1}{2}\int d\mathbf{r}_1\int d\mathbf{r}_2\int d\mathbf{r}\int d\mathbf{r}'\,\boldsymbol{\mathcal{A}}^{-1}(\mathbf{r}_1-\mathbf{r}_2) \\
&\qquad\qquad : \left\{\boldsymbol{\mathcal{A}}(\mathbf{r}_1-\mathbf{r})[\boldsymbol{\mathcal{T}}(\mathbf{r}-\mathbf{r}')+\boldsymbol{\mathcal{A}}(\mathbf{r}-\mathbf{r}')]^{-1}\boldsymbol{\mathcal{A}}(\mathbf{r}'-\mathbf{r}_2)\right\} \\
&\quad -\frac{1}{2}\int d\mathbf{r}_1\int d\mathbf{r}_2\,\boldsymbol{\mathcal{A}}^{-1}(\mathbf{r}_1-\mathbf{r}_2) : \boldsymbol{\mathcal{A}}(\mathbf{r}_1-\mathbf{r}_2) \\
&\quad +\frac{1}{2}\int d\mathbf{r}_1\int d\mathbf{r}_2\int d\mathbf{r}\int d\mathbf{r}'\int d\mathbf{r}''\int d\mathbf{r}'''\,(\boldsymbol{\mathcal{E}}_0(\mathbf{r})-\mathbf{F}(\mathbf{r})) \\
&\qquad\qquad \cdot[\boldsymbol{\mathcal{T}}(\mathbf{r}-\mathbf{r}')+\boldsymbol{\mathcal{A}}(\mathbf{r}-\mathbf{r}')]^{-1}\boldsymbol{\mathcal{A}}(\mathbf{r}'-\mathbf{r}_1)\boldsymbol{\mathcal{A}}^{-1}(\mathbf{r}_1-\mathbf{r}_2)\boldsymbol{\mathcal{A}}(\mathbf{r}_2-\mathbf{r}'') \\
&\qquad\qquad \cdot[\boldsymbol{\mathcal{T}}(\mathbf{r}''-\mathbf{r}''')+\boldsymbol{\mathcal{A}}(\mathbf{r}''-\mathbf{r}''')]^{-1}\,(\boldsymbol{\mathcal{E}}_0(\mathbf{r}''')-\mathbf{F}(\mathbf{r}'''))
\end{aligned}
\tag{3.23}
$$

3.2.3 The Structure of Variational Parameter $\boldsymbol{\mathcal{A}}$

If we expand the last term in the exact effective Hamiltonian in Eq. (3.11), we obtain the following quadratic term:

$$
\sum_{s=A,B}\frac{e^{\beta\mu_s}}{\Lambda_s}\int d\mathbf{r}\int d\mathbf{r}'\mathbf{G}(\mathbf{r})\int d\mathbf{r}_1 h_s(\mathbf{r}-\mathbf{r}_1)h_s(\mathbf{r}_1-\mathbf{r}')\left(\int d\boldsymbol{\mu}_s\,\boldsymbol{\mu}_s\boldsymbol{\mu}_s\right)\mathbf{G}(\mathbf{r}') \tag{3.24}
$$

The integral over $\boldsymbol{\mu}_s$ is a constant times an identity matrix. Thus we may let $\boldsymbol{\mathcal{A}}^{-1}$ to take the form

$$
\boldsymbol{\mathcal{A}}^{-1}(\mathbf{r}-\mathbf{r}') = \frac{1}{a'}\mathbb{1}\sum_{s=A,B}\frac{e^{\beta\mu_s}}{\Lambda_s}\int d\mathbf{r}_1 h_s(\mathbf{r}-\mathbf{r}_1)h_s(\mathbf{r}_1-\mathbf{r}') \tag{3.25}
$$

where a' is some constant from the integral over $\boldsymbol{\mu}_s$. Using the above form would make it difficult for us to exactly evaluate the tensor $[\boldsymbol{\mathcal{T}}+\boldsymbol{\mathcal{A}}]^{-1}$ involved in the variational

grand potential. Therefore, instead, as h_s is a short-ranged function centered around the position of the particle, we take the limit $h_s(\mathbf{r}) \to \delta(\mathbf{r})$ whenever it does not cause a singularity in the free energy. When the limit of δ-function is taken, the operators $\boldsymbol{\mathcal{A}}$ and $\boldsymbol{\mathcal{A}}^{-1}$ becomes

$$\boldsymbol{\mathcal{A}}(\mathbf{r}-\mathbf{r}') = a\mathbb{1}\delta(\mathbf{r}-\mathbf{r}') \tag{3.26}$$

$$\boldsymbol{\mathcal{A}}^{-1}(\mathbf{r}-\mathbf{r}') = \frac{1}{a}\mathbb{1}\delta(\mathbf{r}-\mathbf{r}') \tag{3.27}$$

where $\frac{1}{a'}\sum_{s=A,B}\frac{e^{\beta\mu_s}}{\Lambda_s} = \frac{1}{a}$. Using the δ-function limit of $\boldsymbol{\mathcal{A}}$, we may evaluate the inverse operator of $\boldsymbol{\mathcal{T}}+\boldsymbol{\mathcal{A}}$. Let $\boldsymbol{\mathcal{M}}$ be the inverse of $\boldsymbol{\mathcal{T}}+\boldsymbol{\mathcal{A}}$ such that

$$\int d\mathbf{r}'\left[\boldsymbol{\mathcal{T}}(\mathbf{r}-\mathbf{r}')+\boldsymbol{\mathcal{A}}(\mathbf{r}-\mathbf{r}')\right]\boldsymbol{\mathcal{M}}(\mathbf{r}'-\mathbf{r}'') = \mathbb{1}\delta(\mathbf{r}-\mathbf{r}'') \tag{3.28}$$

To find $\boldsymbol{\mathcal{M}}$, we perform Fourier transform to the above equation

$$\begin{aligned}&\int d\mathbf{r}'\left[\int\frac{d\mathbf{k}}{(2\pi)^3}\left(\tilde{\boldsymbol{\mathcal{T}}}(\mathbf{k})+\tilde{\boldsymbol{\mathcal{A}}}(\mathbf{k})\right)e^{i\mathbf{k}\cdot(\mathbf{r}-\mathbf{r}')}\right]\left[\int\frac{d\mathbf{k}'}{(2\pi)^3}\,\tilde{\boldsymbol{\mathcal{M}}}(\mathbf{k}')e^{i\mathbf{k}'\cdot(\mathbf{r}'-\mathbf{r}'')}\right]\\ &=\int\frac{d\mathbf{k}}{(2\pi)^3}\,\mathbb{1}e^{i\mathbf{k}\cdot(\mathbf{r}-\mathbf{r}'')}\end{aligned} \tag{3.29}$$

which leads to

$$\tilde{\boldsymbol{\mathcal{M}}}(\mathbf{k}) = \left(\tilde{\boldsymbol{\mathcal{T}}}(\mathbf{k})+\tilde{\boldsymbol{\mathcal{A}}}(\mathbf{k})\right)^{-1} \tag{3.30}$$

With $\boldsymbol{\mathcal{A}}(\mathbf{r}) = a\mathbb{1}\delta(\mathbf{r})$ and $\boldsymbol{\mathcal{T}}(\mathbf{k}) = \beta\mathbf{k}\mathbf{k}/\varepsilon_0 k^2$,[52] its Fourier transform is given by

$\tilde{\boldsymbol{\mathcal{A}}}(\mathbf{k}) = a\mathbb{1}$. Thus, $\tilde{\boldsymbol{\mathcal{M}}}(\mathbf{k})$ can be evaluated as

$$\begin{aligned}
\tilde{\boldsymbol{\mathcal{M}}}(\mathbf{k}) &= \left(\tilde{\boldsymbol{\mathcal{T}}}(\mathbf{k}) + a\mathbb{1}\right)^{-1} = a^{-1}\left[\mathbb{1} + a^{-1}\tilde{\boldsymbol{\mathcal{T}}}(\mathbf{k})\right]^{-1} \\
&= a^{-1}\left[\mathbb{1} - \frac{1}{a}\tilde{\boldsymbol{\mathcal{T}}}(\mathbf{k}) + \frac{1}{a^2}\tilde{\boldsymbol{\mathcal{T}}}(\mathbf{k})^2 - \frac{1}{a^3}\tilde{\boldsymbol{\mathcal{T}}}(\mathbf{k})^3 + \ldots\right] \\
&= a^{-1}\left[\mathbb{1} - \frac{1}{a}\left(\frac{\beta}{\varepsilon_0}\right)\left(\frac{\mathbf{kk}}{k^2}\right) + \frac{1}{a^2}\left(\frac{\beta}{\varepsilon_0}\right)^2\left(\frac{\mathbf{kk}}{k^2}\right)^2 - \frac{1}{a^3}\left(\frac{\beta}{\varepsilon_0}\right)^3\left(\frac{\mathbf{kk}}{k^2}\right)^3 + \ldots\right] \\
&= a^{-1}\mathbb{1} - a^{-1}\left(\frac{\beta}{\varepsilon_0 a}\right)\left[1 - \frac{\beta}{\varepsilon_0 a} + \left(\frac{\beta}{\varepsilon_0 a}\right)^2 - \ldots\right]\left(\frac{\mathbf{kk}}{k^2}\right) \\
&= \frac{1}{a}\left[\mathbb{1} - \frac{\varepsilon_0}{\beta + \varepsilon_0 a}\boldsymbol{\mathcal{T}}(\mathbf{k})\right] \qquad (3.31)
\end{aligned}$$

Inverse Fourier transform of the above equation gives

$$\boldsymbol{\mathcal{M}}(\mathbf{r}-\mathbf{r}') = \left[\boldsymbol{\mathcal{T}}(\mathbf{r}-\mathbf{r}') + \boldsymbol{\mathcal{A}}(\mathbf{r}-\mathbf{r}')\right]^{-1} = \frac{1}{a}\left[\mathbb{1}\delta(\mathbf{r}-\mathbf{r}') - \frac{\varepsilon_0}{\beta+\varepsilon_0 a}\boldsymbol{\mathcal{T}}(\mathbf{r}-\mathbf{r}')\right] \quad (3.32)$$

Now, we take the limit of $\boldsymbol{\mathcal{A}}(\mathbf{r}-\mathbf{r}') = a\mathbb{1}\delta(\mathbf{r}-\mathbf{r}')$ in the variational grand potential in Eq. (3.23) wherever a singularity does not arise, and use $\boldsymbol{\mathcal{A}}(\mathbf{r}-\mathbf{r}') = a\mathbb{1}\int d\mathbf{r}_2\, h_s^{-1}(\mathbf{r}-\mathbf{r}_2)h_s^{-1}(\mathbf{r}_2-\mathbf{r}')$ wherever the δ-function creates a singularity. The resulting variational grand potential is given by

$$\begin{aligned}
&\beta W \\
= \;& -\ln\left(\frac{\det\boldsymbol{\mathcal{A}}}{\det(\boldsymbol{\mathcal{T}}+\boldsymbol{\mathcal{A}})}\right)^{\frac{1}{2}} - \frac{1}{2}\frac{\varepsilon_0 a}{\beta+\varepsilon_0 a}\int d\mathbf{r}\int d\mathbf{r}'\,\boldsymbol{\mathcal{A}}^{-1}(\mathbf{r}-\mathbf{r}') : \boldsymbol{\mathcal{T}}(\mathbf{r}-\mathbf{r}') \\
&+\frac{1}{2a}\frac{\varepsilon_0}{\beta+\varepsilon_0 a}\int d\mathbf{r}\int d\mathbf{r}'\,[\boldsymbol{\mathcal{E}}_0(\mathbf{r}) - \mathbf{F}(\mathbf{r})]\boldsymbol{\mathcal{T}}(\mathbf{r}-\mathbf{r}')[\boldsymbol{\mathcal{E}}_0(\mathbf{r}') - \mathbf{F}(\mathbf{r}')] \\
&-\sum_{s=A,B}\frac{e^{\beta\mu_s}}{\Lambda_s}\int d\mathbf{r}\int d\boldsymbol{\mu}_s\,\exp\left[-\frac{\varepsilon_0}{\beta+\varepsilon_0 a}\int d\mathbf{r}_1\,[\boldsymbol{\mathcal{E}}_0(\mathbf{r}_1) - \mathbf{F}(\mathbf{r}_1)]\boldsymbol{\mathcal{T}}(\mathbf{r}_1-\mathbf{r})\boldsymbol{\mu}_s\right. \\
&\left.+\boldsymbol{\mathcal{E}}_0(\mathbf{r})\boldsymbol{\mu}_s - \frac{1}{2}\frac{\varepsilon_0 a}{\beta+\varepsilon_0 a}\int d\mathbf{r}_1\int d\mathbf{r}_2\,\boldsymbol{\mu}_s h_s(\mathbf{r}-\mathbf{r}_1)\boldsymbol{\mathcal{T}}(\mathbf{r}_1-\mathbf{r}_2)h_s(\mathbf{r}_2-\mathbf{r})\boldsymbol{\mu}_s\right] \\
&-\frac{1}{a}\frac{\varepsilon_0}{\beta+\varepsilon_0 a}\int d\mathbf{r}\int d\mathbf{r}'\,(\boldsymbol{\mathcal{E}}_0(\mathbf{r}) - \mathbf{F}(\mathbf{r}))\,\boldsymbol{\mathcal{T}}(\mathbf{r}-\mathbf{r}')\,(\boldsymbol{\mathcal{E}}_0(\mathbf{r}') - \mathbf{F}(\mathbf{r}')) \\
&+\frac{1}{2a}\left(\frac{\varepsilon_0}{\beta+\varepsilon_0 a}\right)^2\int d\mathbf{r}\int d\mathbf{r}'\int d\mathbf{r}''\,(\boldsymbol{\mathcal{E}}_0(\mathbf{r}) - \mathbf{F}(\mathbf{r}))\,\boldsymbol{\mathcal{T}}(\mathbf{r}-\mathbf{r}')\boldsymbol{\mathcal{T}}(\mathbf{r}'-\mathbf{r}'') \\
&\qquad\qquad\cdot(\boldsymbol{\mathcal{E}}_0(\mathbf{r}'') - \mathbf{F}(\mathbf{r}'')) \qquad (3.33)
\end{aligned}$$

We may further simplify the last line above by noting that

$$\begin{aligned}
&\int d\mathbf{r}'\, \boldsymbol{\mathcal{T}}(\mathbf{r}-\mathbf{r}')\boldsymbol{\mathcal{T}}(\mathbf{r}'-\mathbf{r}'') \\
&= \int d\mathbf{r}' \int \frac{d\mathbf{k}_1}{(2\pi)^3} \int \frac{d\mathbf{k}_2}{(2\pi)^3} \tilde{\boldsymbol{\mathcal{T}}}(\mathbf{k}_1)\tilde{\boldsymbol{\mathcal{T}}}(\mathbf{k}_2) e^{i\mathbf{k}_1\cdot(\mathbf{r}-\mathbf{r}')} e^{i\mathbf{k}_2\cdot(\mathbf{r}'-\mathbf{r}'')} \\
&= \int \frac{d\mathbf{k}}{(2\pi)^3} \frac{\beta}{\varepsilon_0} \tilde{\boldsymbol{\mathcal{T}}}(\mathbf{k}) e^{i\mathbf{k}\cdot(\mathbf{r}-\mathbf{r}'')} \\
&= \frac{\beta}{\varepsilon_0} \boldsymbol{\mathcal{T}}(\mathbf{r}-\mathbf{r}'')
\end{aligned} \tag{3.34}$$

Therefore,

$$\begin{aligned}
\beta W &= -\frac{1}{2}\ln\left(\frac{\det \boldsymbol{\mathcal{A}}}{\det(\boldsymbol{\mathcal{T}}+\boldsymbol{\mathcal{A}})}\right) - \frac{1}{2}\frac{\varepsilon_0 a}{\beta+\varepsilon_0 a}\int d\mathbf{r}\int d\mathbf{r}'\, \boldsymbol{\mathcal{A}}^{-1}(\mathbf{r}-\mathbf{r}') : \boldsymbol{\mathcal{T}}(\mathbf{r}-\mathbf{r}') \\
&\quad - \frac{\varepsilon_0^2}{2(\beta+\varepsilon_0 a)^2}\int d\mathbf{r}\int d\mathbf{r}'\, (\boldsymbol{\mathcal{E}}_0(\mathbf{r})-\mathbf{F}(\mathbf{r}))\, \boldsymbol{\mathcal{T}}(\mathbf{r}-\mathbf{r}')\, (\boldsymbol{\mathcal{E}}_0(\mathbf{r}')-\mathbf{F}(\mathbf{r}')) \\
&\quad - \sum_{s=A,B}\frac{e^{\beta\mu_s}}{\Lambda_s}\int d\mathbf{r}\int d\boldsymbol{\mu}_s \\
&\quad \times \exp\left[-\frac{1}{2}\frac{\varepsilon_0 a}{\beta+\varepsilon_0 a}\int d\mathbf{r}_1\int d\mathbf{r}_2\, \boldsymbol{\mu}_s h_s(\mathbf{r}-\mathbf{r}_1)\boldsymbol{\mathcal{T}}(\mathbf{r}_1-\mathbf{r}_2)h_s(\mathbf{r}_2-\mathbf{r})\boldsymbol{\mu}_s \right. \\
&\qquad \left. + \boldsymbol{\mu}_s\cdot\boldsymbol{\mathcal{E}}_0(\mathbf{r}) - \frac{\varepsilon_0}{\beta+\varepsilon_0 a}\int d\mathbf{r}_1\, [\boldsymbol{\mathcal{E}}_0(\mathbf{r}_1)-\mathbf{F}(\mathbf{r}_1)]\boldsymbol{\mathcal{T}}(\mathbf{r}_1-\mathbf{r})\boldsymbol{\mu}_s\right]
\end{aligned} \tag{3.35}$$

The first term in βW, involving the logarithm of a quotient of two determinants, may be evaluated using the procedure outlined in Appendix B of Ref. 19. Let us define a matrix $\boldsymbol{\Lambda}(\lambda) = \boldsymbol{\mathcal{A}} + \lambda\boldsymbol{\mathcal{T}}$, where λ is a scalar parameter. Then, we may rewrite

$$\begin{aligned}
\ln\left(\frac{\det(\boldsymbol{\mathcal{T}}+\boldsymbol{\mathcal{A}})}{\det\boldsymbol{\mathcal{A}}}\right) &= \ln\left(\frac{\det\boldsymbol{\Lambda}(\lambda=1)}{\det\boldsymbol{\Lambda}(\lambda=0)}\right) \\
&= \ln\left(\det\boldsymbol{\Lambda}(\lambda=1)\right) - \ln\left(\det\boldsymbol{\Lambda}(\lambda=0)\right) \\
&= \int d\mathbf{r}\int d\mathbf{r}'\int_{\boldsymbol{\Lambda}(\lambda=0)}^{\boldsymbol{\Lambda}(\lambda=1)} \frac{\delta\ln\det\boldsymbol{\Lambda}}{\delta\boldsymbol{\Lambda}^{-1}(\mathbf{r},\mathbf{r}';\lambda)} : \delta\boldsymbol{\Lambda}^{-1}(\mathbf{r},\mathbf{r}';\lambda)
\end{aligned} \tag{3.36}$$

where the last equality is due to the chain rule. Since $\det\boldsymbol{\Lambda}$ can be written as a

Gaussian integral as in Eq. (3.19), we have

$$\frac{\delta \ln \det \mathbf{\Lambda}}{\delta \mathbf{\Lambda}^{-1}(\mathbf{r},\mathbf{r}';\lambda)} = -\mathbf{\Lambda}(\mathbf{r},\mathbf{r}';\lambda) \tag{3.37}$$

and thus,

$$\ln\left(\frac{\det(\boldsymbol{\mathcal{T}}+\boldsymbol{\mathcal{A}})}{\det \boldsymbol{\mathcal{A}}}\right) = -\int d\mathbf{r}\int d\mathbf{r}'\int_{\mathbf{\Lambda}(\lambda=0)}^{\mathbf{\Lambda}(\lambda=1)} \mathbf{\Lambda}(\mathbf{r},\mathbf{r}';\lambda) : \delta\mathbf{\Lambda}^{-1}(\mathbf{r},\mathbf{r}';\lambda) \tag{3.38}$$

Using a procedure similar to that presented in Eq. (3.31), we may derive an expression for $\mathbf{\Lambda}^{-1}$ as

$$\begin{aligned}\mathbf{\Lambda}^{-1}(\mathbf{r},\mathbf{r}';\lambda) &= [\boldsymbol{\mathcal{A}}(\mathbf{r}-\mathbf{r}')+\lambda\boldsymbol{\mathcal{T}}(\mathbf{r}-\mathbf{r}')]^{-1} \\ &= \frac{1}{a}\left[\mathbb{1}\delta(\mathbf{r}-\mathbf{r}') - \frac{\varepsilon_0}{\beta}\left(\frac{\lambda\beta}{\lambda\beta+\varepsilon_0 a}\right)\boldsymbol{\mathcal{T}}(\mathbf{r}-\mathbf{r}')\right]\end{aligned} \tag{3.39}$$

With this, the differential of the inverse operator may be written as

$$\delta\mathbf{\Lambda}^{-1}(\mathbf{r},\mathbf{r}';\lambda) = \frac{d\mathbf{\Lambda}^{-1}(\mathbf{r},\mathbf{r}';\lambda)}{d\lambda}d\lambda = -\frac{\varepsilon_0^2}{(\lambda\beta+\varepsilon_0 a)^2}\boldsymbol{\mathcal{T}}(\mathbf{r}-\mathbf{r}')d\lambda$$

and therefore,

$$\begin{aligned}&\ln\left(\frac{\det(\boldsymbol{\mathcal{T}}+\boldsymbol{\mathcal{A}})}{\det \boldsymbol{\mathcal{A}}}\right) \\ =\;& \int d\mathbf{r}\int d\mathbf{r}'\int_{\lambda=0}^{1}[\boldsymbol{\mathcal{A}}(\mathbf{r}-\mathbf{r}')+\lambda\boldsymbol{\mathcal{T}}(\mathbf{r}-\mathbf{r}')] : \frac{\varepsilon_0^2}{(\lambda\beta+\varepsilon_0 a)^2}\boldsymbol{\mathcal{T}}(\mathbf{r}-\mathbf{r}')d\lambda \\ =\;& \frac{\varepsilon_0}{a(\beta+a\varepsilon_0)}\int d\mathbf{r}\int d\mathbf{r}'\boldsymbol{\mathcal{A}}(\mathbf{r}-\mathbf{r}') : \boldsymbol{\mathcal{T}}(\mathbf{r}-\mathbf{r}') \\ &-\frac{\varepsilon_0^2}{\beta^2}\left(\ln\left[\frac{a\epsilon_0}{\beta+a\epsilon_0}\right]+\frac{\beta}{\beta+a\epsilon_0}\right)\int d\mathbf{r}\int d\mathbf{r}'\boldsymbol{\mathcal{T}}(\mathbf{r}-\mathbf{r}') : \boldsymbol{\mathcal{T}}(\mathbf{r}-\mathbf{r}')\end{aligned} \tag{3.40}$$

With this result, and taking the δ-function limit for $\boldsymbol{\mathcal{A}}$ and $\boldsymbol{\mathcal{A}}^{-1}$, the variational grand

potential is simplified as

$$\begin{aligned}
\beta W &= -\frac{1}{2}\frac{\varepsilon_0^2}{\beta^2}\left(\ln\left[\frac{a\epsilon_0}{\beta+a\epsilon_0}\right]+\frac{\beta}{\beta+a\epsilon_0}\right)\int d\mathbf{r}\int d\mathbf{r}'\,\boldsymbol{\mathcal{T}}(\mathbf{r}-\mathbf{r}'):\boldsymbol{\mathcal{T}}(\mathbf{r}-\mathbf{r}') \\
&\quad -\frac{\varepsilon_0^2}{2(\beta+\varepsilon_0 a)^2}\int d\mathbf{r}\int d\mathbf{r}'\,(\boldsymbol{\mathcal{E}}_0(\mathbf{r})-\mathbf{F}(\mathbf{r}))\,\boldsymbol{\mathcal{T}}(\mathbf{r}-\mathbf{r}')\,(\boldsymbol{\mathcal{E}}_0(\mathbf{r}')-\mathbf{F}(\mathbf{r}')) \\
&\quad -\sum_{s=A,B}\frac{e^{\beta\mu_s}}{\Lambda_s}\int d\mathbf{r}\int d\boldsymbol{\mu}_s \\
&\quad \times\exp\left[-\frac{1}{2}\frac{\varepsilon_0 a}{\beta+\varepsilon_0 a}\int d\mathbf{r}_1\int d\mathbf{r}_2\,\boldsymbol{\mu}_s h_s(\mathbf{r}-\mathbf{r}_1)\boldsymbol{\mathcal{T}}(\mathbf{r}_1-\mathbf{r}_2)h_s(\mathbf{r}_2-\mathbf{r})\boldsymbol{\mu}_s\right. \\
&\qquad \left.+\boldsymbol{\mu}_s\cdot\boldsymbol{\mathcal{E}}_0(\mathbf{r})-\frac{\varepsilon_0}{\beta+\varepsilon_0 a}\int d\mathbf{r}_1\,[\boldsymbol{\mathcal{E}}_0(\mathbf{r}_1)-\mathbf{F}(\mathbf{r}_1)]\boldsymbol{\mathcal{T}}(\mathbf{r}_1-\mathbf{r})\boldsymbol{\mu}_s\right] \quad (3.41)
\end{aligned}$$

The double dot product of the dipole interaction tensor in the first term can be simplified by considering

$$\begin{aligned}
&\int d\mathbf{r}'\,\boldsymbol{\mathcal{T}}(\mathbf{r}-\mathbf{r}'):\boldsymbol{\mathcal{T}}(\mathbf{r}'-\mathbf{r}'') \\
&= \int d\mathbf{r}'\int\frac{d\mathbf{k}_1}{(2\pi)^3}\int\frac{d\mathbf{k}_2}{(2\pi)^3}\,\boldsymbol{\mathcal{T}}(\mathbf{k}_1):\boldsymbol{\mathcal{T}}(\mathbf{k}_2)e^{i(\mathbf{k}_2-\mathbf{k}_1)\cdot\mathbf{r}'}e^{i\mathbf{k}_1\cdot\mathbf{r}-i\mathbf{k}_2\cdot\mathbf{r}''} \\
&= \left(\frac{\beta}{\varepsilon_0}\right)^2\int\frac{d\mathbf{k}}{(2\pi)^3}\,\frac{\mathbf{k}\mathbf{k}}{k^2}:\frac{\mathbf{k}\mathbf{k}}{k^2}e^{i\mathbf{k}\cdot(\mathbf{r}-\mathbf{r}'')} \\
&= \left(\frac{\beta}{\varepsilon_0}\right)^2\frac{1}{(2\pi)^3}\int dk\int d\theta\int d\phi\,k^2\sin\theta 1 e^{ik|\mathbf{r}-\mathbf{r}''|\cos\theta} \\
&= \left(\frac{\beta}{\varepsilon_0}\right)^2\int\frac{d\mathbf{k}}{(2\pi)^3}\,e^{i\mathbf{k}\cdot(\mathbf{r}-\mathbf{r}'')} \quad (3.42)
\end{aligned}$$

Therefore,

$$\int d\mathbf{r}'\,\boldsymbol{\mathcal{T}}(\mathbf{r}-\mathbf{r}'):\boldsymbol{\mathcal{T}}(\mathbf{r}'-\mathbf{r})=\left(\frac{\beta}{\varepsilon_0}\right)^2\int\frac{d\mathbf{k}}{(2\pi)^3}\,1=\left(\frac{\beta}{\varepsilon_0}\right)^2 n_k \quad (3.43)$$

with n_k being the number of modes in the k-space per unit volume, defined as

$$n_k=\int\frac{d\mathbf{k}}{(2\pi)^3}\,1=\frac{1}{V}\sum_{\mathbf{k}}1 \quad (3.44)$$

where in the second equality, we have represented the integral over k-space as a

discrete sum over the k-space. The details of this can be found in Ref. 57.

With this, the variational grand potential can be simplified as

$$\begin{aligned}
\beta W &= -\frac{1}{2}\left(\ln\left[\frac{a\epsilon_0}{\beta+a\epsilon_0}\right]+\frac{\beta}{\beta+a\epsilon_0}\right)\int d\mathbf{r}\, n_k \\
&\quad -\frac{\varepsilon_0^2}{2(\beta+\varepsilon_0 a)^2}\int d\mathbf{r}\int d\mathbf{r}'\,(\boldsymbol{\mathcal{E}}_0(\mathbf{r})-\mathbf{F}(\mathbf{r}))\,\boldsymbol{\mathcal{T}}(\mathbf{r}-\mathbf{r}')\,(\boldsymbol{\mathcal{E}}_0(\mathbf{r}')-\mathbf{F}(\mathbf{r}')) \\
&\quad -\sum_{s=A,B}\frac{e^{\beta\mu_s}}{\Lambda_s}\int d\mathbf{r}\int d\boldsymbol{\mu}_s \\
&\quad \times\exp\left[-\frac{1}{2}\frac{\varepsilon_0 a}{\beta+\varepsilon_0 a}\int d\mathbf{r}_1\int d\mathbf{r}_2\,\boldsymbol{\mu}_s h_s(\mathbf{r}-\mathbf{r}_1)\boldsymbol{\mathcal{T}}(\mathbf{r}_1-\mathbf{r}_2)h_s(\mathbf{r}_2-\mathbf{r})\boldsymbol{\mu}_s\right. \\
&\qquad \left.+\boldsymbol{\mu}_s\cdot\boldsymbol{\mathcal{E}}_0(\mathbf{r})-\frac{\varepsilon_0}{\beta+\varepsilon_0 a}\int d\mathbf{r}_1\,[\boldsymbol{\mathcal{E}}_0(\mathbf{r}_1)-\mathbf{F}(\mathbf{r}_1)]\boldsymbol{\mathcal{T}}(\mathbf{r}_1-\mathbf{r})\boldsymbol{\mu}_s\right] \quad (3.45)
\end{aligned}$$

3.2.4 Particle Number and Concentration

The average number of particles $\langle N_s\rangle$ can be calculated from the variational grand potential as

$$\begin{aligned}
\langle N_s\rangle &= -\frac{\partial\beta W}{\partial\beta\mu_s} \\
&= \frac{e^{\beta\mu_s}}{\Lambda_s}\int d\mathbf{r}\int d\boldsymbol{\mu}_s \\
&\quad \times\exp\left[-\frac{1}{2}\frac{\varepsilon_0 a}{\beta+\varepsilon_0 a}\int d\mathbf{r}_1\int d\mathbf{r}_2\,\boldsymbol{\mu}_s h_s(\mathbf{r}-\mathbf{r}_1)\boldsymbol{\mathcal{T}}(\mathbf{r}_1-\mathbf{r}_2)h_s(\mathbf{r}_2-\mathbf{r})\boldsymbol{\mu}_s\right. \\
&\qquad \left.+\boldsymbol{\mu}_s\cdot\boldsymbol{\mathcal{E}}_0(\mathbf{r})-\frac{\varepsilon_0}{\beta+\varepsilon_0 a}\int d\mathbf{r}_1\,[\boldsymbol{\mathcal{E}}_0(\mathbf{r}_1)-\mathbf{F}(\mathbf{r}_1)]\boldsymbol{\mathcal{T}}(\mathbf{r}_1-\mathbf{r})\boldsymbol{\mu}_s\right] \quad (3.46)
\end{aligned}$$

The number concentration of particles $\langle c_s(\mathbf{r})\rangle$ can be obtained through the relation $\langle N_s\rangle = \int d\mathbf{r}\,\langle c_s(\mathbf{r})\rangle$, which gives

$$\langle c_s(\mathbf{r})\rangle = \frac{e^{\beta\mu_s}}{\Lambda_s}\int d\boldsymbol{\mu}_s\, e^{-f_s(\boldsymbol{\mu}_s;\mathbf{r})} \quad (3.47)$$

where $f_s(\boldsymbol{\mu}_s;\mathbf{r})$ is given by

$$\begin{aligned} f_s(\boldsymbol{\mu}_s;\mathbf{r}) &= \frac{1}{2}\frac{\varepsilon_0 a}{\beta+\varepsilon_0 a}\int d\mathbf{r}_1\int d\mathbf{r}_2\,\boldsymbol{\mu}_s h_s(\mathbf{r}-\mathbf{r}_1)\boldsymbol{\mathcal{T}}(\mathbf{r}_1-\mathbf{r}_2)h_s(\mathbf{r}_2-\mathbf{r})\boldsymbol{\mu}_s \\ &\quad -\boldsymbol{\mu}_s\cdot\boldsymbol{\mathcal{E}}_0(\mathbf{r})+\frac{\varepsilon_0}{\beta+\varepsilon_0 a}\int d\mathbf{r}_1\,[\boldsymbol{\mathcal{E}}_0(\mathbf{r}_1)-\mathbf{F}(\mathbf{r}_1)]\boldsymbol{\mathcal{T}}(\mathbf{r}_1-\mathbf{r})\boldsymbol{\mu}_s \quad (3.48) \end{aligned}$$

3.2.5 Minimizing the Variational Grand Potential with Respect to the Variational Parameters

We then minimize the variational grand potential with respect to a and $\mathbf{F}$ to obtain its lower bound. Differentiating βW with respect to a gives

$$\begin{aligned} \frac{d\beta W}{da} &= -\frac{1}{2a}\left(\frac{\beta}{\beta+\varepsilon_0 a}\right)^2\int d\mathbf{r}\,n_k \\ &\quad +\left(\frac{\varepsilon_0}{\beta+\varepsilon_0 a}\right)^3\int d\mathbf{r}\int d\mathbf{r}'\,(\boldsymbol{\mathcal{E}}_0(\mathbf{r})-\mathbf{F}(\mathbf{r}))\,\boldsymbol{\mathcal{T}}(\mathbf{r}-\mathbf{r}')\,(\boldsymbol{\mathcal{E}}_0(\mathbf{r}')-\mathbf{F}(\mathbf{r}')) \\ &\quad -\sum_{s=A,B}\int d\mathbf{r}\langle c_s(\mathbf{r})\rangle\left[\left(\frac{\varepsilon_0}{\beta+\varepsilon_0 a}\right)^2\int d\mathbf{r}_1\,[\boldsymbol{\mathcal{E}}_0(\mathbf{r}_1)-\mathbf{F}(\mathbf{r}_1)]\boldsymbol{\mathcal{T}}(\mathbf{r}_1-\mathbf{r})\,\langle\boldsymbol{\mu}_s\rangle_{f_s(\mathbf{r})}\right. \\ &\quad \left.-\frac{1}{2}\frac{\beta\varepsilon_0}{(\beta+\varepsilon_0 a)^2}\int d\mathbf{r}_1\int d\mathbf{r}_2\,\langle\boldsymbol{\mu}_s h_s(\mathbf{r}-\mathbf{r}_1)\boldsymbol{\mathcal{T}}(\mathbf{r}_1-\mathbf{r}_2)h_s(\mathbf{r}_2-\mathbf{r})\boldsymbol{\mu}_s\rangle_{f_s(\mathbf{r})}\right] \quad (3.49) \end{aligned}$$

and differentiating βW with respect to $\mathbf{F}(\mathbf{r})$ gives

$$\begin{aligned} \frac{\delta\beta W}{\delta\mathbf{F}(\mathbf{r})} &= \left(\frac{\varepsilon_0}{\beta+\varepsilon_0 a}\right)^2\int d\mathbf{r}'\boldsymbol{\mathcal{T}}(\mathbf{r}-\mathbf{r}')\,(\boldsymbol{\mathcal{E}}_0(\mathbf{r}')-\mathbf{F}(\mathbf{r}')) \\ &\quad -\sum_{s=A,B}\int d\mathbf{r}'\,\langle c_s(\mathbf{r}')\rangle\left[\frac{\varepsilon_0}{\beta+\varepsilon_0 a}\boldsymbol{\mathcal{T}}(\mathbf{r}-\mathbf{r}')\,\langle\boldsymbol{\mu}_s\rangle_{f_s(\mathbf{r}')}\right] \quad (3.50) \end{aligned}$$

where the expectation value $\langle\mathcal{O}\rangle_{f_s(\mathbf{r})}$ is defined as

$$\langle\mathcal{O}(\boldsymbol{\mu}_s)\rangle_{f_s(\mathbf{r})}=\frac{\int d\boldsymbol{\mu}_s\,\mathcal{O}e^{-f_s(\boldsymbol{\mu}_s;\mathbf{r})}}{\int d\boldsymbol{\mu}_s\,e^{-f_s(\boldsymbol{\mu}_s;\mathbf{r})}} \quad (3.51)$$

Setting $d\beta W/da=0$ and $d\beta W/d\mathbf{F}(\mathbf{r})=0$, we have the following constitutive

relations:

$$\begin{aligned}
&\frac{1}{2a}\left(\frac{\beta}{\beta+\varepsilon_0 a}\right)^2\int d\mathbf{r}\, n_k \\
&+\left(\frac{\varepsilon_0}{\beta+\varepsilon_0 a}\right)^3\int d\mathbf{r}\int d\mathbf{r}'\,(\boldsymbol{\mathcal{E}}_0(\mathbf{r})-\mathbf{F}(\mathbf{r}))\,\boldsymbol{\mathcal{T}}(\mathbf{r}-\mathbf{r}')\,(\boldsymbol{\mathcal{E}}_0(\mathbf{r}')-\mathbf{F}(\mathbf{r}')) \\
&=\sum_{s=A,B}\int d\mathbf{r}\langle c_s(\mathbf{r})\rangle\left[-\left(\frac{\varepsilon_0}{\beta+\varepsilon_0 a}\right)^2\int d\mathbf{r}_1\,[\boldsymbol{\mathcal{E}}_0(\mathbf{r}_1)-\mathbf{F}(\mathbf{r}_1)]\boldsymbol{\mathcal{T}}(\mathbf{r}_1-\mathbf{r})\,\langle\boldsymbol{\mu}_s\rangle_{f_s(\mathbf{r})}\right. \\
&\left.+\frac{1}{2}\frac{\beta\varepsilon_0}{(\beta+\varepsilon_0 a)^2}\int d\mathbf{r}_1\int d\mathbf{r}_2\;\langle\boldsymbol{\mu}_s h_s(\mathbf{r}-\mathbf{r}_1)\boldsymbol{\mathcal{T}}(\mathbf{r}_1-\mathbf{r}_2)h_s(\mathbf{r}_2-\mathbf{r})\boldsymbol{\mu}_s\rangle_{f_s(\mathbf{r})}\right] \qquad (3.52a)
\end{aligned}$$

and

$$\begin{aligned}
&\left(\frac{\varepsilon_0}{\beta+\varepsilon_0 a}\right)\int d\mathbf{r}'\boldsymbol{\mathcal{T}}(\mathbf{r}-\mathbf{r}')\,(\boldsymbol{\mathcal{E}}_0(\mathbf{r}')-\mathbf{F}(\mathbf{r}')) \\
&\qquad=\sum_{s=A,B}\int d\mathbf{r}'\,\langle c_s(\mathbf{r}')\rangle\left[\boldsymbol{\mathcal{T}}(\mathbf{r}-\mathbf{r}')\,\langle\boldsymbol{\mu}_s\rangle_{f_s(\mathbf{r}')}\right] \qquad (3.52b)
\end{aligned}$$

Substitution of Eq. (3.52b) into Eq. (3.52a) simplifies the constitutive relations to

$$\begin{aligned}
&\frac{\beta}{\varepsilon_0 a}\int d\mathbf{r}\, n_k \\
&=\sum_{s=A,B}\int d\mathbf{r}\langle c_s(\mathbf{r})\rangle\left[\int d\mathbf{r}_1\int d\mathbf{r}_2\;\langle\boldsymbol{\mu}_s h_s(\mathbf{r}-\mathbf{r}_1)\boldsymbol{\mathcal{T}}(\mathbf{r}_1-\mathbf{r}_2)h_s(\mathbf{r}_2-\mathbf{r})\boldsymbol{\mu}_s\rangle_{f_s(\mathbf{r})}\right] \qquad (3.53a)
\end{aligned}$$

and

$$\begin{aligned}
&\left(\frac{\varepsilon_0}{\beta+\varepsilon_0 a}\right)\int d\mathbf{r}'\boldsymbol{\mathcal{T}}(\mathbf{r}-\mathbf{r}')\,(\boldsymbol{\mathcal{E}}_0(\mathbf{r}')-\mathbf{F}(\mathbf{r}')) \\
&\qquad=\sum_{s=A,B}\int d\mathbf{r}'\,\langle c_s(\mathbf{r}')\rangle\left[\boldsymbol{\mathcal{T}}(\mathbf{r}-\mathbf{r}')\,\langle\boldsymbol{\mu}_s\rangle_{f_s(\mathbf{r}')}\right] \qquad (3.53b)
\end{aligned}$$

In Eq. (3.53a), taking $h_s(\mathbf{r})\to\delta(\mathbf{r})$ does not result in a singularity, and therefore

we take the δ-function limit for h_s as

$$\begin{aligned}
\frac{\beta}{\varepsilon_0 a}\int d\mathbf{r}\, n_k &= \sum_{s=A,B}\int d\mathbf{r}\langle c_s(\mathbf{r})\rangle \\
&\quad\times\left[\int d\mathbf{r}_1\int d\mathbf{r}_2\ \langle \boldsymbol{\mu}_s\delta(\mathbf{r}-\mathbf{r}_1)\boldsymbol{\mathcal{T}}(\mathbf{r}_1-\mathbf{r}_2)\delta(\mathbf{r}_2-\mathbf{r})\boldsymbol{\mu}_s\rangle_{f_s(\mathbf{r})}\right] \\
\frac{\beta}{\varepsilon_0 a}\int d\mathbf{r}\, n_k &= \sum_{s=A,B}\int d\mathbf{r}\langle c_s(\mathbf{r})\rangle\left[\langle \boldsymbol{\mu}_s\boldsymbol{\mathcal{T}}(\mathbf{r}-\mathbf{r})\boldsymbol{\mu}_s\rangle_{f_s(\mathbf{r})}\right] \\
\frac{\beta}{\varepsilon_0 a}\int d\mathbf{r}\, n_k &= \sum_{s=A,B}\int d\mathbf{r}\langle c_s(\mathbf{r})\rangle\frac{\beta}{3\varepsilon_0}n_k\bar{\mu}_s^2 \\
\frac{1}{a} &= \sum_{s=A,B}\langle c_s(\mathbf{r})\rangle\frac{\bar{\mu}_s^2}{3}
\end{aligned} \tag{3.54}$$

where, in the third equality, we have used the following result:

$$\begin{aligned}
\boldsymbol{\mu}_s\boldsymbol{\mathcal{T}}(\mathbf{r}-\mathbf{r})\boldsymbol{\mu}_s &= \boldsymbol{\mu}_s\left(\int\frac{d\mathbf{k}}{(2\pi)^3}\frac{\beta\mathbf{k}\mathbf{k}}{\varepsilon_0 k^2}e^{i\mathbf{k}\cdot\mathbf{0}}\right)\boldsymbol{\mu}_s = \int\frac{d\mathbf{k}}{(2\pi)^3}\,\boldsymbol{\mu}_s\frac{\beta\mathbf{k}\mathbf{k}}{\varepsilon_0 k^2}\boldsymbol{\mu}_s \\
&= \frac{\beta}{\varepsilon_0}\int\frac{d\mathbf{k}}{(2\pi)^3}\left(\boldsymbol{\mu}_s\cdot\frac{\mathbf{k}}{k}\right)^2 = \frac{\beta}{\varepsilon_0}\bar{\mu}_s^2\int\frac{d\mathbf{k}}{(2\pi)^3}(\cos\theta_k)^2 \\
&= \frac{\beta}{3\varepsilon_0}\bar{\mu}_s^2\int\frac{d\mathbf{k}}{(2\pi)^3}1 \\
&= \frac{\beta}{3\varepsilon_0}\bar{\mu}_s^2 n_k
\end{aligned} \tag{3.55}$$

To solve the second constitutive relation, we need to find an expression for $\langle\boldsymbol{\mu}_s\rangle_{f_s(\mathbf{r})}$, which can be evaluated as

$$\begin{aligned}
\langle\boldsymbol{\mu}_s\rangle_{f_s(\mathbf{r})} &= \frac{\int d\boldsymbol{\mu}_s\,\boldsymbol{\mu}_s e^{-f_s(\boldsymbol{\mu};\mathbf{r})}}{\int d\boldsymbol{\mu}_s\, e^{-f_s(\boldsymbol{\mu};\mathbf{r})}} \\
&= \frac{\int d\boldsymbol{\mu}_s\,\boldsymbol{\mu}_s e^{-\frac{1}{2}\frac{\varepsilon_0 a}{\beta+\varepsilon_0 a}\int d\mathbf{r}_1\int d\mathbf{r}_2\,\boldsymbol{\mu}_s h_s(\mathbf{r}-\mathbf{r}_1)\boldsymbol{\mathcal{T}}(\mathbf{r}_1-\mathbf{r}_2)h_s(\mathbf{r}_2-\mathbf{r})\boldsymbol{\mu}_s+\boldsymbol{\mu}_s\cdot\boldsymbol{\mathcal{E}}_I(\mathbf{r})}}{\int d\boldsymbol{\mu}_s\, e^{-\frac{1}{2}\frac{\varepsilon_0 a}{\beta+\varepsilon_0 a}\int d\mathbf{r}_1\int d\mathbf{r}_2\,\boldsymbol{\mu}_s h_s(\mathbf{r}-\mathbf{r}_1)\boldsymbol{\mathcal{T}}(\mathbf{r}_1-\mathbf{r}_2)h_s(\mathbf{r}_2-\mathbf{r})\boldsymbol{\mu}_s+\boldsymbol{\mu}_s\cdot\boldsymbol{\mathcal{E}}_I(\mathbf{r})}} \\
&= \frac{\int d\boldsymbol{\mu}_s\,\boldsymbol{\mu}_s e^{\boldsymbol{\mu}_s\cdot\boldsymbol{\mathcal{E}}_I(\mathbf{r})}}{\int d\boldsymbol{\mu}_s\, e^{\boldsymbol{\mu}_s\cdot\boldsymbol{\mathcal{E}}_I(\mathbf{r})}} \\
&= \left(\coth(\bar{\mu}_s|\boldsymbol{\mathcal{E}}_I(\mathbf{r})|)-\frac{1}{\bar{\mu}_s|\boldsymbol{\mathcal{E}}_I(\mathbf{r})|}\right)\frac{\bar{\mu}_s\boldsymbol{\mathcal{E}}_I(\mathbf{r})}{|\boldsymbol{\mathcal{E}}_I(\mathbf{r})|}
\end{aligned} \tag{3.56}$$

where the quadratic term in f_s can be ignored as it is a constant that does not depend

on the direction of $\boldsymbol{\mu}_s$, and

$$\boldsymbol{\mathcal{E}}_I(\mathbf{r}) = \boldsymbol{\mathcal{E}}_0(\mathbf{r}) - \frac{\varepsilon_0}{\beta + \varepsilon_0 a} \int d\mathbf{r}' \, \boldsymbol{\mathcal{T}}(\mathbf{r} - \mathbf{r}')[\boldsymbol{\mathcal{E}}_0(\mathbf{r}') - \mathbf{F}(\mathbf{r}')] \tag{3.57}$$

Therefore, Eq. (3.53b) can be simplified as

$$\begin{aligned} & \left(\frac{\varepsilon_0}{\beta + \varepsilon_0 a} \right) (\boldsymbol{\mathcal{E}}_0(\mathbf{r}) - \mathbf{F}(\mathbf{r})) \\ = & \sum_{s=A,B} \langle c_s(\mathbf{r}) \rangle \left[\left(\coth(\bar{\mu}_s |\boldsymbol{\mathcal{E}}_I(\mathbf{r})|) - \frac{1}{\bar{\mu}_s |\boldsymbol{\mathcal{E}}_I(\mathbf{r})|} \right) \frac{\bar{\mu}_s \boldsymbol{\mathcal{E}}_I(\mathbf{r})}{|\boldsymbol{\mathcal{E}}_I(\mathbf{r})|} \right] \end{aligned} \tag{3.58}$$

In summary, in this subsection we have derived the constitutive relations to be

$$\frac{1}{a} = \sum_{s=A,B} \langle c_s(\mathbf{r}) \rangle \frac{\bar{\mu}_s^2}{3} \tag{3.59a}$$

$$\left(\frac{\varepsilon_0}{\beta + \varepsilon_0 a} \right) (\boldsymbol{\mathcal{E}}_0(\mathbf{r}) - \mathbf{F}(\mathbf{r})) = \sum_{s=A,B} \langle c_s(\mathbf{r}) \rangle \left[\left(\coth(\bar{\mu}_s |\boldsymbol{\mathcal{E}}_I(\mathbf{r})|) - \frac{1}{\bar{\mu}_s |\boldsymbol{\mathcal{E}}_I(\mathbf{r})|} \right) \frac{\bar{\mu}_s \boldsymbol{\mathcal{E}}_I(\mathbf{r})}{|\boldsymbol{\mathcal{E}}_I(\mathbf{r})|} \right] \tag{3.59b}$$

3.2.6 Dielectric Constant for a Homogeneous System

To find the dielectric constant of the mixture, we first derive a relation between the polarization of the system and the externally applied field:

$$\begin{aligned} \mathbf{P}(\mathbf{r}) &= -\frac{\delta \beta W}{\delta \boldsymbol{\mathcal{E}}_0(\mathbf{r})} \\ &= \frac{\varepsilon_0^2}{(\beta + \varepsilon_0 a)^2} \int d\mathbf{r}' \int d\mathbf{r}'' \, \boldsymbol{\mathcal{T}}(\mathbf{r} - \mathbf{r}') \left[\mathbb{1} \delta(\mathbf{r}' - \mathbf{r}'') - \frac{\delta \mathbf{F}(\mathbf{r}')}{\delta \boldsymbol{\mathcal{E}}_0(\mathbf{r}'')} \right] (\boldsymbol{\mathcal{E}}_0(\mathbf{r}'') - \mathbf{F}(\mathbf{r}'')) \\ &\quad + \sum_{s=A,B} \int d\mathbf{r}' \int d\mathbf{r}'' \, \langle c_s(\mathbf{r}'') \rangle \\ &\quad \times \left[\mathbb{1} \delta(\mathbf{r} - \mathbf{r}') \delta(\mathbf{r}' - \mathbf{r}'') - \frac{\varepsilon_0}{\beta + \varepsilon_0 a} \boldsymbol{\mathcal{T}}(\mathbf{r} - \mathbf{r}') \left(\mathbb{1} \delta(\mathbf{r}' - \mathbf{r}'') - \frac{\delta \mathbf{F}(\mathbf{r}')}{\delta \boldsymbol{\mathcal{E}}_0(\mathbf{r}'')} \right) \right] \\ &\quad \times \left(\coth(\bar{\mu}_s |\boldsymbol{\mathcal{E}}_I(\mathbf{r}'')|) - \frac{1}{\bar{\mu}_s |\boldsymbol{\mathcal{E}}_I(\mathbf{r}'')|} \right) \frac{\bar{\mu}_s^2 \boldsymbol{\mathcal{E}}_I(\mathbf{r}'')}{\bar{\mu}_s |\boldsymbol{\mathcal{E}}_I(\mathbf{r}'')|} \end{aligned} \tag{3.60}$$

To linear order, we let the solution to the constitutive equation give $\mathbf{F} = -\gamma\boldsymbol{\mathcal{E}}_0$. Then, linearizing Eq. (3.60) gives

$$\begin{aligned}\langle\mathbf{P}(\mathbf{k})\rangle &= \frac{\varepsilon_0^2(1+\gamma)^2}{(\beta+\varepsilon_0 a)^2}\boldsymbol{\mathcal{T}}(\mathbf{k})\boldsymbol{\mathcal{E}}_0(\mathbf{k}) \\ &\quad + \frac{1}{a}\left[\mathbb{1} - \frac{\varepsilon_0(1+\gamma)}{\beta+\varepsilon_0 a}\boldsymbol{\mathcal{T}}(\mathbf{k})\right]\left[\mathbb{1} - \frac{\varepsilon_0(1+\gamma)}{\beta+\varepsilon_0 a}\boldsymbol{\mathcal{T}}(\mathbf{k})\right]\boldsymbol{\mathcal{E}}_0(\mathbf{k}) \qquad (3.61)\end{aligned}$$

which gives an expression for the electric susceptibility of the system

$$\begin{aligned}\chi_0(\mathbf{k}) &= \frac{\beta}{\varepsilon_0}\frac{\varepsilon_0^2(1+\gamma)^2}{(\beta+\varepsilon_0 a)^2}\boldsymbol{\mathcal{T}}(\mathbf{k}) \\ &\quad + \frac{\beta}{\varepsilon_0 a}\left[\mathbb{1} - \frac{\varepsilon_0(1+\gamma)}{\beta+\varepsilon_0 a}\boldsymbol{\mathcal{T}}(\mathbf{k})\right]\left[\mathbb{1} - \frac{\varepsilon_0(1+\gamma)}{\beta+\varepsilon_0 a}\boldsymbol{\mathcal{T}}(\mathbf{k})\right] \qquad (3.62)\end{aligned}$$

Using the relation $\mathrm{tr}\chi_0(\mathbf{k}) = \frac{(\varepsilon-1)(2\varepsilon+1)}{\varepsilon}$, we have

$$\frac{(\varepsilon-1)(2\varepsilon+1)}{\varepsilon} = \frac{\beta}{\varepsilon_0 a}\frac{(2+\gamma^2)\beta + 3\varepsilon_0 a}{\beta+\varepsilon_0 a} \qquad (3.63)$$

In the limit of small electric field, we can solve Eq. (3.59b) to linear order in $\boldsymbol{\mathcal{E}}_0$ as

$$\begin{aligned}\left(\frac{\varepsilon_0}{\beta+\varepsilon_0 a}\right)(\boldsymbol{\mathcal{E}}_0(\mathbf{r}) - \mathbf{F}(\mathbf{r})) &= \sum_{s=A,B}\langle c_s(\mathbf{r})\rangle\frac{1}{3}\bar{\mu}_s|\boldsymbol{\mathcal{E}}_I(\mathbf{r})|\frac{\bar{\mu}_s\boldsymbol{\mathcal{E}}_I(\mathbf{r})}{|\boldsymbol{\mathcal{E}}_I(\mathbf{r})|} \\ \left(\frac{\varepsilon_0}{\beta+\varepsilon_0 a}\right)(\boldsymbol{\mathcal{E}}_0(\mathbf{r}) - \mathbf{F}(\mathbf{r})) &= \sum_{s=A,B}\langle c_s(\mathbf{r})\rangle\frac{1}{3}\bar{\mu}_s^2\boldsymbol{\mathcal{E}}_I(\mathbf{r}) \\ \left(\frac{\varepsilon_0}{\beta+\varepsilon_0 a}\right)(\boldsymbol{\mathcal{E}}_0(\mathbf{r}) - \mathbf{F}(\mathbf{r})) &= \frac{1}{a}\boldsymbol{\mathcal{E}}_I(\mathbf{r}) \qquad (3.64)\end{aligned}$$

For a homogeneous system, the field $\boldsymbol{\mathcal{E}}_I$ in Eq. (3.57) can be evaluated as

$$\begin{aligned}\boldsymbol{\mathcal{E}}_I &= \boldsymbol{\mathcal{E}}_0 - \frac{\varepsilon_0}{\beta+\varepsilon_0 a}\frac{\beta}{3\varepsilon_0}[\boldsymbol{\mathcal{E}}_0 - \mathbf{F}] \\ &= \boldsymbol{\mathcal{E}}_0 - \frac{\beta}{3(\beta+\varepsilon_0 a)}[\boldsymbol{\mathcal{E}}_0 - \mathbf{F}] \qquad (3.65)\end{aligned}$$

Then, in a homogenous system under a very small applied field, we obtain the fol-

lowing relationship between $\mathbf{F}$ and $\boldsymbol{\mathcal{E}}_0$ by solving Eq. (3.64):

$$\begin{aligned} \mathbf{F} &= -\frac{2\beta}{\beta + 3\varepsilon_0 a}\boldsymbol{\mathcal{E}}_0 \\ \gamma &= \frac{2\beta}{\beta + 3\varepsilon_0 a} \end{aligned} \tag{3.66}$$

Therefore, for homogeneous mixture at the limit of small applied field, we have

$$\frac{(\varepsilon - 1)(2\varepsilon + 1)}{\varepsilon} = \frac{3\beta}{\varepsilon_0 a}\left(\frac{2\beta^2 + 3\beta\varepsilon_0 a + 9\varepsilon_0^2 a^2}{(\beta + 3\varepsilon_0 a)^2}\right) \tag{3.67}$$

3.2.7 Legendre Transform of the Variational Grand Potential to the Helmholtz Free Energy

We are hoping to calculate the solubility of two polar liquids in a mixture, and to do so requires the Helmholtz free energy in the canonical ensemble. Before we do the Legendre transform, we need an expression for n_k in the variational grand potential in Eq. (3.45). To regularize the singularity, we make use of the derived constitutive relation in Eq. (3.53a), and write

$$\begin{aligned} &\int d\mathbf{r}\, n_k = \frac{\varepsilon_0 a}{\beta}\sum_{s=A,B}\int d\mathbf{r}\langle c_s(\mathbf{r})\rangle \\ &\times\left[\int d\mathbf{r}_1 \int d\mathbf{r}_2\ \langle \boldsymbol{\mu}_s h_s(\mathbf{r}-\mathbf{r}_1)\boldsymbol{\mathcal{T}}(\mathbf{r}_1-\mathbf{r}_2)h_s(\mathbf{r}_2-\mathbf{r})\boldsymbol{\mu}_s\rangle_{f_s(\mathbf{r})}\right] \end{aligned} \tag{3.68}$$

With this expression, we rewrite the variational grand potential as

$$\begin{aligned}\beta W &= -\frac{1}{2}\left(\ln\left[\frac{a\epsilon_0}{\beta+a\epsilon_0}\right]+\frac{\beta}{\beta+a\epsilon_0}\right)\frac{\varepsilon_0 a}{\beta} \\ &\quad\times\sum_{s=A,B}\int d\mathbf{r}\langle c_s(\mathbf{r})\rangle\left[\int d\mathbf{r}_1\int d\mathbf{r}_2\ \langle\boldsymbol{\mu}_s h_s(\mathbf{r}-\mathbf{r}_1)\boldsymbol{\mathcal{T}}(\mathbf{r}_1-\mathbf{r}_2)h_s(\mathbf{r}_2-\mathbf{r})\boldsymbol{\mu}_s\rangle_{f_s(\mathbf{r})}\right] \\ &\quad-\frac{\varepsilon_0^2}{2(\beta+\varepsilon_0 a)^2}\int d\mathbf{r}\int d\mathbf{r}'\left(\boldsymbol{\mathcal{E}}_0(\mathbf{r})-\mathbf{F}(\mathbf{r})\right)\boldsymbol{\mathcal{T}}(\mathbf{r}-\mathbf{r}')\left(\boldsymbol{\mathcal{E}}_0(\mathbf{r}')-\mathbf{F}(\mathbf{r}')\right) \\ &\quad-\sum_{s=A,B}\frac{e^{\beta\mu_s}}{\Lambda_s}\int d\mathbf{r}\int d\boldsymbol{\mu}_s\,\exp\left[-\frac{\varepsilon_0}{\beta+\varepsilon_0 a}\int d\mathbf{r}_1\left[\boldsymbol{\mathcal{E}}_0(\mathbf{r}_1)-\mathbf{F}(\mathbf{r}_1)\right]\boldsymbol{\mathcal{T}}(\mathbf{r}_1-\mathbf{r})\boldsymbol{\mu}_s\right. \\ &\quad\left.+\boldsymbol{\mu}_s\cdot\boldsymbol{\mathcal{E}}_0(\mathbf{r})-\frac{1}{2}\frac{\varepsilon_0 a}{\beta+\varepsilon_0 a}\int d\mathbf{r}_1\int d\mathbf{r}_2\,\boldsymbol{\mu}_s h_s(\mathbf{r}-\mathbf{r}_1)\boldsymbol{\mathcal{T}}(\mathbf{r}_1-\mathbf{r}_2)h_s(\mathbf{r}_2-\mathbf{r})\boldsymbol{\mu}_s\right]\end{aligned} \tag{3.69}$$

To simplify the grand potential, we introduce the following function for $h_s(\mathbf{r})$ that describes a uniform distribution of the polarization within the spherical volume v_s of the molecule:

$$h_s(\mathbf{r})=\begin{cases}\frac{1}{v_s} & |\mathbf{r}|<\left(\frac{3v_s}{4\pi}\right)^{\frac{1}{3}} \\ 0 & \text{otherwise}\end{cases} \tag{3.70}$$

With this functional form for h_s, we can evaluate the following product as

$$\int d\mathbf{r}_1\int d\mathbf{r}_2\,\boldsymbol{\mu}_s h_s(\mathbf{r}-\mathbf{r}_1)\boldsymbol{\mathcal{T}}(\mathbf{r}_1-\mathbf{r}_2)h_s(\mathbf{r}_2-\mathbf{r})\boldsymbol{\mu}_s=\frac{\beta}{3\varepsilon_0 v_s}\bar{\mu}_s^2 \tag{3.71}$$

The derivation for Eq. (3.71) will be deferred to the Appendix 3.A. The variational grand potential can then be simplified as

$$\begin{aligned}\beta W &= -\frac{1}{2}\left(\ln\left[\frac{a\epsilon_0}{\beta+a\epsilon_0}\right]+\frac{\beta}{\beta+a\epsilon_0}\right)\frac{\varepsilon_0 a}{\beta}\sum_{s=A,B}\int d\mathbf{r}\langle c_s(\mathbf{r})\rangle\frac{\beta}{3\varepsilon_0 v_s}\bar{\mu}_s^2 \\ &\quad-\frac{\varepsilon_0^2}{2(\beta+\varepsilon_0 a)^2}\int d\mathbf{r}\int d\mathbf{r}'\left(\boldsymbol{\mathcal{E}}_0(\mathbf{r})-\mathbf{F}(\mathbf{r})\right)\boldsymbol{\mathcal{T}}(\mathbf{r}-\mathbf{r}')\left(\boldsymbol{\mathcal{E}}_0(\mathbf{r}')-\mathbf{F}(\mathbf{r}')\right) \\ &\quad-\sum_{s=A,B}\frac{e^{\beta\mu_s}}{\Lambda_s}\int d\mathbf{r}\int d\boldsymbol{\mu}_s\,\exp\left[-\frac{1}{2}\frac{\varepsilon_0 a}{\beta+\varepsilon_0 a}\frac{\beta}{3\varepsilon_0 v_s}\bar{\mu}_s^2+\boldsymbol{\mu}_s\cdot\boldsymbol{\mathcal{E}}_I(\mathbf{r})\right]\end{aligned} \tag{3.72}$$

Now we shall perform the Legendre transform on the grand potential. Based on

Eq. (3.46), we can express the chemical potential μ_s as

$$\begin{aligned} e^{-\beta\mu_s} &= \frac{1}{\Lambda_s \int d\mathbf{r}\,\langle c_s(\mathbf{r})\rangle} \int d\mathbf{r} \int d\boldsymbol{\mu}_s \exp\left[-\frac{1}{2}\frac{\varepsilon_0 a}{\beta+\varepsilon_0 a}\frac{\beta}{3\varepsilon_0 v_s}\bar{\mu}_s^2 \right. \\ &\qquad \left. +\boldsymbol{\mu}_s\cdot\boldsymbol{\mathcal{E}}_0(\mathbf{r}) - \frac{\varepsilon_0}{\beta+\varepsilon_0 a}\int d\mathbf{r}_1\,[\boldsymbol{\mathcal{E}}_0(\mathbf{r}_1)-\mathbf{F}(\mathbf{r}_1)]\boldsymbol{\mathcal{T}}(\mathbf{r}_1-\mathbf{r})\boldsymbol{\mu}_s\right] \\ \beta\mu_s &= \ln\Lambda_s + \ln\int d\mathbf{r}\,\langle c_s(\mathbf{r})\rangle \\ &\qquad -\ln\int d\mathbf{r}\int d\boldsymbol{\mu}_s \exp\left[-\frac{1}{2}\frac{\varepsilon_0 a}{\beta+\varepsilon_0 a}\frac{\beta}{3\varepsilon_0 v_s}\bar{\mu}_s^2 + \boldsymbol{\mu}_s\cdot\boldsymbol{\mathcal{E}}_I(\mathbf{r})\right] \end{aligned} \tag{3.73}$$

Thus, the Helmholtz free energy is given by

$$\begin{aligned} \beta F &= \beta W + \sum_{s=A,B}\beta\mu_s\langle N_s\rangle \\ &= -\frac{1}{2}\left(\ln\left[\frac{a\epsilon_0}{\beta+a\epsilon_0}\right]+\frac{\beta}{\beta+a\epsilon_0}\right)\frac{\varepsilon_0 a}{\beta}\sum_{s=A,B}\int d\mathbf{r}\langle c_s(\mathbf{r})\rangle\frac{\beta}{3\varepsilon_0 v_s}\bar{\mu}_s^2 \\ &\quad -\frac{\varepsilon_0^2}{2(\beta+\varepsilon_0 a)^2}\int d\mathbf{r}\int d\mathbf{r}'\,(\boldsymbol{\mathcal{E}}_0(\mathbf{r})-\mathbf{F}(\mathbf{r}))\,\boldsymbol{\mathcal{T}}(\mathbf{r}-\mathbf{r}')\,(\boldsymbol{\mathcal{E}}_0(\mathbf{r}')-\mathbf{F}(\mathbf{r}')) \\ &\quad +\sum_{s=A,B}\left(\int d\mathbf{r}\,\langle c_s(\mathbf{r})\rangle\right)\ln\left(\int d\mathbf{r}\,\langle c_s(\mathbf{r})\rangle\right) \\ &\quad +\sum_{s=A,B}\left(\int d\mathbf{r}\,\langle c_s(\mathbf{r})\rangle\right) \\ &\quad \times\left[\ln\Lambda_s - 1 - \ln\int d\mathbf{r}\,\exp\left(-\frac{1}{6}\frac{\beta a}{v_s(\beta+\varepsilon_0 a)}\bar{\mu}_s^2\right)\frac{4\pi\sinh(\bar{\mu}_s|\boldsymbol{\mathcal{E}}_I(\mathbf{r})|)}{\bar{\mu}_s|\boldsymbol{\mathcal{E}}_I(\mathbf{r})|}\right] \end{aligned} \tag{3.74}$$

In the limit $\boldsymbol{\mathcal{E}}_0 \to 0$, the Helmholtz free energy becomes

$$\begin{aligned} \beta F_{\lim\boldsymbol{\mathcal{E}}_0\to 0} &= -\frac{1}{2}\frac{\varepsilon_0 a}{\beta}\left(\ln\left[\frac{a\epsilon_0}{\beta+a\epsilon_0}\right]\right)\sum_{s=A,B}\int d\mathbf{r}\langle c_s(\mathbf{r})\rangle\frac{\beta}{3\varepsilon_0 v_s}\bar{\mu}_s^2 \\ &\quad +\sum_{s=A,B}\left(\int d\mathbf{r}\,\langle c_s(\mathbf{r})\rangle\right)\ln\left(\int d\mathbf{r}\,\langle c_s(\mathbf{r})\rangle\right) \\ &\quad +\sum_{s=A,B}\left(\int d\mathbf{r}\,\langle c_s(\mathbf{r})\rangle\right)\left[\ln\Lambda_s - 1 - \ln\int d\mathbf{r}\,4\pi\right] \end{aligned} \tag{3.75}$$

For a homogeneous system,

$$\begin{aligned}\beta F_{\lim \boldsymbol{\varepsilon}_0 \to 0} &= -\frac{V}{2}\frac{\varepsilon_0 a}{\beta}\left(\ln\left[\frac{a\epsilon_0}{\beta + a\epsilon_0}\right]\right)\sum_{s=A,B}\langle c_s\rangle \frac{\beta}{3\varepsilon_0 v_s}\bar{\mu}_s^2 \\ &\quad + V\sum_{s=A,B}\langle c_s\rangle \ln\left(\langle c_s\rangle V\right) + V\sum_{s=A,B}\langle c_s\rangle\left[\ln\Lambda_s - 1 - \ln 4\pi\right] \quad (3.76)\end{aligned}$$

For a binary system, let us introduce the volume fraction ϕ_s for the solvent type s. The number concentration relates to the volume fraction through $\langle c_s\rangle = \phi_s/v_s$. Using the volume fraction, we rewrite the free energy as

$$\begin{aligned}\beta F_{\lim \boldsymbol{\varepsilon}_0 \to 0} &= -\frac{V}{2}\frac{\varepsilon_0 a}{\beta}\left(\ln\left[\frac{a\epsilon_0}{\beta + a\epsilon_0}\right]\right)\sum_{s=A,B}\frac{\phi_s}{v_s}\frac{\beta}{3\varepsilon_0 v_s}\bar{\mu}_s^2 \\ &\quad + V\sum_{s=A,B}\left(\frac{\phi_s}{v_s}\right)\ln\phi_s + V\sum_{s=A,B}\left(\frac{\phi_s}{v_s}\right)\left[\ln\frac{\Lambda_s V}{4\pi v_s} - 1\right] \quad (3.77)\end{aligned}$$

where

$$a = \left(\sum_{s=A,B}\frac{\phi_s\bar{\mu}_s^2}{3v_s}\right)^{-1} \quad (3.78)$$

as given by Eq. (3.59a).

Then the mixing free energy can be expressed as

$$\begin{aligned}&\Delta\beta F_{\mathrm{mix},\boldsymbol{\varepsilon}_0\to 0} \\ &= \beta F_{\lim \boldsymbol{\varepsilon}_0 \to 0} - \sum_{s=A,B}\phi_s \beta F_{\lim \boldsymbol{\varepsilon}_0 \to 0}(\phi_s = 1) \\ &= -V\sum_{s=A,B}\frac{\phi_s\bar{\mu}_s^2}{6v_s^2}\left[a\ln\left(\frac{a\epsilon_0}{\beta + a\epsilon_0}\right) - a_s\ln\left(\frac{a_s\epsilon_0}{\beta + a_s\epsilon_0}\right)\right] + V\sum_{s=A,B}\left(\frac{\phi_s}{v_s}\right)\ln\phi_s\end{aligned} \quad (3.79)$$

where $a_s = 3v_s/\bar{\mu}_s^2$.

3.3 Results and Discussions

3.3.1 Dielectric Constants of Polar Liquid Mixtures

In this section, we apply the FTVT to calculate the dielectric constants of liquid mixtures. We assume that the molar volumes and the dielectric constants of the pure solvents are known. The liquid components are assumed to be nonpolarizable, and we determine the effective permanent dipole moment of each liquid from its dielectric constant, molecular volume, and temperature by applying Eq. (3.67) to a pure solvent component. In this work, for simplicity, we do not model the polarizability and the specific molecular correlations explicitly; instead, their effects are renormalized into the effective permanent dipole moment. For simplicity, we also assume that the liquid mixture is incompressible and that the volume change upon mixing is zero.

In Figure 3.1 and 3.2, we plot the mixture dielectric constant vs. the solvent composition calculated by the FTVT for aqueous and non-aqueous mixtures, respectively. In both figures, we compare the values predicted by the FTVT to the experimentally measured dielectric constants, shown as scattered points of the same color for each mixture. In Figure 3.1, we observe that there is very good agreement between the FTVT predicted dielectric constant and the experimental values for all aqueous mixtures considered except the water/DMSO mixture. The general good agreement suggest that the FTVT can serve as a robust and convenient method for calculating the mixture dielectric constants based on pure-solvent dielectric constants and molar volumes. We note that the use of an effective permanent dipole for each solvent component is found to be applicable for the hydrogen-bonding liquids, even though the specific interactions around a molecule, such as the tetrahedral order around a water molecule, are not taken into account. We observe from Figure 3.1 that the FTVT underestimates the dielectric constant of a water/DMSO mixture. This is because the presence of DMSO enhances the hydrogen bonds in water, and the hydrogen bonds between DMSO and water is longer lived that the water-water hydrogen bonds.[58–60] As the additional correlation caused by the hydrogen bonds are not captured with the FTVT, the FTVT underestimates mixture dielectric constant of the water/DMSO

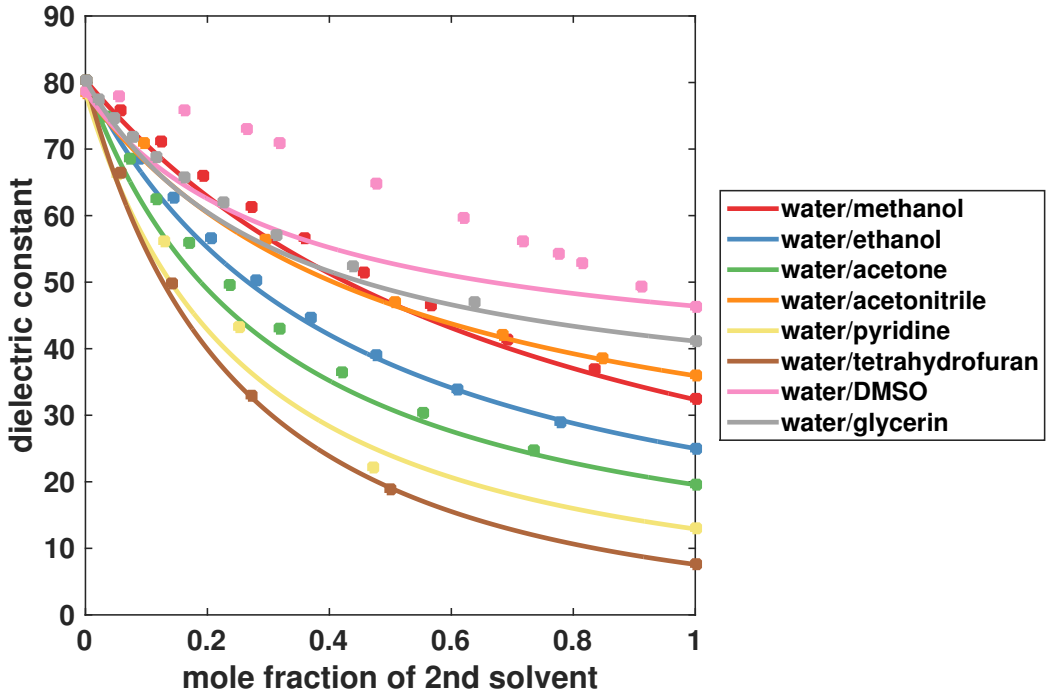

Figure 3.1: Dielectric constants of mixtures calculated by the FTVT (lines) plotted against the mixture composition for a range of aqueous mixtures. The mixtures are distinguished with different colors as indicated by the legend. The results are compared with the experimentally observed values shown as scattered points of the same color.

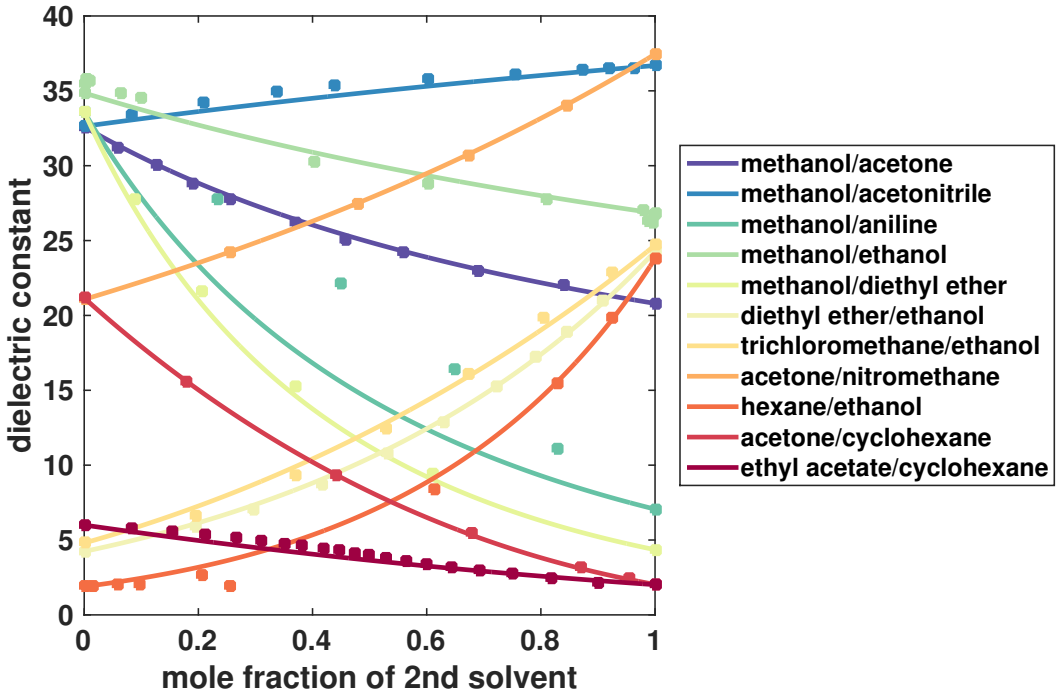

Figure 3.2: Dielectric constants of mixtures calculated by the FTVT (lines) plotted against the mixture composition for a range of nonaqueous mixtures. The mixtures are distinguished with different colors as indicated by the legend. The results are compared with the experimentally observed values shown as scattered points of the same color.

mixture.

For the nonaqueous mixtures considered in Figure 3.2, we observe good agreement between theoretically predicted dielectric constants and experimentally measured values for all mixtures except the methanol/aniline mixture. This again suggests that the FTVT is able to provide reliable predictions for the dielectric constants of general mixtures. In particular, we note that, for nonpolar molecules such as hexane and cyclohexane, the use of an effective permanent dipole moment seems to be able to capture the effects of polarizability. For water/aniline mixture, the deviation between the FTVT-predicted dielectric constants and the experimental results are most probably due to the strong hydrogen-bonding interaction inside the mixture.[61]

3.3.2 Miscibility of Liquids

In this section, we apply the mixing free energy derived in Eq. (3.79) to predict the miscibility of liquids. Using the mixing free energy derived in the FTVT, we can determine whether these two solvents are miscible by looking at the convexity of the mixing free energy: if the mixing free energy is convex for all compositions, the two solvents are miscible; otherwise, there exist compositions at which the mixture separates into two phases of different compositions, and the two solvents are not miscible with each other. Based on Eq. (3.79), the only inputs required for the FTVT to predict the miscibility of two solvents are the effective permanent dipole moments and the molecular volumes of the solvent components. The molecular volume can be computed from the molar volume of the liquid, and the effective permanent dipole moment can be computed from both the molar volume and the dielectric constant by applying Eq. (3.67) to a pure solvent component. Therefore, the miscibility between any liquids can be predicted based on only two macroscopic properties of each component: the dielectric constant and the molar volume.

In Figures 3.3(a) to 3.5(b), we have plotted the miscibility maps for six solvents: water, methanol, ethanol, acetone, cyclohexane, and benzene. We call these solvents the "host solvent" for the miscibility map. These miscibility maps are plotted on

the axes of dielectric constant and molar volume of a second solvent. If the second solvent has molar volume and dielectric constant that falls in the green region of the miscibility map, it is predicted to be miscible with the host solvent; otherwise, if the second solvent falls in the blue region of the miscibility map, it is predicted to be immiscible with the host solvent. On each of the miscibility maps, we also indicate the experimentally observed miscibility for real solvents: a yellow circle indicates that the solvent is observed to be miscible with the host solvent, while a red cross indicates that the solvent is immiscible with the host solvent. The numbers next to the experimentally measured miscibility correspond to the solvent serial numbers listed in Table 3.1.

In Figures 3.3(a) to 3.5(b), we find that there are excellent agreements between the FTVT-predicted miscibility and the experimentally measured miscibility for real solvents. This suggests that the FTVT is able to give good predictions for the miscibility between two liquids. In addition, we observe that water, being a small and highly-polar molecule, is miscible with liquids that have relatively small molar volume and large dielectric constant. On the other end of the spectrum, cyclohexane and benzene, being large in molecular size and nonpolar, are miscible with liquids that have relatively large molar volume and small dielectric constant. In the middle of the spectrum, for molecules such as ethanol and acetone, having intermediate molecular size and intermediate dielectric constant allows them to be miscible with most solvents, as indicated by the largest green region in their miscibility maps. Thus, the FTVT has provided a quantitative explanation to the common saying "like dissolves like, and unlike does not". Here, we have observed that, for two solvents to be miscible, they need to be alike both in their dielectric constants (polarity) and molar volumes (molecular volumes).

From the miscibility map for water in Figures 3.3(a), we find that acetic acid, 1,4-dioxane, and tetrahydrofuran are predicted to be immiscible with water by the FTVT, but are experimentally observed to be miscible with water. We note that acetic acid is known to form dimers in its pure liquid. In a dimer, the permanent dipole moment of the acetic acid cancel out, and therefore, the permanent dipole moment calculated

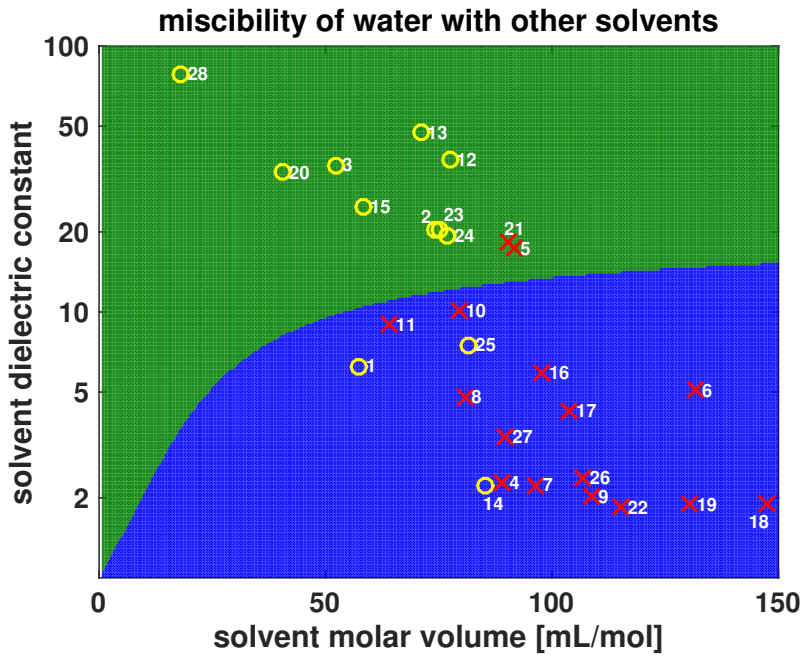

(a)

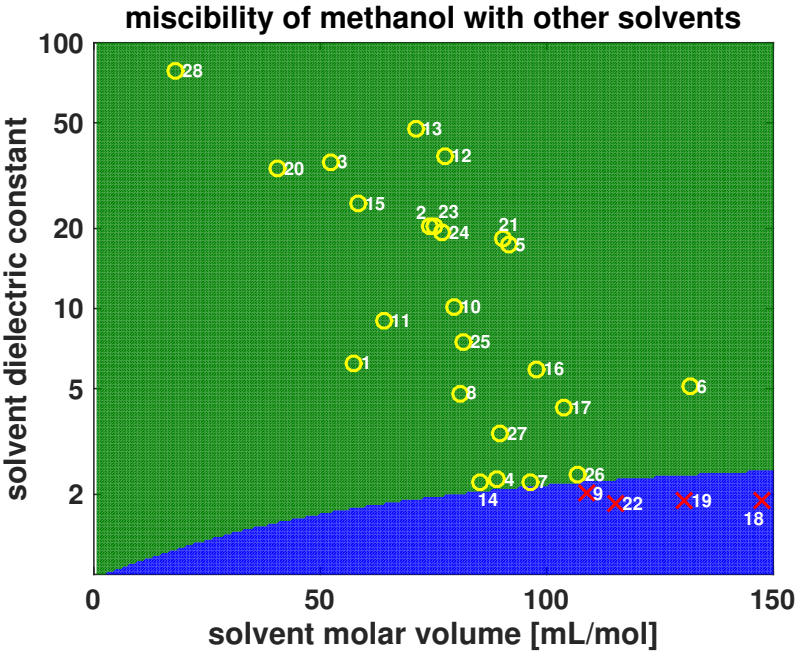

(b)

Figure 3.3: The miscibility maps for host solvents (a) water and (b) methanol plotted on the axes of dielectric constant and molar volume of a second solvent. The green/blue region indicates that a solvent with dielectric constant and molar volume at the point is miscible/immiscible with the host solvent. The yellow circles indicate actual solvents that are miscible with the host solvent, while the red crosses indicate actual solvents that are immiscible with the host solvent. The numbers next to the experimentally measured miscibility correspond to the solvent serial numbers listed in Table 3.1.

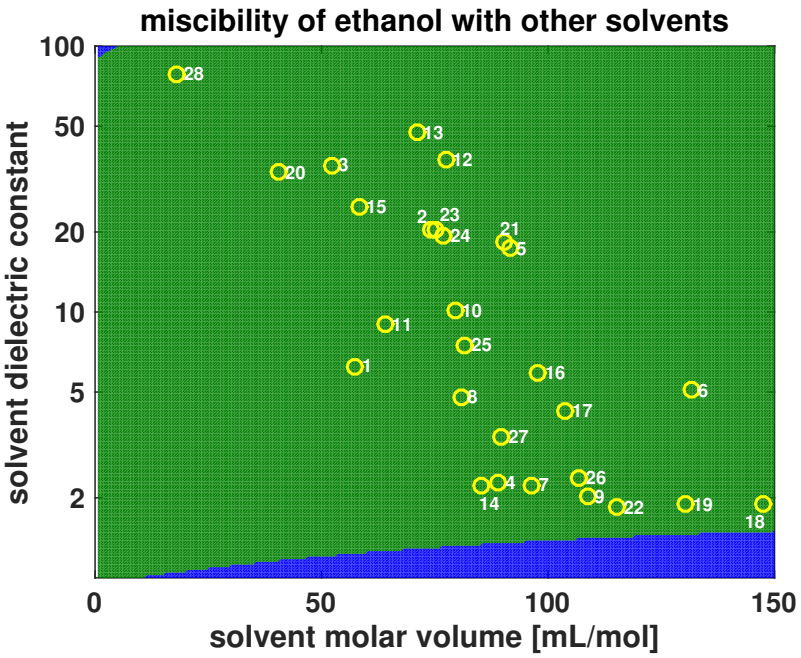

(a)

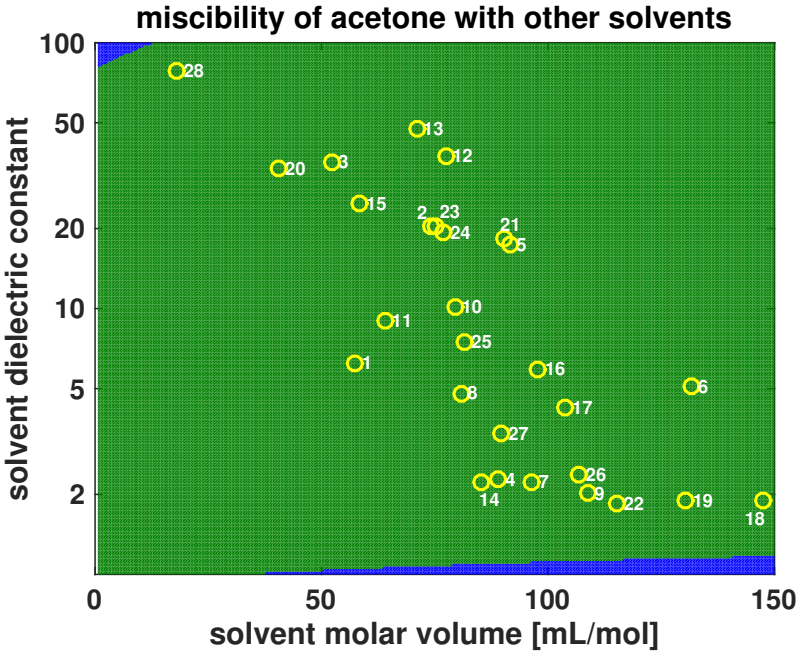

(b)

Figure 3.4: The miscibility maps for host solvents (a) ethanol and (b) acetone plotted on the axes of dielectric constant and molar volume of a second solvent. The green/blue region indicates that a solvent with dielectric constant and molar volume at the point is miscible/immiscible with the host solvent. The yellow circles indicate actual solvents that are miscible with the host solvent, while the red crosses indicate actual solvents that are immiscible with the host solvent. The numbers next to the experimentally measured miscibility correspond to the solvent serial numbers listed in Table 3.1.

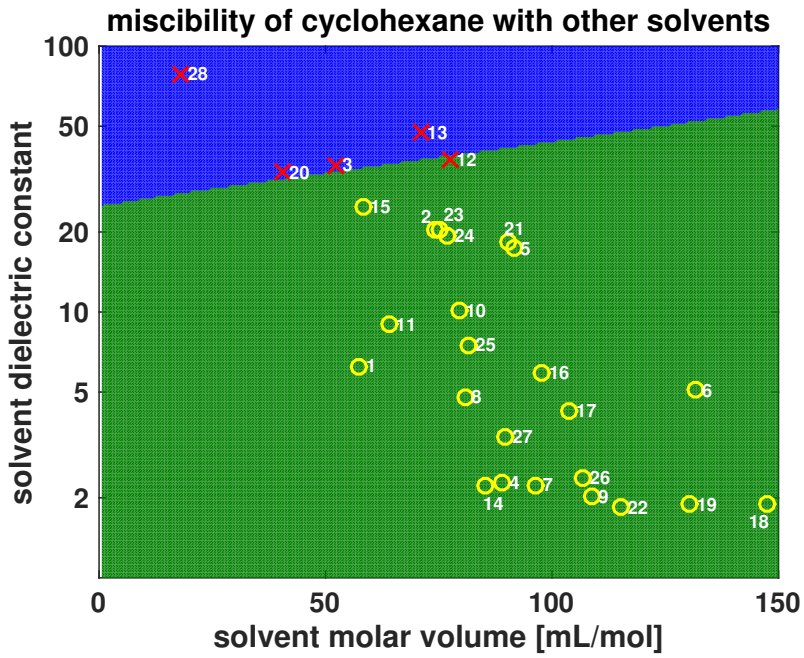

(a)

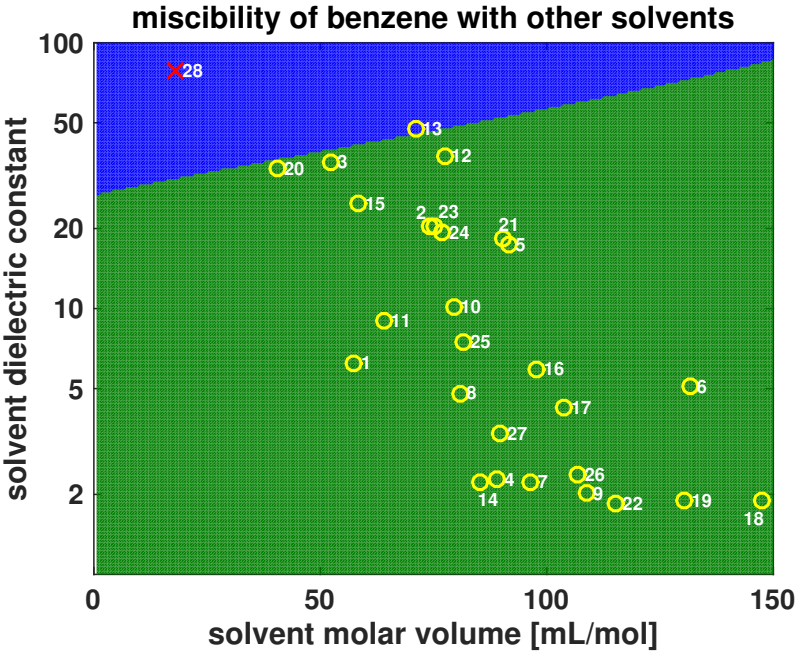

(b)

Figure 3.5: The miscibility maps for host solvents (a) cyclohexane and (b) benzene plotted on the axes of dielectric constant and molar volume of a second solvent. The green/blue region indicates that a solvent with dielectric constant and molar volume at the point is miscible/immiscible with the host solvent. The yellow circles indicate actual solvents that are miscible with the host solvent, while the red crosses indicate actual solvents that are immiscible with the host solvent. The numbers next to the experimentally measured miscibility correspond to the solvent serial numbers listed in Table 3.1.

Table 3.1: The serial numbers (SN), the dielectric constants, and the molar volumes for the solvents considered in the miscibility maps in Figures 3.3(a) to 3.5(b).

SN	Solvent Name	Dielectric Constant	Molar Volume [mL/mol]
1	acetic acid	6.25	57.49
2	acetone	20.51	74.03
3	acetonitrile	35.68	52.25
4	benzene	2.27	89.12
5	1-butanol	17.34	91.56
6	butyl acetate	5.07	131.62
7	tetrachloromethane	2.23	96.50
8	trichloromethane	4.81	80.73
9	cyclohexane	2.02	108.75
10	1,2-dichloroethane	10.12	79.46
11	dichloromethane	8.97	64.02
12	dimethylformamide	37.47	77.39
13	dimethyl sulfoxide	47.24	70.96
14	1,4-dioxane	2.21	85.23
15	ethanol	24.75	58.37
16	ethyl acetate	5.93	97.86
17	diethyl ether	4.24	103.84
18	heptane	1.91	147.46
19	hexane	1.88	130.45
20	methanol	33.45	40.49
21	2-butanone	18.24	90.14
22	pentane	1.84	115.22
23	1-propanol	20.52	75.15
24	2-propanol	19.26	76.96
25	tetrahydrofuran	7.51	81.63
26	toluene	2.38	106.85
27	trichloroethene	3.39	89.73
28	water	78.34	18.07

from the dielectric constant of pure acetic acid significantly underestimates the actual permanent dipole moment of the acetic acid. For 1,4-dioxane and tetrahydrofuran, they do not form hydrogen bonds in their pure solvents, but are able to form hydrogen bonds with water. Therefore, the interactions between 1,4-dioxane or tetrahydrofuran and water are more favorable than that captured by the FTVT theory. On the other hand, for 1-butanol and 2-butanone, the FTVT predicts that they are miscible with water by experimental observations indicate otherwise. However, these two solvents lie close to the miscible-immiscible boundary on water's miscibility map and we can still consider the theory-experiment agreement to be good. The discrepancy between theory and experiment for 1-butanol and 2-butanone may be because of the fact that the effective permanent dipole does not describe their interactions with water most accurately. Since 1-butanol and 2-butanone are large molecules, it may be important to consider their polarizability explicitly.

3.4 Summary and Outlooks

In this chapter, we have developed a variational field theoretical approach for studying polar liquid mixtures, and applied the theory to compute the dielectric constants and miscibility of liquid mixtures. The theory results in a simple analytical expression for the free energy of the mixture. Using only the dielectric constants and the molar volume of the pure-solvent components as inputs, and not any adjustable parameters, the theory predicts the dielectric constants and miscibility of liquid mixtures in impressive agreements with experimentally observed results. In addition, a short-ranged polarization distribution function is introduced for each solvent molecule, removing the divergence problems in the field-theoretic treatment.

The FTVT in this work provides a general and systematic approach for obtaining a free energy for a system of liquid mixtures. While we have only considered binary solvent mixtures in this chapter, it is straightforward to generalize the theory to multi-component mixed solvents. In addition, the shape of the molecule can be incorporated with more details through the short-ranged polarization distribution function. An

important next step is to account for the effects of polarizability of the solvents, as their effects can be crucial for the property of mixtures too. In future work, it will be interesting to consider ionic solutions by including ions into the solvent mixture, and to integrate the treatment of solvent mixture in this work with existing models for charge solvation in computer simulations.

Appendix 3.A Evaluation of the Self-Interaction Factor for Uniformly Polarized Spheres

In this section, we provide the details for the evaluation of Eq. (3.71):

$$\int d\mathbf{r}_1 \int d\mathbf{r}_2 \, \boldsymbol{\mu}_s h_s(\mathbf{r}-\mathbf{r}_1)\boldsymbol{\mathcal{T}}(\mathbf{r}_1-\mathbf{r}_2)h_s(\mathbf{r}_2-\mathbf{r})\boldsymbol{\mu}_s = \frac{\beta}{3\varepsilon_0 v_s}\bar{\mu}_s^2 \tag{3.80}$$

with $h_s(\mathbf{r})$ given by

$$h_s(\mathbf{r}) = \begin{cases} \frac{1}{v_s} & |\mathbf{r}| < \left(\frac{3v_s}{4\pi}\right)^{\frac{1}{3}} \\ 0 & \text{otherwise} \end{cases} \tag{3.81}$$

The integral is essentially the self-interaction energy (multiplied by inverse temperature β) of a uniformly polarized sphere of radius R such that $\frac{4}{3}\pi R^3 = v_s$. One of the easy way to perform the calculation is to make use of the result from Example 4.2 in Ref. 62, which gives the electric field inside the sphere of a uniformly polarized sphere of polarization $\mathbf{P}$ is

$$\mathbf{E} = -\frac{1}{3\varepsilon_0}\mathbf{P} = -\frac{1}{3\varepsilon_0}\frac{\boldsymbol{\mu}_s}{v_s} \tag{3.82}$$

Thus the energy for such a sphere is

$$E = -\boldsymbol{\mu}_s \cdot \mathbf{E} = \frac{\boldsymbol{\mu}_s^2}{3\varepsilon_0 v_s} \tag{3.83}$$

and therefore we arrive at Eq. (3.71).

Part II

Nonequilibrium Properties

Chapter 4

A Molecularly-Based Theory for Electron Transfer Reorganization Energy in Pure Solvents

This chapter includes content from our previously published article:

Zhuang, B.; Wang, Z.-G. A Molecularly Based Theory for Electron Transfer Reorganization Energy. *J. Chem. Phys.* **2015,** *143,* 224502.

4.1 Introduction

Electron transfer (ET) is a ubiquitous mechanism in many chemical, electrochemical and biological processes. The ET kinetics depends on the nonequilibrium free energy surfaces of the reactant and the product states generated by the electron-transferring species and the solvent degrees of freedom.[63–68] The celebrated Marcus theory[69,70] envisions the nonequilibrium free energy surface as two equal-curvature parabolic functions of a one-dimensional macroscopic coordinate – the solvent orientational polarization, based on a linear dielectric treatment of the solvent in terms of its static and optical dielectric constants. This simple picture has had wide successes in many experimental and simulation tests. In particular the prediction – and subsequent experimental observation – of an inverted region in the energy gap law[67] represents a great triumph of the Marcus theory.

The treatment of the solvent as a linear dielectric medium is clearly an approximation, as recognized by Marcus himself and others.[71–73] Two notable discrepancies have been known in the literature. First, computer simulations indicated that the solvent reorganization energy depends on the charges of the donor-acceptor system,[74–80] and not only on the amount of charge transfer as predicted by the Marcus theory. Second, time-resolved spectroscopic measurements of electron-transferring species revealed differences in the energies and shapes of the absorption and the emission bands, while the Marcus picture predicts a perfect symmetry between the two bands.[73,81,82] The explanation of these phenomena requires theoretical methods that account for solvent properties beyond the linear dielectric approximation, such as spatially varying dielectric response and dielectric saturation.

Molecular dynamics (MD) simulations with explicit solvents can include the microscopic molecular structure and interactions, allowing dynamical details of ET processes to be studied.[79,80,83–92] However, multiple long trajectories are required to perform umbrella sampling, making it impractical to perform calculations for general solvents. Integral-equation theories[12,93–99] is a more convenient alternative to the laborious nonequilibrium sampling schemes in MD simulations, but nanosecond MD simulations are still required to compute the solvent correlation functions in these approaches. Also, it is cumbersome to include the induced dipoles of the solvent in simulations and integral-equation theories; as such, these methods often treat solvent molecules as nonpolarizable, with the effects of solvent electronic response approximated or ignored. Furthermore, these methods require specific, well-parameterized solvent models.

On the other hand, phenomenological treatments[73,100–117] are convenient tools that elucidate the essential physics in electron transfer reactions, and provide good explanations for experimental and simulation data by invoking *ad hoc* fitting parameters. However, for any specific ET system, to make *a priori* predictions of the reorganization energy, it is desirable to develop a theory that captures the most important properties of each solvent using only readily-available parameters from physicochemical handbooks.

Recently, Nakamura et al.[44] developed a coarse-grained theory for equilibrium ion solvation in liquids and liquid mixtures using field-theoretic techniques. The term 'coarse-grained' refers to a simplified description of the solvent molecules using a reduced set of degrees of freedom. The theory accounts for the molecular nature of the solvents by using a small number of molecular parameters that are readily available – the permanent dipole, the polarizability, and the molecular volume for the solvent and the ionic radius for the ionic solute. The theory naturally captures spatially varying dielectric responses and dielectric saturation in the close vicinity of the ion. With no adjustable parameters, the theory predicts solvation energies in both single-component liquids and binary liquid mixtures that are in excellent agreement with experimental data. A key insight of the work in Ref. 44 is that the solvation energy of an ion is largely determined by the local response of the permanent and induced dipoles, as well as the local solvent composition in the case of mixtures, and bears no strong correlation with the *bulk* dielectric constant.

In this chapter, we extend the work of Nakamura et al. to the calculation of nonequilibrium solvation energy (the reorganization energy) for electron transfer reactions in simple molecular liquids. In contrast to equilibrium ion solvation where both the electronic and orientational components of the solvent polarization reach full equilibrium, the nonequilibrium solvation energy in ET involves conditions where only the electronic polarization responds to the instantaneous solute charges while the orientational component is kept at nonequilibrium values because of the longer time scales for solvent orientational relaxation compared to the electronic motion. The field theoretical formulation naturally accounts for these two different degrees of freedom by introducing two respective conjugate fields (which become identical under full equilibrium conditions). With the same set molecular input as for equilibrium solvation, and with no adjustable parameters, our theory predicts reorganization energies for a variety of charge transfer reactions involving simple metal ions in good agreement with experimentally obtained data. Furthermore, by treating all solvent molecules on equal footing and representing the solvent polarization as spatially varying quantities, our theory provides a unified description of the solvation energy contributions from

all the solvent molecules, thus avoiding the need to separately treat the inner-sphere and the outer-sphere molecules, as is commonly done in existing ET theories. Our approach allows ET reorganization energy to be calculated with minimal computational effort, typically less than half a minute on a personal computer.

The rest of this chapter is organized as follows. In Section 4.2, after a brief description of the setup of the problem to identify the relevant energies, we formulate our dipolar self-consistent-field theory (DSCFT) for charge solvation under both equilibrium and nonequilibrium conditions for a single-component liquid. (Extension to liquid mixtures will be deferred to a forthcoming work.) The key equations and main steps in the derivation are presented, while some of the technical details are delegated to the two appendices. In Section 4.3, we present the results for the reorganization and activation energies for several prototypical ET reactions. We show that the DSCFT is able to unify the treatment of inner-sphere and outer-sphere solvent molecules to provide a reliable estimate of the total reorganization energy. In addition, we show that the nonequilibrium free energy surface is well described by a parabolic function, but contrary to the prediction by the linear dielectric theory, the curvature of the free energy surface is not independent of the magnitude of charge on the electron-transferring species. Finally, in Section 4.4, we summarize the main points of this work and offer some concluding remarks.

4.2 Dipolar Self-Consistent-Field Theory (DSCFT)

In this section, we derive the DSCFT by extending the equilibrium theory for ion solvation by Nakamura et al. to the case of nonequilibrium solvation with arbitrary solute charge distribution. We start with a brief review of the key concepts in ET theory to define the relevant free energies. Next, we formulate the field-theoretic DSCFT theory for the solvation of a solute with arbitrary charge under equilibrium and nonequilibrium conditions. We then apply the DSCFT to ET between two simple ions, detailing the procedure for calculating the reorganization energy and the free energy change of the reaction.

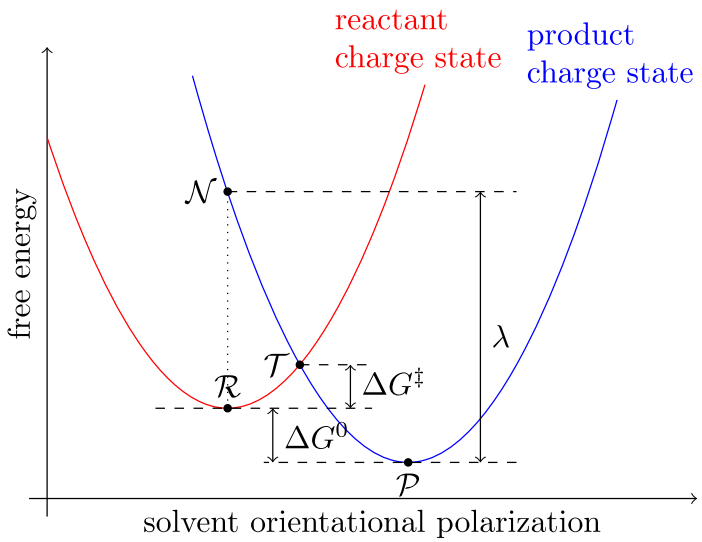

Figure 4.1: Free energy vs. solvent orientational polarization for electron transfer reactions. The linear dielectric theory predicts that the two free energy curves are parabolic and have equal curvature. $\mathcal{R}$ and $\mathcal{P}$ are the equilibrium states when the solute is at the reactant charge state and the product charge state, respectively. $\mathcal{N}$ is the nonequilibrium state in which the solute is in the product charge state while the solvent orientational polarization is in equilibrium with the reactant charge state. $\mathcal{T}$ labels the transition state. The activation energy, the free energy change of the reaction, and the reorganization energy are $\Delta G^{\ddagger}$, ΔG^{0}, and λ, respectively.

4.2.1 Key Concepts in Electron Transfer Theory

We consider the typical ET in a weakly-coupled donor-acceptor complex (the solute) in a polar solvent. The solute has charge distribution $\hat{\rho}_c^{(R)}(\mathbf{r})$ in the reactant state and $\hat{\rho}_c^{(P)}(\mathbf{r})$ in the product state. The macrostate of the solvent can be described by its electronic polarization $\mathbf{P}_{\text{el}}$ and orientational polarization $\mathbf{P}_{\text{or}}$. Due to the separation of timescale between the fast-responding electronic polarization and the slow-responding orientational polarization, the ET kinetics is controlled by the thermally-induced nonequilibrium reorganization in the solvent orientational polarization. Based on the linear dielectric description for the solvent, the free energies in the reactant and the product charge states relate to the nonequilibrium orientational polarization through two parabolas of equal curvature, as sketched in Fig. 4.1.

The key insight in the Marcus theory[69,70] is that a thermally-activated ET process must satisfy both the Franck-Condon principle and energy conservation. As such,

prior to the electron transfer, the solvent orientational polarization must reorganize to a transition state ($\mathcal{T}$) such that the free energy in the reactant state equals the free energy in the product state. The difference in the free energy of the transition state and the reactant equilibrium state ($\mathcal{R}$) defines the activation energy $\Delta G^{\ddagger}$ of the ET process. However, it is generally difficult to directly obtain a simple expression for the orientational polarization at the transition state. Instead, the activation energy is calculated by its relation to the free energy change of the reaction ΔG^0 and the reorganization energy λ through the following expression, based on the double-parabola picture of the free energy surface:

$$\Delta G^{\ddagger} = \frac{\lambda}{4}\left(1 + \frac{\Delta G^0}{\lambda}\right)^2 \tag{4.1}$$

where the free energy change and the reorganization energy are given by

$$\Delta G^0 = G_{\mathcal{P}} - G_{\mathcal{R}} \tag{4.2}$$

$$\lambda = G_{\mathcal{N}} - G_{\mathcal{P}} \tag{4.3}$$

In the above expressions, $G_{\mathcal{S}}$ denotes the free energy of the state $\mathcal{S}$. States $\mathcal{R}$ and $\mathcal{P}$ are the equilibrium states corresponding to the reactant and the product charges, where both the solvent orientational and the electronic polarizations are in full equilibrium with the solute charge. State $\mathcal{N}$ is a nonequilibrium state in which the solute is in the product charge state but the solvent orientational polarization is kept at its previous equilibrium value in state $\mathcal{R}$. In State $\mathcal{N}$, the solvent electronic polarization equilibrates with both the solute charge and the nonequilibrium orientational polarization. These states as well as the relevant energies are indicated in the sketch in Fig. 4.1.

The usual treatment of reorganization energy in the linear dielectric theory involves the separation of the inner-sphere (solute) and the outer-sphere (solvent) contributions. For an ET process between two simple ions, the coordinated metal complexes, instead of the bare ions, are usually treated as the solute in the inner sphere.

For example, for the Fe^{2+}/Fe^{3+} exchange reaction in aqueous medium, the hexaaquo-complexes $[Fe(H_2O)_6]^{2+}$ and $[Fe(H_2O)_6]^{3+}$ are considered as the solutes. The inner-sphere reorganization energy considers the nonequilibrium coordinate bond lengths between the ion and the solvent ligands, while the outer-sphere reorganization energy considers nonequilibrium solvent orientational polarization *outside* the hexaaquocomplexes. Using classical linear dielectric theory, Marcus derived the following expression relating the outer-sphere reorganization energy λ_o and the geometry of the solute:[69]

$$\lambda_o = \frac{(\Delta q)^2}{4\pi\epsilon_0}\left(\frac{1}{2a_D}+\frac{1}{2a_A}-\frac{1}{d}\right)\left(\frac{1}{\epsilon_\infty}-\frac{1}{\epsilon_s}\right) \tag{4.4}$$

where a_D and a_A are respectively the radii of the donor and the acceptor, d is the distance between them, and Δq is the amount of charge transferred. ϵ_∞ and ϵ_s are respectively the bulk optical and the static dielectric constants of the solvent. In this work, we refer to the reorganization energy calculated by Eq. (4.4) as the bulk linear dielectric constant (BLDC) approximation.

The Marcus theory thus establishes that the key to the study of an ET process is to find the free energies of charge solvation under the equilibrium condition, where both the orientational and the electronic polarizations of the solvent are in equilibrium with the solute charge, as well as the nonequilibrium condition, where the solvent orientational polarization is kept at an out-of-equilibrium value. In the following subsection, we formulate a molecularly-based mean-field theory for calculating these free energies.

4.2.2 Dipolar Self-Consistent-Field Theory (DSCFT) for Equilibrium and Nonequilibrium Solvation

In this section, we formulate the DSCFT for charge solvation under both the equilibrium and the nonequilibrium situations. We consider a set of solutes immersed in a polar solvent, as schematically illustrated in Fig. 4.2. The set of solutes is modeled as a charge distribution $\hat{\rho}_c(\mathbf{r})$ inside some solute cavity $\mathcal{C}$ representing the space

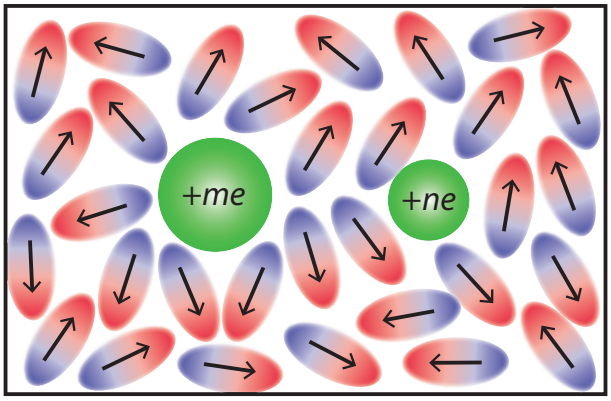

Figure 4.2: A schematic representation of the system of solutes in a dipolar solvent. The solute cavity $\mathcal{C}$ is represented in green and the solvent is represented by the red and blue dipoles.

inaccessible to solvent molecules. The solvent consists of N dipolar molecules, each characterized by its molecular volume v, permanent dipole $\bar{\mu}$, and polarizability α. The state of the ith solvent molecule is described by $\{\mathbf{r}_i, \boldsymbol{\mu}_i, \mathbf{p}_i\}$, which respectively denote its position, permanent dipole (with magnitude $|\boldsymbol{\mu}_i| = \bar{\mu}$), and induced dipole.

We write the total charge density of the solute-solvent system as:

$$\hat{\rho}(\mathbf{r}) = \hat{\rho}_c(\mathbf{r}) + \hat{\rho}_{\text{or}}(\mathbf{r}) + \hat{\rho}_{\text{el}}(\mathbf{r}) \tag{4.5}$$

where $\hat{\rho}_{\text{or}}$ and $\hat{\rho}_{\text{el}}$ are respectively the charge densities due to the orientational and the electronic polarizations. As the solvent orientational polarization is due to the permanent dipole moments that are related to the nuclear degrees of freedom, and the electronic polarization is due to the induced dipole moments that are related to the electronic degrees of freedom, we express $\hat{\rho}_{\text{or}}$ and $\hat{\rho}_{\text{el}}$ in terms of their corresponding dipole moments as[50]

$$\hat{\rho}_{\text{or}}(\mathbf{r}) = -\sum_{i=1}^{N} \boldsymbol{\mu}_i \cdot \nabla\delta(\mathbf{r} - \mathbf{r}_i) \tag{4.6}$$

$$\hat{\rho}_{\text{el}}(\mathbf{r}) = -\sum_{i=1}^{N} \mathbf{p}_i \cdot \nabla\delta(\mathbf{r} - \mathbf{r}_i) \tag{4.7}$$

The energy of the system consists of the Coulomb interaction and the deformation

energy of the induced dipoles, and it can be expressed as

$$U = \frac{1}{2}\int d\mathbf{r}\int d\mathbf{r}'\,\frac{\hat{\rho}(\mathbf{r})\hat{\rho}(\mathbf{r}')}{4\pi\epsilon_0|\mathbf{r}-\mathbf{r}'|} + \sum_{i=1}^{N}\frac{\mathbf{p}_i^2}{2\alpha} \tag{4.8}$$

where the second term is the deformation energy of the induced dipoles in the harmonic approximation.[50,51] For convenience, we work in a semi-grand canonical ensemble of open-solvent and incompressible system with volume V, temperature T, and solvent chemical potential μ, for which the partition function is

$$\begin{aligned}\Xi \;=\; \sum_{N=0}^{\infty}\frac{e^{\beta\mu N}}{N!}\left(\prod_{i=1}^{N}\frac{1}{\eta}\int d\mathbf{r}_i\int d\boldsymbol{\mu}_i\int d\mathbf{p}_i\right)\\ \times\delta[v\hat{n}(\mathbf{r})-1]e^{-\beta U}\end{aligned} \tag{4.9}$$

where $\beta = 1/k_BT$ and η is the analog of thermal de Broglie wavelength that makes the configurational integral dimensionless. The actual value of η is inconsequential as it only contributes to a reference energy. $\delta[f(\mathbf{r})]$ is the δ-functional, which is the generalization of the Dirac delta function to the function space, such that $\delta[f(\mathbf{r})] = 0$ unless $f = 0$ for all $\mathbf{r}$, and the integral of the functional over the function space satisfies $\int \mathcal{D}f\delta[f(\mathbf{r})] = 1$. $\hat{n}(\mathbf{r}) = \sum_{i=1}^{N}\delta(\mathbf{r}-\mathbf{r}_i)$ is the number density operator for the solvent molecules. Rather than accounting for the non-electrostatic interactions between the solvent molecules explicitly, in our coarse-grained approach, we treat the liquid as incompressible and use the δ-functional constraint to enforce a constant density everywhere in the system. The integral runs over the configurational space of solvent molecules; the integral over $\boldsymbol{\mu}_i$ runs over the 4π solid angle as the magnitude of the permanent dipole is fixed.

Next, we transform the particle-based partition function in Eq. (4.9) into a field representation by performing a series of identity transformations.[14] This process introduces coarse-grained particle densities and coarse-grained potentials that decouple the particle-particle interactions. These coarse-grained variables are introduced as

integration variables using the property of the δ-functional:

$$F[f(\mathbf{r})] = \int \mathcal{D}g\, \delta[f(\mathbf{r}) - g(\mathbf{r})] F[g(\mathbf{r})] \tag{4.10}$$

where f represents a general function and F is a general functional. The δ-functionals can be further rewritten using its Fourier representation:

$$\delta[f] = \int \mathcal{D}h\, \exp\left[i \int d\mathbf{r}\, h(\mathbf{r}) f(\mathbf{r}) \right] \tag{4.11}$$

The resulting partition function after the transformations is

$$\begin{aligned}
\Xi \;=& \int \mathcal{D}w \int \mathcal{D}\rho_{\mathrm{or}} \int \mathcal{D}\rho_{\mathrm{el}} \int \mathcal{D}w_{\mathrm{or}} \int \mathcal{D}w_{\mathrm{el}} \\
&\times \sum_{N=0}^{\infty} \frac{e^{\beta\mu N}}{N!} \left(\prod_{i=1}^{N} \frac{1}{\eta} \int d\mathbf{r}_i \int d\boldsymbol{\mu}_i \int d\mathbf{p}_i \right) \\
&\times \exp\left[i \int d\mathbf{r} w(\mathbf{r}) [vn(\mathbf{r}) - 1] - \frac{\beta}{2} \int d\mathbf{r} \int d\mathbf{r}' \frac{\rho(\mathbf{r})\rho(\mathbf{r}')}{4\pi\epsilon_0 |\mathbf{r} - \mathbf{r}'|} \right. \\
&\quad - \sum_{j=1}^{N} \frac{\beta \mathbf{p}_j^2}{2\alpha} + i \int d\mathbf{r}\, w_{\mathrm{or}}(\mathbf{r}) \rho_{\mathrm{or}}(\mathbf{r}) + i \int d\mathbf{r}\, w_{\mathrm{el}}(\mathbf{r}) \rho_{\mathrm{el}}(\mathbf{r}) \\
&\quad \left. - i \int d\mathbf{r}\, w_{\mathrm{or}}(\mathbf{r}) \hat{\rho}_{\mathrm{or}}(\mathbf{r}) - i \int d\mathbf{r}\, w_{\mathrm{el}}(\mathbf{r}) \hat{\rho}_{\mathrm{el}}(\mathbf{r}) \right]
\end{aligned} \tag{4.12}$$

where $\rho(\mathbf{r}) = \hat{\rho}_c(\mathbf{r}) + \rho_{\mathrm{or}}(\mathbf{r}) + \rho_{\mathrm{el}}(\mathbf{r})$. The procedure introduces the coarse-grained orientational and electronic charge densities ρ_{or} and ρ_{el} (represented without a hat) that do not depend explicitly on the solvent microscopic configuration. The identity transformation decouples the interactions terms and makes the partition function into one of a single-particle in effective fluctuating fields. Integration over the microscopic configurational space $\{\mathbf{r}_i, \boldsymbol{\mu}_i, \mathbf{p}_i\}$ leads to the field-theoretic grand partition function, given by

$$\Xi = \int \mathcal{D}w \int \mathcal{D}\rho_{\mathrm{or}} \int \mathcal{D}\rho_{\mathrm{el}} \int \mathcal{D}w_{\mathrm{or}} \int \mathcal{D}w_{\mathrm{el}}\, e^{-\beta H} \tag{4.13}$$

with the field Hamiltonian

$$\begin{aligned}
&\beta H[w, \rho_{\rm or}, \rho_{\rm el}, w_{\rm or}, w_{\rm el}] \\
= \;& i\int d\mathbf{r}\, w(\mathbf{r}) - i\int d\mathbf{r}\, w_{\rm or}(\mathbf{r})\rho_{\rm or}(\mathbf{r}) - i\int d\mathbf{r}\, w_{\rm el}(\mathbf{r})\rho_{\rm el}(\mathbf{r}) \\
&+ \int d\mathbf{r}\int d\mathbf{r}'\frac{\beta\rho(\mathbf{r})\rho(\mathbf{r}')}{8\pi\epsilon_0|\mathbf{r}-\mathbf{r}'|} - e^{\beta\mu}Q[w, w_{\rm or}, w_{\rm el}]
\end{aligned} \tag{4.14}$$

where $Q[w, w_{\rm or}, w_{\rm el}]$ is the single-particle partition function under the fluctuating fields given by

$$\begin{aligned}
&Q[w, w_{\rm or}, w_{\rm el}] \\
&= \frac{4\pi\bar{\mu}^2}{\eta}\left(\frac{2\pi\alpha}{\beta}\right)^{\frac{3}{2}}\int d\mathbf{r}\,\left\{\Gamma(\mathbf{r})\frac{\sin(\bar{\mu}|\nabla w_{\rm or}(\mathbf{r})|)}{\bar{\mu}|\nabla w_{\rm or}(\mathbf{r})|}\right. \\
&\qquad\qquad \left.\exp\left[ivw(\mathbf{r}) - \frac{\alpha}{2\beta}(\nabla w_{\rm el}(\mathbf{r}))^2\right]\right\}
\end{aligned} \tag{4.15}$$

Here, $\Gamma(\mathbf{r})$ serves to limit the integration to space outside of the cavity, with $\Gamma(\mathbf{r}) = 0$ if $\mathbf{r} \in \mathcal{C}$ and $\Gamma(\mathbf{r}) = 1$ otherwise.

The functional integration in the field-theoretic partition function in Eq. (4.13) cannot be evaluated in closed form. To proceed, we make the saddle-point approximation by taking the maximum of the integrand corresponding to the set of functions $\{w^*, \rho^*_{\rm or}, \rho^*_{\rm el}, w^*_{\rm or}, w^*_{\rm el}\}$ that extremizes the Boltzmann factor $\exp(-\beta H)$, i. e. $\Xi \approx \exp\{-H[w^*, \rho^*_{\rm or}, \rho^*_{\rm el}, w^*_{\rm or}, w^*_{\rm el}]\}$. At equilibrium, the saddle-point values of the functional arguments are determined by extremizing H with respect to all of its functional variables. Under the nonequilibrium condition where electronic polarization can respond but the orientational polarization is kept at its previous equilibrium value, we extremize H with respect to all functional variables except $\rho_{\rm or}$ and its conjugate field $w_{\rm or}$. We delegate the details of the extremization procedure to Appendix 4.A. Here, we simply write down the two sets of resulting constitutive relations, one set applicable under equilibrium conditions, and the other set applicable under nonequilibrium conditions. Since the saddle-point values of the functional variables lie on the imaginary axis, in order to work with real quantities and for the convenience of

relating our theory to the classical electrostatics theory, we make a change of variables $w_{\text{or}} = -i\beta\phi_{\text{or}}$, $w_{\text{el}} = -i\beta\phi_{\text{el}}$, and $w = i\beta u$.[1] Upon simplification and rearrangement of the resulting equations, the set of constitutive relations for equilibrium is

$$\nabla \cdot \mathbf{D} = \hat{\rho}_c(\mathbf{r}) \tag{4.16a}$$

$$\chi_{\text{or}}(\mathbf{r}) = \Gamma(\mathbf{r})\frac{\beta\bar{\mu}^2}{\epsilon_0 v} e^{-\beta v u(\mathbf{r}) + \frac{\beta\alpha}{2}|\nabla\phi(\mathbf{r})|^2} G(\beta\bar{\mu}|\nabla\phi(\mathbf{r})|) \tag{4.16b}$$

$$\chi_{\text{el}}(\mathbf{r}) = \Gamma(\mathbf{r})\frac{\alpha}{\epsilon_0 v} \tag{4.16c}$$

$$1 = e^{-\beta v u(\mathbf{r}) + \frac{\beta\alpha}{2}|\nabla\phi(\mathbf{r})|^2} \frac{\sinh(\beta\bar{\mu}|\nabla\phi(\mathbf{r})|)}{\beta\bar{\mu}|\nabla\phi(\mathbf{r})|} \tag{4.16d}$$

where $G(x) = [1/\tanh(x) - 1/x]\sinh(x)/x^2$. $\mathbf{D}$ is electric displacement given by $\mathbf{D} = -\epsilon_0[1 + \chi_{\text{el}} + \chi_{\text{or}}(\mathbf{r})]\nabla\phi(\mathbf{r})$, and χ_{or} and χ_{el} are respectively the orientational and electronic electric susceptibilities. χ_{or} and χ_{el} are zero inside the solute cavity, which is a vacuum with no solvent. The electric susceptibilities relate to the local static dielectric function $\varepsilon_s(\mathbf{r})$ and the local optical dielectric function $\varepsilon_\infty(\mathbf{r})$ through $\chi_{\text{or}}(\mathbf{r})$ and $\chi_{\text{el}}(\mathbf{r})$ through $\varepsilon_s(\mathbf{r}) = 1 + \chi_{\text{or}}(\mathbf{r}) + \chi_{\text{el}}(\mathbf{r})$ and $\varepsilon_\infty(\mathbf{r}) = 1 + \chi_{\text{el}}(\mathbf{r})$. At the saddle-point level, the bulk dielectric constant is only accounted for in the limit of dilute gases, but the effect of this approximation is inconsequential as the solvation energy is determined by the local dielectric response and not directly related to the bulk dielectric constant.[44] We have dropped the superscripts * in these equations for notational simplicity, but it should be understood that the effective charge densities and potentials are at their saddle-point values. The subscripts on the electric potentials are dropped because $\phi(\mathbf{r}) = \phi_{\text{el}}(\mathbf{r}) = \phi_{\text{or}}(\mathbf{r})$ from the minimization of H, as evident from Eqs. (4.28) and (4.29).

[1] The saddle-point approximation is also known as the method of steepest descents. Roughly speaking, it involves the deformation of the integration path to the complex plane, and we expect the integral to be dominated by the stationary point of the integrand in the complex plane. The detailed analytical structure is out of scope for this manuscript. We refer interested readers to pp. 203-209 of Ref. 14.

For nonequilibrium situations, the constitutive relations become

$$\nabla \cdot \mathbf{D} = \hat{\rho}_c(\mathbf{r}) \tag{4.17a}$$

$$\chi_{\mathrm{el}}(\mathbf{r}) = \Gamma(\mathbf{r}) \frac{\alpha}{\epsilon_0 v} \tag{4.17b}$$

$$1 = e^{-\beta v u(\mathbf{r}) + \frac{\beta\alpha}{2}|\nabla\phi_{\mathrm{el}}(\mathbf{r})|^2} \frac{\sinh(\beta\bar{\mu}|\nabla\phi_{\mathrm{or}}(\mathbf{r})|)}{\beta\bar{\mu}|\nabla\phi_{\mathrm{or}}(\mathbf{r})|} \tag{4.17c}$$

where the values of ϕ_{or} and χ_{or} for the nonequilibrium state $\mathcal{N}$ are from their values at the reactant equilibrium state $\mathcal{R}$. The electric displacement is given by $\mathbf{D} = -\epsilon_0(1+\chi_{\mathrm{el}})\nabla\phi_{\mathrm{el}}(\mathbf{r}) - \epsilon_0\chi_{\mathrm{or}}(\mathbf{r})\nabla\phi_{\mathrm{or}}(\mathbf{r})$, since ϕ_{or} and ϕ_{el} must now be distinguished because the relation $\phi_{\mathrm{or}} = \phi_{\mathrm{el}}$ no longer holds under the nonequilibrium condition.

The free energy of solvation can be obtained by substituting the saddle-point values of the functional arguments into the Hamiltonian in Eq. (4.14). Upon simplification, for which the details are given in Appendix 4.A, the free energy of solvation is written as

$$\begin{aligned} & G[\mathbb{C}, \hat{\rho}_c(\mathbf{r})] \\ = & \int d\mathbf{r} \left\{ \frac{1}{2}\epsilon_0(1+\chi_{\mathrm{el}}(\mathbf{r}))|\nabla\phi_{\mathrm{el}}(\mathbf{r})|^2 + \epsilon_0\chi_{\mathrm{or}}(\mathbf{r})|\nabla\phi_{\mathrm{or}}(\mathbf{r})|^2 \right. \\ & \left. -\frac{1}{\beta v}\Gamma(\mathbf{r}) \log\left[\frac{\sinh\beta\bar{\mu}|\nabla\phi_{\mathrm{or}}(\mathbf{r})|}{\beta\bar{\mu}|\nabla\phi_{\mathrm{or}}(\mathbf{r})|}\right] - \frac{1}{\beta v}\Gamma(\mathbf{r}) \right\} \end{aligned} \tag{4.18}$$

where $\mathbb{C} = \{\chi_{\mathrm{or}}, \phi_{\mathrm{or}}, \Gamma\}$ is the nuclear configuration set that contain all necessary information describing the nuclear configuration, and χ_{el} and ϕ_{el} are calculated using the constitutive relations. The saddle-point free energy as an integral over the whole space is infinite, but the divergent parts cancel in the evaluation of reorganization energy as presented in Appendix 4.B.

It is known that field-theoretic treatment of electrostatically interacting systems at the saddle-point level leads to the Poisson equation, as in Eqs. (4.16a) and (4.17a).[44,46,47] The spatially-varying orientational and electronic electric susceptibilities $\chi_{\mathrm{or}}(\mathbf{r})$ and $\chi_{\mathrm{el}}(\mathbf{r})$ describe the collective response of the permanent dipoles and the induced dipoles, respectively, given by Eqs. (4.16b), (4.16c), and (4.17b). The equations for

electric susceptibilities are equivalent to the nonlinear Langevin-Debye model when the field $-\nabla\phi$ is taken as the local field.[24,118–120] The incompressibility condition is accounted for at the mean-field level by Eqs. (4.16d) and (4.17c). Eqs. (4.16) to (4.18) are the key equations in the DSCFT. In the next section, we apply the DSCFT to a simple ET process between two ions and present results of our numerical calculations.

4.2.3 Application of DSCFT to Simple Electron Transfer Between Two Ions

In this section, we apply the DSCFT framework to a simple ET reaction $D^m + A^n \rightarrow D^{m+1} + A^{n-1}$ between two ions. Following Marcus's two-sphere model, the donor (D) and the acceptor (A) are modeled as two spherical cavities, each with a point charge at the center. The reactant state has charge distribution $\hat{\rho}_c^{(R)}(\mathbf{r}) = me\delta(\mathbf{r}-\mathbf{R}_D) + ne\delta(\mathbf{r}-\mathbf{R}_A)$, and the product state has charge distribution $\hat{\rho}_c^{(P)}(\mathbf{r}) = (m+1)e\delta(\mathbf{r}-\mathbf{R}_D)+(n-1)e\delta(\mathbf{r}-\mathbf{R}_A)$, where $\mathbf{R}_D$ and $\mathbf{R}_A$ are respectively the positions of the donor and the acceptor, and e is the elementary charge. The distance between the donor and the acceptor is $d = |\mathbf{R}_D - \mathbf{R}_A|$. The solute cavity $\mathcal{C}_\mathcal{S}(S = \mathcal{P}, \mathcal{R}, \mathcal{N})$ is represented by the set $\{\mathbf{r} : |\mathbf{r}-\mathbf{R}_D| < a_D^\mathcal{S} \text{ or } |\mathbf{r}-\mathbf{R}_A| < a_A^\mathcal{S}\}$, where $a_D^\mathcal{S}$ and $a_A^\mathcal{S}$ are, respectively, the radii of the species D and A in State $\mathcal{S}$.[2] For the equilibrium state $\mathcal{R}/\mathcal{P}$, $a_D^{\mathcal{R}/\mathcal{P}}$ and $a_A^{\mathcal{R}/\mathcal{P}}$ are taken to be the ionic radii of D^m/D^{m+1} and A^n/A^{n-1}, respectively. For the nonequilibrium State $\mathcal{N}$, the solute cavity takes the ionic radii of the species in State $\mathcal{R}$, such that $a_{D/A}^\mathcal{N} = a_{D/A}^\mathcal{R}$, because States $\mathcal{N}$ and $\mathcal{R}$, having the same solvent nuclear configuration, have the same region inaccessible to the solvent. $\Gamma^\mathcal{S}(\mathbf{r})$, the indicator function of the solute cavity $\mathcal{C}_\mathcal{S}$, equals 0 when $\mathbf{r} \in \mathcal{C}_\mathcal{S}$ and 1 otherwise.

Under a particular distribution of the solute charge, the nonequilibrium free energy can be evaluated with respect to the free energy at the equilibrium state for the same solute charge distribution. In doing so, the free energy surface $G^{(R)}$ in the reactant

[2]For solutes with a more complex structure, it may be the most convenient to describe the solute cavity as a union of van der Waals spheres of the atoms. The topic of solute cavity has been extensively reviewed in Ref. 121.

charge state and the free energy surface $G^{(P)}$ in the product charge state are expressed as

$$G^{(R)} = G[\mathbb{C}, \hat{\rho}_c^{(R)}] - G_{\rm eq}^{(R)} \tag{4.19}$$

$$G^{(P)} = G[\mathbb{C}, \hat{\rho}_c^{(P)}] - G_{\rm eq}^{(P)} + \Delta G^0 \tag{4.20}$$

where ΔG^0 is the free energy of the reaction. $G_{\rm eq}^{(R)}$ and $G_{\rm eq}^{(P)}$ are the free energies at the equilibrium states $\mathcal{R}$ and $\mathcal{P}$, respectively, given by $G_{\rm eq}^{(R)} = G[\mathbb{C}^{\mathcal{R}}, \hat{\rho}_c^{(R)}]$ and $G_{\rm eq}^{(P)} = G[\mathbb{C}^{\mathcal{P}}, \hat{\rho}_c^{(P)}]$, where $\mathbb{C}^{\mathcal{S}} = \{\chi_{\rm or}^{\mathcal{S}}, \phi_{\rm or}^{\mathcal{S}}, \Gamma^{\mathcal{S}}\}$ ($\mathcal{S} = \mathcal{R}, \mathcal{P}$) is the nuclear configuration set of state $\mathcal{S}$. $\chi_{\rm or}^{\mathcal{R}}$, $\phi_{\rm or}^{\mathcal{R}}$, and $\Gamma^{\mathcal{R}}$ are the values of $\chi_{\rm or}$, $\phi_{\rm or}$, and Γ in the reactant equilibrium state $\mathcal{R}$; $\chi_{\rm or}^{\mathcal{P}}$, $\phi_{\rm or}^{\mathcal{P}}$, and $\Gamma^{\mathcal{P}}$ are defined similarly. The reorganization energy λ is then

$$\lambda = G[\mathbb{C}^{\mathcal{R}}, \hat{\rho}_c^{(P)}] - G[\mathbb{C}^{\mathcal{P}}, \hat{\rho}_c^{(P)}] \tag{4.21}$$

A strategy for evaluating λ is presented in Appendix 4.B, where allowance is made for the solute cavities in the reactant and the product states to be different (i. e. $\Gamma^{\mathcal{R}} = \Gamma^{\mathcal{P}}$ is not required).

To simplify the calculation further, we approximate the solution to Eqs. (4.16a) and (4.17a) by assuming that the electric displacement $\mathbf{D}$ can be written as the superposition of the displacement due to each individual point charge as [3]

$$\mathbf{D}(\mathbf{r}) = \frac{q_1}{4\pi r_D^2}\hat{\mathbf{r}}_D + \frac{q_2}{4\pi r_A^2}\hat{\mathbf{r}}_A \tag{4.22}$$

where $\mathbf{r}_{D/A} = \mathbf{r} - \mathbf{R}_{D/A}$ and $\hat{\mathbf{r}}_{D/A}$ indicates the unit vector in the direction of $\mathbf{r}_{D/A}$. We expect that the error due to this approximation is small, as the jump in dielectric constant at the boundary of the solute cavity is not significant because of dielectric saturation.

For each state, we perform numerical calculations on a bispherical coordinate

[3] We note that the equation $\nabla \cdot \mathbf{D} = \hat{\rho}_c(\mathbf{r})$ does not imply the superposition principle. The superposition principle holds for the electric displacement $\mathbf{D}$ only when the dielectric continuum is uniform.

(σ, τ, φ), which is related to the cylindrical coordinate (r, z, φ) by $z = a_0 \sinh\sigma/(\cosh\sigma - \cos\tau)$ and $r = a_0 \sin\tau/(\cosh\sigma - \cos\tau)$.[122] Each constant-$\sigma$ surface in the bispherical coordinate is circle of radius $a_0/|\sinh\sigma|$ with its center located at $z = a_0 \coth\sigma$. The value of a_0 is determined by the ionic radii of the donor and the acceptor and their distance, and by requiring that the cavity boundaries of the donor and the acceptor are each a surface of constant σ, and that the region accessible by the solvent is simply described by $\sigma_A < \sigma < \sigma_D$. This is achieved by simultaneously solving

$$\frac{a_0}{|\sinh\sigma_D|} = a_D \tag{4.23a}$$

$$\frac{a_0}{|\sinh\sigma_A|} = a_A \tag{4.23b}$$

$$a_0 \coth\sigma_D - a_0 \coth\sigma_A = d \tag{4.23c}$$

That is, the donor cavity surface is $\sigma = \sigma_D = \cosh^{-1}\left(\frac{a_D^2 - a_A^2 + d^2}{2a_D d}\right)$, and the acceptor cavity surface is $\sigma = \sigma_A = -\cosh^{-1}\left(\frac{a_A^2 - a_D^2 + d^2}{2a_A d}\right)$, and $a_0 = a_D \sinh\sigma_D$. Due to the cylindrical symmetry in the problem, we only have to perform calculations on the two-dimensional $\sigma\tau$-plane. The integration for the free energy is carried out on a 240×680 $\sigma\tau$-grid between $\sigma \in (\sigma_A, \sigma_D)$ and $\tau \in (0, \pi)$. The potential ϕ in the equilibrium state is found by iteration until the next iteration produces a reduced electric field $\nabla\phi/[\frac{e}{4\pi\epsilon_0(2a_D a_A/(a_D + a_A))}]$ within 10^{-6} from its current value at all grid points.

4.3 Results and Discussions

In this section, we consider ET reactions in water, for which the molecules have a vacuum permanent dipole moment $\bar{\mu} = 1.85\,\mathrm{D}$, polarizability $\alpha = 1.45\,\text{Å}^3$, and molecular volume $v = 30.0\,\text{Å}^3$. The temperature is $T = 298.15\,\mathrm{K}$. Here, we consider self-exchange reactions, which involve only two species before and after the reaction, and thus, we simplify the notation for the solute radii as $a_D = a_D^{\mathcal{R}} = a_A^{\mathcal{P}}$ and $a_A = a_A^{\mathcal{R}} = a_D^{\mathcal{P}}$.

4.3.1 A Unified Description of Solvent Molecules

As a first step, we evaluate the outer-sphere solvent reorganization energy using the DSCFT for the Fe^{2+}/Fe^{3+} exchange reaction. We set the radii of the solute cavities to be $a_D = 3.31\,\text{Å}$ and $a_A = 3.18\,\text{Å}$, which are the radii of $[Fe(H_2O)_6]^{2+}$ and $[Fe(H_2O)_6]^{3+}$, respectively.[4] We note that in the product equilibrium state $\mathcal{P}$, the radii of the ET species are switched. For self-exchange reactions, the reorganization energy can be calculated as the free energy difference between the nonequilibrium state $\mathcal{N}$ and reactant equilibrium state $\mathcal{R}$, both involving the same nuclear configuration, and thus the same solvent accessible space. At the contact distance of $d = 6.5$ Å between the two spherical ions, the DSCFT predicts the outer-sphere solvent reorganization to be 26.2 kcal/mol, in good agreement with the earlier value of 27.6 kcal/mol given in the literature.[65]

Even though the separation of the inner- and the outer-sphere contributions is a widely-used strategy for evaluating reorganization energies, the discrimination between the inner- and the outer-sphere molecules introduces additional parameters to the theory . Furthermore, the treatment ignores dipolar interactions between the inner- and the outer-sphere solvent molecules. In contrast, MD simulations do not distinguish between the inner- and the outer-sphere molecules – the same forcefield is used on all solvent molecules, regardless of their distances from the ions. A theory based on molecular-level interactions around the ions should be able to treat all solvent molecules on equal footing. Since the DSCFT is able to account for the spatial variation in the solvent response at the molecular length scale, we expect that distinction of the inner- and the outer-sphere solvent molecules may not be necessary, and the reorganization energy due to *all* solvent molecules can be directly evaluated.

To test how well DSCFT can predict the reorganization energy by treating all solvent molecules in a unified manner, we calculate the *total* reorganization energy for a variety of ET reactions between simple ions. We set the cavity radii a_D and a_A to be the crystal ionic radii of the donor and the acceptor, and use earlier litera-

[4]The radii of $Fe(H_2O)_6^{2+}$ and $Fe(H_2O)_6^{3+}$ are calculated based on their sum (contact distance) 6.5 Å and their difference 0.13 Å. See Ref. 65 and 88.

ture values of the donor-acceptor distance for the value of d. Table 4.1 tabulates the reorganization energy and the activation energy for selected ET reactions calculated by the DSCFT, together with values from earlier calculations in the literature that treat the inner- and outer-sphere reorganization energies separately, as well as values obtained from experiments.[5] In reality, the electron transfer occurs at a range of donor-acceptor separation d (e. g. around 4.5 Å to 5.5 Å for Fe^{2+}/Fe^{3+} exchange),[123] and thus, the comparison between the calculated value based on a typical value of d within this range and the experimentally-measured values serves only to provide qualitative validation of our approach. We observe that the activation energies calculated using DSCFT are generally within a few kilocalorie per mole from literature values. This suggests that the DSCFT, with readily-available parameters describing the solvent and the solutes, can make reliable predictions for the direct evaluation of the *total* reorganization energy by a unified treatment of the inner-sphere and the outer-sphere solvent molecules. We note in addition that, even though explicit solvent structure and molecular specific interactions have not been taken into account in the DSCFT, the DSCFT predicts the value of 20.3 kcal/mol for ET activation energy for Fe^{2+}/Fe^{3+} exchange in water, in excellent agreement with the value of 20 kcal/mol from atomistic simulations by Kuharski et al.[88]

[5]The activation free energy $\Delta G^{\ddagger}$ is calculated from the values of temperature T, enthalpy of activation $\Delta H^{\ddagger}$, and entropy of activation $\Delta S^{\ddagger}$ compiled in Ref. 63 through $\Delta G^{\ddagger} = \Delta H^{\ddagger} - T\Delta S^{\ddagger}$.

Table 4.1: The DSCFT-calculated reorganization energy λ_{DSCFT} and activation energy $\Delta G^{\ddagger}_{\mathrm{DSCFT}}$, as well as the total activation energy $\Delta G^{\ddagger}_{\mathrm{cal}}$ from earlier calculations in the literature that treat the inner- and outer-sphere reorganization energies separately, and experimentally obtained activation energy $\Delta G^{\ddagger}_{\mathrm{exp}}$ for a range of ET reactions. The crystal ionic radii in Ref. 1 are used for the cavity radii of the solutes. High-spin and low-spin species are denoted by hs and ls, respectively.

Donor/Acceptor	a_D [Å]	a_A [Å]	d [Å]	λ_{DSCFT} [kcal/mol]	$\Delta G^{\ddagger}_{\mathrm{DSCFT}}$ [kcal/mol]	$\Delta G^{\ddagger}_{\mathrm{cal}}$ [kcal/mol]	$\Delta G^{\ddagger}_{\mathrm{exp}}$ [kcal/mol]
Fe^{2+}/Fe^{3+}(hs)	0.92	0.785	5.25[6]	81.4	20.3	19.3[7],14.8[8]	16.6[2],14.9[3]
Fe^{2+}/Fe^{3+}(ls)	0.75	0.69	5.25[1]	57.2	14.3		
Co^{2+}/Co^{3+}(hs)	0.885	0.75	6.6[9]	90.9	22.7	21.7[4]	16.5[2]
Co^{2+}/Co^{3+}(ls)	0.79	0.685	6.6[4]	87.1	21.8		
Mn^{2+}/Mn^{3+}(hs)	0.97	0.785	5.36[5]	101	25.2	20.2[2]	$\geq$16.6[2]
Mn^{2+}/Mn^{3+}(ls)	0.81	0.72	5.36[5]	70.4	17.6		
V^{2+}/V^{3+}	0.93	0.78	5.33[10]	88.3	22.1	16.7[2]	20.2[2]
Cr^{2+}/Cr^{3+}	0.94	0.755	5.32[5]	106	26.5	20.3[2]	$\geq$23.9[2]
Ru^{2+}/Ru^{3+}	0.87	0.82	6.5[4]	46.3	11.6	10.5[4]	-
Ce^{3+}/Ce^{4+}	1.15	1.01	7.36[2]	75.6	18.9	19.3[2]	19.0[2]
Pu^{3+}/Pu^{4+}	1.14	1.00	7.24[2]	76.3	19.1	20.9[2]	16.3[2]
Pa^{3+}/Pa^{4+}	1.16	1.04	7.34[2]	65.7	16.4	20.4[2]	-
U^{3+}/U^{4+}	1.165	1.03	7.3[2]	71.7	17.9	20.5[2]	-
Am^{3+}/Am^{4+}	1.115	0.99	7.22[2]	71.6	17.9	21.0[2]	-

Some ionic solutes have a high-spin state and a low-spin state. It has been proposed that spin-exchange may couple to ET reactions, such that the less prevalent spin state serves as the reaction intermediate.[126] Therefore, for ionic species that have a high-spin state and a low-spin state, we calculate the activation energy of electron transfer for both the high-spin and the low-spin species. For the Fe^{2+}/Fe^{3+} exchange, the Co^{2+}/Co^{3+} exchange, and the Mn^{2+}/Mn^{3+} exchange considered in this work, we found that the ET processes between ions of low-spin states have lower activation energies than those between ions in the high-spin state. By comparing the calculated ET activation energies and the experimentally obtained value, our result suggests that the Mn^{2+}/Mn^{3+} exchange may primarily occur between the low-spin Mn^{2+} and Mn^{3+}, as the experimentally obtained activation energy is comparable to the DSCFT-calculated activation energy between the low-spin Mn^{2+} and Mn^{3+}. For the Fe^{2+}/Fe^{3+} exchange, the experimentally obtained activation energy is in between the DSCFT-calculated activation energies for the high-spin and the low-spin Fe ions, thus our result suggests that both the exchange between the high-spin ions and the exchange between the low-spin ions occur under experimental conditions. For the Co^{2+}/Co^{3+} exchange, the DSCFT-calculated activation energy, as well as the activation energy calculated in earlier literature, are much higher than the experimentally obtained activation energy. The reason for this may be the presence of an alternative pathway for electron transfer, as discussed in several earlier papers[127,128] and reviewed by Sutin in Ref. 65.

Since the DSCFT is able to compute the all-solvent contribution towards the reorganization energy, we further investigate its dependence on the size of the solutes. In the immediate vicinity of an ion, the effect of dielectric saturation causes the static dielectric constant ϵ_s to approach the optical dielectric constant ϵ_∞, and thus the Pekar factor $(1/\epsilon_\infty - 1/\epsilon_s)$ in this region is small compared to its bulk value. Such effect of dielectric saturation is not accounted for in the linear dielectric theory, which predicts /the solvent reorganization energy to be proportional to the Pekar factor of the bulk solvent as given by Eq. (4.4). When the ionic radius of the solute is small or the charge on the solute is large, the effect of dielectric saturation is significant,

and we expect that the actual solvent reorganization energy in these situations will be much smaller than that predicted by the linear dielectric theory.

Here, we compare the solvent reorganization energies calculated using the DSCFT and the linear dielectric theory for the reaction $M^m + M^{m+1} \rightarrow M^{m+1} + M^m$ at $m = 0, 1$ and 2. We fix the donor-acceptor distance at $d = 10$ Å, and ignore the size difference between the donor and the acceptor by assuming $a_D = a_A = a$. In Fig. 4.3, we plot the reorganization energy as a function of solute radius a. We observe that the linear dielectric theory works well only for solute radius more than approximately 3.5 Å, comparable to the radii of typical coordinated ion complexes. This is probably the reason for separating the inner- and the outer-sphere treatments for the solvent in the linear dielectric theory, since solvent molecules in the outer-sphere are at a sufficient distance away from the ion to be reasonably treated using linear dielectric theory. For smaller solutes with radii less than 3.5 Å, the reorganization energy not only depends on the amount of charge transferred, but also on the magnitude of charge on the solutes, contrary to the prediction of linear dielectric theory. Furthermore, it is intriguing that the solvent reorganization energy for self-exchange between charged solutes stays constant for $a \lessapprox 2.5$ Å, but this effect is absent for the 0/1+ exchange reaction. This can be understood as a manifestation of dielectric saturation – as the orientational dipoles are fully saturated within $a \lessapprox 2.5$ Å from an ion, this saturated region is not much affected if the charge on the ion changes by e, and therefore, the polarization in this region does not contribute to the reorganization energy.

The unified treatment of the inner-sphere and the outer-sphere solvent molecules considerably simplifies the calculation of reorganization energies. Although we have ignored the specific interactions between the ions and their coordinated solvent molecules, by treating the spatially dependent electrostatic interaction between the ions and the solvent molecules, we are able to capture the energetics of the coordination bonds. This is most likely because electrostatic interaction is the main factor in determining the energetics of ion-solvent interactions. We also note that while the DSCFT accounts for the excluded volume of the solvent molecules by the incompressibility constrain, it does not account for the liquid-state packing structure of the solvent

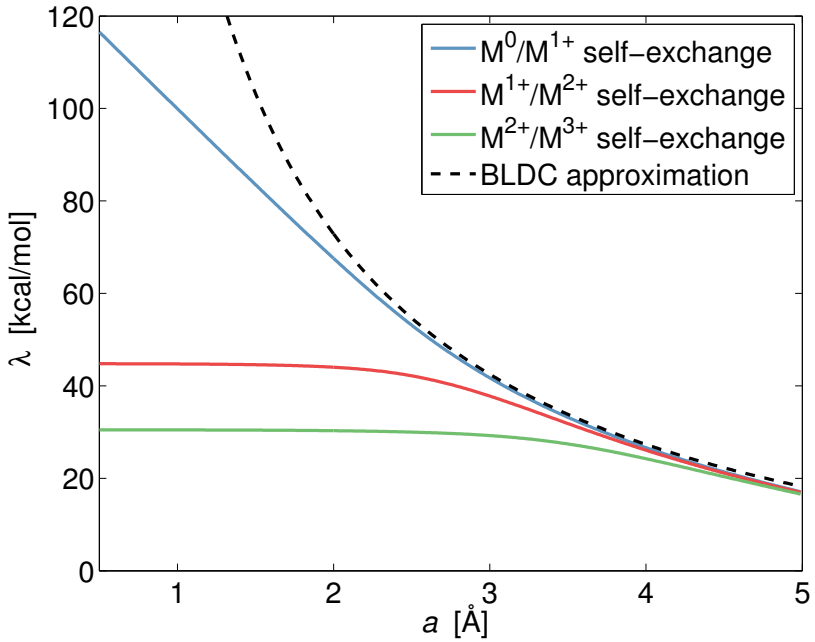

Figure 4.3: The reorganization energy λ as a function of the radius of solutes a for fixed interionic separation 10 Å in water. The bulk linear dielectric constant (BLDC) approximation is calculated using Eq. (4.4), with static dielectric constant $\epsilon_s = 80.1$ and optical dielectric constant $\epsilon_\infty = n^2 = 1.33^2$, where n denotes the refractive index.

molecules. Yet the previous success of the DSCFT in capturing the equilibrium solvation free energy of ions in both single-component liquids and binary mixtures[44] and the current success in describing the reorganization energy for ET reactions, seem to suggest that geometric packing of the solvent, at least for simple molecules, may not be important, due to the long-range nature of the electrostatic interactions, which is not much affected by smearing out the local molecular density.

4.3.2 The Nonequilibrium Solvation Free Energy Surface

A consequence of the linear dielectric description for the solvent is that the nonequilibrium free energy surfaces in the reactant and the product charge states are two parabolas of equal curvature. This leads to Eq. (4.1), a simple relationship between the activation energy and the reorganization energy, and Eq. (4.4), the prediction that the solvent reorganization energy depends on the amount of charge transfer but not

on the magnitude of charge on the electron-transferring species. In this section, we apply the DSCFT to calculate the nonequilibrium free energy surface as a function of the reaction coordinate, and explore the alterations to predictions of the linear dielectric theory as a result of a more refined description of solvent response.

We calculate the free energy surfaces for two model reactions of the form $M^m + M^n \rightarrow M^{m+1} + M^{n-1}$ with (i) $m = +2$ and $n = +3$, and (ii) $m = 0$ and $n = +1$. For simplicity, we set the radii of all solute species to be $a = 1\,\text{Å}$, regardless of their charge states, so that $\Gamma(\mathbf{r})$ is independent of the states. The distance between the donor and the acceptor is set to be $d = 5.25\,\text{Å}$ apart. It is common to calculate the free energy as a function of a charging parameter ζ, with $\chi_{\text{or}}(\zeta)$ and $\phi_{\text{or}}(\zeta)$ representing the equilibrium value of χ_{or} and ϕ_{or} when the solute is $M^{m+\zeta} + A^{n-\zeta}$. We write $G^{(R)}$ and $G^{(P)}$ as a function of ζ as

$$G^{(R)}(\zeta) = G[\mathbb{C}(\zeta), \hat{\rho}_c^{(R)}] - G_{\text{eq}}^{(R)} \tag{4.24}$$

$$G^{(P)}(\zeta) = G[\mathbb{C}(\zeta), \hat{\rho}_c^{(P)}] - G_{\text{eq}}^{(P)} + \Delta G^o \tag{4.25}$$

where $\mathbb{C}(\zeta) = \{\chi_{\text{or}}(\zeta), \phi_{\text{or}}(\zeta), \Gamma\}$.

In Fig. 4.4, we plot $G^{(R)}(\zeta)$ and $G^{(P)}(\zeta)$ for the exchange reactions between M^{2+} and M^{3+} and between M^0 and M^{1+}. We note that for both reactions, the free energy curves are well represented as parabolas in the relevant part of the reaction coordinate. This is because, for a self-exchange reaction, anharmonicity in solvent response cancels out due to the symmetry of the reaction.[71] Our result is in agreement with earlier MD simulations, which have also found the parabolic free energy surfaces to be a good description for self-exchange reactions.[88,129]

However, the curvature of the free energy parabola depends strongly on the charge on the electron-transferring species, contrary to the prediction of linear dielectric theory. The reorganization energy for the electron exchange between M^0 and M^{1+} is larger than that between M^{2+} and M^{3+} by about a factor of four. Our results are consistent with earlier findings in molecular simulations of ET reaction in nonpolarizable solvents.[79,80]

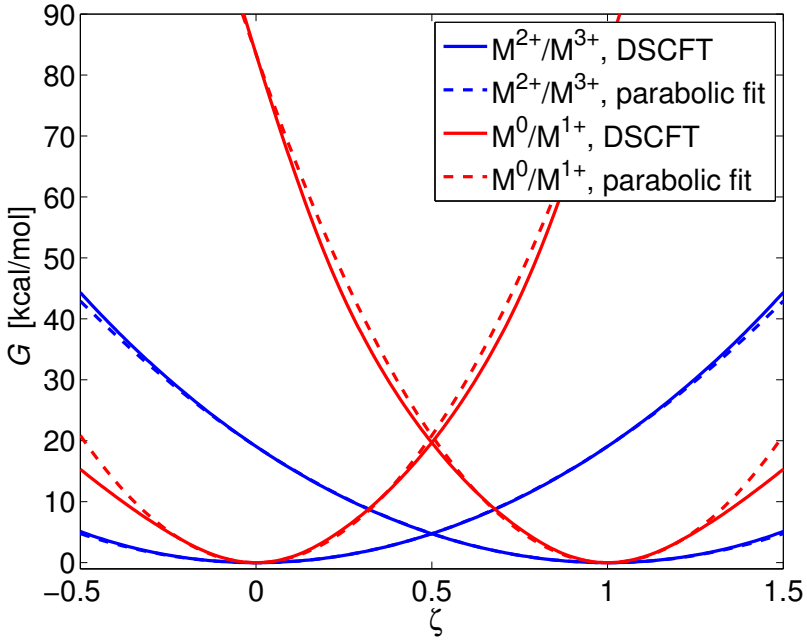

Figure 4.4: Free energy curves vs. the charging parameter ζ for self-exchange reactions. Each dashed line is a parabolic fit to the corresponding free energy curve that passes through the values of $G(\zeta = 0)$ and $G(\zeta = 1)$.

We expect that the change in the solvent orientational polarization between the reactant and the product states is a key factor determining the magnitude of reorganization energy. To gain insight on how the reorganization energy depends on the charge of the solutes, we examine the change in the solvent orientational polarization $\Delta\mathbf{P}_{\rm or}$ between the reactant and the product equilibrium state given by

$$\begin{aligned} \Delta\mathbf{P}_{\rm or} &= \mathbf{P}^{(P)}_{\rm or,eq} - \mathbf{P}^{(R)}_{\rm or,eq} \\ &= -\epsilon_0 \chi^{\mathcal{P}}_{\rm or} \nabla\phi^{\mathcal{P}}_{\rm or} + \epsilon_0 \chi^{\mathcal{R}}_{\rm or} \nabla\phi^{\mathcal{R}}_{\rm or} \end{aligned} \tag{4.26}$$

where $\mathbf{P}^{(R)}_{\rm or,eq}$ and $\mathbf{P}^{(P)}_{\rm or,eq}$ denote the equilibrium solvent orientational polarization in the reactant and the product charge states. Fig. 4.5 plots the spatial variation of $|\Delta\mathbf{P}_{\rm or}|$ around the donor and the acceptor. As suggested by the figure, the change in orientational polarization in the M^0/M^{1+} exchange reaction is more substantial in magnitude and more extensive in space than that in the M^{2+}/M^{3+} reaction, resulting in the larger reorganization energy in the M^0/M^{1+} exchange reaction.

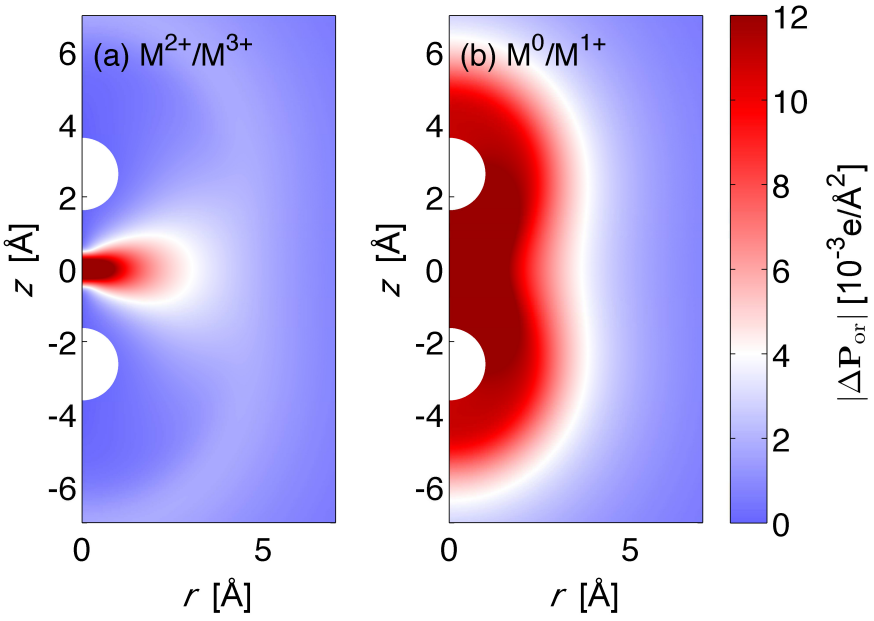

Figure 4.5: The magnitude of change in the orientational polarization $|\Delta \mathbf{P}_{\mathrm{or}}|$ between the reactant and the product equilibrium states for (a) the M^{2+}/M^{3+} exchange reaction and (b) the M^{0}/M^{1+} exchange reaction. The values of polarization change has unit $10^{-3}e/\text{Å}^2$ on a cross section around the donor and the acceptor in the cylindrical coordinate.

4.4 Conclusions

Using field-theoretic techniques, we have developed a dipolar self-consistent-field theory (DSCFT) for treating charge solvation under both equilibrium and nonequilibrium conditions, and applied the theory to study solvent reorganization in ET reactions. The central result of the DSCFT theory consists of two sets of easily-solvable constitutive relations, one applicable under the equilibrium condition and the other under the nonequilibrium condition, as well as an expression for the free energy of the system. With readily available parameters, the DSCFT provides a coarse-grained molecular theory for the reorganization energies and activation energies in self-exchange ET reactions.

Because the DSCFT naturally accounts for the spatial variation in the solvent response, it can be used to directly calculate the total solvent reorganization energy without making a distinction between the inner-sphere and outer-sphere solvent molecules. The activation energies of a range of simple ET reactions calculated with the DSCFT are within a few kilocalories per mole from previous calculated or experimentally-obtained values. The dependence of the reorganization energy on the size of the solutes suggests that a saturation zone within approximately 2.5 Å from the center of the charged solutes contributes insignificantly to the reorganization energy. In addition, we find that for solutes with radii larger than approximately 3.5 Å, the solvent can be reasonably described by the bulk optical and static dielectric constants. Furthermore, by calculating the free energy landscape for model charge-exchange reactions, we find that the free energy surfaces are well described by two equal-curvature parabolas. However, contrary to the prediction of linear dielectric theory, the reorganization energy depends strongly on the magnitude of charge on the solutes. In fact, for the geometry considered in this work, there is a four-fold difference between the solvent reorganization energies of the M^0/M^{1+} exchange and the M^{2+}/M^{3+} exchange. This large difference in reorganization energy would be very significant for the kinetics of ET reactions.

We have focused on applying the DSCFT to ET reactions between two simple

ions in this chapter, but the method can be extended to solutes with more complicated geometries, such as multiatom molecules and proteins, by altering the solute charge distribution $\hat{\rho}_c(\mathbf{r})$ and the solute cavity $\mathcal{C}$. Furthermore, while in this work we have only applied the DSCFT to self-exchange reactions, the theory can be applied to asymmetric ET reactions where there is a change in charge and/or solute cavity, provided that the free energy change of the reaction ΔG^0 is given. Since the DSCFT makes no assumptions on the form of the reorganization energy, it is a suitable tool for studying nonlinearity and asymmetry in the solvent response for general ET processes.[100] In addition, the framework of the DSCFT can be easily extended to ET reactions in solvent mixtures, where preferential solvation is expected to have significant effects in the solvent reorganization.[44,130–132] We will examine such effects on ET reactions in solvent mixtures in a forthcoming work.

Finally, we note that while field-theoretical techniques are widely used in soft-matter and polymeric systems, we are not aware of its application to chemical reactions. We believe the application of field-theoretical techniques to chemical systems is a fruitful direction, particularly in cases where there are a large number of fluctuating environmental degrees of freedom.

Appendix 4.A Extremization of the Field Hamiltonian

Starting from Eq. (4.14), extremization of H with respect to w, ρ_{or}, ρ_{el}, w_{or}, and w_{el} respectively gives

$$\begin{aligned} 1 &= \frac{e^{\beta\mu}}{\eta} 4\pi\bar{\mu}^2 \left(\frac{2\pi\alpha}{\beta}\right)^{\frac{3}{2}} v \\ &\quad \times e^{ivw(\mathbf{r})} \frac{\sin(\bar{\mu}|\nabla w_{\mathrm{or}}(\mathbf{r})|)}{\bar{\mu}|\nabla w_{\mathrm{or}}(\mathbf{r})|} e^{-\frac{\alpha}{2\beta}(\nabla w_{\mathrm{el}}(\mathbf{r}))^2} \end{aligned} \tag{4.27}$$

$$iw_{\mathrm{or}}(\mathbf{r}) = \beta \int d\mathbf{r}' \frac{\hat{\rho}_c(\mathbf{r}') + \rho_{\mathrm{or}}(\mathbf{r}') + \rho_{\mathrm{el}}(\mathbf{r}')}{4\pi\epsilon_0|\mathbf{r}-\mathbf{r}'|} \tag{4.28}$$

$$iw_{\rm el}(\mathbf{r}) = \beta \int d\mathbf{r}' \frac{\hat{\rho}_c(\mathbf{r}') + \rho_{\rm or}(\mathbf{r}') + \rho_{\rm el}(\mathbf{r}')}{4\pi\epsilon_0|\mathbf{r}-\mathbf{r}'|} \tag{4.29}$$

$$\begin{aligned}\rho_{\rm or}(\mathbf{r}) &= -i\frac{e^{\beta\mu}}{\eta}4\pi\bar{\mu}^2\left(\frac{2\pi\alpha}{\beta}\right)^{\frac{3}{2}} \\ &\times\nabla\cdot\left[\Gamma(\mathbf{r})e^{ivw(\mathbf{r})}e^{-\frac{\alpha}{2\beta}(\nabla w_{\rm el})^2}\mathcal{G}(\bar{\mu}|\nabla w_{\rm or}|)\bar{\mu}^2\nabla w_{\rm or}\right]\end{aligned} \tag{4.30}$$

$$\begin{aligned}\rho_{\rm el}(\mathbf{r}) &= i\frac{e^{\beta\mu}}{\eta}4\pi\bar{\mu}^2\left(\frac{2\pi\alpha}{\beta}\right)^{\frac{3}{2}}\left(\frac{\alpha}{\beta}\right) \\ &\times\nabla\cdot\left[\Gamma(\mathbf{r})e^{ivw(\mathbf{r})}e^{-\frac{\alpha}{2\beta}(\nabla w_{\rm el})^2}\frac{\sin(\bar{\mu}|\nabla w_{\rm or}|)}{\bar{\mu}|\nabla w_{\rm or}|}\nabla w_{\rm el}\right]\end{aligned} \tag{4.31}$$

where $\mathcal{G}(x) = (1/\tan x - 1/x)(\sin x)/x^2$.

Eq. (4.27) is obtained by extremizing w outside the solute cavity. Inside the solute cavity where w is not defined, we set $w = 0$. Furthermore, by letting the fields u, $w_{\rm or}$, and $w_{\rm el}$ goes to zero as $|\mathbf{r}| \to \infty$, Eq. (4.27) gives

$$1 = \frac{e^{\beta\mu}}{\eta}4\pi\bar{\mu}^2\left(\frac{2\pi\alpha}{\beta}\right)^{\frac{3}{2}} v \tag{4.32}$$

Furthermore, Eqs. (4.28) and (4.29) can be rewritten by taking the Laplacian on both sides of the equation:

$$-i\frac{\epsilon_0}{\beta}\nabla^2 w_{\rm or}(\mathbf{r}) = \hat{\rho}_c(\mathbf{r}) + \rho_{\rm or}(\mathbf{r}) + \rho_{\rm el}(\mathbf{r}) \tag{4.33}$$

$$-i\frac{\epsilon_0}{\beta}\nabla^2 w_{\rm el}(\mathbf{r}) = \hat{\rho}_c(\mathbf{r}) + \rho_{\rm or}(\mathbf{r}) + \rho_{\rm el}(\mathbf{r}) \tag{4.34}$$

With these, the constitutive relations in Eq. (4.16) can be derived by noting that Eqs. (4.27) to (4.31) all hold under the equilibrium condition. On the other hand, Eq. (4.17) can be derived by noting that $\rho_{\rm or}$ and $w_{\rm or}$ are out of equilibrium under the nonequilibrium condition, and therefore only Eqs. (4.27), (4.29), and (4.31) holds.

To derive the saddle-point free energy, we substitute the nonequilibrium set of constitutive relations and the out-of-equilibrium value of $\rho_{\rm or}$ into the field Hamiltonian

in Eq. (4.14). Following integration by parts, we arrive at

$$\begin{aligned} G &= \int d\mathbf{r} \left\{ \frac{1}{2}\epsilon_0 |\nabla\phi_{\rm el}(\mathbf{r})|^2 + \epsilon_0\chi_{\rm el}(\mathbf{r})|\nabla\phi_{\rm el}(\mathbf{r})|^2 \right. \\ &\qquad \left. + \epsilon_0\chi_{\rm or}(\mathbf{r})|\nabla\phi_{\rm or}(\mathbf{r})|^2 - \Gamma(\mathbf{r})u(\mathbf{r}) - \Gamma(\mathbf{r})\frac{1}{\beta v} \right\} \\ &= \int d\mathbf{r} \left\{ \frac{1}{2}\epsilon_0 |\nabla\phi_{\rm el}(\mathbf{r})|^2 + \epsilon_0\chi_{\rm el}(\mathbf{r})|\nabla\phi_{\rm el}(\mathbf{r})|^2 \right. \\ &\qquad + \epsilon_0\chi_{\rm or}(\mathbf{r})|\nabla\phi_{\rm or}(\mathbf{r})|^2 - \frac{1}{\beta v}\Gamma(\mathbf{r}) \\ &\qquad \left. - \frac{1}{\beta v}\Gamma(\mathbf{r}) \log\left[\frac{\sinh \beta\bar{\mu}|\nabla\phi_{\rm or}(\mathbf{r})|}{\beta\bar{\mu}|\nabla\phi_{\rm or}(\mathbf{r})|} e^{\frac{\beta\alpha}{2}(\nabla\phi_{\rm el}(\mathbf{r}))^2} \right] \right\} \\ &= \int d\mathbf{r} \left\{ \frac{1}{2}\epsilon_0 (1+\chi_{\rm el}(\mathbf{r}))|\nabla\phi_{\rm el}(\mathbf{r})|^2 + \epsilon_0\chi_{\rm or}(\mathbf{r})|\nabla\phi_{\rm or}(\mathbf{r})|^2 \right. \\ &\qquad \left. - \frac{1}{\beta v}\Gamma(\mathbf{r}) \log\left[\frac{\sinh \beta\bar{\mu}|\nabla\phi_{\rm or}(\mathbf{r})|}{\beta\bar{\mu}|\nabla\phi_{\rm or}(\mathbf{r})|} \right] - \frac{1}{\beta v}\Gamma(\mathbf{r}) \right\} \end{aligned} \tag{4.35}$$

which is the expression for saddle-point free energy, Eq. (4.18). The last term in the integrand describes the translational entropy of the solvent molecules.[14]

Appendix 4.B Treatment of the Solute Cavity in the Evaluation of Reorganization Energy

In this section, we present the general strategy for evaluating the reorganization energy and show that the divergent part in the saddle-point free energy G is canceled in the evaluation. In this work, the solute cavity is treated as part of the nuclear configuration parameter $\mathbb{C}$ to the saddle-point free energy. To allow for difference in solute cavities in the reactant and the product states, we reference each free energy to that of a state in vacuum with the same charge distribution, so that the free energy contribution from within the cavity is canceled. The resulting dependence of reorganization energy λ on the solute cavities $\Gamma^{\mathcal{R}}$ and $\Gamma^{\mathcal{P}}$ is explicitly included in Eq. (4.39).

Let $G_0[\hat{\rho}_c]$ be the free energy of the charged distribution $\hat{\rho}_c(\mathbf{r})$ in vacuum. In a vacuum, $\chi_{\rm or} = \chi_{\rm el} = 0$, and the saddle-point free energy reduces to

$$G_0 = \int d\mathbf{r}\, \frac{1}{2}\epsilon_0 |\nabla\phi_0(\mathbf{r})|^2 \tag{4.36}$$

where $\phi_0(\mathbf{r})$ is the electric potential in the vacuum calculated through the Poisson equation Eq. (4.16a), or

$$\phi_0(\mathbf{r}) = \int d\mathbf{r}' \frac{\hat{\rho}_c(\mathbf{r})}{4\pi\epsilon_0|\mathbf{r}-\mathbf{r}'|} \tag{4.37}$$

Starting from Eq. (4.21), we subtract and add the free energy of vacuum charge distribution $\hat{\rho}_c^{\mathcal{P}}$, i. e.,

$$\lambda \;=\; (G[\mathbb{C}^{\mathcal{R}}, \hat{\rho}_c^{(P)}] - G_0[\hat{\rho}_c^{(P)}]) - (G[\mathbb{C}^{\mathcal{P}}, \hat{\rho}_c^{(P)}] - G_0[\hat{\rho}_c^{(P)}]) \tag{4.38}$$

In each of the brackets in the above equation, the contributions to the free energy from the region within the solute cavity cancel off, so the integral in each bracket only needs to be evaluated outside the solute cavity. Therefore, the reorganization energy can be calculated as

$$\begin{aligned}
\lambda \;=\; & \int d\mathbf{r}\, \Gamma^{\mathcal{R}}(\mathbf{r}) \left\{ \frac{1}{2}\epsilon_0(1+\chi_{\rm el}^{\mathcal{N}}(\mathbf{r}))|\nabla\phi_{\rm el}^{\mathcal{N}}(\mathbf{r})|^2 \right. \\
& \left. +\epsilon_0\chi_{\rm or}^{\mathcal{R}}(\mathbf{r})|\nabla\phi_{\rm or}^{\mathcal{R}}(\mathbf{r})|^2 - \frac{1}{\beta v}\log\left[\frac{\sinh\beta\bar{\mu}|\nabla\phi_{\rm or}^{\mathcal{R}}(\mathbf{r})|}{\beta\bar{\mu}|\nabla\phi_{\rm or}^{\mathcal{R}}(\mathbf{r})|}\right] - \frac{1}{2}\epsilon_0|\nabla\phi_0^{(P)}(\mathbf{r})|^2 \right\} \\
& - \int d\mathbf{r}\, \Gamma^{\mathcal{P}}(\mathbf{r}) \left\{ \frac{1}{2}\epsilon_0(1+\chi_{\rm el}^{\mathcal{P}}(\mathbf{r}))|\nabla\phi_{\rm el}^{\mathcal{P}}(\mathbf{r})|^2 \right. \\
& \left. +\epsilon_0\chi_{\rm or}^{\mathcal{P}}(\mathbf{r})|\nabla\phi_{\rm or}^{\mathcal{P}}(\mathbf{r})|^2 - \frac{1}{\beta v}\log\left[\frac{\sinh\beta\bar{\mu}|\nabla\phi_{\rm or}^{\mathcal{P}}(\mathbf{r})|}{\beta\bar{\mu}|\nabla\phi_{\rm or}^{\mathcal{P}}(\mathbf{r})|}\right] - \frac{1}{2}\epsilon_0|\nabla\phi_0^{(P)}(\mathbf{r})|^2 \right\} \\
& - \int d\mathbf{r}\, \frac{1}{\beta v}(\Gamma^{\mathcal{R}}(\mathbf{r}) - \Gamma^{\mathcal{P}}(\mathbf{r}))
\end{aligned} \tag{4.39}$$

where the superscripts $\mathcal{R}$, $\mathcal{N}$, and $\mathcal{P}$ refers to the states (indicated in Fig. 4.1) at which the susceptibilities, potentials, and solute cavities are defined, and $\phi_0^{(P)}$ denotes the potential in a vacuum with the product charge distribution $\hat{\rho}_c^{(P)}$.

Chapter 5

A Molecularly-Based Theory for Electron Transfer Reorganization Energy in Solvent Mixtures

This chapter includes content from our previously published article:

Zhuang, B.; Wang, Z.-G. Molecular-Based Theory for Electron-Transfer Reorganization Energy in Solvent Mixtures. *J. Phys. Chem. B* **2016,** *120,* 6373-6382.

5.1 Introduction

It has long been established that solvent fluctuation plays a central role in the kinetics and dynamics of electron transfer (ET) processes. The groundbreaking work by Marcus in 1956 envisioned fluctuation of solvent orientational polarization on two crossing parabolic nonequilibrium free energy surfaces – whose curvature is determined by a linear dielectric treatment of the solvent – and elucidated the relationship between the free energy for solvent reorganization and the rate of ET processes.[69,70] Since then, the area of ET has seen much research activity and growth,[67,68] for example, with subsequent theoretical work on dynamical[85,133–139] and quantum-mechanical effects,[83,113,140–148] experimental confirmation of the inverted region,[149] and characterization of ET mechanism in proteins and photosynthetic systems.[150–153] However, relatively little attention has been given to solvent mixtures, despite their common

usage as solvent media, for instance, in recent developments of lithium-ion batteries.[154] Solvent mixtures are paramount to technological and industrial applications, since they offer virtually endless possibilities as reaction media, allowing continuous tuning of the macroscopic solvent properties for optimal performance. To facilitate the search of new reaction media for technological applications, a convenient and predictive theoretical framework for solvent reorganization in liquid mixtures is desirable.

The lack of understanding for ET processes in solvent mixtures is due in large part to the complex effects mixed solvents have on the ET rates.[155] Experimental studies have shown distinctive behaviors in the ET rates depending on the specific electron transferring species and the solvent components. However, no systematic trend has emerged for understanding the observed behaviors and for predicting the behaviors in general mixtures.[138,156–165] Moreover, the kinetic,[160,166] dynamic,[167,168] and spectroscopic behaviors[169] for ET processes in solvent mixtures cannot be directly correlated with the corresponding properties in the pure solvent components. It is generally recognized that ET in mixed solvents is not controlled by macroscopic solvent parameters because of preferential solvation,[132,166,169–174] as the local composition of the solvent around a charged solute is significantly different from the bulk composition.[2]

Despite its importance, there have been very few theoretical studies for ET in liquid mixtures. Zusman developed an analytical theory to study the dynamical solvent effect in ET, connecting the ET rate to the solvent diffusion coefficients and the mixture correlation functions.[175] For the solvent reorganization energy, Chandra considered a nonpolarizable solvent mixture model using density functional theory with a constrained variational approach, and found that preferential solvation of the reacting system by the more polar species of the mixture is crucial.[176] One current theoretical challenge, in order to better understand the effect of solvent on ET kinetics, is to take into account the electronic polarizability of the solvent mixture, which is responsible for the solvent induced dipoles that respond on the same time scale as the charge transfer. Furthermore, as mixture correlation functions, which are required inputs

in density functional approaches, are not readily available, it is desirable to develop a simple analytical theory based on readily-available pure-solvent properties, which can be efficiently used for surveying the vast number of possible solvent mixtures.

Recently, we developed a molecularly-based dipolar self-consistent-field theory (DSCFT) for calculating reorganization energies in pure liquids using statistical-field techniques.[177] The theory models the polarizable solvent molecules using a few readily-available molecular parameters, including the permanent dipole moment, the polarizability, and the molecular volume. The statistical-field transformations yield orientational and electronic polarizations of the solvent that are continuous, spatially dependent functions. The resulting theory naturally accounts for the effect of dielectric saturation around the reacting species, and as a result, it is unnecessary to distinguish between the inner-sphere and the outer-sphere solvent molecules in the calculations. Despite the simplicity of the theory, the solvent reorganization energies predicted by the DSCFT, with no adjustable parameters, are in good agreement with previous calculations and experimental measurements for a range of reactions.

In this chapter, we extend the DSCFT to charge solvation in liquid mixtures under equilibrium and nonequilibrium conditions, and apply the theory to the solvent reorganization energy of ET processes. For ET in solvent mixtures, the slow-responding nuclear degrees of freedom not only relate to the solvent orientational polarization – as in earlier works for pure solvents – but also to the solvent composition around the reacting species. In constructing the nonequilibrium free energy, we keep both the orientational polarization and the solvent composition at their values in the reactant state, and perform a constrained extremization on the free energy with the reacting species at the product state. The resulting theory naturally accounts for the spatially-varying solvent composition and response. Our theory suggests three general categories of binary mixtures, classified by the relative static and optical dielectric constants of the solvent components. We explore the relationship between the reorganization energy and the bulk solvent composition in these three mixture categories. We find that each category of mixture produces a distinctive local solvent composition profile in the vicinity of the reacting species, which gives rise to

the distinctive composition dependence of the reorganization energy that cannot be predicted using the dielectric constants of the homogeneous solvent mixtures.

The rest of the chapter is organized as follows. In Section 5.2, we present the formulation of the DSCFT for solvation of a general solute under both equilibrium and nonequilibrium conditions in a binary liquid mixture. The free energy of solvation as well as two sets of constitutive relations, one applicable under equilibrium conditions and the other applicable under out-of-equilibrium conditions, are derived. In Section 5.3, we apply the general DSCFT to solvent reorganization energy in ET reactions. For comparison, we also briefly describe a uniform dielectric treatment for calculating the solvent composition dependence of the reorganization energy, based on the dielectric constants of the homogeneous solvent mixtures. In Section 5.4, we study the relationship between the solvent composition and the reorganization energy for electron exchange reactions between Fe^{2+} and Fe^{3+}, where both the donor and acceptor are charged, and between Ag^{0} and Ag^{1+}, where the ET occurs between a neutral and a charged species, in three general categories of binary solvent mixtures. We highlight the connection between the reorganization energy and the local solvent composition profile around the reacting species. Finally, in Section 5.5, we recapitulate the main points in this work and offer some concluding remarks and outlook.

5.2 Dipolar Self-Consistent-Field Theory (DSCFT) for Charge Solvation in Solvent Mixtures

In this section, we formulate the dipolar self-consistent-field theory (DSCFT) for charge solvation in liquid mixtures under equilibrium and nonequilibrium conditions. Here, equilibrium refers to a condition in which both the nuclear and the electronic degrees of freedom of the solvent are in equilibrium with the charge on the solute; nonequilibrium refers to a condition where the nuclear degrees of freedom of the solvent are out-of-equilibrium due to their longer relaxation times while the electronic degrees of freedom are allowed to equilibrate.

For simplicity, we consider a charged solute in a binary mixture consisting of solvent A and solvent B, with a bulk composition specified by the mole fraction of one of the species (A for concreteness), x_A; the theory can be easily generalized to multi-component mixtures. We characterize each solvent molecule by its permanent dipole moment $\bar{\mu}_S$, polarizability α_S, and molecular volume v_S ($S = A, B$). The solute is described by its charge distribution $\hat{\rho}_c(\mathbf{r})$ inside a cavity $\mathcal{C}$ that is inaccessible to the solvent molecules. The charge distribution of the system can be described as

$$\hat{\rho}(\mathbf{r}) = \hat{\rho}_c(\mathbf{r}) + \hat{\rho}_{\text{or}}(\mathbf{r}) + \hat{\rho}_{\text{el}}(\mathbf{r}) \tag{5.1}$$

where $\hat{\rho}_{\text{or}}$ and $\hat{\rho}_{\text{or}}$ are the charge densities due to the permanent and the induce dipole moments, respectively, given by

$$\hat{\rho}_{\text{or}}(\mathbf{r}) = -\sum_{S,i} \boldsymbol{\mu}_{S,i} \cdot \nabla\delta(\mathbf{r} - \mathbf{r}_{S,i}) \tag{5.2}$$

$$\hat{\rho}_{\text{el}}(\mathbf{r}) = -\sum_{S,i} \mathbf{p}_{S,i} \cdot \nabla\delta(\mathbf{r} - \mathbf{r}_{S,i}) \tag{5.3}$$

In the above expressions, $\mathbf{r}_{S,i}$, $\boldsymbol{\mu}_{S,i}$, and $\mathbf{p}_{S,i}$ respectively denote the position, the permanent dipole moment, and the induced dipole of the ith molecule of type S, and the summation runs over all solvent molecules. The permanent dipole moments have fixed magnitude $|\boldsymbol{\mu}_{S,i}| = \bar{\mu}_S$.

The energy of the system consists of the Coulomb interaction and the deformation cost of the induced dipoles, and it can be written as

$$U = \frac{1}{2}\int d\mathbf{r} \int d\mathbf{r}' \frac{\hat{\rho}(\mathbf{r})\hat{\rho}(\mathbf{r}')}{4\pi\epsilon_0|\mathbf{r} - \mathbf{r}'|} + \sum_{S,i} \frac{\mathbf{p}_{S,i}^2}{2\alpha_S} \tag{5.4}$$

where ϵ_0 is the permittivity of the vacuum.

To proceed, we consider a large enough volume V around the charged solute at temperature T that is open to both solvent species, each with chemical potential μ_S.

The particle-based grand partition function is given by

$$\begin{aligned}\Xi &= \sum_{N_A=0}^{\infty}\sum_{N_B=0}^{\infty}\frac{1}{N_A!}\frac{1}{N_B!}e^{\beta\mu_A N_A}e^{\beta\mu_B N_B} \\ &\quad\times\prod_{S=A,B}\left(\prod_{i=1}^{N_S}\frac{1}{\eta_S}\int d\mathbf{r}_{S,i}\int d\boldsymbol{\mu}_{S,i}\int d\mathbf{p}_{S,i}\right) \\ &\quad\times\delta\left[\sum_S v_S\hat{n}_S(\mathbf{r})-1\right]e^{-\beta U} \end{aligned} \tag{5.5}$$

where N_S is the number of molecules of solvent S, $\beta = 1/k_BT$, and η_S is the analog of thermal de Broglie wavelength that makes the configurational integral dimensionless. The value of η_S is inconsequential as it only contributes to a reference energy. The integral runs over the configurational space of the solvent molecules, with integration over $\mathbf{r}_{S,i}$ extends the space outside the solute cavity, and integration over $\boldsymbol{\mu}_{S,i}$ spans the 4π solid angle (as the magnitude of the permanent dipole is fixed). $\hat{n}_S(\mathbf{r}) = \sum_{i=1}^{N_S}\delta(\mathbf{r}-\mathbf{r}_{S,i})$ is the number density operator for solvent S. v_S is the molecular volume of solvent S which reflects the effects of the non-electrostatic intermolecular forces in giving rise to the particular density of the liquid at a given temperature and pressure. The δ-functional in Eq. (5.5) enforces an incompressibility condition for the liquid mixture, and amounts to assuming no volume change upon mixing.

Using statistical field techniques, we decouple the quadratic interactions between the charge density with a series of identity transformations. The procedure for the transformations is similar to that presented in our early work in Ref. 177, and it leads to the following exact field-theoretic partition function:

$$\begin{aligned}\Xi &= \int\mathcal{D}\rho_{\text{or}}\int\mathcal{D}w_{\text{or}}\int\mathcal{D}\rho_{\text{el}}\int\mathcal{D}w_{\text{el}}\int\mathcal{D}w \\ &\quad\times\left(\prod_S\int\mathcal{D}\varphi_S\int\mathcal{D}w_S\right)e^{-\beta H}\end{aligned} \tag{5.6}$$

with the effective field Hamiltonian H given by

$$\begin{aligned}
&\beta H[\rho_{\rm or}, w_{\rm or}, \rho_{\rm el}, w_{\rm el}, w, \varphi_S, w_S] \\
= &\int d\mathbf{r} \int d\mathbf{r}' \, \frac{\beta\rho(\mathbf{r})\rho(\mathbf{r}')}{8\pi\epsilon_0|\mathbf{r}-\mathbf{r}'|} + i\sum_S \int d\mathbf{r}\, w_S(\mathbf{r})\varphi_S(\mathbf{r}) \\
&-i\int d\mathbf{r}\, w_{\rm or}(\mathbf{r})\rho_{\rm or}(\mathbf{r}) - i\int d\mathbf{r}\, w_{\rm el}(\mathbf{r})\rho_{\rm el}(\mathbf{r}) \\
&-i\int d\mathbf{r}\, w(\mathbf{r})\left(\sum_S \varphi_S(\mathbf{r}) - 1\right) - \sum_S e^{\beta\mu_S} Q_S
\end{aligned} \tag{5.7}$$

where $\rho(\mathbf{r}) = \hat{\rho}_c(\mathbf{r}) + \rho_{\rm or}(\mathbf{r}) + \rho_{\rm el}(\mathbf{r})$, and Q_S is the single-particle partition function in the fields $w_S(\mathbf{r})$, $w_{\rm or}(\mathbf{r})$ and $w_{\rm el}(\mathbf{r})$,

$$\begin{aligned}
Q_S = &\frac{4\pi\bar{\mu}_S^2}{\eta_S}\left(\frac{2\pi\alpha_S}{\beta}\right)^{\frac{3}{2}} \int d\mathbf{r}\, \left\{\Gamma(\mathbf{r})\frac{\sin(\bar{\mu}_S|\nabla w_{\rm or}(\mathbf{r})|)}{\bar{\mu}_S|\nabla w_{\rm or}(\mathbf{r})|}\right. \\
&\left.\times \exp\left[iv_S w_S(\mathbf{r}) - \frac{\alpha_S}{2\beta}(\nabla w_{\rm el}(\mathbf{r}))^2\right]\right\}
\end{aligned} \tag{5.8}$$

Here, $\Gamma(\mathbf{r})$ serves to limit the integration to space outside the solute cavity, with $\Gamma(\mathbf{r}) = 0$ if $\mathbf{r} \in \mathcal{C}$ and 1 otherwise. The transformation to the field-theoretic partition function has introduced the coarse-grained charge density fields $\rho_{\rm or}$ and $\rho_{\rm el}$ for the solvent permanent and induced dipoles, respectively; $w_{\rm or}$ and $w_{\rm el}$ are the scaled orientational and electronic electric potentials that are the conjugate fluctuating fields to $\rho_{\rm or}$ and $\rho_{\rm el}$, respectively. w is a coarse-grained pressure-like field arising from the incompressibility condition. φ_S is the coarse-grained spatially-dependent volume fraction of species S, with w_S being the volume fraction potential that is conjugate to φ_S.

The functional integration in the field-based partition function in Eq. (5.6) cannot be evaluated exactly in closed form. To proceed, we take the saddle-point approximation by extremizing the effective Hamiltonian H with respect to its functional arguments. In the equilibrium condition, we obtain the constitutive relations by extremizing H with respect to all of its functional arguments. In the nonequilibrium condition, the solvent composition in the system and the orientational polarization are

out of equilibrium because of the longer response time of nuclear degrees of freedom; therefore, the functions $\rho_{\rm or}$ and φ_S keep their values from the previous equilibrium state, and we perform a constrained extremization of H with respect to the rest of the functional arguments. Details of the derivation are provided in the supporting information. In order to work with real quantities and for the convenience of relating our theory to classical electrostatics, we make a change of variables $w_{\rm or} = -i\beta\phi_{\rm or}$, $w_{\rm el} = -i\beta\phi_{\rm el}$, and $w_S = i\beta u_S$. The resulting set of constitutive relations for charge solvation under equilibrium condition is

$$\nabla \cdot \mathbf{D} = \hat{\rho}_c(\mathbf{r}) \tag{5.9}$$

$$\varphi_S(\mathbf{r}) \;=\; \Gamma(\mathbf{r})\varphi_S^{(\infty)} \exp\left[-\beta u(\mathbf{r}) v_S + \frac{\beta\alpha_S}{2}|\nabla\phi(\mathbf{r})|^2\right] \frac{\sinh(\beta\bar{\mu}_S|\nabla\phi(\mathbf{r})|)}{\beta\bar{\mu}_S|\nabla\phi(\mathbf{r})|} \tag{5.10}$$

$$\sum_S \varphi_S(\mathbf{r}) = 1 \tag{5.11}$$

where $\mathbf{D}$ is the electric displacement given by

$$\mathbf{D} = -\epsilon_0[1 + \chi_{\rm el}(\mathbf{r}) + \chi_{\rm or}(\mathbf{r})]\nabla\phi(\mathbf{r}) \tag{5.12}$$

and $\chi_{\rm or}(\mathbf{r})$ and $\chi_{\rm el}(\mathbf{r})$ are the electric susceptibilities due to the permanent and the induced dipoles, respectively, given by

$$\chi_{\rm or}(\mathbf{r}) = \Gamma(\mathbf{r}) \sum_S \frac{\beta\bar{\mu}_S^2\varphi_S(\mathbf{r})}{\epsilon_0 v_s} \frac{\mathcal{L}(\beta\bar{\mu}_S|\nabla\phi(\mathbf{r})|)}{\beta\bar{\mu}_S|\nabla\phi(\mathbf{r})|} \tag{5.13}$$

$$\chi_{\rm el}(\mathbf{r}) = \Gamma(\mathbf{r}) \sum_S \frac{\varphi_S(\mathbf{r})\alpha_S}{v_S\epsilon_0} \tag{5.14}$$

with $\mathcal{L}(x) = (\coth x - 1/x)$ being the Langevin function. We recognize that Eq. (5.9) is just the Poisson equation. Eqs. (5.9) – (5.11) are to be solved for the fields ϕ, φ_S and u. The bulk volume fraction $\varphi_S^{(\infty)}$ of solvent S is related to the mole fractions of the species through $\varphi_S^{(\infty)} = x_S v_S / \left(\sum_{S'} x_{S'} v_{S'}\right)$. The subscripts on the functions ϕ

and u are omitted because at full equilibrium the extremization procedure results in $\phi = \phi_{\text{or}} = \phi_{\text{el}}$ and $u = u_A = u_B$.

Under the nonequilibrium condition in which the nuclear degrees of freedom (reflected in the values of φ_S and ϕ_{or}) are fixed from the corresponding equilibrium state, the constitutive relations are

$$\nabla \cdot \mathbf{D} = \hat{\rho}_c(\mathbf{r}) \tag{5.15}$$

$$\varphi_S(\mathbf{r}) \;=\; \Gamma(\mathbf{r})\varphi_S^{(\infty)} \exp\left[-\beta u_S(\mathbf{r}) v_S + \frac{\beta\alpha_S}{2}|\nabla\phi_{\text{el}}(\mathbf{r})|^2\right] \frac{\sinh(\beta\bar{\mu}_S|\nabla\phi_{\text{or}}(\mathbf{r})|)}{\beta\bar{\mu}_S|\nabla\phi_{\text{or}}(\mathbf{r})|} \tag{5.16}$$

where the electric displacement $\mathbf{D}$ is now given by

$$\mathbf{D} = -\epsilon_0 \left[(1 + \chi_{\text{el}}(\mathbf{r}))\nabla\phi_{\text{el}}(\mathbf{r}) + \chi_{\text{or}}(\mathbf{r})\nabla\phi_{\text{or}}(\mathbf{r})\right] \tag{5.17}$$

Note that Eqs. (5.15) and (5.16) have similar form to Eqs. (5.9) and (5.10), except that we have to distinguish between the electric potentials ϕ_{el} and ϕ_{or}, and between the conjugate fields to the composition u_A and u_B. The value for χ_{el} is given by Eq. (5.14). Eqs. (5.15) and (5.16) are then solved for the values of ϕ_{el} and u_S, with χ_{or}, ϕ_{or}, φ_S, and Γ from the corresponding equilibrium state that has the same nuclear configuration.[1] We note that Γ describes the space accessible to solvent molecules, and therefore, it is related to the nuclear configuration of the solvent. Since φ_S remains unchanged from the corresponding equilibrium value, Eq. (5.11) is automatically satisfied, and the electric susceptibilities χ_{el} and χ_{or} in the nonequilibrium state turn out to be equal to those in the corresponding equilibrium state.

The free energy of solvation is obtained by evaluating the field-theoretic Hamiltonian H at the saddle-point values of its functional arguments. Upon simplification,

[1] While the effective Hamiltonian H is extremized over ϕ_{or} in the nonequilibrium state, it can be shown from the constitutive relations that ϕ_{or} in the nonequilibrium state has the same value as itself in the corresponding equilibrium state where the orientational polarization and solvent composition are in equilibrium with the solute charge distribution. See supporting information.

the free energy of solvation G can be written as

$$\begin{aligned} & G[\mathbb{C}, \hat{\rho}_c] \\ & = \int d\mathbf{r} \left[-\sum_S \left(u_S(\mathbf{r})\varphi_S(\mathbf{r}) + \frac{\varphi_S(\mathbf{r})}{\beta v_S} \right) \right. \\ & \left. +\epsilon_0 \left(\frac{1}{2} + \chi_{\mathrm{el}}(\mathbf{r}) \right) |\nabla\phi_{\mathrm{el}}(\mathbf{r})|^2 + \epsilon_0\chi_{\mathrm{or}}|\nabla\phi_{\mathrm{or}}(\mathbf{r})|^2 \right] \end{aligned} \tag{5.18}$$

where $\mathbb{C} = \{\varphi_S, \phi_{\mathrm{or}}, \chi_{\mathrm{or}}, \mathcal{C}\}$ is the nuclear configuration set, which contains all necessary information describing the solvent nuclear configuration. In the above free energy expression, the values of χ_{el}, ϕ_{el}, and u_S used for evaluating G are to be calculated using the set of constitutive relations appropriate for the solvation condition (i.e., equilibrium vs. nonequilibrium).

The constitutive relations under equilibrium condition (Eqs. (5.9) – (5.11)) and nonequilibrium condition (Eqs (5.15) and (5.16)), and the free energy of solvation (Eq. (5.18)) are the key equations in the theory, and can be applied to study the energetics of general ET processes in solvent mixtures. In the following section, we focus on electron transfer between simple ions, and outline the calculation of the solvent reorganization energy.

5.3 Calculation of Solvent Reorganization Energy

Broadly speaking, the solvent composition impacts the ET kinetics through two main effects: first, the composition-dependent dielectric properties of the solvent affects the donor-acceptor association constant; second, the local composition of the solvents around the reacting species strongly influences the solvent reorganization energy. Both effects are important for the rate of ET reactions. However, in this chapter, we focus on how the local solvent composition around the donor-acceptor complex affects the solvent reorganization energy.

5.3.1 The DSCFT Calculation

We consider electron transfer between two simple ions in the form $D^m + A^n \rightarrow D^{m+1} + A^{n-1}$, where D and A respectively denote the electron donor and the acceptor, with their centers located at $\mathbf{R}_D$ and $\mathbf{R}_A$, respectively. The solute charge distribution is described by $\hat{\rho}_c^{(\mathcal{R})}(\mathbf{r}) = me\delta(\mathbf{r} - \mathbf{R}_D) + ne\delta(\mathbf{r} - \mathbf{R}_A)$ in the reactant state, and $\hat{\rho}_c^{(\mathcal{P})}(\mathbf{r}) = (m+1)e\delta(\mathbf{r} - \mathbf{R}_D) + (n-1)e\delta(\mathbf{r} - \mathbf{R}_A)$ in the product state, where e is the elementary charge. The solute cavity $\mathcal{C}^{(\mathcal{R})}$ in the reactant state has the shape of two spheres, described by $\{\mathbf{r} : |\mathbf{r} - \mathbf{R}_D| < a_D^{(\mathcal{R})}$ or $|\mathbf{r} - \mathbf{R}_A| < a_A^{(\mathcal{R})}\}$, where $a_D^{(\mathcal{R})}$ and $a_A^{(\mathcal{R})}$ are the ionic radii (or atomic radii if the species is neutral) of D^m and A^n. The solute cavity $\mathcal{C}^{(\mathcal{P})}$ in the product state is defined similarly, with $a_D^{(\mathcal{P})}$ and $a_A^{(\mathcal{P})}$ being the ionic radii of D^{m+1} and A^{n-1}.[2]

The solvent reorganization energy λ is the free energy difference between the following two states: (i) the equilibrium state under the product charge distribution and (ii) the nonequilibrium state under the product charge distribution but with the nuclear configuration from the reactant state. The nuclear configuration of a state includes the solvent composition, orientational polarization, and the accessible space to the solvent outside the solute cavity, and we denote this information in a nuclear configuration set $\mathbb{C}^{(\mathcal{S})} = \{\varphi_S^{(\mathcal{S})}, \phi_{\text{or}}^{(\mathcal{S})}, \chi_{\text{or}}^{(\mathcal{S})}, \mathcal{C}^{(\mathcal{S})}\}, (\mathcal{S} = \mathcal{R}, \mathcal{P})$. Algebraically, we express λ as

$$\lambda = G[\mathbb{C}^{(\mathcal{R})}, \hat{\rho}_c^{(\mathcal{P})}] - G[\mathbb{C}^{(\mathcal{P})}, \hat{\rho}_c^{(\mathcal{P})}] \tag{5.19}$$

In computing the reorganization energy, the integral only needs to be evaluated for the region outside the cavity by referencing the free energy to a vacuum state with the same charge distribution. Details for the procedure are given in Appendix B of Ref. 177.

To simplify the calculation, we solve Eqs. (5.9) and (5.15) by assuming that the

[2]For calculating the reorganization energy, one only needs the ionic radii in the reactant and the product states. The determination of the variation of ionic radii with the reaction coordinate is intrinsically a quantum mechanical problem, which is beyond the scope of the current work. As far as charge solvation is concerned, Eq. 18 allows us to calculate the nonequilibrium solvation free energy for any ionic radii/solute cavity. More details for the treatment of solute cavity are described in Appendix B of our earlier work in in Ref. 177.

electric displacement $\mathbf{D}$ can be written as a superposition of the displacement due to each individual point charge as

$$\mathbf{D}(\mathbf{r}) = \frac{q_D}{4\pi r_D^2}\hat{\mathbf{r}}_D + \frac{q_A}{4\pi r_A^2}\hat{\mathbf{r}}_A \tag{5.20}$$

where $\mathbf{r}_{D/A} = \mathbf{r} - \mathbf{R}_{D/A}$ and $\hat{\mathbf{r}}_{D/A}$ indicates the unit vector in the direction of $\mathbf{r}_{D/A}$.

We perform numerical evaluations on a two-center bispherical coordinate (σ, τ, φ), which relates to the cylindrical coordinate (r, z, φ) by $z = a_0 \sinh\sigma/(\cosh\sigma - \cos\tau)$ and $r = a_0 \sin\sigma/(\cosh\sigma - \cos\tau)$. Each constant-$\sigma$ surface in the bispherical coordinate is a circle of radius $a_0/|\sinh\sigma|$ with its center located at $z = a_0 \coth\sigma$. The value of a_0 is determined by the ionic radii of the donor and the acceptor and their distance, and by requiring that the cavity boundaries of the donor and the acceptor are each a surface of constant σ, and that the region accessible by the solvent is simply described by $\sigma_A < \sigma < \sigma_D$. This is achieved by simultaneously solving

$$\frac{a_0}{|\sinh\sigma_D|} = a_D \tag{5.21a}$$

$$\frac{a_0}{|\sinh\sigma_A|} = a_A \tag{5.21b}$$

$$a_0 \coth\sigma_D - a_0 \coth\sigma_A = d \tag{5.21c}$$

Geometrically, these set of equations describe the donor cavity surface by $\sigma = \sigma_D = \cosh^{-1}\left(\frac{a_D^2 - a_A^2 + d^2}{2a_D d}\right)$, and the acceptor cavity surface by $\sigma = \sigma_A = -\cosh^{-1}\left(\frac{a_A^2 - a_D^2 + d^2}{2a_A d}\right)$, and $a_0 = a_D \sinh\sigma_D$. Due to the cylindrical symmetry in the problem, we only have to perform calculations on the two-dimensional $\sigma\tau$-plane. The integration for the free energy is carried out on a 60×170 $\sigma\tau$-grid between $\sigma \in (\sigma_A, \sigma_D)$ and $\tau \in (0, \pi)$. The electric potential field ϕ in the equilibrium state is found by iteration until the next iteration produces a reduced potential field $\nabla\phi/[\frac{e}{4\pi\epsilon_0(2a_D a_A/(a_D + a_A))}]$ within 10^{-8} from its current value at all grid points.

5.3.2 The Uniform Dielectric Treatment

As mentioned in the introduction, a key effect that influences the ET reorganization energy in a mixture is preferential solvation due to the difference in the local solvent composition around the charged redox species from the bulk. In order to highlight the effects of preferential solvation in a liquid mixture, in this subsection we examine the consequence of ignoring the preferential solvation on the reorganization energy by assuming the solvent to be a uniform dielectric medium. In Section 5.4, we will compare results from our DSCFT calculation with results from the uniform dielectric treatment presented in this subsection. We start with the familiar Marcus equation[70] for reorganization energy

$$\lambda_{\mathrm{cl}} = (\Delta e)^2 \left(\frac{1}{2a_D} + \frac{1}{2a_A} - \frac{1}{d}\right)\left(\frac{1}{\epsilon_\infty} - \frac{1}{\epsilon_s}\right) \tag{5.22}$$

where ε_∞ and ε_s are respectively the optical and static dielectric constants of the solvent. If we assume the solvent mixture to be spatially uniform, then the dielectric response can be characterized by the optical and static dielectric constants of a homogeneous bulk mixture, which are commonly approximated using the Clausius-Mossotti equation[27,178] and the Onsager equation[26,179], respectively given by

$$\frac{\epsilon_\infty - 1}{\epsilon_\infty + 2} = \sum_{S=A,B} \varphi_S^{(\infty)} \frac{\epsilon_{\infty,S} - 1}{\epsilon_{\infty,S} + 2} \tag{5.23}$$

and

$$\frac{(\epsilon_s - 1)(2\epsilon_s + 1)}{\epsilon_s} = \sum_{S=A,B} \varphi_S^{(\infty)} \frac{(\epsilon_{s,S} - 1)(2\epsilon_{s,S} + 1)}{\epsilon_{s,S}} \tag{5.24}$$

where $\epsilon_{\infty,S}$ and $\epsilon_{s,S}$ are respectively the corresponding optical and static dielectric constants of pure solvent S.

The Pekar factor $P = 1/\epsilon_\infty - 1/\epsilon_s$ is the only solvent-dependent factor in the expression for reorganization energy in Eq. (5.22). Given the reorganization energies λ_A and λ_B in pure solvents A and B, respectively, the reorganization energy in an

A/B mixture follows from Eq. (5.22) to be

$$\lambda_{\rm cl} = \lambda_A + \frac{P - P_A}{P_B - P_A}(\lambda_B - \lambda_A) \tag{5.25}$$

where P_S is the Pekar factor for the pure solvent S. Here, for consistency and to provide a meaningful interpolation that matches the pure solvent results, we use the DSCFT-predicted reorganization energies for the pure solvents.[3] Note that Eq. (5.25) is invariant with respect to switching labels A and B. We refer to Eq. (5.25) as the uniform dielectric treatment for calculating the mixture reorganization energy.

5.4 Solvent Reorganization Energy of Self-Exchange Reactions in Binary Mixtures

In this section, we study the solvent reorganization energy for electron transfer in binary liquid mixtures. We consider two simple electron-exchange reactions: (i) $Fe^{2+} + Fe^{3+} \rightarrow Fe^{3+} + Fe^{2+}$ and (ii) $Ag^0 + Ag^{1+} \rightarrow Ag^{1+} + Ag^0$. In case (i), the electron transfer occurs between two multiply-charged species, whereas in case (ii) the electron transfer occurs between a singly-charged species and a neutral species. We note that, even though we apply the DSCFT to self-exchange reactions in the present work, the calculation of reorganization energy with the DSCFT is applicable to general reactions. The radii of the electron-transferring species are taken to be their crystallographic ionic or atomic radii, whose values are 0.92 Å, 0.785 Å, 1.29 Å, and 1.60 Å for Fe^{2+}, Fe^{3+}, Ag^{1+}, and Ag^0, respectively. The distance between the centers of the donor and the acceptor is kept at $d = 5.5$ Å.

Because charge solvation has different time and length scale dependence on the permanent and induced dipoles, we classify binary solvent mixtures into the following three general categories based on the relative static and optical dielectric constants of the two liquid components, and examine a representative solvent mixture from each

[3]One may substitute the radii a_D and a_A as well as the donor-acceptor distance d into Eq. (22) to obtain the reorganization energy. However, we have shown in Ref. 177 that the use of bare ion radius significantly overestimates the reorganization energy in a pure solvent.

Table 5.1: Parameters for the pure solvents involved in the binary mixed solvents considered in this work. The permanent dipole $\bar{\mu}$, the molecular polarizability α, and the molecular volume v are used in the DSCFT calculation. v is the volume per molecule calculated from the liquid density at 25°C. The static and optical dielectric constants, ϵ_s and ϵ_∞ are listed here for reference and for calculations using the uniform dielectric treatment.

	DSCFT			Bulk	
Solvent	$\bar{\mu}$ [D]	α [Å^3]	v [Å^3]	ϵ_s	ϵ_∞
Water	1.85	1.45	30.0	80.1	1.78
Methanol	1.70	3.29	67.2	33.0	1.77
DMSO	3.96	8.00	117.8	47.2	2.19
2-Propanol	1.58	6.97	127.8	20.2	1.90
Pyridine	2.22	9.65	133.8	13.3	2.28

category:

1. The two components have comparable optical dielectric constants, but one component has a higher static dielectric constant than the other; e.g. *water/methanol mixture*

2. The two components have comparable static dielectric constants, but one component has a higher optical dielectric constant than the other; e.g. *2-propanol/pyridine mixture*

3. One of the components has a higher static dielectric constant but a lower optical dielectric constant than the other component; e.g. *water/DMSO mixture*

We note that, in comparing the dielectric constants of polar liquids, a difference of 10 in static dielectric constant is considered quite moderate, while a difference of 0.1 in optical dielectric constant can be considered quite large. In referring to the binary solvent mixtures, we adopt the notation that the component with a higher static dielectric is followed by the component with the lower static dielectric constant, separation by a slash. For example, an A/B mixture is one where A has a higher static dielectric constant than B. Henceforth, we use the mole fraction to denote the mixture composition. We calculate the solvent composition and the reorganization energy in the chosen example of solvent mixture mentioned in each category. In

Table 5.1, we list the permanent dipole $\bar{\mu}$, the molecular polarizability α, and the molecular volume v for the five solvent species studied in this work, together with their experimental static dielectric constants ϵ_s and optical dielectric constants ϵ_∞.

5.4.1 Electron Self-Exchange Between Charged Species

We first examine the self-exchange reaction $Fe^{2+} + Fe^{3+} \rightarrow Fe^{3+} + Fe^{2+}$ in binary mixtures. Since both the donor and the acceptor are multiply charged, preferential solvation takes place around both the donor and the acceptor. The local solvent composition in the immediate vicinity of the donor and acceptor is insensitive to the global solvent composition. We thus expect that the electron transfer reorganization energy – which is largely determined by the local composition of the solvent around the donor-acceptor complex – to be a weak function of the bulk solvent composition in a broad composition range.

The first case we consider is the water/methanol mixture. Since the two solvent components have similar optical dielectric constants, water is expected to be enriched around both the donor and the acceptor because of its higher static dielectric constant. In Fig. 5.1(a), we plot the equilibrium solvent composition around the donor-acceptor complex for a 50:50 water/methanol mixture in cylindrical coordinate, in which the centers of Fe^{2+} and Fe^{3+} are located on the z-axis. The solute cavity is represented by the white semispherical region, labeled with the charge of the ion. The region around the electron-transferring species appears bright-yellow, indicating that the ET species is essentially surrounded by pure water. As a result, the solvent reorganization energy in a water/methanol mixture over most of the composition range approximately equals to that in pure water, except at exceedingly low water concentration. This is shown in the plot of solvent reorganization energy vs. mole fraction of water in Fig. 5.2(a).

The observation here provides a qualitative explanation to the experimental result by Wada and Endo.[160]. These authors found that the rate of Fe^{2+}/Fe^{3+} exchange in the water/methanol mixture stays constant for mole fraction of methanol between 0 and 0.3. At higher concentrations of methanol, however, the experiment observed a

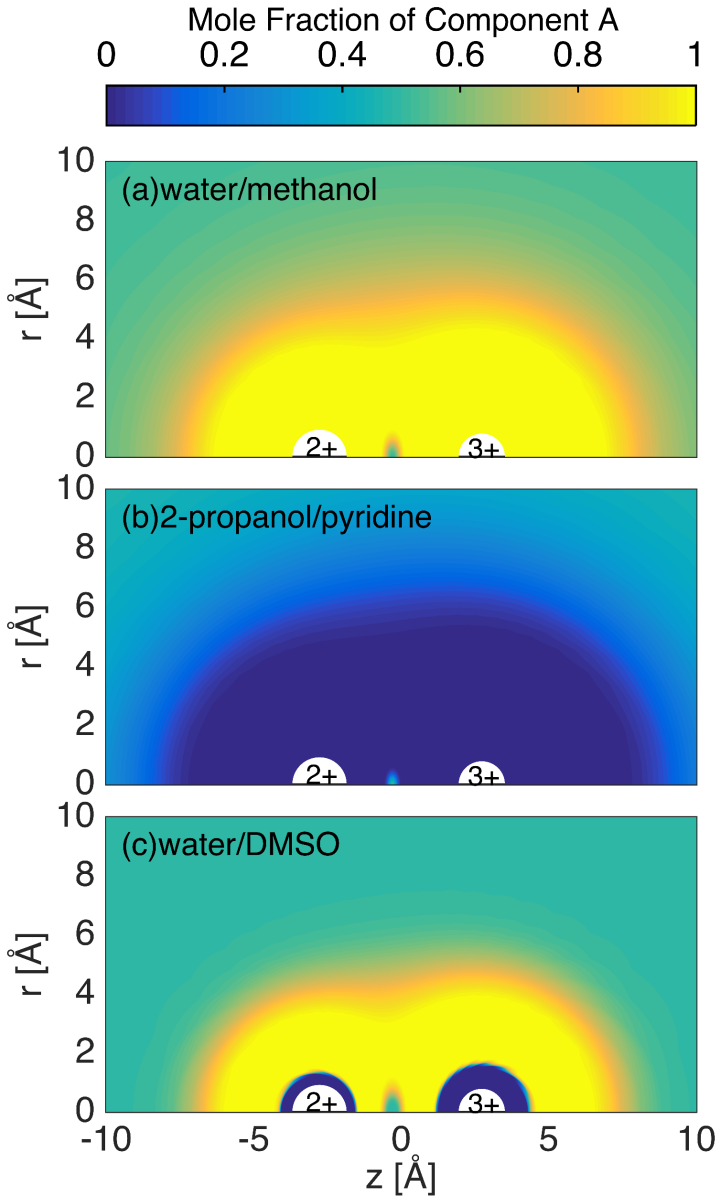

Figure 5.1: Equilibrium composition (mole fraction of solvent component A) around the donor-acceptor complex at the reactant state for the $Fe^{2+} + Fe^{3+} \rightarrow Fe^{3+} + Fe^{2+}$ reaction in a 50:50 mixture of (a) water and methanol, (b) 2-propanol and pyridine, and (c) water and DMSO. The mole fraction of A is plotted on a cylindrical r-z coordinate with the centers of the donor and the acceptor located on the $r = 0$ axis. The center of the donor (Fe^{2+}) and the acceptor (Fe^{3+}) are located at $z = -2.75$ Å and $z = 2.75$ Å respectively. The white semispherical region indicates the space occupied by the donor and the acceptor, which is inaccessible to the solvent molecules.

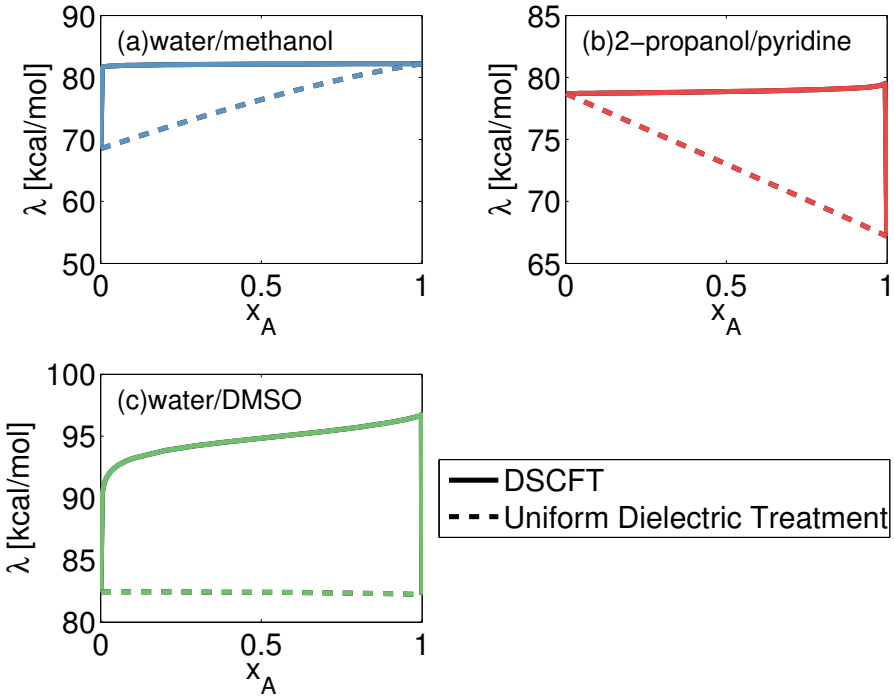

Figure 5.2: Solvent reorganization energy (λ) vs. the mole fraction of component A (x_A) for electron self-exchange reaction $Fe^{2+} + Fe^{3+} \rightarrow Fe^{3+} + Fe^{2+}$ in (a) water/methanol, (b)2-propanol/pyridine, and (c) water/DMSO mixtures. The solid squares are results calculated with the DSCFT, while the dashed lines are results calculated from the uniform dielectric treatment using Eq. (5.25).

gradual decrease in the rate of reaction with increasing methanol content. A likely explanation is the increased energy penalty for Fe^{2+} and Fe^{3+} to approach to a reactive distance (of approximately 6 Å) from each other, as a result of the decreased solvent dielectric constant with increasing methanol content.

The second case is the 2-propanol/pyridine mixture. While 2-propanol and pyridine have comparable static dielectric constants, pyridine has a significantly higher optical dielectric constant, and therefore is more polarizable. Under the strong electric fields around a multiply-charged ion, the more polarizable pyridine molecule develops a significantly larger induced dipole. As a result, pyridine interacts more favorably with the ions and is enriched around the ions. In Fig. 5.1(b), we present the equilibrium solvent composition in a 50:50 2-propanol/pyridine mixture. The blue region suggests that pyridine is enriched around the donor-acceptor complex, despite having a smaller static dielectric constant than 2-propanol. As the immediate vicinity of Fe^{2+} and Fe^{3+} are exclusively occupied by pyridine, the solvent reorganization energy for Fe^{2+}/Fe^{3+} exchange in 2-propanol/pyridine mixtures should be nearly equal to that in pure pyridine, except at very low pyridine concentration. This behavior is confirmed by the plot of solvent reorganization energy vs. mole fraction of 2-propanol shown in Fig. 5.2(b).

The third case is Fe^{2+}/Fe^{3+} self-exchange process in the water/DMSO mixture. In this case, water has a higher static dielectric constant, but DMSO has a higher optical dielectric constant. Because both larger permanent dipole moment and larger polarizability lead to favorable interactions with the ions, we expect both water and DMSO to be present in the immediate vicinity of both Fe^{2+} and Fe^{3+}. Fig. 5.1(c) shows the equilibrium solvent composition around the $Fe^{2+} - Fe^{3+}$ complex in a 50:50 water/DMSO mixture. The composition profile clearly indicates the presence of both water and DMSO in the neighborhood of the donor and the acceptor – while water is the preferred solvent in most region within about 5 Å from the centers of the ions, DMSO is enriched in the immediate vicinity of the ions, where the electric field is the strongest. We should caution that such coarse-grained composition profile must be interpreted with discretion, as the size of individual solvent molecules could be bigger

than the structural features in the composition profile. Nevertheless, if we average the composition over the typical size of a molecule, the composition profile in Fig. 5.1(c) suggests that there are more DMSO molecules around the Fe^{3+} than the Fe^{2+} because of the stronger electric field around the charge +3 ion. The unequal solvent concentration around the donor and the acceptor gives rise to a compositional contribution to the solvent reorganization energy, in addition to the contribution from the orientational polarization. Consequently, the solvent reorganization energy for Fe^{2+}/Fe^{3+} exchange in water/DMSO is significantly higher than that in either of the pure components, as shown in Fig. 5.2(c). These results provide a qualitative understanding for the earlier experimental observation by Wada and Aoki, who found the rate of reaction for the Fe^{2+}/Fe^{3+} exchange vary nonmonotonically with the solvent composition in a water/DMSO mixture, with a minima in the reaction rate at some intermediate concentration of DMSO.[159]

To highlight the effect of preferential solvation, in Fig. 5.2 we include results for the reorganization energy calculated using the uniform dielectric treatment, Eq. (5.25) (shown as dashed lines in the figure). In all cases, the reorganization energy calculated by the DSCFT is larger than that predicted by the uniform dielectric treatment. This suggests that the solvent reorganization energy for the Fe^{2+}/Fe^{3+} exchange reaction is primarily determined by the local solvent composition around the donor-acceptor complex, and is insensitive to the global solvent composition.

5.4.2 Electron Self-Exchange Between a Charged and a Neutral Species

In contrast to Fe^{2+}/Fe^{3+} exchange reaction studied in the last subsection where both the donor and acceptors carry multiple charges, in this subsection we explore the reaction $Ag^{1+} + Ag^0 \rightarrow Ag^0 + Ag^{1+}$, an exchange between a singly-charged and a neutral species, again in the three classes of binary solvent mixtures. In this reaction, the vicinity of the charged Ag^{1+} is enriched in the preferred solvent component, while the surrounding of the neutral Ag^0 is mostly at the bulk solvent composition.

Unlike the previous case of charge transfer between multiply-charged solutes, where the solvent reorganization energy primarily depends on the local solvent composition, this reaction, involving a neutral species, is expected to exhibit a stronger dependence of its reorganization energy on the bulk solvent composition.

First, we consider the Ag^{1+}/Ag^0 exchange in the water/methanol mixture. At equilibrium, water is enriched around the Ag^{1+} ion, while the solvent composition around the Ag^0 atom is essentially at the bulk composition, as presented in the equilibrium solvent composition profile for a 50:50 water/methanol mixture in Fig. 5.3(a). Because of the enrichment of water around Ag^{1+}, addition of a small amount of water to pure methanol should lead to a large increase in the solvent reorganization energy. Further addition of water continues to change the solvent composition around the Ag^0, causing a gradual increase in reorganization energy with increasing water content in the solvent. This dependence of reorganization energy on the solvent composition is observed in Fig. 5.4(a). Because of the preferential solvation around Ag^{1+}, the reorganization energy at all compositions are above that predicted by the uniform dielectric treatment shown as a dashed curve in Fig. 5.4(a).

We now consider the 2-propanol/pyridine mixture. In this case, pyridine is enriched around the Ag^{1+} ion because of its higher optical dielectric constant, as observed in the equilibrium composition of a 50:50 2-propanol/pyridine mixture in Fig. 5.3(b). We plot the solvent reorganization energy vs. the bulk mole fraction of 2-propanol in Fig. 5.4(b). Because of preferential solvation of pyridine around the Ag^{1+} ion, addition of a small amount of pyridine to pure 2-propanol leads to a steep increase in the solvent reorganization energy. Further addition of pyridine gradually change the solvent reorganization energy towards the value in pure pyridine. As in the previous cases, preferential solvation results in a larger solvent reorganization energy than that predicted by the uniform dielectric treatment.

Next we consider the water/DMSO mixture. Since water has a higher static dielectric constant and DMSO has a higher optical dielectric constant, it is not obvious which component in enriched in the vicinity of Ag^{1+}. Our DSCFT calculation indicates that it is water that is enriched around Ag^{1+}, as shown in Fig. 5.3(c), because

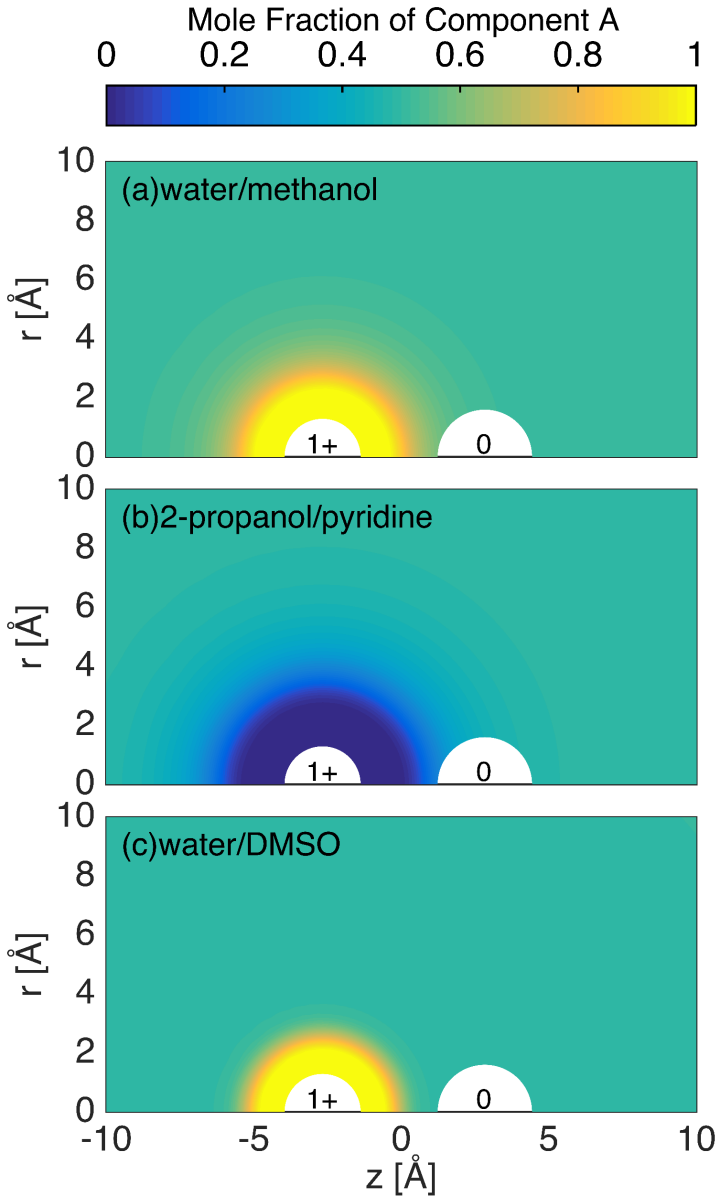

Figure 5.3: Equilibrium composition (mole fraction of solvent component A) around the donor-acceptor complex at the reactant state for the $Ag^{1+} + Ag^{0} \rightarrow Ag^{0} + Ag^{1+}$ reaction in a 50:50 mixture of (a) water and methanol, (b) 2-propanol and pyridine, and (c) water and DMSO. The mole fraction of A is plotted on a cylindrical r-z coordinate with the centers of the donor and the acceptor located on the $r = 0$ axis. The center of the donor (Ag^{1+}) and the acceptor (Ag^{0}) are located at $z = -2.75$ Å and $z = 2.75$ Å respectively. The white semispherical region indicates the space occupied by the donor and the acceptor, which is inaccessible to the solvent molecules.

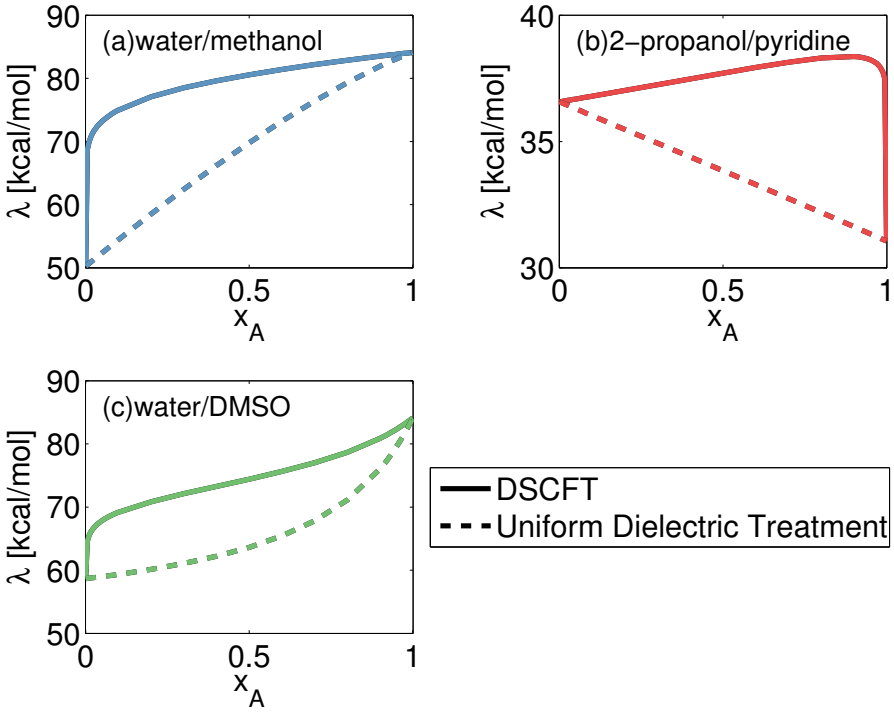

Figure 5.4: Solvent reorganization energy (λ) vs. the mole fraction of component A (x_A) for electron self-exchange reaction $Ag^{1+} + Ag^0 \rightarrow Ag^0 + Ag^{1+}$ in (a) water/methanol, (b)2-propanol/pyridine, and (c) water/DMSO mixtures. The solid squares are results calculated with the DSCFT, while the dashed line are results calculated from the uniform dielectric treatment using Eq. (5.25).

the DMSO molecules are not sufficiently polarized by the low charge on Ag^{1+} to outweigh the Ag^{1+}-water interaction. Therefore, as shown in Fig. 5.4(c), the addition of a small amount of water to pure DMSO creates a sharp increase in the solvent reorganization energy, while further addition leads to gradual increase in the solvent reorganization energy towards the value in pure water.

5.5 Conclusion

In this work, we have developed a molecularly-based theory for equilibrium and nonequilibrium charge solvation in mixed solvents, and applied the theory to the solvent reorganization energy of ET reactions. Using statistical field methods with the saddle-point approximation, the theory naturally leads to two sets of constitutive relations, one applicable under full equilibrium condition and the other applicable under nonequilibrium condition, as well as a simple, analytical expression for the solvation free energy. The theory considers both the nuclear and the electronic degrees of freedom of the solvent dipoles, and self-consistently accounts for the spatially-varying composition and dielectric response of the mixed solvent around the reacting species. As numerically solving the constitutive relations requires minimal computational effort, the theory provides a convenient and efficient tool for evaluating the ET reorganization energy in mixed solvents.

Our results show that the composition dependence of the solvent reorganization energy is largely determined by the local solvent composition around the reacting species, which is often very different from the bulk solvent composition due to preferential solvation. This observation is in agreement with Ref. 44, which compared the DSCFT-predicted solvation energies to experimental values and found that the equilibrium ion solvation energy in a mixture is predominantly attributed to the solvent composition in vicinity of the ion. Generally, the solvent component with the larger static or optical dielectric constant is enriched around the charged solutes, and the solvent reorganization energy is dominated by the contribution from the enriched component. However, if one component has a larger static dielectric constant and the

other has a larger optical dielectric constant, as in the case of water/DMSO mixture, the local solvent composition is sensitive to the the solute charge: the solvent composition around the donor and the acceptor can be quite different. Most interestingly, for the Fe^{2+}/Fe^{3+} exchange in water/DMSO mixture, we predict a reorganization energy that is much larger than that in either of the pure components. Such compositional contribution to the reorganization energy is significant in magnitude and represents a new feature addressed by our work.

By consideration of the local solvent composition profiles around the charged solutes, we identify three classes of binary solvent mixtures, each characterized by the different relative magnitudes of the static and optical dielectric constants of the two components. This classification can serve as a convenient guide for the general behavior in the composition dependence of reorganization energy in mixed solvents. In all three classes of solvent mixtures considered, we observe large deviation in solvent reorganization energy from the value predicted by the uniform dielectric treatment, illustrating the important effects of preferential solvation.

The DSCFT in this work provides a general and systematic approach for calculating solvent effects on the ET reorganization energy. While we have only considered ET processes in binary solvent mixtures in this work, it is straightforward to generalize the theory to multi-component mixed solvents. In addition, the shape and the charge distribution of the donor-acceptor complex can be generalized to describe intermolecular or intramolecular charge transfer of macromolecules. At present, the effects of mixed solvent on ET reaction rate remain largely unexplored; we hope that our theory can facilitate further exploration in the subject by providing a fast and reliable approximation to the solvent reorganization energy. An important direction is to combine the DSCFT with transition state sampling methods, such as the string method,[180,181] to locate the reaction path of ET. It will be useful to understand how coupled changes in local solvent composition and orientational polarization influence the activation as the reaction proceeds from the equilibrium to the transition state. Furthermore, we note that as a simple coarse-grained theory, the DSCFT involves several assumptions and approximations that can be improved with further devel-

opment. For instance, the local liquid structure around the reacting species can be incorporated using liquid-state density functional theory.[182,183] Due to the small number of solvent molecules in the first solvation shell of the ions, such local structures can lead to more pronounced solvent composition effects than captured in the current theory. It will be interesting to explore these effects in future work.

Appendix 5.A Derivation of the Constitutive Relations

In this supporting information, we derive the constitutive relations under equilibrium condition (Eqs. (5.9) – (5.11)) and nonequilibrium condition (Eqs. (5.15) and (5.16)). We start by extremizing the effective Hamiltonian H in Eq. (5.7) with respect to its functional arguments. Under full equilibrium H is extremized with respect to all the field variables φ_S, $\rho_{\rm or}$, $\rho_{\rm el}$, $w_{\rm or}$, $w_{\rm el}$, w_S, and w, respectively giving rise to the following seven relations:

$$w(\mathbf{r}) = w_S(\mathbf{r}) \tag{5.26}$$

$$iw_{\rm or}(\mathbf{r}) = \beta \int d\mathbf{r}' \frac{[\hat{\rho}_c(\mathbf{r}) + \rho_{\rm or}(\mathbf{r}) + \rho_{\rm el}(\mathbf{r})]}{4\pi\epsilon_0|\mathbf{r}-\mathbf{r}'|} \tag{5.27}$$

$$iw_{\rm el}(\mathbf{r}) = \beta \int d\mathbf{r}' \frac{[\hat{\rho}_c(\mathbf{r}) + \rho_{\rm or}(\mathbf{r}) + \rho_{\rm el}(\mathbf{r})]}{4\pi\epsilon_0|\mathbf{r}-\mathbf{r}'|} \tag{5.28}$$

$$\begin{aligned}\rho_{\rm or}(\mathbf{r}) = & -i\sum_S \frac{e^{\beta\mu_S}}{\eta_S} 4\pi\bar{\mu}_S^2 \left(\frac{2\pi\alpha_S}{\beta}\right)^{\frac{3}{2}} \nabla\cdot\Big[\Gamma(\mathbf{r}) e^{iw_S(\mathbf{r})v_S - \frac{\alpha_S}{2\beta}(\nabla w_{\rm el}(\mathbf{r}))^2} \\ & \times \left(\cot(\bar{\mu}_S|\nabla w_{\rm or}(\mathbf{r})|) - \frac{1}{\bar{\mu}_S|\nabla w_{\rm or}(\mathbf{r})|}\right) \frac{\sin(\bar{\mu}_S|\nabla w_{\rm or}(\mathbf{r})|)}{(\bar{\mu}_S|\nabla w_{\rm or}(\mathbf{r})|)^2} \bar{\mu}_S^2 \nabla w_{\rm or}(\mathbf{r})\Big]\end{aligned} \tag{5.29}$$

$$\rho_{\rm el}(\mathbf{r}) = i\sum_S \frac{e^{\beta\mu_S}}{\eta_S} 4\pi\bar{\mu}_S^2 \left(\frac{2\pi\alpha_S}{\beta}\right)^{\frac{3}{2}} \frac{\alpha_S}{\beta}\nabla\cdot\Big[\Gamma(\mathbf{r}) e^{iw_S(\mathbf{r})v_S - \frac{\alpha_S}{2\beta}(\nabla w_{\rm el}(\mathbf{r}))^2} \times \frac{\sin(\bar{\mu}_S|\nabla w_{\rm or}(\mathbf{r})|)}{\bar{\mu}_S|\nabla w_{\rm or}(\mathbf{r})|}\nabla w_{\rm or}(\mathbf{r})\Big] \tag{5.30}$$

$$\varphi_S(\mathbf{r}) = \frac{e^{\beta\mu_S}}{\eta_S} 4\pi\bar{\mu}_S^2 \left(\frac{2\pi\alpha_S}{\beta}\right)^{\frac{3}{2}} v_S\Gamma(\mathbf{r}) e^{iw_S(\mathbf{r})v_S - \frac{\alpha_S}{2\beta}(\nabla w_{\rm el}(\mathbf{r}))^2} \frac{\sin(\bar{\mu}_S|\nabla w_{\rm or}(\mathbf{r})|)}{\bar{\mu}_S|\nabla w_{\rm or}(\mathbf{r})|} \tag{5.31}$$

$$\sum_S \varphi_S(\mathbf{r}) = 1 \tag{5.32}$$

Under nonequilibrium condition in which $\rho_{\rm or}$ and φ_S are fixed at their out-of-equilibrium values, H is extremized with respect to $\rho_{\rm el}$, $w_{\rm or}$, $w_{\rm el}$, w_S, and w, and therefore, only Eqs. (5.28) – (5.32) are applicable.

To further simplify the equations, we substitute Eq. (5.31) into Eqs. (5.29) and (5.30), and rewrite Eqs. (5.29) and (5.30) respectively as

$$\rho_{\rm or}(\mathbf{r}) = -i\nabla\cdot\left[\sum_S \frac{\varphi_S(\mathbf{r})}{v_S}\left(\cot(\bar{\mu}_S|\nabla w_{\rm or}(\mathbf{r})|) - \frac{1}{\bar{\mu}_S|\nabla w_{\rm or}(\mathbf{r})|}\right)\frac{1}{\bar{\mu}_S|\nabla w_{\rm or}(\mathbf{r})|}\bar{\mu}_S^2\nabla w_{\rm or}(\mathbf{r})\right] \tag{5.33}$$

and

$$\rho_{\rm el}(\mathbf{r}) = i\nabla\cdot\left[\sum_S \frac{\alpha_S}{\beta}\frac{\varphi_S(\mathbf{r})}{v_S}\nabla w_{\rm or}(\mathbf{r})\right] \tag{5.34}$$

Because Eq. (5.33) holds under both equilibrium and nonequilibrium conditions, one can show that the conjugate field to the orientational polarization $w_{\rm or}$ is determined once $\rho_{\rm or}$ and φ_S are specified. Therefore, when an equilibrium state and a nonequilibrium state have equal values for $\rho_{\rm or}$ and φ_S due to their unchanged nuclear configurations, the two states have the same values for $w_{\rm or}$ as well. To simplify the expressions further, we introduce the the orientational and electronic electric susceptibilities $\chi_{\rm or}(\mathbf{r})$ and $\chi_{\rm el}(\mathbf{r})$, and rewrite Eqs. (5.33) and (5.34) as

$$\rho_{\rm or}(\mathbf{r}) = i\nabla\cdot\left[\frac{\epsilon_0}{\beta}\chi_{\rm or}(\mathbf{r})\nabla w_{\rm or}(\mathbf{r})\right] \tag{5.35}$$

and

$$\rho_{\mathrm{el}}(\mathbf{r}) = i\nabla \cdot \left[\frac{\epsilon_0}{\beta}\chi_{\mathrm{el}}(\mathbf{r})\nabla w_{\mathrm{el}}(\mathbf{r})\right] \tag{5.36}$$

where $\chi_{\mathrm{or}}(\mathbf{r})$ and $\chi_{\mathrm{el}}(\mathbf{r})$ are, respectively, given by

$$\chi_{\mathrm{or}}(\mathbf{r}) = -\frac{\beta}{\epsilon_0}\sum_S \frac{\varphi_S(\mathbf{r})}{v_S}\left(\cot(\bar{\mu}_S|\nabla w_{\mathrm{or}}(\mathbf{r})|) - \frac{1}{\bar{\mu}_S|\nabla w_{\mathrm{or}}(\mathbf{r})|}\right)\frac{1}{\bar{\mu}_S|\nabla w_{\mathrm{or}}(\mathbf{r})|}\bar{\mu}_S^2 \tag{5.37}$$

and

$$\chi_{\mathrm{el}}(\mathbf{r}) = \frac{\beta}{\epsilon_0}\sum_S \frac{\alpha_S}{\beta}\frac{\varphi_S(\mathbf{r})}{v_S} \tag{5.38}$$

Furthermore, upon taking the Laplacian on both sides of Eqs. (5.27) and (5.28), we can write these equations respectively as

$$-i\frac{\epsilon_0}{\beta}\nabla^2 w_{\mathrm{or}}(\mathbf{r}) = \hat{\rho}_c(\mathbf{r}) + \rho_{\mathrm{or}}(\mathbf{r}) + \rho_{\mathrm{el}}(\mathbf{r}) \tag{5.39}$$

$$-i\frac{\epsilon_0}{\beta}\nabla^2 w_{\mathrm{el}}(\mathbf{r}) = \hat{\rho}_c(\mathbf{r}) + \rho_{\mathrm{or}}(\mathbf{r}) + \rho_{\mathrm{el}}(\mathbf{r}) \tag{5.40}$$

To make the calculations more convenient, we remove ρ_{or} and ρ_{el} from Eqs. (5.39) and (5.40) equations using Eqs. (5.35) and (5.36). The resulting equations are

$$-i\frac{\epsilon_0}{\beta}\nabla \cdot [\nabla w_{\mathrm{or}}(\mathbf{r}) + \chi_{\mathrm{or}}(\mathbf{r})\nabla w_{\mathrm{or}}(\mathbf{r}) + \chi_{\mathrm{el}}(\mathbf{r})\nabla w_{\mathrm{el}}(\mathbf{r})] = \hat{\rho}_c(\mathbf{r}) \tag{5.41}$$

$$-i\frac{\epsilon_0}{\beta}\nabla \cdot [\nabla w_{\mathrm{el}}(\mathbf{r}) + \chi_{\mathrm{or}}(\mathbf{r})\nabla w_{\mathrm{or}}(\mathbf{r}) + \chi_{\mathrm{el}}(\mathbf{r})\nabla w_{\mathrm{el}}(\mathbf{r})] = \hat{\rho}_c(\mathbf{r}) \tag{5.42}$$

Furthermore, by letting the fields w_S, w_{el}, and w_{or} go to zero as $|\mathbf{r}| \to \infty$ in Eq. (5.31), we may equate the bulk volume fraction $\varphi_S^{(\infty)}$ with the following factor

$$\varphi_S^{(\infty)} = \frac{e^{\beta\mu_S}}{\eta_S}4\pi\bar{\mu}_S^2\left(\frac{2\pi\alpha_S}{\beta}\right)^{\frac{3}{2}}v_S \tag{5.43}$$

With these simplifications, we summarize the constitutive relations as follows:

$$w(\mathbf{r}) = w_S(\mathbf{r}) \tag{5.44}$$

$$-i\frac{\epsilon_0}{\beta}\nabla\cdot[\nabla w_{\rm or}(\mathbf{r})+\chi_{\rm or}(\mathbf{r})\nabla w_{\rm or}(\mathbf{r})+\chi_{\rm el}(\mathbf{r})\nabla w_{\rm el}(\mathbf{r})]=\hat{\rho}_c(\mathbf{r}) \tag{5.45}$$

$$-i\frac{\epsilon_0}{\beta}\nabla\cdot[\nabla w_{\rm el}(\mathbf{r})+\chi_{\rm or}(\mathbf{r})\nabla w_{\rm or}(\mathbf{r})+\chi_{\rm el}(\mathbf{r})\nabla w_{\rm el}(\mathbf{r})]=\hat{\rho}_c(\mathbf{r}) \tag{5.46}$$

$$\varphi_S(\mathbf{r})=\Gamma(\mathbf{r})\varphi_S^{(\infty)}e^{iw_S(\mathbf{r})v_S-\frac{\alpha_S}{2\beta}(\nabla w_{\rm el}(\mathbf{r}))^2}\frac{\sin(\bar{\mu}_S|\nabla w_{\rm or}(\mathbf{r})|)}{\bar{\mu}_S|\nabla w_{\rm or}(\mathbf{r})|} \tag{5.47}$$

$$\sum_S\varphi_S(\mathbf{r})=1 \tag{5.48}$$

where

$$\chi_{\rm or}(\mathbf{r})=-\frac{\beta}{\epsilon_0}\sum_S\frac{\varphi_S(\mathbf{r})}{v_S}\left(\cot(\bar{\mu}_S|\nabla w_{\rm or}(\mathbf{r})|)-\frac{1}{\bar{\mu}_S|\nabla w_{\rm or}(\mathbf{r})|}\right)\frac{1}{\bar{\mu}_S|\nabla w_{\rm or}(\mathbf{r})|}\bar{\mu}_S^2 \tag{5.49}$$

and

$$\chi_{\rm el}(\mathbf{r})=\frac{\beta}{\epsilon_0}\sum_S\frac{\alpha_S}{\beta}\frac{\varphi_S(\mathbf{r})}{v_S} \tag{5.50}$$

The saddle-point condition yields purely imaginary values for the fields $w_{\rm or}$, $w_{\rm el}$, w, and w_S. In order to work with real quantities and for the convenience of relating our theory to classical electrostatics, we make a change of variables $w_{\rm or}=-i\beta\phi_{\rm or}$, $w_{\rm el}=-i\beta\phi_{\rm el}$, $w=i\beta u$, and $w_S=i\beta u_S$ in Eqs. (5.44) – (5.48). This results in Eq. (9) – (11) in main text. The nonequilibrium constitutive relations in Eqs. (15) and (16) correspond to Eqs. (5.46) – (5.48).

Chapter 6

Electron Transfer Reorganization Energy in Solvent Mixtures: Theory and Simulations

Solvent mixtures are commonly used as the medium for electron transfer (ET) reactions, such as in recent developments of lithium-ion batteries,[154] as one can tune the mixture composition for optimal performance.[132,161,162,168,172,174,175,184] However, even though a mature theoretical framework has been developed for ET in pure solvents since the landmark work by Marcus in 1956,[68–70] the chemical physics of ET in solvent mixtures is far from being elucidated. In a solvent mixture, the ET dynamics would be influenced by the phenomenon of preferential solvation, where the local composition of the solvent around the charged redox centers differs from the bulk composition.[2,173,185] In addition, the solvent reorganization energy not only have contributions from the nonequilibrium solvent orientational polarization as in a pure solvent, but also from the nonequilibrium solvent composition.[186] As the variation in the solvent composition occurs at molecular length scale,[44,131] one must use a molecularly-based method that accounts for both the nuclear and electronic degrees of freedom of the molecules to study ET dynamics in mixed solvents.[187]

In a recent work, we developed the dipolar self-consistent-field theory (DSCFT) for calculating the ET reorganization energy in solvent mixtures using field-theoretic techniques.[177,186] The theory describes each solvent molecule by its permanent dipole moment, polarizability, and molecular volume, all of which are readily-available pa-

rameters in physicochemical tables. The coarse-graining procedure provides a convenient way to separate the fast electronic and the slow nuclear response in the mixed solvent. Under saddle-point approximations, we self-consistently determine the composition and dielectric response of the solvent, and the solvent property in the vicinity of the redox centers is found to have a predominant effect on the reorganization energy.[186] However, as a coarse-grained theory, the DSCFT does not take into account the specific molecular structures and interactions. In this work, we examine equilibrium and nonequilibrium solvation of charged redox centers using molecular dynamics (MD) simulations with explicit solvent molecules. The solvent reorganization energy and the solvent compositions calculated using the MD simulations will be directly compared with the predictions from the DSCFT to evaluate the robustness of our previous field-theoretic coarse-grained approach. As the solvent electronic response is due to the induced dipoles of solvent molecules, we employ polarizable solvent models with the Drude polarizable force field; to the best of our knowledge, this is the first MD simulation for studying nonequilibrium solvation and ET reorganization energy in *polarizable* solvent mixtures.

In this work, we study the Fe^{2+}/Fe^{3+} electron exchange in mixed solvents, with the distance between Fe^{2+} and Fe^{3+} fixed at 5.5 Å.[88] To demonstrate the essential behaviors of charge solvation in mixed solvents, we consider the reaction in three binary solvent mixtures, each consisting of water and one of the three prototype molecules that has the same structure as water by differs from water only in its permanent dipole moment and/or polarizability. The three prototype molecules are named MODEL-A, MODEL-B, and MODEL-C; their relative permanent dipole moment $\tilde{\mu}$ and the relative polarizability $\tilde{\alpha}$ to that of water are listed in Table 6.1. In particular, MODEL-A has the same polarizability as water but a smaller permanent dipole moment, MODEL-B has the same permanent dipole moment as water but a larger polarizability, and MODEL-C has a smaller permanent dipole moment but a larger polarizability than water. The mixture of water and MODEL-X is correspondingly denoted as Mixture X ($X = A, B, C$).

Table 6.1: The permanent dipole and the polarizability of the prototype solvent models relative to water.

Prototype Model	MODEL-A	MODEL-B	MODEL-C
$\tilde{\mu}$	0.616	1	0.628
$\tilde{\alpha}$	1	1.300	1.711

6.1 The DSCFT

The DSCFT is a field-theoretic coarse-grained theory for calculating the energy for charge solvation under equilibrium and nonequilibrium conditions. The nonequilibrium condition refers to situation at which the solvent orientational polarization and composition are out of equilibrium. The theory describes the electron-transferring solute by its charge distribution $\rho_c(\mathbf{r})$ in a region $\mathcal{C}$ that is inaccessible to the solvent molecules. Each solvent molecule of type s is characterized by its permanent dipole moment $\bar{\mu}_s$, polarizability α_s, and volume v_s. We formulate the theory by transforming the particle-based partition function of the system into a field representation in the grand canonical ensemble of open solvent, introducing coarse-grained fields including the orientational polarization (due to permanent dipoles) and the electronic polarization (due to induced dipoles), their conjugate fields, and the solvent composition. We then extremize the Boltzmann factor in the partition function according to procedures of saddle-point approximation: under the equilibrium condition, we perform a full extremization with respect to all coarse-grained fields; under the nonequilibrium condition, we perform a constrained extremization instead, keeping the orientational polarization, its conjugate field, and the solvent composition fixed at their values from the previous equilibrium state. The details of the derivation are provided in Refs. 177 and 186. Here, we present the key equations obtained in the theory. In the equilibrium condition, the following set of constitutive relations is satisfied:

$$\nabla \cdot \mathbf{D}(\mathbf{r}) = \rho_c(\mathbf{r}) \tag{6.1a}$$

$$\mathbf{D}(\mathbf{r}) = -\epsilon_0[1 + \chi_{\mathrm{el}}(\mathbf{r}) + \chi_{\mathrm{or}}(\mathbf{r})]\nabla\phi(\mathbf{r}) \tag{6.1b}$$

$$\chi_{\rm or}(\mathbf{r}) = \Gamma(\mathbf{r})\frac{\beta}{\epsilon_0}\sum_s \frac{\varphi_s^{(\infty)}}{v_s}\bar{\mu}_s^2 B_s[u(\mathbf{r}),\phi(\mathbf{r})]G(\beta\bar{\mu}_s|\nabla\phi(\mathbf{r})|) \tag{6.1c}$$

$$\chi_{\rm el}(\mathbf{r}) = \Gamma(\mathbf{r})\sum_s \frac{\varphi_s(\mathbf{r})\alpha_s}{v_s\epsilon_0} \tag{6.1d}$$

$$\varphi_s(\mathbf{r}) = \Gamma(\mathbf{r})\varphi_s^{(\infty)} B_s[u(\mathbf{r}),\phi(\mathbf{r})]\frac{\sinh(\beta\bar{\mu}_s|\nabla\phi(\mathbf{r})|)}{\beta\bar{\mu}_s|\nabla\phi(\mathbf{r})|} \tag{6.1e}$$

where $\beta = 1/k_BT$ is the inverse temperature, ϵ_0 is the vacuum permittivity, $G(x) = (1/\tanh x - 1/x)\sinh x/x^2$, and $B_s[u(\mathbf{r}),\phi(\mathbf{r})] = \exp[-\beta u(\mathbf{r})v_s + \frac{\beta\alpha_s}{2}|\nabla\phi(\mathbf{r})|^2]$. $\mathbf{D}$ denotes the electric displacement, while $\chi_{\rm or}$ and $\chi_{\rm el}$ are the electric susceptibilities due to the permanent and the induced dipoles, respectively. $\varphi_s^{(\infty)}$ and $\varphi_s(\mathbf{r})$ are respectively the bulk and the local volume fractions of the $s^{\rm th}$ solvent component, satisfying $\sum_s \varphi_s = 1$. ϕ and u are the electrostatic potential and the incompressibility potential to be solved through the set of equations. $\Gamma(\mathbf{r})$ is the indicator function for the space outside the solute cavity that is accessible to the solvent, such that $\Gamma(\mathbf{r}) = 0$ if $\mathbf{r} \in \mathcal{C}$ and 1 otherwise.

In addition, the following set of constitutive relations holds under the nonequilibrium condition:

$$\nabla\cdot\mathbf{D} = \rho_c(\mathbf{r}) \tag{6.2a}$$

$$\mathbf{D} = -\epsilon_0\left[(1+\chi_{\rm el}(\mathbf{r}))\nabla\phi_{\rm el}(\mathbf{r}) + \chi_{\rm or}(\mathbf{r})\nabla\phi_{\rm or}(\mathbf{r})\right] \tag{6.2b}$$

$$\chi_{\rm el}(\mathbf{r}) = \Gamma(\mathbf{r})\sum_s \frac{\varphi_s(\mathbf{r})\alpha_s}{v_s\epsilon_0} \tag{6.2c}$$

$$\varphi_s(\mathbf{r}) = \Gamma(\mathbf{r})\varphi_s^{(\infty)} B_s[u_s(\mathbf{r}),\phi_{\rm el}(\mathbf{r})]\frac{\sinh(\beta\bar{\mu}_s|\nabla\phi_{\rm or}(\mathbf{r})|)}{\beta\bar{\mu}_s|\nabla\phi_{\rm or}(\mathbf{r})|} \tag{6.2d}$$

where the values $\chi_{\rm or}$, $\phi_{\rm or}$, and φ_s are from the corresponding equilibrium state. Superscripts are added to ϕ and u under the nonequilibrium condition as the conditions $\phi = \phi_{\rm or} = \phi_{\rm el}$ and $u = u_s$ holds in the equilibrium condition but not in the nonequilibrium condition.

Using the saddle-point values for the coarse-grained field variables obtained by

solving the constitutive relations, the free energy of solvation is

$$G[\rho_c, \mathbb{C}] = \int d\mathbf{r} \left[-\sum_s \left(u_s(\mathbf{r})\varphi_s(\mathbf{r}) + \frac{\varphi_s(\mathbf{r})}{\beta v_s} \right) + \epsilon_0 \left(\frac{1}{2} + \chi_{\mathrm{el}}(\mathbf{r}) \right) |\nabla\phi_{\mathrm{el}}(\mathbf{r})|^2 + \epsilon_0 \chi_{\mathrm{or}} |\nabla\phi_{\mathrm{or}}(\mathbf{r})|^2 \right] \tag{6.3}$$

where $\mathbb{C} = \{\varphi_s, \chi_{\mathrm{or}}, \phi_{\mathrm{or}}, \mathcal{C}\}$ is the nuclear configuration set that includes all information specifying the coarse-grained nuclear configuration. In evaluating the solvation energy with Eq. (6.3), the fields χ_{el}, ϕ_{el}, and u_s are solved with Eq. (6.1) under the equilibrium condition or Eq. (6.2) under the nonequilibrium condition.

For the electron exchange reaction $Fe^{2+} + Fe^{3+} \rightarrow Fe^{3+} + Fe^{2+}$, the solute charge distribution in the reactant and the product states are $\rho_c^{(R)}(\mathbf{r}) = 2e\delta(\mathbf{r} - \mathbf{R}_D) + 3e\delta(\mathbf{r} - \mathbf{R}_A)$ and $\rho_c^{(P)}(\mathbf{r}) = 3e\delta(\mathbf{r} - \mathbf{R}_D) + 2e\delta(\mathbf{r} - \mathbf{R}_A)$, respectively, where e is the elementary charge and $\mathbf{R}_D$ and $\mathbf{R}_A$ are the positions of the donor and the acceptor. The solute cavity $\mathcal{C}^{(R)}$ in the reactant state is a region of two spheres described by $\{\mathbf{r} : |\mathbf{r} - \mathbf{R}_D| < a_2 \text{ or } |\mathbf{r} - \mathbf{R}_A| < a_3\}$, where $a_2 = 0.92\,\text{Å}$ and $a_3 = 0.785\,\text{Å}$ are the ionic radii of Fe^{2+} and Fe^{3+} respectively. Similarly, the solute cavity in the product state is given by $\mathcal{C}^{(P)} = \{\mathbf{r} : |\mathbf{r} - \mathbf{R}_D| < a_3 \text{ or } |\mathbf{r} - \mathbf{R}_A| < a_2\}$, with the radii of the charge-transferring species exchanged after the reaction. The reorganization energy of the reaction is given by

$$\lambda = G[\rho_c^{(P)}, \mathbb{C}^{(R)}] - G[\rho_c^{(P)}, \mathbb{C}^{(P)}] \tag{6.4}$$

where the superscript $(R)/(P)$ indicates that the quantity is in equilibrium with the reactant/product's charge distribution. We solve Eqs. (6.1a) and (6.2a) by assuming that $\mathbf{D}$ can be written as a superposition of the displacements due to the individual solute charges. The detailed procedure for the numerical evaluation is given in Ref. 186. In our calculation, the solvent parameters for water are $\bar{\mu}_{\mathrm{w}} = 1.85\,\text{D}$, $\alpha_{\mathrm{w}} = 0.978\,\text{Å}^3$, and $v_{\mathrm{w}} = 30.0053\,\text{Å}^3$ (with subscript w stand for water), corresponding to the values for the SWM4-NDP model used in MD simulations. The solvent parameters for the prototype molecules are scaled accordingly.

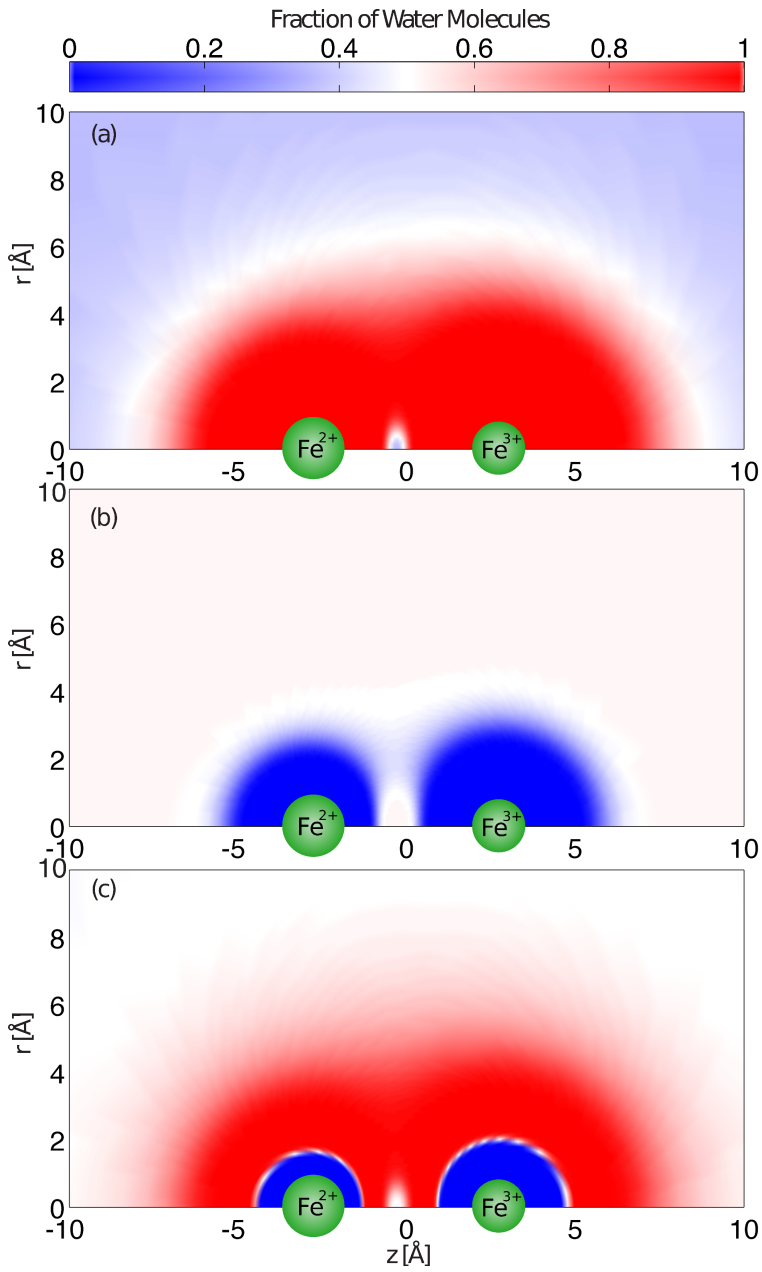

Figure 6.1: The fraction of water molecules around the donor-acceptor pair in (a) Mixture A at $\varphi_{\mathrm{w}}^{(\infty)} = 0.35$, (b) Mixture B at $\varphi_{\mathrm{w}}^{(\infty)} = 0.53$, and (c) Mixture C at $\varphi_{\mathrm{w}}^{(\infty)} = 0.48$ at the equilibrium state calculated by the DSCFT. The fraction of water is displayed in the cylindrical $rz-$coordinate where the centers of the Fe^{2+} and Fe^{3+} ions are located at $(r, z) = (0, -2.75)$ and $(0, 2.75)$ respectively.

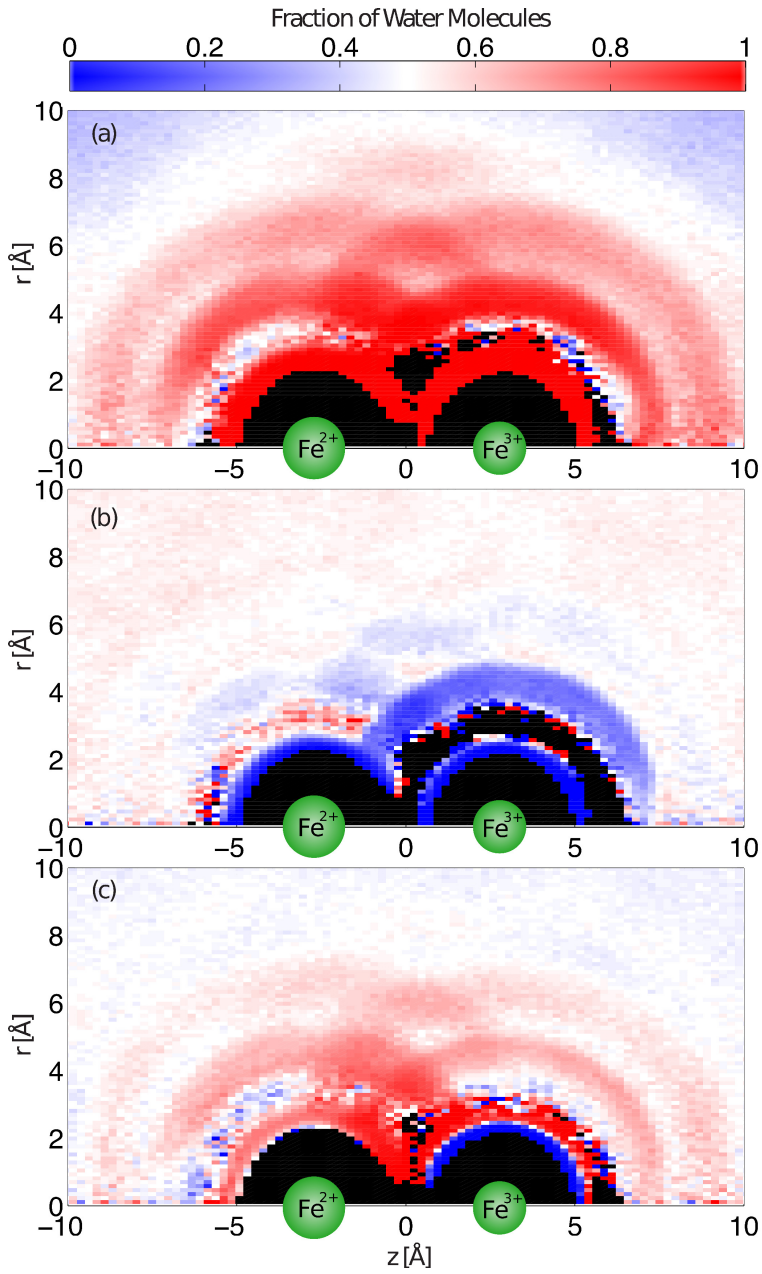

Figure 6.2: The fraction of water molecules around the donor-acceptor pair in (a) Mixture A at $\varphi_{\mathrm{w}}^{(\infty)} = 0.35$, (b) Mixture B at $\varphi_{\mathrm{w}}^{(\infty)} = 0.53$, and (c) Mixture C at $\varphi_{\mathrm{w}}^{(\infty)} = 0.48$ at the equilibrium state from the MD simulation. The fraction of water molecules is calculated based on the frequency of appearance of oxygen atoms in an $rz-$grid in the cylindrical coordinate. The centers of the Fe^{2+} and Fe^{3+} ions are located at $(r, z) = (0, -2.75)$ and $(0, 2.75)$ respectively. The grids points that do not have any appearance of the oxygen atom are colored in black.

6.2 MD Simulations

We perform MD simulations using the Drude polarizable force field with the SWM4-NDP model for water.[188–190] To create the models for the prototype solvents, the charges on the SWM4-NDP water responsible for the permanent and the induced dipoles are scaled according to $\tilde{\mu}$ and $\tilde{\alpha}$ correspondingly. The description of the force field and the parameters are provided in the supporting information. The Fe ions are described by the Lennard-Jones parameters ($\sigma_{\mathrm{FeO}} = 2.53\,\text{Å}$, $\epsilon_{\mathrm{FeO}} = -1.2\text{kcal/mol}$ for the FeO interaction only) with point charges $+2e/+3e$ at the center.[79,88] We perform the simulation using the OpenMM package.[191] The trajectory is propagated using the extended Lagrangian dynamics with a dual-Langevin thermostat scheme, where the relative position of each Drude-nucleus pair is simulated at temperature 1 K and damping coefficient $5.0\,\text{ps}^{-1}$, and the rest of the degrees of freedom are at 298.15 K and damping coefficients 20.0 ps^{-1}.[192] All simulations are carried out with a pair of Fe ions and 430 solvent molecules in a cubic simulation cell of size $23.46\,\text{Å} \times 23.46\,\text{Å} \times 23.46\,\text{Å}$ under periodic boundary condition. Following initial equilibration for 1300 ps, the microstate of the system is collected every picosecond for 3000 ps. For each solvent composition, 12 repeated simulations are carried out starting from different randomly-generated initial configurations.

In the MD simulation, the nuclear degrees of freedom of the solvent are represented by the positions of all atomic sites $\{\mathbf{r}_{\gamma,i}\}$, where $\mathbf{r}_{\gamma,i}$ is the position of the γth atomic site on the ith solvent molecule. The electronic degrees of freedom due to the induced dipoles are represented by the positions of all Drude particles $\{\mathbf{r}_{D,i}\}$, with $\mathbf{r}_{D,i}$ denoting the position of the Drude particle on the ith molecule. The solvent reorganization energy can be calculated as a function of the energy gap $\Delta\epsilon$ between the reactant state and the product state at given nuclear configuration $\{\mathbf{r}_{\gamma,i}\}$, which

can be expressed as

$$\Delta\epsilon(\{\mathbf{r}_{\gamma,i}\}) = \min_{\{\mathbf{r}_{D,i}\}} U\left(\rho_c^{(R)}, \{\mathbf{r}_{\gamma,i}\}, \{\mathbf{r}_{D,i}\}\right) - \min_{\{\mathbf{r}_{D,i}\}} U\left(\rho_c^{(P)}, \{\mathbf{r}_{\gamma,i}\}, \{\mathbf{r}_{D,i}\}\right) \tag{6.5}$$

where U is the potential energy of the microstate. The minima of the potential energy with respect to $\{\mathbf{r}_{D,i}\}$ is taken so that the induced dipoles are equilibrated with the charge distribution and the nuclear configuration. We use the free energy perturbation (FEP) method[193,194] to sample the free energy surface away from equilibrium using intermediate values of charges on the two redox centers. The details of the FEP method are provided in the supporting information. By using intermediate solute charge given by $\rho_c^{(m)} = \rho_c^{(R)} + m(\rho_c^{(P)} - \rho_c^{(R)})$ with m being a coefficient between 0 and 1, the FEP method calculates the nonequilibrium free energy surface $\Delta G_R(x)$ over the reactant state and $\Delta G_P(x)$ over the product state using the following expressions:

$$\Delta G_R(x) = -\beta^{-1} \ln \left\langle \delta(\Delta\epsilon - x) e^{-\beta[U_R - U_m]} \right\rangle_m + \Delta G_{mr} \tag{6.6}$$

$$\Delta G_P(x) = -\beta^{-1} \ln \left\langle \delta(\Delta\epsilon - x) e^{-\beta[U_P - U_m]} \right\rangle_m + \Delta G_{mr} \tag{6.7}$$

where $U_s = U\left(\rho_c^{(s)}, \{\mathbf{r}_{\gamma,i}\}, \{\mathbf{r}_{D,i}\}\right)$ for $s = R, P, m$, and ΔG_{mr} is the free energy difference between the equilibrium states under charge distributions $\rho_c^{(m)}$ and $\rho_c^{(R)}$ (whose actual value can be found by connecting the free energy surfaces calculated at different values of m). In addition, $\langle \mathcal{O} \rangle_m$ is the time average of the observable $\mathcal{O}$ in a system with solute charge $\rho_c^{(m)}$. In our calculation, we have used $m = 0, 0.17, 0.32, 0.5$. Assuming parabolicity in the free energy surfaces, the reorganization energy is given by four times the free energy difference between the transition state at $\Delta\epsilon = 0$ and the product equilibrium state as[69]

$$\lambda = 4(\Delta G(0) - \Delta G^{(P)}) \tag{6.8}$$

where $G^{(P)}$ is the free energy of the product equilibrium state.

To calculate the volume fraction of the solvent φ_s at the position (r, z) in the cylindrical coordinate, we count the total number $\mathcal{N}_s$ of oxygen atoms of solvent s appearing in the space bounded by $(r - h/2, r + h/2)$ and $(z - h/2, z + h/2)$ in all sampled microstates, with h being the grid size. The volume fraction φ_X for an X/Y mixture is given by $\varphi_X = \mathcal{N}_X/(\mathcal{N}_X + \mathcal{N}_Y)$. In addition, as the simulations are performed in canonical ensemble with fixed volume fraction in a box, we find the bulk composition by averaging the volume fraction in the region $r > 10\,\text{Å}$ in the cylindrical coordinate.

6.3 Effects of Preferential Solvation on the Solvent Reorganization Energy

In a mixed solvent, the solvent component with the larger permanent dipole moment or the larger polarizability is enriched around the charged solutes to lower the free energy of the system. We expect that the local solvent composition around the charged redox centers, instead of the bulk solvent composition, would have a dominant effect over the ET dynamics in mixed solvents. Here, we examine the connection between the solvent composition around the donor-acceptor complex and the solvent reorganization energy in Mixtures A, B, and C. The three mixtures have different relative permanent dipole moments and polarizabilities between the two components, and each represents a class of binary solvent mixtures. Using both the DSCFT and the MD simulations, we calculate the equilibrium solvent composition profiles around the redox centers, with results displayed in Figs. 6.1 and 6.2. In addition, the solvent reorganization energy as a function of the bulk solvent composition for the Fe^{2+}/Fe^{3+} exchange reaction are computed using both methods, with results plotted in Fig. 6.3. Below, we discuss the connection between the local solvent composition and the reorganization energy in each of the three mixtures.

Mixture A can be described as *permanent-dipole dominated*, as water has a larger permanent dipole moment than MODEL-A while the two have equal polarizability.

The larger permanent dipole moment on water interacts more favorably with the the strong electric field around the multiply-charged solutes, causing water to be enriched around the charged species. In Figs. 6.1(a) and 6.2(a), both the DSCFT and the MD simulation predict that, in Mixture A at $\varphi_{\mathrm{w}}^{(\infty)} = 0.35$, the region around the redox centers is predominantly water. The enrichment of water around the redox centers results in water dominating the solvent reorganization energy in Mixture A. As we observe in Fig. 6.3, both the DSCFT and the MD simulations predict that the solvent reorganization energy at intermediate compositions of Mixture A is approximately equal to that in the pure water.

Mixture B is a *induced-dipole dominated* mixture, as the two components have equal permanent dipole moments but MODEL-B has a much larger polarizability. As observed in Figs. 6.1(b) and 6.2(b), MODEL-B is enriched around the redox centers in this case, because its higher polarizability allows larger induced dipole moments to be developed in very strong electric field around the ions. We also find that the region where MODEL-B is enriched is more extensive around the Fe^{3+} than the Fe^{2+}, as the larger ionic charge on Fe^{3+} polarizes MODEL-B to a greater extent. Due to the enrichment of MODEL-B around the donor-acceptor complex, the solvent reorganization energy in Mixture B is predominantly determined by MODEL-B, as Fig. 6.3 shows that the solvent reorganization energy at intermediate compositions of Mixture B is comparable to that in the pure MODEL-B.

Mixture C represents a more interesting case, as MODEL-C has a larger polarizability but a smaller permanent dipole moment than water, resulting in *permanent- and induced-dipole competition* around the charged solute. In this case, both water and MODEL-C may be enriched around the redox centers. In Fig. 6.1(c), the DSCFT predicts that the region within approximately 2 Å from the ions is favored by the more polarizable MODEL-C, while water is favored in the region between 2 Å to 5 Å from the ions. Additionally, the MODEL-C-enriched region is larger around the Fe^{3+} than around the Fe^{2+}, suggesting that MODEL-C is more favorable around Fe^{3+}. On the other hand, with explicit molecular structures taken into account, the MD simulation predicts that there is a region enriched with MODEL-C in the immediate vicinity of

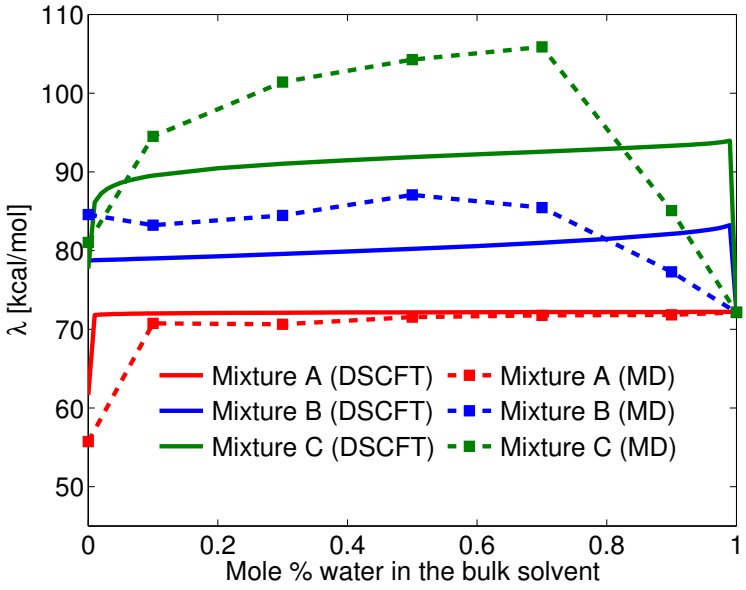

Figure 6.3: The solvent reorganization energy vs. the bulk solvent composition as calculated by the DSCFT and the MD simulations.

Fe^{3+}, but not around the Fe^{2+}. Both the DSCFT and the MD simulations suggest that, at equilibrium, the solvent compositions in the immediate vicinity of the donor and the acceptor are unequal. The spatial inhomogeneity in the solvent composition would lead to an additional contribution to the solvent reorganization energy beyond that contributed by the orientational polarization. As observed in Fig. 6.3, both the DSCFT and the MD simulations predict that the solvent reorganization energy in mixtures of water and MODEL-C are significantly greater than that in either of the pure solvents due to the additional compositional contribution.

6.4 Effects of Polarizability on Solvent Reorganization Energy

In comparing the solvent reorganization energies for Fe^{2+}/Fe^{3+} exchange in pure water and MODEL-B, we find that both the DSCFT and the MD simulations suggest that the reorganization energy is larger in the more polarizable MODEL-B (Fig. 6.3). This is in contrast to the prediction of the commonly-used Marcus theory for re-

organization energy, which predicts that the solvent reorganization decreases with increasing solvent polarizability.[1] There are two competing effects at work when the polarizability increases: on one hand, a more polarizable solvent is able to respond to electronic transitions more easily, and thus reduces the free energy for reorganization; on the other hand, a more polarizable solvent may also interacts with the charged solutes more favorably at the equilibrium state, which lowers the equilibrium free energy and results in a larger energy barrier for the ET process. In this case, the later outpowers the former because of the favorable nonlinear solvent-induced dipole interaction around the redox centers; this nonlinear solvent-solute interaction can be captured with MD simulations or the molecularly-based DSCFT, but not by a linear-dielectric description of solvent as in the Marcus theory.

6.5 On the Validity of Field-Theoretic Coarse-Grained Approach

Comparing the equilibrium solvent composition around the redox centers calculated by the DSCFT (Fig. 6.1) and by the MD simulations (Fig. 6.2), we find that the MD simulations, with specific molecular structures and interactions taken into account, produces more compositional details such as solvation shells. Additionally, as the DSCFT only accounts for the molecular volume at the self-consistent-field level, the solvent compositional features produced may be unphysical, such as in Fig. 6.1(c), where the region enriched with MODEL-C is narrower than the size of solvent molecules. Such compositional features must be interpreted with discretion by averaging the solvent compositional features over molecular sizes. Nevertheless, the DSCFT correctly predicts the asymmetry of solvent composition around the donor and the acceptor in Mixture C. Furthermore, with the additional steric constraints

[1] The Marcus theory predicts that the solvent reorganization energy is proportional to the Pekar factor $(1/\varepsilon_\infty - 1/\varepsilon_s)$, where ε_∞ and ε_s are the solvent optical and static dielectric constants, respectively. The dielectric constants can be further expressed in terms of the orientational electric susceptibility $\chi_{\rm or}$ and the electronic electric susceptibility $\chi_{\rm el}$ as $\varepsilon_\infty = 1 + \chi_{\rm el}$ and $\varepsilon_s = 1 + \chi_{\rm or} + \chi_{\rm el}$. With increasing polarizability, $\chi_{\rm el}$ increases and the Pekar factor decreases.

included in MD simulations, the compositional contribution to the solvent reorganization energy is more significant, as we observe that the reorganization energy at intermediate concentrations of Mixture C is much greater in the MD simulations than in the DSCFT (Fig. 6.3).

For the solvent reorganization energy in the pure solvents as well as in Mixtures A and B, we observe in Fig. 6.3 that the DSCFT predicted value agrees well with the full-atom MD simulations. The solvent compositional profile predicted by the DSCFT also bear many similarities with that sampled by the MD simulations. This is remarkable as the DSCFT is a highly coarse-grained theory with no adjustable parameters. The computational time for the DSCFT is only about an hour on a personal computer, while the MD simulations take weeks of computation time on a GPU cluster.

We note that the DSCFT may predict a sharp change in the solvent reorganization energy on addition of a small amount of one solvent component. This is because the DSCFT is formulated in a grand canonical ensemble, where there is an infinite particle reservoir for the solvent molecules. In comparison, the MD simulations are performed in a simulation cell with a finite number of solvent molecules, and the small and finite simulation box may not provide sufficient number of particles to be comparable to the system in the grand canonical ensemble. Therefore, the predictions of DSCFT and the MD simulations may be more differing when the composition of solvent is highly asymmetric.

6.6 Conclusion

The DSCFT and the MD simulations suggest that the solvent reorganization energy for an ET reaction is largely determined by the local solvent composition around the electron-transferring species. Based on the relative permanent dipole moments and the relative polarizabilities of the solvent components in the mixture, we classify binary mixtures into three categories: permanent-dipole dominant, induced-dipole dominant, as well as one that involves permanent- and induced-dipole competition.

Each class of mixtures produce a distinct compositional profile around the donor-acceptor complex, which predominantly determines the solvent reorganization energy. While the MD simulations provide greater structural details in the solvent composition around the redox centers, the DSCFT, at the self-consistent-field level, is able to capture the general behavior in the solvent composition and the reorganization energy remarkably well.

Appendix 6.A The Drude Polarizable Force Field

The SWM4-NDP model[189,190] has four interaction sites: an oxygen atom, two hydrogen atoms, and an additional massless site "M" located at a fixed distance l_{OM} from the oxygen atom along the bisector of the HOH angle. The OH bond length and the HOH angle are kept fixed. A Drude particle with a small mass is attached to the oxygen atom through a harmonic spring with force constant k_D to describe the induced dipole of the molecule.

All pairwise interactions are truncated at $r_{\mathrm{cut}} = L/2$, where L is the dimension of the simulation box. The Lennard-Jones interactions are exerted between O-O pairs and O-Fe pairs. All other pairs of atomic sites have zero Lennard-Jones interaction energy. The Coulomb interactions between all interaction sites are multiplied by a damping function $S(r)$, such that both the potential and the derivative vanish smoothly at $r = r_{\mathrm{cut}}$:[83]

$$S(r) = \begin{cases} 1 - \dfrac{2r}{r_{\mathrm{cut}}} + \dfrac{r^2}{r_{\mathrm{cut}}^2} & r \le r_{\mathrm{cut}} \\ 0 & r > r_{\mathrm{cut}} \end{cases} \tag{6.9}$$

The total interaction energy of the system can be written as

$$\begin{aligned} U &= \sum_i \frac{1}{2} k_D |\mathbf{r}_{\mathrm{O},i} - \mathbf{r}_{\mathrm{D},i}|^2 + \sum_{i<j} \sum_{\gamma,\gamma'} S(|\mathbf{r}_{\gamma,i} - \mathbf{r}_{\gamma',j}|) \frac{q_\gamma q_{\gamma'}}{4\pi\epsilon_0 |\mathbf{r}_{\gamma,i} - \mathbf{r}_{\gamma',j}|} \\ & \sum_{i<j} \sum_{\gamma,\gamma'} 4\epsilon_{\gamma,\gamma'} \left[\left(\frac{\sigma_{\gamma,\gamma'}}{|\mathbf{r}_{\gamma,i} - \mathbf{r}_{\gamma',j}|} \right)^{12} - \left(\frac{\sigma_{\gamma,\gamma'}}{|\mathbf{r}_{\gamma,i} - \mathbf{r}_{\gamma',j}|} \right)^{6} \right] \end{aligned} \tag{6.10}$$

where $\epsilon_{\gamma,\gamma'}$ and $\sigma_{\gamma,\gamma'}$ are the Lennard-Jones coefficients between atomic sites of type γ and type γ'. The index i and j counts over the molecules (including the Fe ions and the solvent molecules) in the system.

Appendix 6.B The Model Parameters for the Solvents

The parameters for the solvent molecules are provided in 6.2. To avoid polarization catastrophe when the molecules approach the multiply charged Fe^{2+} and Fe^{3+} ions, the spring constant for the Drude particle has been set to $k_D = 5000\,[\mathrm{kcal/mol/\AA^2}]$, with the charges on the O and the D particles adjusted accordingly to keep the polarizability of the molecule constant.

Appendix 6.C The Free Energy Perturbation Method (FEP)

In this section, we derive the free energy perturbation method (FEP) for calculating the free energy surface as a function of the energy gap in the MD simulations. Let ϵ_r and ϵ_p be the energies when the solute charge is at the reactant state and the product state respectively. ϵ_r and ϵ_p are functions of the nuclear configurations denoted by the set of all atomic sites $\{\mathbf{r}_{\gamma,i}\}$. In addition, we denote the potential energy of system by U, which is specified by the charge on the solute $\rho_c(\mathbf{r})$, the positions of all atomic

Table 6.2: Parameters for water and the prototype solvent models used in the MD simulation and the DSCFT

Model	SWM4-NDP(water)	MODEL-A	MODEL-B	MODEL-C
Relative parameters				
$\tilde{\mu}$	1	0.616	1	0.628
$\tilde{\alpha}$	1	1	1.300	1.711
MD simulation parameters				
$\bar{\mu}$ [D]	1.85	1.14	1.85	1.16
α [Å^3]	0.978	0.978	1.27	1.67
$q_{\mathrm{O}}[e]$	3.8379	3.8379	4.9893	6.5663
$q_{\mathrm{D}}[e]$	-3.8379	-3.8379	-4.9893	-6.5663
$q_{\mathrm{H}}[e]$	0.5573	0.3434	0.5573	0.3500
$q_{\mathrm{M}}[e]$	-1.1146	-0.6868	-1.1146	-0.7000
ϵ_{OO} [kcal/mol]	0.21094	0.21094	0.21094	0.21094
σ_{OO} [Å]	3.18395	3.18395	3.18395	3.18395
l_{OH} [Å]	0.9572	0.9572	0.9572	0.9572
$\theta_{\mathrm{HOH}}[^{\mathrm{o}}]$	104.52	104.52	104.52	104.52
l_{OM} [Å]	0.240304	0.240304	0.240304	0.240304
k_D [kcal/mol/Å^2]	5000	5000	5000	5000
DSCFT parameters				
$\bar{\mu}$ [D]	1.85	1.14	1.85	1.16
α [Å^3]	0.978	0.978	1.27	1.67
v [Å^3]	30.0053	30.0053	30.0053	30.0053

sites $\{\mathbf{r}_{\gamma,i}\}$, and the positions of all Drude particles $\{\mathbf{r}_{D,i}\}$. With these, the energy of the reactant and the product states are given by

$$\epsilon_r(\{\mathbf{r}_{\gamma,i}\}) = \min_{\{\mathbf{r}_{D,i}\}} U\left(\rho_c^{(R)}, \{\mathbf{r}_{\gamma,i}\}, \{\mathbf{r}_{D,i}\}\right) \tag{6.11}$$

$$\epsilon_p(\{\mathbf{r}_{\gamma,i}\}) = \min_{\{\mathbf{r}_{D,i}\}} U\left(\rho_c^{(P)}, \{\mathbf{r}_{\gamma,i}\}, \{\mathbf{r}_{D,i}\}\right) \tag{6.12}$$

and the energy gap is given by

$$\Delta\epsilon(\{\mathbf{r}_{\gamma,i}\}) = \epsilon_p(\{\mathbf{r}_{\gamma,i}\}) - \epsilon_r(\{\mathbf{r}_{\gamma,i}\}) \tag{6.13}$$

and the electron transfer process occurs at $\Delta\epsilon = 0$ on the reaction coordinate.

Let us first find the free energy curve when the donor-acceptor pair is in the

reactant state. The probability for finding the system in a configuration with $\Delta\epsilon = x$ can be expressed as a time average over the trajectory as

$$p_r(x) = \frac{n_r(x)}{n_{\text{total}}} = \frac{1}{n_{\text{total}}} \sum_{i=1}^{n_{\text{total}}} \delta(\Delta\epsilon(t_i) - x) \tag{6.14}$$

where $n_r(x)$ is the number of frames in the trajectory when the configuration gives $\Delta\epsilon = x$ when the solute is in the reactant state, and n_{total} is the total number of frames. $\Delta\epsilon(t_i)$ denotes the energy gap at the i^{th} timestep in the trajectory. The operational definition of the delta function in the simulation is $\delta(\Delta\epsilon(t_i) - x) = 1$ when $|\Delta\epsilon(t_i) - x| \leq \Delta x/2$, with $\Delta x = (x_{\max} - x_{\min})/n_{\text{bins}}$ being the size of bins.

On the other hand, $p_r(x)$ may also be written as a configurational average as

$$p_r(x) = \frac{\int d\xi\, \delta(\Delta\epsilon(\{\mathbf{r}_{\gamma,i}\}) - x) e^{-\beta U\left(\rho_c^{(R)}, \{\mathbf{r}_{\gamma,i}\}, \{\mathbf{r}_{D,i}\}\right)}}{\int d\xi\, e^{-\beta U\left(\rho_c^{(R)}, \{\mathbf{r}_{\gamma,i}\}, \{\mathbf{r}_{D,i}\}\right)}} \tag{6.15}$$

where $\int d\xi = \prod_{\gamma,i} \int d\mathbf{r}_{\gamma,i} \prod_i \int d\mathbf{r}_{D,i}$ denotes the integral over the configuration space.

To derive an equation for the FEP method, we perform identity transformation on 6.15 by multiplying the same factor simultaneously to the numerator and the denominator as

$$\begin{aligned}
& p_r(x) \\
= \; & \frac{\int d\xi\, \delta(\Delta\epsilon(\{\mathbf{r}_{\gamma,i}\}) - x) e^{-\beta\left[U\left(\rho_c^{(R)}, \{\mathbf{r}_{\gamma,i}\}, \{\mathbf{r}_{D,i}\}\right) - U\left(\rho_c^{(m)}, \{\mathbf{r}_{\gamma,i}\}, \{\mathbf{r}_{D,i}\}\right)\right] - \beta U\left(\rho_c^{(m)}, \{\mathbf{r}_{\gamma,i}\}, \{\mathbf{r}_{D,i}\}\right)}}{\int d\xi\, e^{-\beta U\left(\rho_c^{(m)}, \{\mathbf{r}_{\gamma,i}\}, \{\mathbf{r}_{D,i}\}\right)}} \\
& \times \frac{\int d\xi\, e^{-\beta\left[U\left(\rho_c^{(m)}, \{\mathbf{r}_{\gamma,i}\}, \{\mathbf{r}_{D,i}\}\right) - U\left(\rho_c^{(R)}, \{\mathbf{r}_{\gamma,i}\}, \{\mathbf{r}_{D,i}\}\right)\right] - \beta U\left(\rho_c^{(R)}, \{\mathbf{r}_{\gamma,i}\}, \{\mathbf{r}_{D,i}\}\right)}}{\int d\xi\, e^{-\beta U\left(\rho_c^{(R)}, \{\mathbf{r}_{\gamma,i}\}, \{\mathbf{r}_{D,i}\}\right)}} \\
= \; & \left\langle \delta(\Delta\epsilon(\{\mathbf{r}_{\gamma,i}\}) - x) e^{-\beta\left[U\left(\rho_c^{(R)}, \{\mathbf{r}_{\gamma,i}\}, \{\mathbf{r}_{D,i}\}\right) - U\left(\rho_c^{(m)}, \{\mathbf{r}_{\gamma,i}\}, \{\mathbf{r}_{D,i}\}\right)\right]} \right\rangle_m \\
& \times \left\langle e^{-\beta\left[U\left(\rho_c^{(m)}, \{\mathbf{r}_{\gamma,i}\}, \{\mathbf{r}_{D,i}\}\right) - U\left(\rho_c^{(R)}, \{\mathbf{r}_{\gamma,i}\}, \{\mathbf{r}_{D,i}\}\right)\right]} \right\rangle_R
\end{aligned} \tag{6.16}$$

where $\rho_c^{(m)}$ is an intermediate value of the charge distribution on the solute given by

$$\rho_c^{(m)} = \rho_c^{(R)} + m(\rho_c^{(P)} - \rho_c^{(R)}) \tag{6.17}$$

and the average $\langle \mathcal{O} \rangle_s$ is defined as

$$\langle \mathcal{O} \rangle_s = \frac{\int d\xi \mathcal{O} e^{-\beta U\left(\rho_c^{(s)}, \{\mathbf{r}_{\gamma,i}\}, \{\mathbf{r}_{D,i}\}\right)}}{\int d\xi e^{-\beta U\left(\rho_c^{(s)}, \{\mathbf{r}_{\gamma,i}\}, \{\mathbf{r}_{D,i}\}\right)}} \tag{6.18}$$

with $s = R, m$ describing the charge state of the solute. The average $\langle \mathcal{O} \rangle_s$ can be sampled as a time average from the trajectory in an MD simulation with the corresponding charge state of the solute.

The free energy of the system when the solute is at the reactant state can be calculated by

$$\begin{aligned} & \Delta G_r(x) \\ = \; & -\beta^{-1} \ln p_r(x) \\ = \; & -\beta^{-1} \ln \left\langle \delta(\Delta\epsilon(\{\mathbf{r}_{\gamma,i}\}) - x) e^{-\beta\left[U\left(\rho_c^{(R)}, \{\mathbf{r}_{\gamma,i}\}, \{\mathbf{r}_{D,i}\}\right) - U\left(\rho_c^{(m)}, \{\mathbf{r}_{\gamma,i}\}, \{\mathbf{r}_{D,i}\}\right)\right]} \right\rangle_m + \Delta G_{mr} \end{aligned} \tag{6.19}$$

where

$$\Delta G_{mr} = -\beta^{-1} \ln \left[\frac{\int d\xi e^{-\beta U\left(\rho_c^{(m)}, \{\mathbf{r}_{\gamma,i}\}, \{\mathbf{r}_{D,i}\}\right)}}{\int d\xi e^{-\beta U\left(\rho_c^{(R)}, \{\mathbf{r}_{\gamma,i}\}, \{\mathbf{r}_{D,i}\}\right)}} \right] \tag{6.20}$$

Similarly,

$$\begin{aligned} & \Delta G_p(x) \\ = \; & -\beta^{-1} \ln p_p(x) + \Delta G_{pr} \\ = \; & -\beta^{-1} \ln \left\langle \delta(\Delta\epsilon(\{\mathbf{r}_{\gamma,i}\}) - x) e^{-\beta\left[U\left(\rho_c^{(P)}, \{\mathbf{r}_{\gamma,i}\}, \{\mathbf{r}_{D,i}\}\right) - U\left(\rho_c^{(m)}, \{\mathbf{r}_{\gamma,i}\}, \{\mathbf{r}_{D,i}\}\right)\right]} \right\rangle_m + \Delta G_{mr} \end{aligned} \tag{6.21}$$

This page is intentionally left blank to signify the end of Part II.

Chapter 7

Summary and Outlook

This thesis has presented field-theoretic treatments for two main systems: an equilibrium system with polar liquids and their mixtures, as well as a nonequilibrium system in the context of electron transfer reactions, where the solvent orientational polarization and composition are out of equilibrium with the charge on the electron-transferring solute. For the equilibrium system of polar liquids and their mixtures, we have introduced a variational approach, such that the effects of reaction field in the system can be accounted for. We have compared the dielectric constants of the liquids and their mixtures and the miscibility of liquids predicted by our theory to experimental results, and found that the agreements between theoretical predictions and experimental observations are impressive. For the nonequilibrium system where the solvent orientation polarization is out-of-equilibrium with the solute charge, we have employed a self-consistent-field approach with a constrained orientational polarization and solvent composition to derive a nonequilibrium solvation energy for the situation. In particular, for nonequilibrium charge solvation in solvent mixtures, we have identified three classes of binary solvent mixtures, each characterized by the different relative magnitudes of the static and optical dielectric constants of the two components. This classification can serve as a convenient guide for the general behavior in the composition dependence of reorganization energy in mixed solvents. In all three classes of solvent mixtures considered, we observe large deviation in solvent reorganization energy from the value predicted by the uniform dielectric treatment, illustrating the important effects of preferential solvation.

The field-theoretic treatments for solvent presented in this thesis represent a particularly systematic and convenient approach to perform coarse-graining for the pure solvents and their mixtures. With a small number of readily-available, non-adjustable molecular parameters, the basic physics of the solvent is captured. The resulting free energy expressions and constitutive relations derived from the theories are also simple and convenient to use. Since the field-theoretic approaches present a convenient way for coarse-graining the solvent while capturing the basic solvent properties, such as the effect of preferential solvation in the immediate vicinity of the charged solute, we see the potential of incorporating the field-theoretic treatment for the solvent in computer simulations. We expect that the approach can help to improve on some of the current implicit solvent models without significantly increasing the computational cost, and yet capture certain properties can could only be captured by explicit solvent models previously. In particular, spectra for electronic transitions in liquid mixtures is still an area that is poorly understood, and we believe that integrating our self-consistent-field approach for nonequilibrium solvent mixtures and electronic structure calculation will be a fruitful direction to achieve a better understanding for the electronic spectra.

As field-theoretic techniques have been applied to a wide range of soft matter and complex fluid systems, we also see the potential of integrating our treatment of solvents in this thesis with existing field-theoretic description of other systems. For example, presently, the field-theoretic approaches for polyelectrolyte solution generally describe the dipolar solvent at the mean-field level;[195–199] it will be interesting to incorporate the effects of reaction field in the solvent. Our variational approach for dipolar mixtures also provide an idea for incorporating the reaction field effects in condensed-phase liquid systems; such an idea would be useful for other systems where the dipolar interactions are important, for example, in the phase separation induced by dipolar interactions in polymer blends.[197]

The methods presented in this thesis also represent a step forward in accounting for polarizability effects in solvents. In the popular integral equation theories and density functional theories for liquids, the consideration for liquid polarizability

has been a challenging issue. In this thesis, we have seen that the field-theoretic approach can provide a particularly convenient treatment for the polarizability of solvent molecules. In the near future, we expect to see the strength of field-theoretic approach to be combined with other existing theories for liquids. Currently, the application of field-theoretic approaches to liquid systems is still a relatively nascent field; many important effects, including hard-sphere interactions and specific correlations between molecules, have yet to be accounted for. We hope that the continued development of field-theoretic approaches can help to bring a more complete statistical-mechanical theory for liquids.

Bibliography

[1] Shannon, R. D. Revised Effective Ionic Radii and Systematic Studies of Interatomic Distances in Halides and Chalcogenides. *Acta Crystallogr., Sect. A: Found. Adv.* **1976,** *32,* 751–767.

[2] Marcus, Y. *Solvent Mixtures: Properties and Selective Solvation;* Marcel Dekker, Inc.: New York, 2002.

[3] Gray, C. G.; Gubbins, K. E. *Theory of Molecular Fluids;* The International Series of Monographs on Chemistry Oxford University Press: Oxford, UK, 1984.

[4] Barker, J. A. *Lattice Theories of the Liquid State;* Pergamon Press: Oxford, UK, 1963.

[5] Reed, T. M.; Gubbins, K. E. *Applied Statistical Mechanics: Thermodynamic and Transport Properties of Fluids;* McGraw-Hill: New York, 1973.

[6] Watts, R. O. Integral Equation Approximations in the Theory of Fluids. In *Statistical Mechanics : Volume 1*; Singer, K., Ed.; Specialist Periodical Reports The Chemical Society: London, 1973.

[7] Barker, J. A.; Henderson, D. What Is "Liquid"? Understanding the States of Matter. *Rev. Mod. Phys.* **1976,** *48,* 587–671.

[8] Hansen, J.-P.; McDonald, I. R. *Theory of Simple Liquids;* Academic Press: Burlington, 3 ed.; 2006.

[9] Smith, W. R. Perturbation Theory in Classical Statistical Mechanics of Fluids.

In *Statistical Mechanics: Volume 1*, Vol. 1; Singer, K., Ed.; The Royal Society of Chemistry: London, 1973.

[10] Boublík, T. Progress in Statistical Thermodynamics Applied to Fluid Phase. *Fluid Phase Equilib.* **1977,** *1,* 37–87.

[11] *New Perspectives in Liquid State Theories for Complex Molecular Systems,* ; Institute Henri Poincaré, Paris, France, 2013.

[12] Jeanmairet, G.; Levesque, M.; Vuilleumier, R.; Borgis, D. Molecular Density Functional Theory of Water. *J. Phys. Chem. Lett.* **2013,** *4,* 619–624.

[13] Carnie, S. L.; Patey, G. N. Fluids of Polarizable Hard Spheres with Dipoles and Tetrahedral Quadrupoles Integral Equation Results with Application to Liquid Water. *Mol. Phys.* **1982,** *47,* 1129-1151.

[14] Fredrickson, G. H. *The Equilibrium Theory of Inhomogeneous Polymers;* Oxford University Press: Oxford, UK, 2006.

[15] Schmid, F. Self-Consistent-Field Theories for Complex Fluids. *J. Phys.: Condens. Matter* **1998,** *10,* 8105.

[16] Fredrickson, G. H.; Ganesan, V.; Drolet, F. Field-Theoretic Computer Simulation Methods for Polymers and Complex Fluids. *Macromolecules* **2002,** *35,* 16–39.

[17] Ting, C. L.; Appelö, D.; Wang, Z.-G. Minimum Energy Path to Membrane Pore Formation and Rupture. *Phys. Rev. Lett.* **2011,** *106,* 168101.

[18] Ting, C. L.; Wu, J.; Wang, Z.-G. Thermodynamic Basis for the Genome to Capsid Charge Relationship in Viral Encapsidation. *P. Natl. Acad. Sci. USA* **2011,** *108,* 16986-16991.

[19] Wang, R.; Wang, Z.-G. On the Theoretical Description of Weakly Charged Surfaces. *J. Chem. Phys.* **2015,** *142,* 104705.

[20] Thompson, R. B.; Jebb, T.; Wen, Y. Benchmarking a Self-Consistent Field Theory for Small Amphiphilic Molecules. *Soft Matter* **2012,** *8,* 9877–9885.

[21] Lee, W. B.; Mezzenga, R.; Fredrickson, G. H. Self-Consistent Field Theory for Lipid-Based Liquid Crystals: Hydrogen Bonding Effect. *J. Chem. Phys.* **2008,** *128,* 074504.

[22] Fröhlich, H. *Theory of Dielectrics;* Oxford University Press: London, 1958.

[23] Mandel, M.; Mazur, P. On the Molecular Theory of Dielectric Polarization. *Physica* **1958,** *24,* 116–128.

[24] Debye, P. J. W. Einige Resultate Einer Kinetischen Theorie Der Isolatoren. *Phys. Z.* **1912,** *13,* 97–100.

[25] Debye, P. J. W. *Polar Molecules;* Chemical Catalog Company: New York, 1929.

[26] Onsager, L. Electric Moments of Molecules in Liquids. *J. Am. Chem. Soc.* **1936,** *58,* 1486-1493.

[27] Böttcher, C. J. F. *Theory of Electric Polarization;* volume 1 Elsevier: Amsterdam, 2 ed.; 1973.

[28] Kirkwood, J. G. The Dielectric Polarization of Polar Liquids. *J. Chem. Phys.* **1939,** *7,* 911–919.

[29] Neumann, M. Dipole Moment Fluctuation Formulas in Computer Simulations of Polar Systems. *Mol. Phys.* **1983,** *50,* 841–858.

[30] Wilson, J. N. The Dielectric Constants of Polar Liquids.. *Chem. Rev.* **1939,** *25,* 377–406.

[31] Matyushov, D. V.; Ladanyi, B. M. A Perturbation Theory and Simulations of the Dipole Solvation Thermodynamics: Dipolar Hard Spheres. *J. Chem. Phys.* **1999,** *110,* 994.

[32] Tani, A.; Henderson, D.; Barker, J. A.; Hecht, C. E. Application of Perturbation Theory to the Calculation of the Dielectric Constant of a Dipolar Hard Sphere Fluid. *Mol. Phys.* **1983,** *48,* 863–869.

[33] Goldman, S.; Joslin, C. The Static Dielectric Constant of SPC and TIP4P Water by Perturbation Theory. *J. Chem. Phys.* **1993,** *99,* 3021–3029.

[34] Chandler, D. The Dielectric Constant and Related Equilibrium Properties of Molecular Fluids: Interaction Site Cluster Theory Analysis. *J. Chem. Phys.* **1977,** *67,* 1113–1124.

[35] Nienhuis, G.; Deutch, J. Structure of Dielectric Fluids. I. the Two-Particle Distribution Function of Polar Fluids. *J. Chem. Phys.* **1971,** *55,* 4213.

[36] Hoye, J. S.; Stell, G. Statistical Mechanics of Polar Systems: Dielectric Constant for Dipolar Fluids. *J. Chem. Phys.* **1974,** *61,* 562-572.

[37] Wertheim, M. S. Exact Solution of the Mean Spherical Model for Fluids of Hard Spheres with Permanent Electric Dipole Moments. *J. Chem. Phys.* **1971,** *55,* 4291–4298.

[38] Fries, P. H.; Patey, G. N. The Solution of the Hypernettedchain Approximation for Fluids of Nonspherical Particles. a General Method with Application to Dipolar Hard Spheres. *J. Chem. Phys.* **1985,** *82,* 429–440.

[39] Adelman, S. A.; Deutch, J. M. The Structure of Polar Fluids. *Advances in Chemical Physics: Non-Simple Liquids, Volume 31* **1975,** 103–153.

[40] Gray, C. G.; Gubbins, K. E.; Joslin, C. G. *Theory of Molecular Fluids Volume 2: Applications.;* International Series of Monographs on Chemistry Oxford University Press: Oxford, UK, 2011.

[41] Pollock, E.; Alder, B.; Patey, G. Static Dielectric Properties of Polarizable Stockmayer Fluids. *Physica A* **1981,** *108,* 14-26.

[42] Mandel, M. The Static Electric Permittivity for Liquids of Polarizable Dipoles. *Physica* **1973,** *66,* 180–194.

[43] Yu, H.; van Gunsteren, W. F. Accounting for Polarization in Molecular Simulation. *Comput. Phys. Commun.* **2005,** *172,* 69–85.

[44] Nakamura, I.; Shi, A.-C.; Wang, Z.-G. Ion Solvation in Liquid Mixtures: Effects of Solvent Reorganization. *Phys. Rev. Lett.* **2012,** *109,* 257802.

[45] Abrashkin, A.; Andelman, D.; Orland, H. Dipolar Poisson-Boltzmann Equation: Ions and Dipoles Close to Charge Interfaces. *Phys. Rev. Lett.* **2007,** *99,* 077801.

[46] Levy, A.; Andelman, D.; Orland, H. Dipolar Poisson-Boltzmann Approach to Ionic Solutions: A Mean Field and Loop Expansion Analysis. *J. Chem. Phys.* **2013,** *139,* 164909.

[47] Levy, A.; Andelman, D.; Orland, H. Dielectric Constant of Ionic Solutions: A Field-Theory Approach. *Phys. Rev. Lett.* **2012,** *108,* 227801.

[48] Wang, Z.-G. Fluctuation in Electrolyte Solutions: The Self Energy. *Phys. Rev. E* **2010,** *81,* 021501.

[49] Netz, R. R.; Orland, H. Variational Charge Renormalization in Charged Systems. *Eur. Phys. J. E* **2003,** *11,* 301-311.

[50] Coalson, R. D.; Duncan, A. Statistical Mechanics of a Multipolar Gas: a Lattice Field Theory Approach. *J. Phys. Chem.* **1996,** *100,* 2612-2620.

[51] Jackson, J. D. *Classical Electrodynamics;* Wiley: New York, 2 ed.; 1998.

[52] Ramshaw, J. D. Comments on the Theory of Dipolar Fluids. *J. Chem. Phys.* **1979,** *70,* 1577–1578.

[53] Qi, S.; Behringer, H.; Schmid, F. Using Field Theory to Construct Hybrid Particle–Continuum Simulation Schemes with Adaptive Resolution for Soft Matter Systems. *New J. Phys.* **2013,** *15,* 125009.

[54] Feynman, R. P. *Statistical Mechanics: A Set of Lectures;* W. A. Benjamin, Inc.: Reading, Massachusetts, 1972.

[55] Goldman, S.; Joslin, C. Why Hydrogen-Bonded Liquids Tend to Have High Static Dielectric Constants. *J. Phys. Chem.* **1993,** *97,* 12349–12355.

[56] Kleinert, H. *Path Integrals in Quantum Mechanics, Statistics, Polymer Physics, and Financial Markets;* World Scientific: Singapore, 2009.

[57] Kardar, M. *Statistical Physics of Fields;* Cambridge University Press: Cambridge, UK, 2007.

[58] Luzar, A.; Stefan, J. Dielectric Behaviour of DMSO-Water Mixtures. A Hydrogen-Bonding Model. *J. Mol. Liq.* **1990,** *46,* 221–238.

[59] Luzar, A.; Chandler, D. Structure and Hydrogen Bond Dynamics of Water–Dimethyl Sulfoxide Mixtures by Computer Simulations. *J. Chem. Phys.* **1993,** *98,* 8160–8173.

[60] Yang, L.-J.; Yang, X.-Q.; Huang, K.-M.; Jia, G.-Z.; Shang, H. Dielectric Properties of Binary Solvent Mixtures of Dimethyl Sulfoxide with Water. *Int. J. Mol. Sci.* **2009,** *10,* 1261–1270.

[61] Fattepur, R. H.; Hosamani, M. T.; Deshpande, D. K.; Mehrotra, S. C. Dielectric Relaxation and Structural Study of Aniline–Methanol Mixture Using Picosecond Time Domain Reflectometry. *J. Chem. Phys.* **1994,** *101,* 9956–9960.

[62] Griffiths, D. J. *Introduction to Electrodynamics;* Prentice Hall: Upper Saddle River, NJ, 1999.

[63] Sutin, N. Electron Exchange Reactions. *Annu. Rev. Nucl. Sci.* **1962,** *12,* 285–328.

[64] Marcus, R. A. Chemical and Electrochemical Electron-Transfer Theory. *Annu. Rev. Phys. Chem.* **1964,** *15,* 155–196.

[65] Sutin, N. Theory of Electron Transfer Reactions: Insights and Hindsights. *Prog. Inorg. Chem.* **1983,** *30,* 441–498.

[66] Marcus, R. A.; Sutin, N. Electron Transfers in Chemistry and Biology. *Biochim. Biophys. Acta.* **1985,** *811,* 265–322.

[67] Marcus, R. A. Electron Transfer Reactions in Chemistry. Theory and Experiment. *Rev. Mod. Phys.* **1993,** *65,* 599–610.

[68] Barbara, P. F.; Meyer, T. J.; Ratner, M. A. Contemporary Issues in Electron Transfer Research. *J. Phys. Chem.* **1996,** *100,* 13148–13168.

[69] Marcus, R. A. Electrostatic Free Energy and Other Properties of States Having Nonequilibrium Polarization. I. *J. Chem. Phys.* **1956,** *24,* 979-989.

[70] Marcus, R. A. On the Theory of Oxidation-Reduction Reactions Involving Electron Transfer. I. *J. Chem. Phys.* **1956,** *24,* 966–978.

[71] Marcus, R. A. On the Theory of Electron-Transfer Reactions. VI. Unified Treatment for Homogeneous and Electrode Reactions. *J. Chem. Phys.* **1965,** *43,* 679-701.

[72] Ichiye, T. Solvent Free Energy Curves for Electron Transfer Reactions: A Nonlinear Solvent Response Model. *J. Chem. Phys.* **1996,** *104,* 7561-7571.

[73] Small, D. W.; Matyushov, D. V.; Voth, G. A. The Theory of Electron Transfer Reactions: What May Be Missing?. *J. Am. Chem. Soc.* **2003,** *125,* 7470-7478.

[74] Kakitani, T.; Mataga, N. On the Possibility of Dielectric Saturation in Molecular Systems. *Chem. Phys. Lett.* **1986,** *124,* 437-441.

[75] Kakitani, T.; Mataga, N. Photoinduced Electron Transfer in Polar Solutions. I. New Aspects of the Role of the Solvent Mode in Electron-Transfer Processes in Charge-Separation Reactions. *Chem. Phys.* **1985,** *93,* 381-397.

[76] Kakitani, T.; Mataga, N. Comprehensive Study on the Role of Coordinated Solvent Mode Played in Electron-Transfer Reactions in Polar Solutions. *J. Phys. Chem.* **1987,** *91,* 6277-6285.

[77] Hatano, Y.; Saito, M.; Kakitani, T.; Mataga, N. Monte Carlo Study of the Dielectric Saturation in Molecular Solutions: Physical Basis of the C Mode in Electron-Transfer Reaction. *J. Phys. Chem.* **1988,** *92,* 1008–1010.

[78] Carter, E. A.; Hynes, J. T. Solute-Dependent Solvent Force Constants for Ion Pairs and Neutral Pairs in a Polar Solvent. *J. Phys. Chem.* **1989,** *93,* 2184-2187.

[79] Yelle, R. B.; Ichiye, T. Solvation Free Energy Reaction Curves for Electron Transfer in Aqueous Solution: Theory and Simulation. *J. Phys. Chem. B* **1997,** *101,* 4127-4135.

[80] Hartnig, C.; Koper, M. T. M. Molecular Dynamics Simulations of Solvent Reorganization in Electron-Transfer Reactions. *J. Chem. Phys.* **2001,** *115,* 8540-8546.

[81] van der Meulen, P.; Jonkman, A. M.; Glasbeek, M. Simulations of Solvation Dynamics Using a Nonlinear Response Approach. *J. Phys. Chem. A* **1998,** *102,* 1906-1911.

[82] Endicott, J. F.; Uddin, M. D. J.; Schlegel, H. B. Some Spectroscopic Aspects of Electron Transfer in Ruthenium(II) Polypyridyl Complexes. *Res. Chem. Intermediat.* **2002,** *28,* 761–777.

[83] Menzeleev, A. R.; Ananth, N.; Miller III, T. F. Direct Simulation of Electron Transfer Using Ring Polymer Molecular Dynamics: Comparison with Semiclassical Instanton Theory and Exact Quantum Methods. *J. Chem. Phys.* **2011,** *135,* 074106.

[84] Kowalczyk, T.; Wang, L.-P.; Van Voorhis, T. Simulation of Solution Phase Electron Transfer in a Compact Donor–Acceptor Dyad. *J. Phys. Chem. B* **2011,** *115,* 12135-12144.

[85] Phelps, D. K.; Weaver, M. J.; Ladanyi, B. M. Solvent Dynamical Effects in Electron Transfer: Molecular Dynamics Simulations of Reactions in Methanol. *Chem. Phys.* **1993,** *176,* 575–588.

[86] Rustad, J. R.; Rosso, K. M.; Felmy, A. R. Molecular Dynamics Investigation of Ferrous–Ferric Electron Transfer in a Hydrolyzing Aqueous Solution: Calculation of the PH Dependence of the Diabatic Transfer Barrier and the Potential of Mean Force. *J. Chem. Phys.* **2004,** *120,* 7607-7615.

[87] Zichi, D. A.; Ciccotti, G.; Hynes, J. T.; Ferrario, M. Molecular Dynamics Simulation of Electron-Transfer Reactions in Solution. *J. Phys. Chem.* **1989,** *93,* 6261-6265.

[88] Kuharski, R. A.; Bader, J. S.; Chandler, D.; Sprik, M.; Klein, M. L.; Impey, R. W. Molecular Model for Aqueous Ferrous–Ferric Electron Transfer. *J. Chem. Phys.* **1988,** *89,* 3248-3257.

[89] Warshel, A.; Hwang, J.-K. Simulation of the Dynamics of Electron Transfer Reactions in Polar Solvents: Semiclassical Trajectories and Dispersed Polaron Approaches. *J. Chem. Phys.* **1986,** *84,* 4938–4957.

[90] Enomoto, Y.; Kakitani, T.; Yoshimori, A.; Hatano, Y.; Saito, M. Monte Carlo Simulation Study on Reorganization Energy of Electron-Transfer Reactions in Polar Solution. *Chem. Phys. Lett.* **1991,** *178,* 235-240.

[91] Rosso, K. M.; Rustad, J. R. Ab Initio Calculation of Homogeneous Outer Sphere Electron Transfer Rates: Application to M(OH2)63+/2+ Redox Couples. *J. Phys. Chem. A* **2000,** *104,* 6718-6725.

[92] Ando, K. A Stable Fluctuating-Charge Polarizable Model for Molecular Dynamics Simulations: Application to Aqueous Electron Transfers. *J. Chem. Phys.* **2001,** *115,* 5228-5237.

[93] Perng, B.-C.; Newton, M. D.; Raineri, F. O.; Friedman, H. L. Energetics of Charge Transfer Reactions in Solvents of Dipolar and Higher Order Multipolar Character. II. Results. *J. Chem. Phys.* **1996,** *104,* 7177–7204.

[94] Perng, B.-C.; Newton, M. D.; Raineri, F. O.; Friedman, H. L. Energetics of Charge Transfer Reactions in Solvents of Dipolar and Higher Order Multipolar Character. I. Theory. *J. Chem. Phys.* **1996,** *104,* 7153-7176.

[95] Ishida, T.; Rossky, P. J. Solvent Effects on Solute Electronic Structure and Properties: Theoretical Study of a Betaine Dye Molecule in Polar Solvents. *J. Phys. Chem. A* **2001,** *105,* 558–565.

[96] Ramirez, R.; Gebauer, R.; Mareschal, M.; Borgis, D. Density Functional Theory of Solvation in a Polar Solvent: Extracting the Functional from Homogeneous Solvent Simulations. *Phys. Rev. E* **2002,** *66,* 031206.

[97] Naka, K.; Morita, A.; Kato, S. Solvent Electronic Polarization Effect on the Electronic Transitions in Solution: Charge Polarizable Reference Interaction Site Model Self-Consistent Field Approach. *J. Chem. Phys.* **1999,** *111,* 481–491.

[98] Akiyama, R.; Kinoshita, M.; Hirata, F. Free Energy Profiles of Electron Transfer at Water–Electrode Interface Studied by the Reference Interaction Site Model Theory. *Chem. Phys. Lett.* **1999,** *305,* 251–257.

[99] Raineri, F. O.; Perng, B.-C.; Friedman, H. L. A Fluctuating Charge Density Formulation of the Dielectric Behavior of Liquids—with Applications to Equilibrium and Nonequilibrium Solvation. *Electrochim. Acta* **1997,** *42,* 2749–2761.

[100] Matyushov, D. V. Energetics of Electron-Transfer Reactions in Soft Condensed Media. *Acc. Chem. Res.* **2007,** *40,* 294-301.

[101] Gupta, S.; Matyushov, D. V. Effects of Solvent and Solute Polarizability on the Reorganization Energy of Electron Transfer. *J. Phys. Chem. A* **2004,** *108,* 2087-2096.

[102] Matyushov, D. V.; Voth, G. A. A Theory of Electron Transfer and Steady-State Optical Spectra of Chromophores with Varying Electronic Polarizability. *J. Phys. Chem. A* **1999,** *103,* 10981-10992.

[103] Matyushov, D. V. Nonergodic Activated Kinetics in Polar Media. *J. Chem. Phys.* **2009,** *130,* 164522.

[104] Matyushov, D. V. Dipole Solvation in Dielectrics. *J. Chem. Phys.* **2004,** *120,* 1375-1382.

[105] Matyushov, D. V. Standard Electrode Potential, Tafel Equation, and the Solvation Thermodynamics. *J. Chem. Phys.* **2009,** *130,* 234704.

[106] Ghorai, P. K.; Matyushov, D. V. Solvent Reorganization Entropy of Electron Transfer in Polar Solvents. *J. Phys. Chem. A* **2006,** *110,* 8857-8863.

[107] Matyushov, D. V.; Voth, G. A. Modeling the Free Energy Surfaces of Electron Transfer in Condensed Phases. *J. Chem. Phys.* **2000,** *113,* 5413-5424.

[108] Newton, M. D.; Basilevsky, M. V.; Rostov, I. V. A Frequency-Resolved Cavity Model (FRCM) for Treating Equilibrium and Non-Equilibrium Solvation Energies: 2: Evaluation of Solvent Reorganization Energies. *Chem. Phys.* **1998,** *232,* 201 - 210.

[109] Basilevsky, M. V.; Rostov, I. V.; Newton, M. D. A Frequency-Resolved Cavity Model (FRCM) for Treating Equilibrium and Non-Equilibrium Solvation Energies. *Chem. Phys.* **1998,** *232,* 189 - 199.

[110] Zarzycki, P.; Kerisit, S.; Rosso, K. Computational Methods for Intramolecular Electron Transfer in a Ferrous–Ferric Iron Complex. *J. Colloid Interface Sci.* **2011,** *361,* 293–306.

[111] German, E. D.; Kuznetsov, A. M. Outer Sphere Energy of Reorganization in Charge Transfer Processes. *Electrochim. Acta* **1981,** *26,* 1595–1608.

[112] Liu, Y.-P.; Newton, M. D. Solvent Reorganization and Donor/acceptor Coupling in Electron-Transfer Processes: Self-Consistent Reaction Field Theory and Ab Initio Applications. *J. Phys. Chem.* **1995,** *99,* 12382–12386.

[113] Kuznetsov, A. M.; Medvedev, I. G. Activation Free Energy of the Nonadiabatic Processes of Electron Transfer and the Reorganization Energy of the Inhomogeneous Nonlocal Medium. *J. Phys. Chem.* **1996,** *100,* 5721–5728.

[114] Newton, M. D. Control of Electron Transfer Kinetics: Models for Medium Reorganization and Donor–Acceptor Coupling. In *Electron Transfer - from Isolated Molecules to Biomolecules. Part 1.*, Vol. 106; JOSHUA Jortner, J.; Bixon, M., Eds.; John Wiley & Sons, Inc.: New York, 1999.

[115] Zarzycki, P.; Rustad, J. R. Theoretical Determination of the NMR Spectrum of Liquid Ethanol. *J. Phys. Chem. A* **2009,** *113,* 291–297.

[116] Jeon, J.; Kim, H. J. Free Energies of Electron Transfer Reactions in Polarizable, Nondipolar, Quadrupolar Solvents. *J. Phys. Chem. A* **2000,** *104,* 9812-9815.

[117] Barzykin, A. V.; Frantsuzov, P. A.; Seki, K.; Tachiya, M. Solvent Effects in Nonadiabatic Electron-Transfer Reactions: Theoretical Aspects. In *Advances in Chemical Physics*, Vol. 123; Prigogine, I.; Rice, S. A., Eds.; John Wiley & Sons, Inc.: New York, 2002.

[118] Langevin, P. Magnétisme et Théorie Des électrons. *Annales de Chimie et de Physique* **1905,** *5,* 70–127.

[119] Langevin, P. Sur La Théorie Du Magnétisme. *J. Phys. Theor. Appl.* **1905,** *4,* 678–693.

[120] Gong, H.; Freed, K. F. Langevin-Debye Model for Nonlinear Electrostatic Screening of Solvated Ions. *Phys. Rev. Lett.* **2009,** *102,* 057603.

[121] Tomasi, J.; Persico, M. Molecular Interactions in Solution: An Overview of

Methods Based on Continuous Distributions of the Solvent. *Chem. Rev.* **1994,** *94,* 2027–2094.

[122] Weisstein, E. W. *CRC Concise Encyclopedia of Mathematics;* CRC press: Boca Raton, Florida, 2 ed.; 2002.

[123] Tembe, B. L.; Friedman, H. L.; Newton, M. D. The Theory of the Fe[sup 2+]–Fe[sup 3+] Electron Exchange in Water. *J. Chem. Phys.* **1982,** *76,* 1490-1507.

[124] Friedman, H. L.; Newton, M. D. Theory of Fe2+-Fe3+ Electron Exchange in Water. *Faraday Discuss. Chem. Soc.* **1982,** *74,* 73-81.

[125] Brunschwig, B. S.; Logan, J.; Newton, M. D.; Sutin, N. A Semiclassical Treatment of Electron-Exchange Reactions. Application to the Hexaaquoiron(II)-Hexaaquoiron(III) System. *J. Am. Chem. Soc.* **1980,** *102,* 5798–5809.

[126] Turner, J. W.; Schultz, F. A. Coupled Electron-Transfer and Spin-Exchange Reactions. *Coordin. Chem. Rev.* **2001,** *219–221,* 81–97.

[127] Endicott, J. F.; Durham, B.; Kumar, K. Examination of the Intrinsic Barrier to Electron Transfer in Hexaaquacobalt(III): Evidence for Very Slow Outer-Sphere Self-Exchange Resulting from Contributions of Franck-Condon and Electronic Terms. *Inorg. Chem.* **1982,** *21,* 2437-2444.

[128] Hush, N. S. Parameters of Electron-Transfer Kinetics. In *Mechanistic Aspects of Inorganic Reactions*; B., R. D.; F., E. J., Eds.; Mechanistic Aspects of Inorganic Reactions American Chemical Society: Wahington, D. C., 1982; Chapter 14, pages 301–332.

[129] Hwang, J. K.; Warshel, A. Microscopic Examination of Free-Energy Relationships for Electron Transfer in Polar Solvents. *J. Am. Chem. Soc.* **1987,** *109,* 715-720.

[130] Wang, Z.-G. Variational Electrostatics for Charge Solvation. *J. Theor. and Comput. Chem.* **2008,** *7,* 397–419.

[131] Day, T. J. F.; Patey, G. N. Ion Solvation Dynamics in Water–Methanol and Water– Dimethylsulfoxide Mixtures. *J. Chem. Phys.* **1999,** *110,* 10937-10944.

[132] Morillo, M.; Denk, C.; Pérez, P.; López, M.; Sánchez, A.; Prado, R.; Sánchez, F. Electron Transfer Reactions in Solvent Mixtures: The Excess Component of Solvent Reorganization Free Energy. *Coordin. Chem. Rev.* **2000,** *204,* 173–198.

[133] Zusman, L. D. The Dynamic Effects of the Solvent in Electron Transfer Reactions. *Russ. Chem. Rev.* **1992,** *61,* 15–24.

[134] Heitele, H. Dynamic Solvent Effects on Electron-Transfer Reactions. *Angew. Chem. Int. Ed. Engl.* **1993,** *32,* 359-377.

[135] Weaver, M. J.; McManis, G. E. Dynamical Solvent Effects on Electron-Transfer Processes: Recent Progress and Perspectives. *Acc. Chem. Res.* **1990,** *23,* 294-300.

[136] Weaver, M. J. Dynamical Solvent Effects on Activated Electron-Transfer Reactions: Dynamical Solvent Effects on Activated Electron-Transfer Reactions: Principles, Pitfalls, and Progress. *Chem. Rev.* **1992,** *92,* 463-480.

[137] Maroncelli, M.; MacInnis, J.; Fleming, G. Polar Solvent Dynamics and Electron-Transfer Reactions. *Science* **1989,** *243,* 1674–1681.

[138] Zagrebin, P. A.; Buchner, R.; Nazmutdinov, R. R.; Tsirlina, G. A. Dynamic Solvent Effects in Electrochemical Kinetics: Indications for a Switch of the Relevant Solvent Mode. *J. Phys. Chem. B* **2010,** *114,* 311-320.

[139] Zusman, L. D. Outer-Sphere Electron Transfer in Polar Solvents. *Chem. Phys.* **1980,** *49,* 295–304.

[140] Kestner, N. R.; Logan, J.; Jortner, J. Thermal Electron Transfer Reactions in Polar Solvents. *J. Phys. Chem.* **1974,** *78,* 2148-2166.

[141] Newton, M. D. Quantum Chemical Probes of Electron-Transfer Kinetics: The Nature of Donor-Acceptor Interactions. *Chem. Rev.* **1991,** *91,* 767-792.

[142] Blumberger, J.; Sprik, M. Quantum Versus Classical Electron Transfer Energy As Reaction Coordinate for the Aqueous Ru^{2+}/Ru^{3+} Redox Reaction. *Theor. Chem. Acc.* **2006,** *115,* 113-126.

[143] Marcus, R. A. Interactions in Polar Media. I. Interparticle Interaction Energy. *J. Chem. Phys.* **1963,** *38,* 1335–1340.

[144] Ando, K. Quantum Energy Gap Law of Outer-Sphere Electron Transfer Reactions: A Molecular Dynamics Study on Aqueous Solution. *J. Chem. Phys.* **1997,** *106,* 116–126.

[145] Ando, K. Solvent Nuclear Quantum Effects in Electron Transfer Reactions. II. Molecular Dynamics Study on Methanol Solution. *J. Chem. Phys.* **2001,** *114,* 9040–9047.

[146] Gehlen, J. N.; Chandler, D. Quantum Theory for Free Energies of Electron Transfer. *J. Chem. Phys.* **1992,** *97,* 4958–4963.

[147] Song, X.; Marcus, R. A. Quantum Correction for Electron Transfer Rates. Comparison of Polarizable Versus Nonpolarizable Descriptions of Solvent. *J. Chem. Phys.* **1993,** *99,* 7768–7773.

[148] Kim, H. J.; Hynes, J. T. Equilibrium and Nonequilibrium Solvation and Solute Electronic Structure. III. Quantum Theory. *J. Chem. Phys.* **1992,** *96,* 5088–5110.

[149] Miller, J. R.; Calcaterra, L. T.; Closs, G. L. Intramolecular Long-Distance Electron Transfer in Radical Anions. The Effects of Free Energy and Solvent on the Reaction Rates. *J. Am. Chem. Soc.* **1984,** *106,* 3047–3049.

[150] Gray, H. B.; Winkler, J. R. Long-Range Electron Transfer. *P. Natl. Acad. Sci. USA* **2005,** *102,* 3534-3539.

[151] Marchi, M.; Gehlen, J. N.; Chandler, D.; Newton, M. Diabatic Surfaces and the Pathway for Primary Electron Transfer in a Photosynthetic Reaction Center. *J. Am. Chem. Soc.* **1993,** *115,* 4178–4190.

[152] Blumberger, J. Recent Advances in the Theory and Molecular Simulation of Biological Electron Transfer Reactions. *Chem. Rev.* **2015,** *115,* 11191–11238.

[153] Gray, H. B.; Winkler, J. R. Electron Transfer in Proteins. *Annu. Rev. Biochem.* **1996,** *65,* 537–561.

[154] Xu, K. Nonaqueous Liquid Electrolytes for Lithium-Based Rechargeable Batteries. *Chem. Rev.* **2004,** *104,* 4303–4418.

[155] Hupp, J. T.; Weydert, J. Optical Electron Transfer in Mixed Solvents. Major Energetic Effects from Unsymmetrical Secondary Coordination. *Inorg. Chem.* **1987,** *26,* 2657-2660.

[156] Cohen, D.; Sullivan, J. C.; Amis, E. S.; Hindman, J. C. Isotopic Exchange Reactions of Neptunium Ions in Solution. IV. the Effect of Variation of Dielectric Constant on the Rate of the Np(V)-Np(VI) Exchange. *J. Am. Chem. Soc.* **1956,** *78,* 1543-1545.

[157] Horne, R. A. Kinetics and Mechanism of the Iron(II)-Iron(III) Electron-Exchange Reaction in Mixed Solvent Media. In *Exchange Reactions*; Proceedings Series International Atomic Energy Agency: Vienna, 1965.

[158] Brandon, J. R.; Dorfman, L. M. Pulse Radiolysis Studies. XIX. Solvent Effects in Electron Transfer and Proton Transfer Reactions of Aromatic Molecule Ions. *J. Chem. Phys.* **1970,** *53,* 3849-3856.

[159] Wada, G.; Aoki, M. Kinetic Studies of the Electron Transfer Reaction in Iron(II) and Iron(III) Systems. IV, the Reaction in Mixed Solvents of Dimethyl Sulfoxide and Water. *B. Chem. Soc. Jpn.* **1971,** *44,* 3056-3060.

[160] Wada, G.; Endo, A. Kinetic Studies of the Electron-Transfer Reaction in Iron(II) and Iron(III) Systems. V. the Reaction in Mixed Solvents of Methanol and Water. *B. Chem. Soc. Jpn.* **1972,** *45,* 1073-1078.

[161] Lipkowski, J.; Czerwiński, A.; Cieszyńska, E.; Galus, Z.; Sobkowski, J. Solvent Effect on Electron Transfer Reactions: Comparison of Homogeneous and Heterogeneous Electron Exchange Between V^{3+} and V^{2+} in Water + *t*-Butanol Mixtures. *J. Electroanal. Chem.* **1981,** *119,* 261-274.

[162] Eichhorn, E.; Rieker, A.; Speiser, B.; Stahl, H. Electrochemistry of Oxygenation Catalysts. 3. Thermodynamic Characterization of Electron Transfer and Solvent Exchange Reactions of Co(salen)/$[Co(salen)]^+$ in DMF, Pyridine, and Their Mixtures. *Inorg. Chem.* **1997,** *36,* 3307–3317.

[163] Muriel, F.; Jiménez, R.; López, M.; Prado-Gotor, R.; Sánchez, F. Solvent Effects on the Oxidation (electron Transfer) Reaction of $[Fe(CN)_6]^{4-}$ by $[Co(NH_3)_5pz]^{3+}$. *Chem. Phys.* **2004,** *298,* 317–325.

[164] Pérez, F.; Hernández, M.; Prado-Gotor, R.; Lopes-Costa, T.; López-Cornejo, P. Method for the Evaluation of the Reorganization Energy of Electron Transfer Reactions in Water–Methanol Mixtures. *Chem. Phys. Lett.* **2005,** *407,* 342–346.

[165] Anbalagan, K.; Lydia, I. S. Solvent Control on the Electron Transfer Reaction Between $Co^{III}(en)_2Br(L)^{2+}$–$Fe(CN)_6^{4-}$ (L=aryl Amines) by Regression Relationships: The PXRD and Electrochemical Investigations. *J. Phys. Org. Chem.* **2011,** *24,* 45–53.

[166] Sánchez, F.; Rodríguez, A.; Muriel, F.; Burgess, J.; López-Cornejo, P. Kinetic Study of the Electron Transfer Process Between $Ru(NH_3)_5pz^{2+}$ and $S_2O_8^{2-}$ in Water–Cosolvent Mixtures: A New Component of Reorganization Energy. *Chem. Phys.* **1999,** *243,* 159–168.

[167] Sarkar, S.; Pramanik, R.; Ghatak, C.; Setua, P.; Sarkar, N. Probing the Interaction of 1-Ethyl-3-Methylimidazolium Ethyl Sulfate ([Emim][$EtSO_4$]) with Alcohols and Water by Solvent and Rotational Relaxation. *J. Phys. Chem. B* **2010,** *114,* 2779-2789.

[168] Pugžlys, A.; den Hartog, H. P.; Baltuška, A.; Pshenichnikov, M. S.; Umapathy, S.; Wiersma, D. A. Solvent-Controlled Acceleration of Electron Transfer in Binary Mixtures. *J. Phys. Chem. A* **2001,** *105,* 11407–11413.

[169] Józefowicz, M. Spectroscopic Determination of Solvation Shell Composition of Fluorenone and 4-Hydroxyfluorenone in Binary Solvent Mixtures. *Spectrochim. Acta A* **2008,** *71,* 537–542.

[170] Ismailova, O.; Berezin, A. S.; Probst, M.; Nazmutdinov, R. R. Interfacial Bond-Breaking Electron Transfer in Mixed Water–Ethylene Glycol Solutions: Reorganization Energy and Interplay Between Different Solvent Modes. *J. Phys. Chem. B* **2013,** *117,* 8793–8801.

[171] Denk, C.; Morillo, M.; Sanchez-Burgos, F.; Sanchez, A. Reorganization Energies for Charge Transfer Reactions in Binary Mixtures of Dipolar Hard Sphere Solvents: A Monte Carlo Study. *J. Chem. Phys.* **1999,** *110,* 473-483.

[172] Pelizzetti, E.; Giordano, R. Solvent Effect on Electron Transfer Reactions. the System $Co(phen)_3^{3+}$-Ferrocene in Water-Alcohol Mixtures. *J. Inorg. Nucl. Chem.* **1981,** *43,* 2463–2466.

[173] Józefowicz, M. Determination of Reorganization Energy of Fluorenone and 4-Hydroxyfluorenone in Neat and Binary Solvent Mixtures. *Spectrochim. Acta A* **2007,** *67,* 444–449.

[174] Matamoros-Fontenla, M. S.; López-Cornejo, P.; Perez, P.; Prado-Gotor, R.; Vega, R. d. l.; Moyá, M. L.; Francisco, S. A Study of the Electron-Transfer Reaction Between $Fe(CN)_2(bpy)_2$ and $S_2O_8^{2-}$ in Solvent Mixtures: The Translational Component of Solvent Reorganization. *New J. Chem.* **1998,** *22,* 39–44.

[175] Zusman, L. Dynamical Solvent Effect in Electron-Transfer Reactions Occurring in a Mixture of 2 Polar-Solvents. *J. Chem. Phys.* **1995,** *102,* 2580–2584.

[176] Chandra, A. Solvent Effects on Outersphere Electron Transfer Reactions in Mixed Dipolar Liquids. *Chem. Phys.* **1998,** *238,* 285-300.

[177] Zhuang, B.; Wang, Z.-G. A Molecularly Based Theory for Electron Transfer Reorganization Energy. *J. Chem. Phys.* **2015,** *143,* 224502.

[178] Lorentz, H. A. *The Theory of Electrons;* Dover: New York, 1952.

[179] Oster, G. The Dielectric Properties of Liquid Mixtures. *J. Am. Chem. Soc.* **1946,** *68,* 2036-2041.

[180] E, W.; Ren, W.; Vanden-Eijnden, E. Finite Temperature String Method for the Study of Rare Events. *J. Phys. Chem. B* **2005,** *109,* 6688–6693.

[181] E, W.; Ren, W.; Vanden-Eijnden, E. Simplified and Improved String Method for Computing the Minimum Energy Paths in Barrier-Crossing Events. *J. Chem. Phys.* **2007,** *126,* 164103.

[182] Borgis, D.; Gendre, L.; Ramirez, R. Molecular Density Functional Theory: Application to Solvation and Electron-Transfer Thermodynamics in Polar Solvents. *J. Phys. Chem. B* **2012,** *116,* 2504–2512.

[183] Zhao, S.; Jin, Z.; Wu, J. New Theoretical Method for Rapid Prediction of Solvation Free Energy in Water. *J. Phys. Chem. B* **2011,** *115,* 6971–6975.

[184] Pelizzetti, E.; Pramauro, E. Solvent Effects on Electron Transfer Reactions. the System Iron(III)-Phenothiazine in Water-Alcohol Mixtures. *Transition Met. Chem.* **1981,** *6,* 334-336.

[185] Marcus, Y. The Use of Chemical Probes for the Characterization of Solvent Mixtures. Part 2. Aqueous Mixtures. *J. Chem. Soc., Perkin Trans. 2* **1994,** 1751–1758.

[186] Zhuang, B.; Wang, Z.-G. Molecular-Based Theory for Electron-Transfer Reorganization Energy in Solvent Mixtures. *J. Phys. Chem. B* **2016,** *120,* 6373–6382.

[187] Blumberger, J.; Lamoureux, G. Reorganization Free Energies and Quantum Corrections for a Model Electron Self-Exchange Reaction: Comparison of Polarizable and Non-Polarizable Solvent Models. *Mol. Phys.* **2008,** *106,* 1597–1611.

[188] Lamoureux, G.; Roux, B. Modeling Induced Polarization with Classical Drude Oscillators: Theory and Molecular Dynamics Simulation Algorithm. *J. Chem. Phys.* **2003,** *119,* 3025-3039.

[189] Lamoureux, G.; Alexander D. MacKerell, J.; Roux, B. A Simple Polarizable Model of Water Based on Classical Drude Oscillators. *J. Chem. Phys.* **2003,** *119,* 5185-5197.

[190] Lamoureux, G.; Harder, E.; Vorobyov, I. V.; Roux, B.; MacKerell Jr., A. D. A Polarizable Model of Water for Molecular Dynamics Simulations of Biomolecules. *Chem. Phys. Lett.* **2006,** *418,* 245 - 249.

[191] Eastman, P. *et al.* OpenMM 4: A Reusable, Extensible, Hardware Independent Library for High Performance Molecular Simulation. *J. Chem. Theory Comput.* **2013,** *9,* 461-469.

[192] Jiang, W.; Hardy, D. J.; Phillips, J. C.; MacKerell, A. D.; Schulten, K.; Roux, B. High-Performance Scalable Molecular Dynamics Simulations of a Polarizable Force Field Based on Classical Drude Oscillators in NAMD. *J. Phys. Chem.Letters* **2011,** *2,* 87-92.

[193] Warshel, A. Dynamics of Reactions in Polar Solvents. Semiclassical Trajectory Studies of Electron-Transfer and Proton-Transfer Reactions. *J. Phys. Chem.* **1982,** *86,* 2218-2224.

[194] King, G.; Warshel, A. Investigation of the Free Energy Functions for Electron Transfer Reactions. *J. Chem. Phys.* **1990,** *93,* 8682-8692.

[195] Lee, C.-L.; Muthukumar, M. Phase Behavior of Polyelectrolyte Solutions with Salt. *J. Chem. Phys.* **2009,** *130,* 024904.

[196] Muthukumar, M. Phase Diagram of Polyelectrolyte Solutions: Weak Polymer Effect. *Macromolecules* **2002,** *35,* 9142–9145.

[197] Kumar, R.; Sumpter, B. G.; Muthukumar, M. Enhanced Phase Segregation Induced by Dipolar Interactions in Polymer Blends. *Macromolecules* **2014,** *47,* 6491–6502.

[198] Ermoshkin, A. V.; Olvera de la Cruz, M. A Modified Random Phase Approximation of Polyelectrolyte Solutions. *Macromolecules* **2003,** *36,* 7824–7832.

[199] Dobrynin, A. V. Solutions of Charged Polymers. In *Polymer Science: A Comprehensive Reference*; Matyjaszewski, K.; Möller, M., Eds.; Elsevier: Amsterdam, 2012.